The role of PML and PML nuclear bodies in FADD-mediated apoptosis

Kirsten Ellerup Jensen

Imperial College London
Macromolecular Structure and Function Research Group

Submitted for a degree of Doctor of Philosophy of Imperial College London

April 2014

Declaration of originality

I hereby declare that all the research associated with my PhD is a product of my own work unless otherwise stated. Ideas or quotations from other people, published or through personnel communication, are fully acknowledged or referenced according to the standard practices.

Copyright declaration

Acknowledgements

My special thanks go to my supervisor Professor Paul Freemont for all his help and support over the *many* years of my project. I want to thank him for his advice and always very useful and constructive discussions. I never lacked the feeling of receiving support and pastoral consideration. He always made sure my glass was full.

My second order of thanks must go to my old bosses in Hamburg, Hans Will, Klaus Harbers and Peter Nobis. They bravely introduced me to science. Hans especially taught me how to survive in research.

I would like to thank many of my colleagues who have supported me on my journey, particularly Ciaran McKeown for teaching me how to do protein purification and showing me all the tricks, and James Chappell for many helpful discussions through the years: I miss our meetings over coffee in the SCR; Alexander Webb for useful advice; Ke Yan likewise, and for putting my brain back into gear at the end of my write-up; Elizabeth Batty for helpful discussions in the early stages of my project; Suhail Islam for assisting me with 3D reconstructions; and Rajika Perera for helping with the CK1 structures. I would also like to thank all the other members of the MSF lab for their support and advice through the years, particularly David Charles for all his help in the final stages.

I would particularly like to thank Paul Hitchen for his help with the MS of SUMO-modified CK1 delta.

Lastly I thank my family for putting up with me, especially during my writing-up period, and never complaining when my experiments took longer than planned so that often I arrived home later than promised.

And I will have to thank my parents for all their support through my life.

Dedicated to my parents

Project motivation

A major focus of Professor Paul Freemont's research group is nuclear organization in the cell. We are using PML and PML nuclear bodies (NBs) together with other nuclear compartments to investigate the relationships between the NBs and how they are organized. This means that functional studies of the PML protein and associated factors are important to us, and they have informed the thesis I have been working on.
When I began to study the PML field around 20 years ago in Hans Will's group in Hamburg, PML NBs were called 'nuclear dots' and it was only Sp100 that was known to localize to nuclear bodies. The second nuclear body protein to be identified was PML. PML was discovered as a fusion protein with the retinoid acid receptor in acute promyelytic leukaemia and is now probably the most prominent NB constituent of all. We now know that PML NBs contain more than 80 constituents, most of them showing only a partial and transient colocalisation. For many years research groups failed to distinguish between the various PML isoforms they were working with and naturally obtained diverse results. Around 10 years ago, when I joined Paul Freemont's group in London, we wrote a review naming all the different PML isoforms and splice variants, making clear the high number of PML proteins expressed in the cell and hence the variety their functions.
Today our main interest is the involvement of PML and PML NBs in apoptosis. There is no formation of PML NBs in PML -/- cells because PML is necessary for PML NB formation and SUMO is important for the formation of mature PML NBs.
We are also interested in SUMO-modification of proteins and the regulatory functions where SUMO-modification is involved. Many research groups have speculated that SUMO-modification takes place within the PML NBs, partly because many of the constituents are being SUMO-modified but also because many of the constituents are part of the SUMO-modification machinery. PML has been shown to be a SUMO E3 ligase and to bind to the SUMO-conjugating enzyme Ubc9.
Our overall is aim to discover more about the function of PML NBs and PML NB constituents. This will give us a better insight into how the disruption of the organisation of PML NBs can cause human disease. After more than 20 years of investigation, PML NBs have turned out to be very complex – and extremely interesting.

Abstract

PML nuclear bodies (NBs) consist of more than 80 constituents and are involved in many cellular processes such as apoptosis, DNA repair, cell cycle, transcriptional regulation and development. PML NBs are associated with the 'nuclear matrix' and vary in size from 0.3 to 1.0 μm in diameter. PML NBs came to prominence when PML, expressed as an oncogenic fusion protein with the retinoic acid receptor, was found in patients with acute promyelocytic leukaemia. PML is the major PML NB constituent and is involved in cellular activities such as apoptosis, growth suppression, antiviral defence and DNA repair, among many others. PML can be modified by the Small Ubiquitin-like MOdifier (SUMO) and contains a SUMO-interacting motif (SIM). Both SUMO-modification and SUMO-interaction play an important role in the formation of PML NBs.

The aim of this study is to gain deeper knowledge about PML, PML NBs and associated factors. Preliminary data show that PML is interacting with TRAF4-associated factor 1 (TFAF-1). The TRAF family of proteins forms part of a signalling pathway via the TNF receptor and is implicated in growth regulation. When TFAF-1 is expressed as a fusion protein with a red fluorescent protein it forms filamentous structures. These structures colocalise with death-effector filaments (DEFs). DEFs are formed by the Fas-associated death domain (FADD) and the prodomain of caspase-8.

The main focus of this study was to discover more about how PML and PML NBs regulate apoptotic pathways, and thereby gain a better insight into the organisation of PML and PML NBs and how their disruption contributes to human disease. The association between TFAF-1, PML, PML NBs and DEFs was investigated further. DEFs were found to disrupt PML NBs and phosphorylation of FADD was found to be necessary for the disruption. Casein kinase 1 alpha (CK1 alpha) phosphorylates FADD at S194, which has been shown to regulate the apoptotic activities of FADD. Thus the regulation of the kinase activity and the phosphorylation of FADD, together with PML and PML NBs were investigated. Preliminary data shows that CK1 is modified by SUMO. This might take place at the PML NBs and adds a whole new aspect to the already very complex story of PML NBs and PML NB constituents.

Abbreviations

aa	amino acid
AML	acute myeloid leukaemia
APL	acute promyelocytic leukaemia
ATRA	all-trans retinoid acid
CARD	caspase recruitment domain
CBs	cajal bodies
CHX	cyclohexamide
CK1	casein kinase 1
CML	chronic myeloid leukemia
cPML	cytoplasmic PML
CrmA	cytokine response modifier A
CT	chromosome territories
Daxx	death domain-associated protein
DD	death domain
DED	death-effector domain
DEF	death-effector filaments
DISC	death-inducing signalling complex
ECL	enhanced chemi-luminescence
EDTA	ethylenediamine tetra-acetic acid
ER	endoplasmatic reticulum
FAB	French-American-British system (of cancer classification)
FADD	Fas-associated death domain
FCS	foetal calf serum
FLASH	Caspase-8-binding FLICE-associated huge protein
GFP	green fluorescent protein
IFN	interferon
IC	interchromatin compartment
ICD	interchromosomal domain compartment
IFN	interferon
IMAGE	Integrated Molecular Analysis of Genomes and their Expression
IPTG	isopropyl β-D-1-thiogalactopyranoside

MAM	mitochondria-associated membrane
MEF	mouse embryonic fibroblast
min	minute(s)
NES	nuclear export signal
NLS	nuclear localisation signal
NPM	nucleophosmin
NuMA	nuclear mitotic apparatus
PAGE	polyacrylamide gel electrophoresis
PBC	primary billiary cirrhosis
PBS	phosphate buffered saline
PcG	polycomb group (bodies)
PCR	polymerase chain reaction
PI	propidium iodide
PIC1	PML interacting clone 1
PLZF	promyelocytic leukaemia zinc finger
PML	promyelocytic leukaemia
PML NBs	promyelotic leukaemia nuclear bodies
RARα	retinoic acid receptor alpha
SBM	SUMO-binding motif
SDS	sodium dodecyl sulphate
SIM	SUMO-interacting motif
SNURF	small nuclear RING-finger protein (or RNF4)
STAT5b	signal transducer and activator of transcription 5b
SUMO	small ubiquitin modifier
TAE	Tris-acetate/EDTA buffer
TFAF	TRAF associated factor
TNF	tumor necrosis factor
TNFR	tumor necrosis factor receptor
TRADD	TNFR-associated death domain
TRAF	TNF receptor associated factor
TRIM	TRIpartite Motif
Tris	2-amino-2(hydroxymethyl)-1,3-propandiol
UV	ultraviolet
WHO	World Health Organization

Table of contents

List of figures

List of tables

1 Introduction

1.1 The mammalian nucleus

1.1.1 The mammalian nucleus and subcompartments of the nucleus

The most prominent organelle of the eukaryotic cell is the nucleus. It contains all the machinery essential for gene expression. It is surrounded by the nuclear envelope, which consists of two membranes. The two membranes are fused together at nuclear pores, which allow smaller molecules to diffuse freely while regulating the transport of larger molecules such as proteins. The nucleus contains all the genetic information necessary for division and maintenance of the cell. This information is stored on chromosomes. Chromosomes are packed into chromatin and their structure varies throughout the cell cycle. For example, chromosomes condense in the M phase of the cell cycle, whereas in interphase, specific regions of chromosomes decondense, becoming accessible for gene expression. Chromatin consists of DNA wrapped around histones, forming nucleosomes, and is organised into chromosome territories. The location of these territories relates to gene density and expression (Cremer and Cremer, 2001). Chromatin consists of the lesser-condensed, active euchromatin and the highly condensed, mostly inactive heterochromatin. Euchromatin is usually located on the interior of the nuclear space whereas heterochromatin is located at the nuclear periphery, often close to the nucleolus. Gene positioning might be self-organising, dependent not only on expression but also on interactions between chromosomes, e.g. co-regulated genes and the association of regulatory elements with their target genes (Misteli, 2008). An overview of the mammalian nucleus and its organisation can be seen in Figure 1.1.

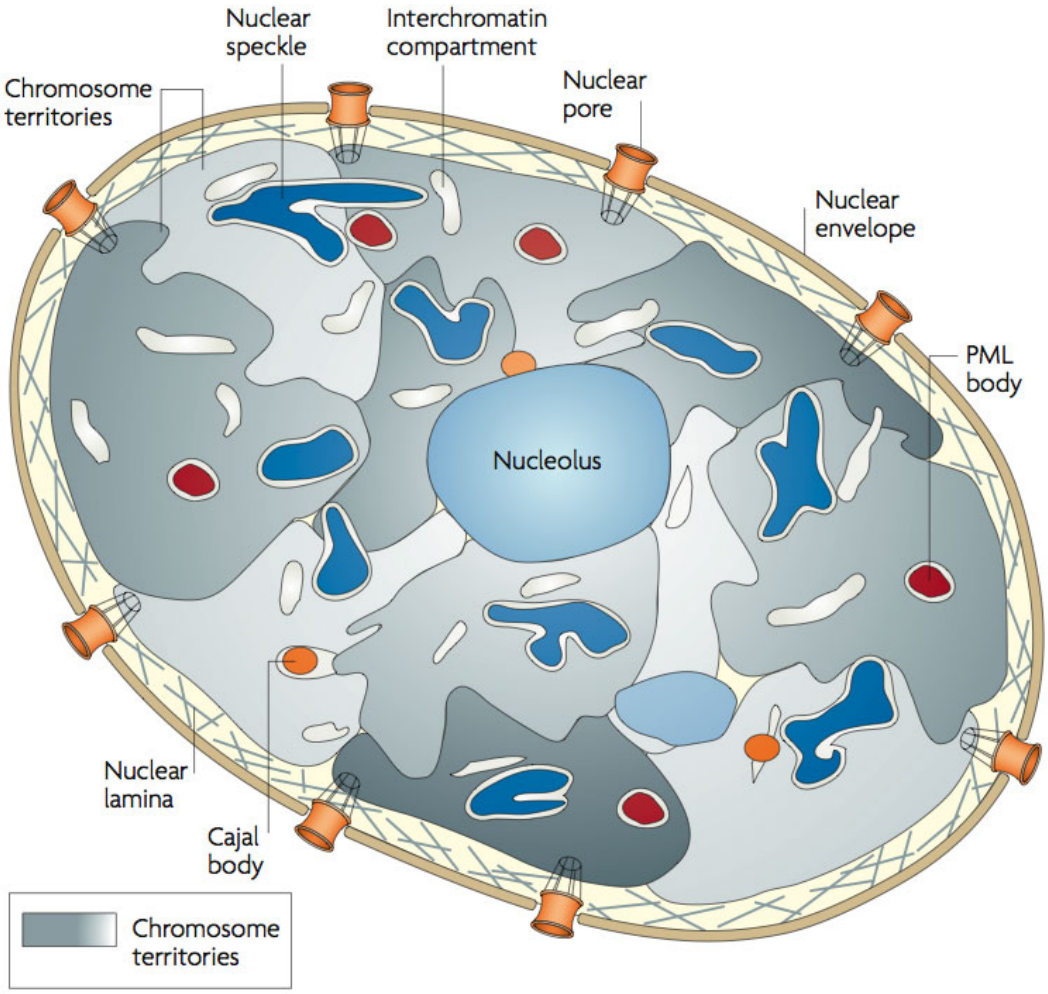

Figure 1.1. An overview of the mammalian nucleus and its organisation

The nucleus is surrounded by the nuclear envelope, which contains nuclear pores. PML nuclear bodies (PML NBs), Cajal bodies (CBs) and nuclear speckles localise to the interchromatin compartment (IC) or interchromosomal domain compartment (ICD). This compartment forms outside the chromosome territories (CT), which are a major feature of nuclear organisation. Adapted from (Lanctot et al., 2007).

1.1.2 Nuclear bodies and dynamics of the nuclear compartments

Several studies have identified an increasing number of specialised domains within the nucleus (Lamond and Earnshaw, 1998). These compartments are often referred to as nuclear bodies. They are defined by distinct sets of residual proteins and include nucleoli, Cajal bodies (CBs), promyelocytic leukaemia nuclear bodies (PML NBs), nuclear speckles, active sites of transcription, polycomb group (PcG) bodies, gemini bodies (gems) and 53BP1 NBs, amongst many others. Nuclear compartments are non

membrane-bound, which was previously thought to lead to their random distribution. Although it is now known that the nucleus is highly organised, the formation of nuclear compartments is still not fully understood. In some cases, the domains have been shown to be dynamic structures and a rapid protein exchange occurs between them and the nucleoplasm (Misteli, 2001; Misteli, 2007). New microscopy techniques have helped in studying the systemic organisation of the nucleus, and further studies might help us to understand how disruption of this organisation can contribute to human disease (Misteli, 2010). How and why such nuclear structures form is far from clear, but two differing models have been discussed in the literature (Kaiser et al., 2008; Matera et al., 2009; Mao et al., 2011). While both involve recruitment of components from the soluble nucleoplasmic pool, one model is ordered and built around a single scaffolding component and the other is stochastic: its components assemble in a random order. Although the assembly is stochastic, it can still be predicted through known interactions. Loss of one component of the complex can lead to the failure to incorporate another component and therefore to disruption of the nuclear organisation (Kaiser et al., 2008; Matera et al., 2009; Mao et al., 2011).

1.2 PML and PML nuclear bodies

1.2.1 Identification of PML and PML nuclear bodies

PML NBs (also known as ND10 or PODs) were first identified over 50 years ago (de The et al., 1960) and comprise a multi-protein heterogeneous complex of over 80 proteins (see Figure 1.2) that is implicated in numerous cellular activities such as ageing, apoptosis, the cell cycle, stress response, hormone signalling, transcriptional regulation and development (reviewed in Negorev and Maul, 2001; Lallemand-Breitenbach and de The, 2010). Thirty years later, the first PML NB component, Sp100, was discovered using autoimmune sera from primary billiary cirrhosis (PBC) patients (Szostecki et al., 1990). PML NBs are associated with the 'nuclear matrix' and are found in nearly all cell types, varying both in size (from 0.3 to 1.0 μm in diameter) and number (10 to 30 structures per cell). PML NBs came to attention with the discovery that PML, a major protein constituent, was associated with acute promyelocytic leukaemia (APL), a type of cancer characterised by a reciprocal chromosomal translocation of chromosomes 15 and 17 resulting in a fusion protein comprising PML and the retinoic acid receptor α (RARα) (reviewed in Zelent et al.,

2001). In APL patients, it is observed that PML NBs are disrupted into smaller and more dispersed bodies whereas in treated patients the bodies reform, suggesting that the integrity of PML is directly correlated with the APL disease phenotype (Koken et al., 1995; Le et al., 1996).

In APL patients treated with arsenic trioxide the PML NBs reform. Arsenic trioxide binds to PML and PML/RARα in the B2-domain of PML and induces the formation of intermolecular disulfate bonds (Jeanne et al., 2010) followed by SUMO-modification and degradation of PML (Lallemand-Breitenbach et al., 2008; Tatham et al., 2008); whereas the treatment with all-trans-retinoic acid causes mostly differentiation of the APL blasts but also degradation of of RARα and PML/RARα via the RARα moiety (reviewed in Dos Santos et al., 2013).

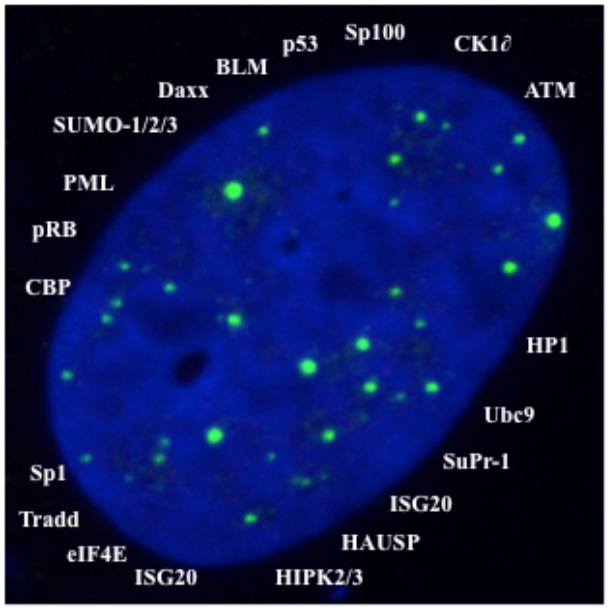

Figure 1.2. A list of cellular proteins identified to localise to PML nuclear bodies

PML and Sp100 are two major components of PML NBs and always co-localise. The other components are either recruited or localise transiently to the PML NBs under specific conditions.

1.2.2 PML

In the following sections and in my studies I concentrated on PML, Sp100, Daxx and SUMO because these are the major components of PML NBs and usually colocalise,

whereas many of the other PML NB components are either recruited or localise transiently to PML NBs under specific conditions.

PML is the key organizer of PML NBs and it has been shown that PML -/- mice cannot assemble PML NBs (Zhong et al., 2000). The *PML* genomic locus is approximately 35 kb in length. It is subdivided into nine exons and a large number of alternative spliced transcripts are synthesized from the *PML* gene, resulting in a variety of PML proteins ranging in molecular weight from 48–97 kDa (Jensen et al., 2001). The *PML* gene encodes six distinct groups of isoforms, all of which contain a conserved TRIpartite Motif or TRIM (Reymond et al., 2001), consisting of a RING finger, two B-boxes and a coiled-coil domain – also named the RBCC motif (Jensen et al., 2001). Studies of the RBCC/TRIM motif have included both biophysical and functional approaches, resulting in the first description of the structure of the PML RING-finger domain (Borden et al., 1995). By using this structure as strategy for further experiments, it was shown that point mutations in the RING finger had severe effects on the structure and integrity of PML NBs *in vivo* (Boddy et al., 1997). Further studies on the RBCC/TRIM motif showed that mutations in the B-box also disrupted PML NB formation *in vivo* and that homo-oligomerisation via the coiled-coil domain was not sufficient for NB formation (Borden et al., 1996).

A yeast two-hybrid protein screen for PML led to the first description of PIC1 (PML interacting clone 1), now known as Small Ubiquitin-like Modifier (SUMO)-1 (Boddy et al., 1996). PML was the first NB protein shown to be modified by SUMO-1 (Kamitani et al., 1998c, Muller et al., 1998, Sternsdorf et al., 1997). At least three lysine residues can serve as SUMO-1 modification sites in the PML protein (Duprez et al., 1999; Kamitani et al., 1998b). A detailed study showed one major modification site, K490, was part of the nuclear localisation signal (NLS) and another site, K65, was where the SUMO-specific E2 conjugating enzyme UBC9 interacted with PML via the RING finger domain (Duprez et al., 1999).

PML is expressed as several different isoforms (Fagioli et al., 1992; Jensen et al., 2001). The isoforms are divided into groups on the basis of sequence differences found at the C-terminus (Jensen et al., 2001). A further division into subgroups has been made which reflects the alternative splicing of exons 4, 5 and 6 (Fagioli et al., 1992; Jensen et al., 2001). A NLS is located in exon 6 (Jensen et al., 2001) and two splice variants that lack exon 6, PML VIb and PML VIIb, have been identified (Reymond et al., 2001). PML I, the longest isoform, contains a nuclear export signal

(NES) (Henderson and Eleftheriou, 2000) and has a nuclear and cytoplasmic distribution when overexpressed in PML -/- cells (Condemine et al., 2006). All PML isoforms except for b/c variants (variants without exon 5 and 6 or exon 4, 5 and 6) contain the three SUMO modification sites and a NLS, suggesting that the functionality of these motifs is relevant to most PML isoforms. Another relevant motif in the PML protein is the SUMO interacting motif (SIM) (Shen et al., 2006). The SIM is localised in exon 7a and found in all PML isoforms except for PML VI (Brand et al., 2010). (See Figure 1.3 for an overview of the PML domain structure.)

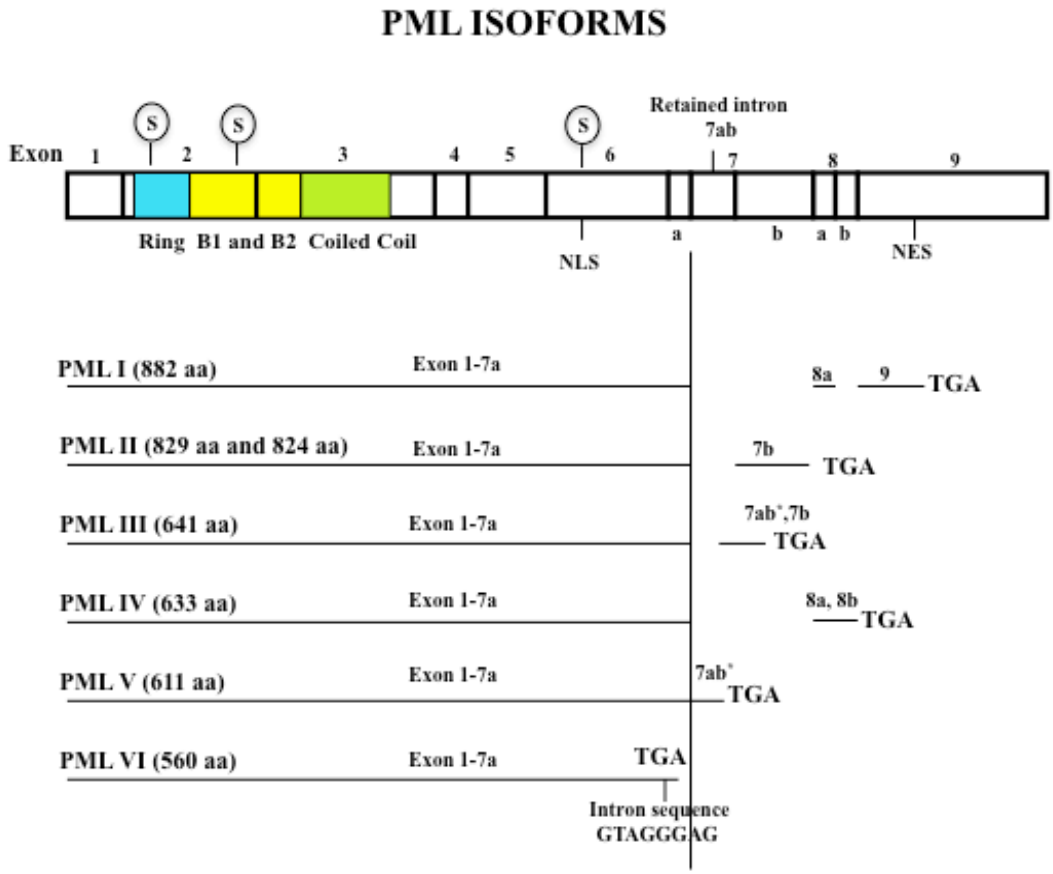

Figure 1.3. PML domain structure

All PML isoform share the N-terminal domain containing the RBCC/TRIM motif. PML isoforms are made by alternative splicing at the C-terminus, resulting in altered sizes of each isoform. SUMO modification sites (S) are located at positions K65, K160 and K490. *Retained intron sequence.

1.2.3 Sp100

A large number of cellular proteins have been identified as localising to PML NBs. All components, except for Sp100, localise transiently to PML NBs or are recruited to them under certain conditions. The Sp100 protein which was the first PML NB component identified (Szostecki et al., 1990) is expressed as many C-terminal-spliced variants (Guldner et al., 1999). Sp100, like PML, is an interferon-inducible protein (Guldner et al., 1992; Grotzinger et al., 1996b) and can also be modified by SUMO-1 (Sternsdorf et al., 1997). Interestingly, modification of Sp100 is dependent on a functional NLS but is not necessary for nuclear import or targeting to PML NBs (Sternsdorf et al., 1999). Sp100 has also been shown to interact with SUMO via a SUMO interaction motif. It was identified as a SUMO-1/2 interaction partner in a yeast two-hybrid assay (Hecker et al., 2006). Furthermore, the SIM in Sp100 is essential for *in vivo* Sp100 SUMO modification (Knipscheer et al., 2008).

Sp100 is a PML NB component that links PML NBs to apoptosis. Caspase-8-binding FLICE-associated huge protein (FLASH) has been shown to interact with Sp100. FLASH localises to the nucleus in the PML NBs but is translocated to the cytoplasm upon CD95 activation, where it interacts with caspase-8 at the mitochondria and subsequently activates the mitochondrial apoptosis pathway (Milovic-Holm et al., 2007). Sp100 has also been shown to contain a potential caspase recruitment domain (CARD) (Sanchez-Pulido et al., 2007), also known as the HSR domain (Grotzinger et al., 1996a; Sternsdorf et al., 1999). It has been speculated that Sp100 can interact with caspase-2 via this domain (Sanchez-Pulido et al., 2007). Caspase-2 also localises to PML NBs (Tang et al., 2005) and the CARD in procaspase-2 is modified by SUMO-1 (Shirakura et al., 2005). It is possible that SUMO-1 modification might play a critical role in the maturation/activation and nuclear localisation of procaspase-2 (Shirakura et al., 2005).

1.2.4 Daxx

The death domain-associated protein (Daxx) was originally discovered as a Fas-receptor interacting protein (Torii et al., 1999; Yang et al., 1997), and also links PML NBs to apoptosis. Daxx localises to the cytoplasm, as well as the nucleus where it is found as a component of PML NBs. It can be modified by SUMO-1 (Jang et al., 2002) and has also been shown to interact with SUMO-modified PML (Ishov et al.,

1999). Localisation of Daxx to PML NBs correlates with the proapoptotic activity of Daxx, and Daxx mutants that fail to localise to PML NBs do not facilitate Fas-induced cell death (Torii et al., 1999). Daxx is also found in the nucleoplasm and within heterochromatic regions of the nucleus in PML -/- cells, where it also fails to facilitate apoptosis (Ishov et al., 1999). Several studies suggest a role for Daxx in promoting apoptosis (Torii et al., 1999; Yang et al., 1997), which is in apparent conflict with the results obtained from mutation of the *Daxx* gene *in vivo* (Michaelson et al., 1999). Surprisingly, Daxx-deficient mice show extensive apoptosis and embryonic lethality. The role of Daxx in preventing and/or inducing apoptosis remains unclear (Salomoni and Khelifi, 2006).

Daxx has also been shown to interact with SUMO (Ryu et al., 2000) and this interaction is necessary for SUMO-modification of Daxx (Lin et al., 2006). It has been speculated that the interaction with SUMO might target Daxx to PML NBs where it can be modified by SUMO, although levels of SUMO-modified Daxx did not change in cells transfected with PML siRNA (Lin et al., 2006). The SIM in Daxx is also important for transrepression of several SUMO-modified transcription factors (Lin et al., 2006). Recently it was shown that the Daxx SIM is phosphorylated by CK2 kinase (Chang et al., 2011). This phosphorylation promotes binding affinity towards SUMO-1 over SUMO-2/3 and results in Daxx interacting with SUMO-1-modified proteins, implying a preference (Chang et al., 2011).

At the moment there are two models proposed for the proapoptotic function of Daxx associated with PML NBs. The first suggests that Daxx represses expression of antiapoptotic genes at PML NBs and the second suggests that Daxx could act as a transcriptional coactivator of proapoptotic genes (Bernardi et al., 2008). Further studies will have to be performed to understand the role of Daxx and PML, and Daxx PML NBs in apoptosis.

Recently Daxx has been shown to act as a chaperone for the H3.3 histone (Drane et al., 2010). H3.3 interacts with Daxx directly and Daxx is essential for targeting H3.3 to PML NBs (Drane et al., 2010). The chromatin remodelling factor ATRX, which also interacts with Daxx and associates with PML NBs (Ishov et al., 2004) assists Daxx in targeting H3.3 onto pericentric DNA repeats (Drane et al., 2010). These findings open a whole new area for the function of Daxx and PML NBs (reviewed in Salomoni, 2013).

1.2.5 SUMO

SUMO was simultaneously discovered by several laboratories in 1996 and given a variety of names: GMP-1, PIC1, Sentrin, HSMT3 and Ubl1 (Matunis et al., 1996; Boddy et al., 1996; Okura et al., 1996; Mannen et al., 1996; Shen et al., 1996). SUMO is now the most commonly used name. SUMO binds covalently to other proteins in a similar way to ubiquitin (Figure 1.4) and is involved in several different cellular events, such as progression through the cell cycle, apoptosis, protein stability, transcriptional regulation, response to viral infection and DNA repair (Johnson and Blobel, 1999; Seeler and Dejean, 2003; Gareau and Lima, 2010; Wilkinson and Henley, 2010). SUMO contains a Gly–Gly motif at the C-terminus, which is essential for its conjugation to other proteins. SUMO binds to a lysine within the consensus sequence ΦKXE/D, where Φ is a hydrophobic amino acid, K the modified lysine, X any amino acid and E/D an acidic amino acid. SUMO-1 only shows 18% homology to ubiquitin but both proteins have a very similar three-dimensional structure (Bayer et al., 1998). The SUMO-1 protein does not contain a lysine residue that corresponds to lysine 48 in ubiquitin, which is responsible for forming ubiquitin chains (Bayer et al., 1998). Therefore, SUMO-1 is unable to form SUMO chains.

Soon after SUMO-1, two further familial proteins were discovered: SUMO-2 (also named SMT3A or Sentrin-3 (Lapenta et al., 1997); and SUMO-3 (SMT3B or Sentrin-2) (Kamitani et al., 1998a). SUMO-2 and SUMO-3 share 95% sequence identity with each other but only 50% sequence identity with SUMO-1. SUMO-2 and SUMO-3 contain the FKXE/D motif and – unlike SUMO-1 – can form SUMO chains (Tatham et al., 2001). Another difference is the flexible N-terminal extension of SUMO-1, which the other SUMO isoforms lack. This is probably important for protein/protein interactions (Bayer et al., 1998) and has been shown to be phosphorylated at serine 2 (Matic et al., 2008).

SUMO has also been shown to interact non-covalently with proteins via a SIM: motif 1 h-h-X-S-X-S/T-a-a-a (h, hydrophobic; a, acidic) (Minty et al., 2000); motif 2 V/I/L-X-V/I/L-V/I/L (Song et al., 2004); and motif 3 K-X_{3-5} –I/V-I/L-I/L-X_3-D/E/Q/N-D/E-D/E (Hannich et al., 2005; Hecker et al., 2006). Recently, RING domain-containing proteins possessing one or more SIMs have been shown to target SUMO-modified proteins for ubiquitin-mediated proteolysis (Prudden et al., 2007; Sun et al., 2007; Uzunova et al., 2007; Tatham et al., 2008; Lallemand-Breitenbach et al., 2008).

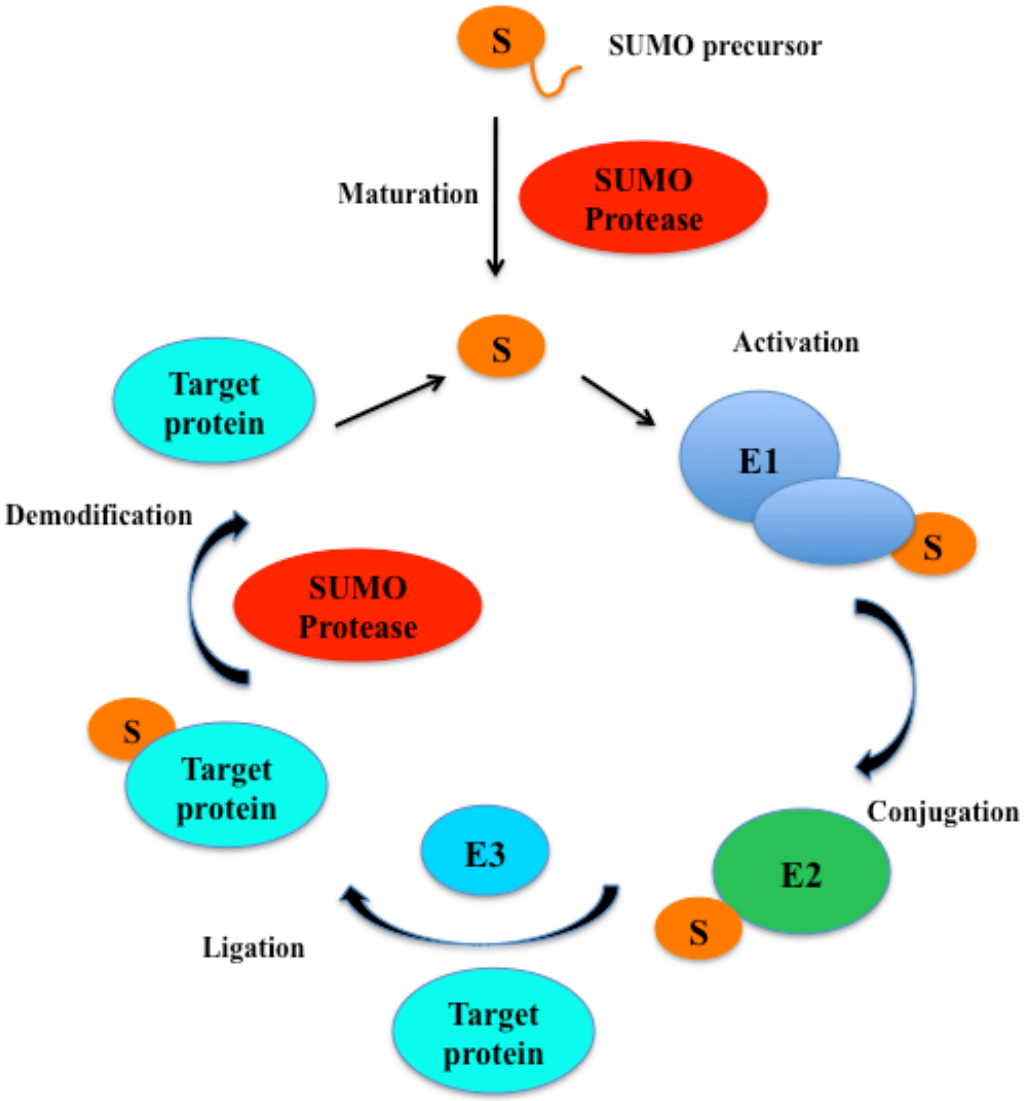

Figure 1.4. Schematic representation of the SUMO cycle

The SUMO protease cleaves the SUMO precursor, leaving two essential glycine residues at the C-terminus. SUMO is activated by formation of a thioester bond between the C-terminal glycine and a cysteine in the SUMO-activating enzyme E1. It is then transferred to the conjugating enzyme E2 and finally passed onto the ε–amino group of specific lysine residues in the target protein by a SUMO-specific ligase E3. S (SUMO), E1 SUMO-activating enzyme (Uba2, Aos1), E2 conjugating enzyme (Ubc9) and E3 SUMO-specific ligase.

1.2.6 RNF4

RNF4, also known as small nuclear RING-finger protein (SNURF), has been linked to transcriptional regulation (Moilanen et al., 1998) and shown to have ubiquitin E3 ligase activity (Hakli et al., 2004). It localises partially to PML NBs (Hakli et al., 2005) and is recruited to them when co-expressed with a specific PML isoform, PML IV, but not with PML III. The recruitment is enhanced by SUMO-1 (Hakli et al., 2005). PML IV is able to repress the transcriptional activity of RNF4, probably by recruiting it to the bodies in a SUMO-dependent way (Hakli et al., 2005). Later it was discovered that RNF4 is a poly-SUMO-specific E3 ubiquitin ligase that is required for arsenic–induced degradation of PML and PML/RARα (Lallemand-Breitenbach et al., 2008; Tatham et al., 2008). Arsenic induces SUMO-modification, ubiquitination and degradation of PML protein. Lysine 160, one of the major SUMO-modification sites in PML, is necessary for this process (Lallemand-Breitenbach et al., 2008). PML is modified by SUMO-1 and SUMO-2/3 after arsenic treatment and it is speculated that both SUMO-1 and SUMO-2/3 contribute to PML degradation but on different levels (Lallemand-Breitenbach et al., 2008). Lysine 160 primarily appears to be a site for SUMO-2 chains and RNF4 binding whereas Lysine 65, which is found in the RING-finger domain of PML, could stabilise the RING-Ubc9 interaction (Knipscheer et al., 2007) and/or stabilise RNF4 binding.

RNF4 was found to bind to and ubiquitinate SUMO-2 chains (Tatham et al., 2008). Cells depleted for RNF4 have increased levels of PML and SUMO-2. PML fails to be degraded in arsenic-treated cells when RNF4 is depleted (Tatham et al., 2008).

To find out more about arsenic-induced degradation of PML, stable cells lines were created (Percherancier et al., 2009; Geoffroy et al., 2010). After treating PML III-expressing cells with arsenic, PML is recruited to the PML NBs, modified by SUMO and targeted for ubiquitin-mediated proteolysis (Geoffroy et al., 2010). Cells expressing PML III but depleted for RNF4 show an accumulation of PML in large bodies (Geoffroy et al., 2010). Depletion of RNF4 in a SUMO-2-expressing cell line treated with arsenic also results in formation of large PML-containing bodies (Geoffroy et al., 2010). RNF4 may interact with poly-SUMO-2 chains attached to PML, but not directly with PML, leading to ubiquitin-mediated degradation of PML (Geoffroy et al., 2010).

By further investigation of the involvement of SUMO in RNF4-mediated degradation of PML, it was shown that the PML SIM is required for arsenic-induced degradation

of PML but not for the arsenic-enhanced SUMO-modification of PML (Percherancier et al., 2009). Serine phosphorylation sites next to the SIM are required for SIM-dependent non-covalent interactions of PML with SUMO-modified partners but are not required for arsenic- and RNF4-induced degradation of PML (Percherancier et al., 2009). Interestingly, this stretch of serines has also been shown to be important in CK2-dependent phosphorylation and ubiquitin-mediated degradation of PML (Scaglioni et al., 2006).

1.3 PML nuclear body formation

PML is essential for PML NB formation and required for NB localisation of other NB components such as Sp100, Daxx and SUMO-1 (Zhong et al., 2000). In PML -/- cells, Daxx and SUMO-1 show a speckled pattern whereas Sp100 forms large aggregates, probably by interacting with itself through the HSR domain. The normal NB pattern can be restored by co-transfection of PML (Zhong et al., 2000). PML has been shown to be covalently modified by SUMO (Sternsdorf et al., 1997) at three lysines: K65, K160 and K490 (Duprez et al., 1999; Kamitani et al., 1998b). PML I and PML IV are additionally C-terminally SUMO-modified at lysine K616 (Boutell et al., 2011; Cuchet-Lourenco et al., 2011). SUMO modification of PML is necessary for the formation of a mature PML NB (Lallemand-Breitenbach et al., 2001). SUMO-modified PML forms a doughnut-like shape whereas the PML mutant PML-3K forms dense aggregates (Lallemand-Breitenbach et al., 2001). Both SUMO binding and modification are necessary for PML NB formation and a model for the assembly of PML NBs has been proposed (Shen et al., 2006; Bernardi and Pandolfi, 2007, Figure 1.5). However, it has been shown that all PML isoforms, including PML VI, which does not contain a SIM, are able to form PML NBs in PML -/- cells (Brand et al., 2010). Thus, the SIM is not essential for nuclear formation of PML but is probably critical for the recruitment of other PML NB components (Brand et al., 2010).

The common feature of PML NB components, i.e. their ability to be modified by SUMO, has led to speculation about PML NBs being the site where SUMO-modification takes place. Another feature is that many PML NB components or RBCC/TRIM proteins are SUMO E3 ligases, important for the SUMO-modification machinery (Chu and Yang, 2011). Some RBCC/TRIM proteins also bind the similarly

important SUMO-conjugating enzyme Ubc9 and enhance the transfer of SUMO from Ubc9 to the substrate (Chu and Yang, 2011).

In mitotic cells, PML is de-SUMO-modified (Everett et al., 1999) and other NB components dissociate from PML. PML forms aggregates through multimerisation of the coiled-coil domain. During interphase, PML is modified again and the nucleation of PML NBs is triggered by the interaction of SUMO-modified PML and other SUMO-modified proteins, such as Sp100 and Daxx, through SUMO moieties and SUMO binding motifs (Shen et al., 2006).

PML NBs localise to the interchromosomal domain compartment (ICD) in the cell (Bridger et al., 1998). This compartment forms outside the chromosomes and co-localises not only with PML NBs but also with coiled bodies and specific nuclear RNAs (Bridger et al., 1998).

The different PML isoforms have been shown to accumulate in various nuclear domains (Condemine et al., 2006). This difference in localisation might be due to variations in the C-terminus of the PML isoforms, resulting in interactions with different nuclear proteins. All PML isoforms colocalise when co-expressed due to PML protein interacting with itself through the coiled-coil domain (Condemine et al., 2006). This results in the PML NBs appearing to be uniform but recent evidence shows that they are structurally and functionally heterogeneous structures (Bernardi and Pandolfi, 2007; Weidtkamp-Peters et al., 2008). It has also recently been shown that the C-terminus of PML II and V can form PML NBs independently of their N-terminus and that the PML NBs formed by PML V can recruit other PML NB components like Sp100 and Daxx (Geng et al., 2012). This suggests that the C-terminus of PML V is important for PML NB formation and adds to the complexity of the assembly of PML NBs (Geng et al., 2012). PML NB formation seems to be influenced by many different mechanisms, including SUMO-modification and SUMO interactions, PML isoform interactions and the presence of other PML NB components (Weidtkamp-Peters et al., 2008). (See Figure 1.5 for a suggested model for PML NB assembly.)

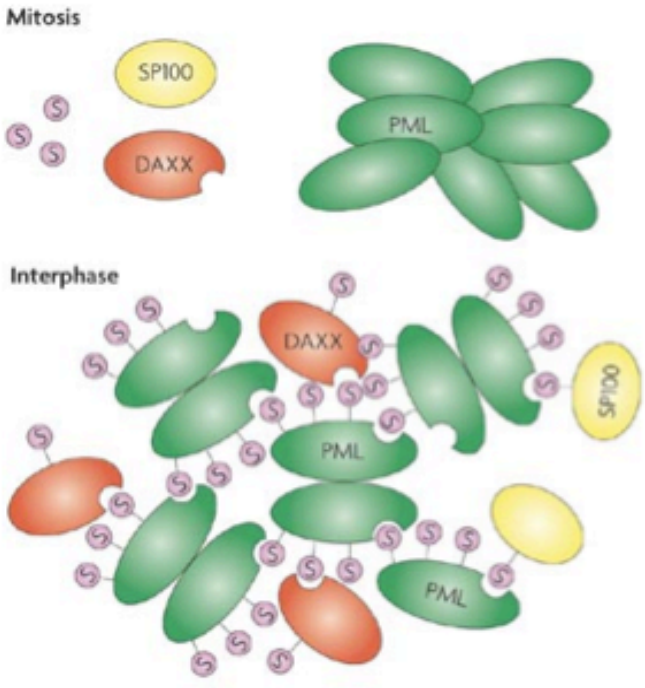

Figure 1.5. A model for the assembly of PML NBs

Many PML NB components are not only covalently modified by SUMO but also contain a SIM. PML NB components interact with themselves or with SUMO, which can subsequently be covalently attached to another PML NB component. (Adapted from Bernardi and Pandolfi, 2007).

1.4 Proposed PML functions

Given the heterogeneous mix of proteins found in PML NBs, the function of the NBs, and thus PML itself (since PML is essential for the formation of PML NBs) (Zhong et al., 2000), has remained elusive. They have been linked to many different functions such as transcriptional regulation, tumour suppression, the regulation of apoptosis, the antiviral response and DNA damage (Bernardi and Pandolfi, 2007; Lallemand-Breitenbach and de The, 2010).

Several models for PML NB function have emerged. One proposes that PML NBs act as 'nuclear depots' where proteins, including those covalently modified by SUMO-1, can be recruited and, under certain conditions, released at sites of action elsewhere (Negorev and Maul, 2001). Support for this model comes from the non-essential nature of the bodies such as their existence as aggregations of concentrated proteins and the discrepancy between functions of NB proteins. Another model suggests that

PML NBs act as sites of nuclear protein turnover, supported by the observations that proteasomes, associated co-factors and mis-folded viral proteins are localised to the bodies under certain conditions (Anton et al., 1999; Lallemand-Breitenbach et al., 2001). As mentioned earlier, the SUMO-dependent ubiquitin ligase RNF4 was found to colocalise to PML NBs (Hakli et al., 2005), which fits this model very well. RNF4 has been shown to target the arsenic-induced SUMO-modified lysine 160 in PML for polyubiquitination and proteasome-mediated degradation in PML NBs (Tatham et al., 2008). Neither of these models is mutually exclusive and many other functions of PML NBs have also been suggested, which is unsurprising when taking into account the many different proteins that localise to PML NBs. However, it is clear that PML NBs form a part of a nuclear/cellular defence mechanism against viral attack and other external insults. Many viruses have been shown to alter the levels, modification and localisation of PML (reviewed in Geoffroy and Chelbi-Alix, 2011).

1.4.1 PML forms part of an anti-viral response

It has emerged that PML nuclear bodies are the targets of viral infection (reviewed in (Everett, 2001). For nuclear replicating DNA viruses, including herpesviruses, adenoviruses and papovaviruses, the viral genome associates with PML NBs, and initial sites of transcription and replication are frequently close to PML NBs (Everett, 2001). In addition, several viral regulatory proteins disrupt PML NB structure and these events are directly correlated with the efficiency of infection. For RNA viruses, including the hepatitis delta virus, lymphocytic choriomeningitis virus and rabies virus, PML NBs are disrupted by a range of mechanisms including the relocalisation of PML NBs to the cytoplasm (reviewed in Regad and Chelbi-Alix, 2001). Interestingly, the *PML* gene contains interferon response elements, and PML expression is upregulated by interferon α, β, and γ treatment, resulting in an increase in the number of PML NBs per cell (Stadler et al., 1995; Lavau et al., 1995; Chelbi-Alix et al., 1998). Several studies have shown that PML expression enables resistance to viral infection and that PML NBs form part of a cellular antiviral response (Chelbi-Alix et al., 1998; Djavani et al., 2001; Bonilla et al., 2002).

One PML isoform, PML II, has been shown to interact directly with adenovirus type 5 E4 Orf3 protein (Hoppe et al., 2006). This interaction is isoform specific as only PML II was rearranged by E4 Orf3 (Hoppe et al., 2006). The PML II interacting sequence has been mapped to aa 645-684 in exon 7b (Leppard et al., 2009). E4 Orf3 has been

shown to self-associate to mediate the formation of nuclear tracks, and PML is not necessary for E4 Orf3 track formation (Hoppe et al., 2006). The E4 Orf3 protein inhibits the cellular viral response, as do many other viral proteins, by disrupting PML NBs (Ullman et al., 2007).

It has been speculated that cytoplasmic PML consists of either newly made cytoplasmic PML or nuclear PML that has been recruited to the cytoplasm (McNally et al., 2008). A PML splice variant lacking exon 5 and 6, PML Ib accumulates in the cytoplasm in HSV-1-infected cells, sequestering ICP0 and thereby decreasing viral gene expression (McNally et al., 2008).

Different viruses use different mechanisms to regulate PML and PML NBs. Some disrupt the bodies by changing the SUMO-modification of PML, thus changing the stability and localisation of PML. Viruses probably disrupt PML NBs to avoid cellular defence mechanisms (reviewed in Everett and Chelbi-Alix, 2007; Reineke and Kao, 2009).

1.4.2 Acute promyelocytic leukaemia

Acute promyelocytic leukaemia (APL) belongs to the acute myeloid leukaemia (AML) family of cancers and is classified as AML-M3 in the old French-American-British (FAB) system and AML with characteristic genetic abnormalities in the newer World Health Organization (WHO) system. APL accounts for 10% of adult AML patients and currently 90% of APL patients are disease free at 5 years. However, APL used to be a fatal disease with a severe prognosis. APL is the most malignant form of acute leukaemia with severe bleeding tendency and a very rapid fatal course of only a few weeks. Cells from APL patients contain a reciprocal translocation of chromosome 15 and 17 which fuses the *PML* gene and the RARα (de The et al., 1991; Goddard et al., 1991; Kakizuka et al., 1991; Pandolfi et al., 1991). This translocation generates the PML-RARα fusion protein and accounts for 99% of all cases. (See Figure 1.6 for an overview of the breakpoints in PML and RARα.) Four other genes have been described as rare fusions with RARα in APL: promyelocytic leukaemia zinc finger (PLZF) (Chen et al., 1993), nucleophosmin (NPM) (Redner et al., 1996), nuclear mitotic apparatus (NuMA) (Wells et al., 1997) and signal transducer and activator of transcription 5b (STAT5b) (Arnould et al., 1999). While the *RARα* gene always

breaks within the same intron and the reciprocal translocations X-RARα and RARα-X are expressed in the APL blasts, X does not bear any structural similarities.

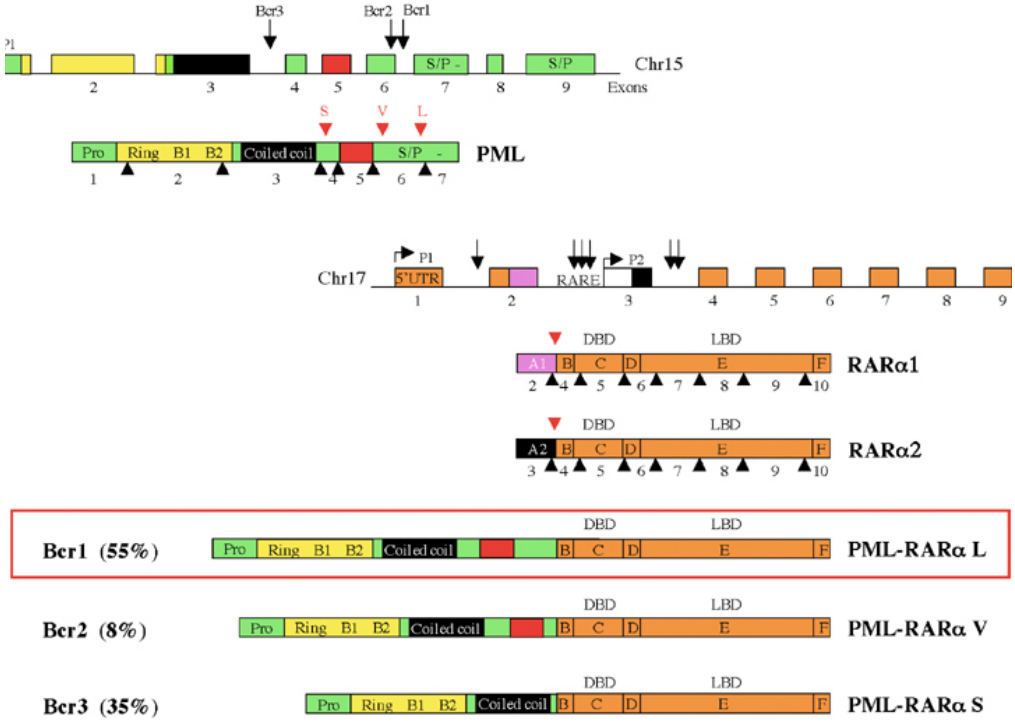

Figure 1.6. Breakpoints in RARα and PML

The PML breakpoint positions are located between exons 3 and 4 and between exons 6 and 7. All PML-RARα fusion proteins contain the RBCC/TRIM motif. The *RARα* gene always breaks within the second intron. (Adapted from Tussie-Luna et al., 2006).

1.4.3 Treatment of acute promyelocytic leukaemia

The prevalence of most cancers increases with age, due to the accumulation of mutations in cells. However, the prevalence of APL appears to remain constant with age, suggesting that it is caused by a single, rate-limiting genetic event (Vickers et al., 2000). APL can be treated with all-trans retinoid acid (ATRA) in association with chemotherapy, with arsenic alone or with arsenic and ATRA.

ATRA induces differentiation of APL blasts (Castaigne et al., 1990) and proteasome-mediated degradation of PML/RARα (Zhu et al., 1999). Degradation of PML/RARα allows for the restoration of PML NBs (Zhu et al., 1997). Only a few patients are cured with ATRA alone (Castaigne et al., 1990) and a combination therapy of ATRA with chemotherapy is often used (Fenaux et al., 1999). Clinical trials have shown that

arsenic on its own delivers a 70% cure rate whereas arsenic and ATRA gives a 90% cure rate (Lallemand-Breitenbach et al., 2012). Arsenic degrades PML/RARα by targeting PML (Zhu et al., 1997) whereas RARα degrades through ATRA (Zhu et al., 1999). Arsenic recruits diffuse PML to PML NBs (Zhu et al., 1997) where PML is then modified by SUMO and targeted for arsenic-induced proteolysis (Lallemand-Breitenbach et al., 2001; Geoffroy et al., 2010). Recently it has been shown that PML gets poly-sumoylated and targeted by RNF4, a SUMO-dependent ubiquitin ligase, then polyubiquinated and degraded by the proteasome (Tatham et al., 2008). Recruitment of PML to the bodies is not dependent on RNF4, but RNF4 follows shortly after and interacts with SUMO, though not with PML, at the NBs (Geoffroy et al., 2010).

Despite there being several different treatments for APL, the main therapies used are ATRA together with chemotherapy, arsenic alone, or arsenic together with ATRA (reviewed in de The and Chen, 2010). Recently a study showed that degradation of PML/RARα, and not differentiation of the APL blasts, as often thought, is responsible for curing APL (Nasr et al., 2008).

1.4.4 PML and cancer

PML has been shown to be involved in tumour suppression (Koken et al., 1995) and increasing evidence suggests that PML expression is altered in various tumours. Loss of PML expression is often associated with increased grade and progression in many tumour types.

Tissue microarrays with samples from normal tissue and cancer tissue were analysed for PML expression and it was found that PML protein expression was lost in 17% of colon adenocarcinoma, 21% of lung carcinoma, 28% of prostate adenocarcinoma, 32% of breast carcinoma, 49% of central nervous carcinoma, 48% of germ cell tumours, 0% of thyroid carcinoma, 0% of adrenal cortical carcinoma and 68% of non-Hodgkin's lymphoma (Gurrieri et al., 2004) tumours. Complete loss of PML expression is often associated with advanced cancers in breast, prostate and central nervous system tumours (Gurrieri et al., 2004). PML mRNA was detected in cells negative for PML protein expression and samples were tested for mutations at the *PML* locus. However, the *PML* gene was rarely mutated and was not subject to loss of heterozygosity (Gurrieri et al., 2004). In a germ cell tumour line where PML protein

expression was partially lost, two other NB components, SUMO and Daxx, were found at normal protein levels but with an aberrant nuclear localisation pattern. Furthermore, PML mRNA was expressed at normal levels and the *PML* gene was not mutated (Gurrieri et al., 2004). The proteasome inhibitor MG132 was used to treat cancer cell lines in order to investigate the effects of proteasome-dependent mechanisms on PML protein expression. After treatment with MG132, the normal NB pattern of PML was restored and SUMO-1 and Daxx were found in the NBs once again (Gurrieri et al., 2004). This suggests that the stability of PML is regulated in a proteasome-dependent way (Gurrieri et al., 2004).

Other studies have also shown that PML protein expression is altered in cancers. An almost complete loss of PML protein was demonstrated in small-cell lung carcinomas (Zhang et al., 2000) and gastric cancers (Lee et al., 2007; Kim et al., 2011). In gastric cancers, PML loss was associated with greater lymphatic invasion and a lower survival rate (Lee et al., 2007; Kim et al., 2011). Loss of PML protein expression can also be used as an independent prognostic marker in patients with oesophageal squamous cell carcinoma (Yen et al., 2011). Different levels of PML expression in cancer cells might mirror the stage and aggressiveness of the tumour.

Other groups have even found overexpression of PML protein in some cancer cells (Chan et al., 1998; Gambacorta et al., 1996; Yoon and Yu, 2001). When PML is highly expressed in chronic myeloid leukemia (CML) it has been shown to result in a less favourable outcome (Ito et al., 2008). PML/RARα is able to act as a potential oncogene and the SUMO-modifaction site lysine 160 in PML is essential for transcriptional repression and transformation (Zhu et al., 2005). It seems to be clear that PML can act as a tumor suppressor in many cancers but in other cases also facilitate cancer cell survial (Martin-Martin et al., 2013).

For immunostaining of PML the monoclonal antibody PG-M3 is often used (Falini et al., 1997). This is a species-specific and fixative-resistant antibody that detects the N-terminal region of PML (Flenghi et al., 1995), which is present in all known PML splice variants. It is often used for rapid diagnosis for APL (Alayed et al., 2013), recognising all APL cases characterised by the three major breakpoints bcr1, bcr2 and bcr3.

1.4.5 Cytoplasmic PML

Nuclear PML has most commonly been studied but accumulating evidence shows that PML also seems to play a role in the cytoplasm. PML was shown to be involved in TGF-β-signalling (Lin et al., 2004). TGF-β induces senescence in wild-type mouse embryonic fibroblasts whereas in PML -/- cells this effect is completely abrogated. It was only possible to partially restore the activity of TGF-β in PML -/- cells by expressing PML IV, a nuclear PML isoform, whereas expression of PML IV ΔNLS or PML RBCC rescued the transcriptional activity of TFG-β. Cytoplasmic PML (cPML) interacts with the signalling proteins SMAD2/3 and SARA (Smad anchor for receptor activation), regulating their localisation (Lin et al., 2004). Also PML/RARα is able to disrupt the complex and thereby interfere with the TGF- β signalling (Lin et al., 2004).

Cytoplasmic PML has also been found to associate with the endoplasmatic reticulum (ER) and the mitochondria-associated membranes (MAMs) (Giorgi et al., 2010). These domains are involved in calcium-dependent apoptotic cell death. PML -/- cells treated with endoplasmic reticulum stress inducers are less responsive to apoptosis when compared with PML +/+ cells (Giorgi et al., 2010). Expression of a PML chimera that localises to the outer surface of the ER restores the mitochondrial calcium signals and the sensitivity to apoptosis (Giorgi et al., 2010). This shows that cytoplasmic PML regulates apoptosis at the ER by controlling calcium release (Giorgi et al., 2010).

APL-associated PML mutations (1272delAG and IVS3-IG-A) cause both of these mutant PML proteins to localise to the cytoplasm and form doughnut-shaped cytoplasmic bodies (Bellodi et al., 2006). The cytoplasmic PML mutants interact with PML/RARα and counteract differentiation induced by retinoic acid (RA). A PML/RARα mutant that localises to the cytoplasm also inhibits RA-dependent transcription and differentiation. These results suggest that the cytoplasmic localisation of PML/RARα might contribute to transformation. The same PML mutants have been used to study the relationship between cPML and p53 (Bellodi et al., 2006). It has been shown that cPML sequesters nuclear PML to the cytoplasm, disrupts the NBs and inhibits p53's transcriptional, growth suppressive and apoptotic functions (Bellodi et al., 2006). Further studies will hopefully bring more insight to

the function of cPML (reviewed in Salomoni and Bellodi, 2007; Carracedo et al., 2011).

1.5 PML and regulation of apoptosis

PML has been involved in many apoptotic pathways such as a caspase-independent and -dependent pathways. PML has been shown to be an important regulator of p53-dependent and -independent apoptotic pathways and PML recruits p53 to the PML NBs upon certain stimuli. As mentioned earlier, PML is able to regulate apoptosis at ER-mitochodria sites showing it has a function outside the PML NBs.

The literature on PML and apoptosis is vast and therefore only relevant aspects – those involving PML and death receptor-mediated apoptosis – have been included here, as this was the main interest of my studies.

1.5.1 PML knockout mice

The availability of embryonic fibroblasts from PML -/- mice has provided opportunities for studying the functional role of PML and PML NBs (Wang et al., 1998a). Homozygous mice for the PML mutation are fertile, born with the expected Mendelian frequency and are indistinguishable at the phenotypic level from PML +/+ mice. However, PML -/- mice are extremely susceptible to bacterial infections, suggesting that PML may indeed play a role in an anti-infection response. PML -/- MEFs grow faster than PML +/+ MEFs and show loss of contact inhibition, suggesting that PML is involved in cell growth control (Wang et al., 1998a). PML -/- mice and cells are protected from the lethal effects of ionizing radiation and anti-Fas antibodies and PML is required for caspase-1 and caspase-3 activation (Wang et al., 1998b). It has also been shown that PML is crucial for the induction of apoptosis by Fas, TNF α, ceramide and type I and II interferons (IFNs) (Wang et al., 1998b). This might also explain the resistance of APL cells to Fas-, TNF- and IFN-induced apoptosis with a lack of caspase-3 activation.

PML -/- MEFs do not show any PML nuclear staining, and other PML NB components such as Sp100, Daxx and SUMO-1 fail to localise to PML NBs in the absence of PML. However, the normal localisation of the other PML NB components can be restored by transfection of PML (Zhong et al., 2000). This shows that PML is

required for the proper nuclear compartmentalisation of other NB components and therefore NB formation (Zhong et al., 2000).

1.5.2 CD95/Fas-mediated apoptosis and death-effector filaments

The CD95/Fas death receptor triggers apoptosis following its activation through the binding of Fas ligand (FasL) (Nagata, 1999). CD95/Fas ligation leads to formation of a death-inducing signalling complex (DISC) by recruitment of Fas-associated death domain (FADD) to its intracellular death domain (DD) (Kischkel et al., 1995). Interaction of the death-effector domain (DED) of FADD and caspase-8 (Boldin et al., 1996) leads to recruitment and proteolytic activation of procaspase-8 at the DISC (Medema et al., 1997).

FADD forms a 3:3 complex with the CD95/Fas receptor via the DD but it has been suggested that the DED in FADD is involved in forming the complex as well (Sandu et al., 2006). Self-association of FADD through the DED is required for the formation of a stable complex with the CD95/Fas receptor (Sandu et al., 2006). After the formation of the complex, procaspase-8 binds to FADD via their respective DEDs and it has been suggested to be a preferential interaction with one of the DEDs in procaspase-8 (Carrington et al., 2006).

CD95/Fas triggers apoptosis via two signalling pathways, which are determined by the amount of caspase-8 activated at the DISC (Scaffidi et al., 1998). In type I cells, a large amount of caspase-8 is activated at the DISC, causing activation of caspase-3 and resulting in apoptosis. In type II cells, the activation of caspase-8 is low and these cells depend on the mitochondrial pathway to activate caspase-3 (Scaffidi et al., 1998). Low concentrations of caspsase-8 results in cleavage of Bid which produces tBid. tBid translocates to the mitchondria where it activates Bax/Bak. This results in cytochrome c being released to the cytosol and activation of the apoptosome follows (Sessler et al., 2013). For a review please see Tourneur and Chiocchia, 2010. An overview of PML NBs and death-receptor-mediated apoptosis is presented in Figure 1.7.

DED-containing proteins such as FADD and the prodomain of caspase-8 can cause apoptosis by forming death-effector filaments (DEFs) (Siegel et al., 1998). DEFs recruit and activate pro-caspase zymogens (Siegel et al., 1998) and viral DED-containing proteins can inhibit apoptosis by preventing formation of the DEFs. The data show that assembly of apoptosis-signalling complexes can occur intracellularly

as well as at the plasma membrane (Siegel et al., 1998).

FADD has been shown to be phosphoryalted at S194 by casein kinase 1 alpha (CK1 alpha) (Alappat et al., 2005). Phosphorylation of FADD correlates with the cell cycle (Scaffidi et al., 2000) and non-phosphorylated FADD is found in G1/S whereas phosphoryalted FADD is found in G2/M (Scaffidi et al., 2000). Phosphorylation of FADD is important for the regulation of cell cycle progression as phosphorylation of FADD was found to be necessary for G2/M cell cycle arrest in non-tumour cell lines (Alappat et al., 2003), and overview in Figure 1.8). This suggests that FADD might not only affect apoptosis by binding to the death receptors but also by interfering with the cell cycle.

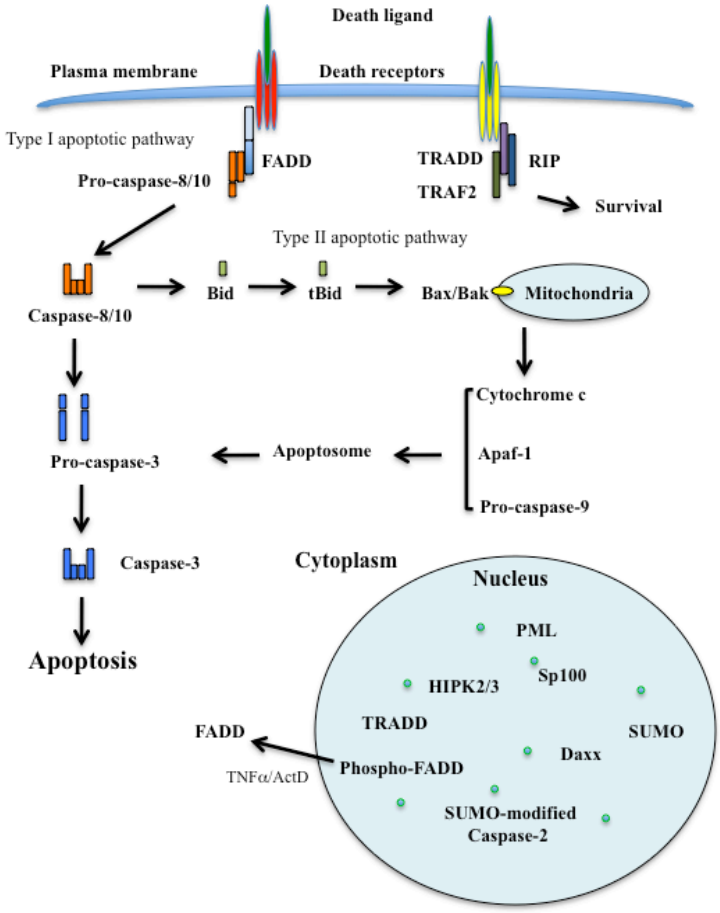

Figure 1.7. PML nuclear bodies and death receptor-mediated apoptosis

Many proteins shown to be part of the death-receptor-mediated apoptotic pathway also localise to the nucleus and some of them partially to PML NBs. Often, post-translational modifications like phosphorylation or SUMO-modification affect the localisation of the proteins.

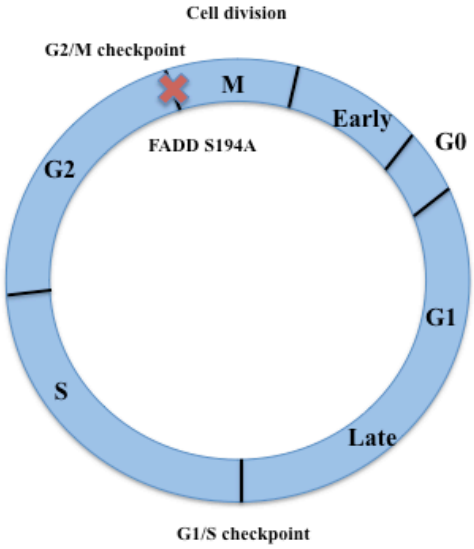

Figure 1.8. Phosphorylation of FADD is important for G2/M arrest in non-tumour cell lines

FADD needs an intact phosphorylation site to arrest cells in G2/M. FADD but not the mutant FADD S194A arrests cells in GS/M. G2/M is an important checkpoint before mitosis. G1/S is important before chromosome duplication.

1.5.3 PML and death receptor-mediated apoptosis

Mounting evidence suggests PML NBs and PML NB components play a very important role in the death receptor-induced cell-death pathway, including CD95-mediated apoptosis (Wang et al., 1998b; Torii et al., 1999).

In addition to Daxx, another protein called tumor necrosis factor receptor (TNFR) type 1-associated death domain (TRADD) has been shown to localise to both the cytoplasm and the nucleus. TRADD contains an NLS and an NES domain and is able to shuttle between the cytoplasm and the nucleus (Morgan et al., 2002). It localises to PML NBs in the nucleus in the absence of export and the DD in TRADD has been shown to be responsible for the localisation. At PML NBs, the DD in TRADD can activate PML- and p53-dependent apoptosis. The apoptotic pathway induced by TRADD-DD is not sensitive to caspase inhibitors (Morgan et al., 2002).

A third protein, known as HIPK3, has also been shown to localise to both the PML NBs and the cytoplasm. It was initially identified as a Fas-interacting protein and has

also been shown to interact with Daxx and FADD (Rochat-Steiner et al., 2000). Interestingly, overexpression of HIPK3 did not show any effect on Fas-induced apoptosis.

Recently, PML and PML/RARα have also been identified as Fas-associated proteins (Tao et al., 2011). PML and PML/RARα bind to Fas through the B-box domain in PML, and the DD in Fas is necessary for Fas/PML and Fas/PML/RARα complex formation (Tao et al., 2011). The Fas/PML/RARα complex formation recruits the anti-apoptotic regulator c-FLIP and inhibits Fas-mediated apoptosis. In addition, PML/RARα prevents binding of the Fas ligand and agonistic antibody CH-11 to the Fas receptor (Tao et al., 2011). The authors speculate that PML might stabilise the Fas-FADD-procaspase-8 complex or destabilise the Fas-FADD-cFLIP complex, with PML/RARα having the opposite effect. This is an important discovery as many cancers feature altered PML expression, which could then result in defective Fas signalling.

1.5.4 PML and SUMO-modified caspases

PML has been shown to be involved in apoptosis via a caspase-independent pathway (Quignon et al., 1998). Caspase inhibitors do not prevent PML-induced cell death and caspase-3 is not activated upon PML overexpression (Quignon et al., 1998), although there is now growing evidence to support a connection between PML/PML NBs and caspases. One initiator caspase, caspase-2, has been shown to localise to PML NBs (Tang et al., 2005) and to be modified by SUMO (Shirakura et al., 2005). SUMO-modification of procaspase-2 at lysine K60 is necessary not only for nuclear localisation but also for activation/maturation of procaspase-2 (Shirakura et al., 2005). Another initiator caspase, caspase-8, can also be modified by SUMO. Caspase-8 can be SUMO-modified at lysine 156, and in this case although the modification is also associated with nuclear localisation it does not seem to interfere with the processing of caspase-8 (Besnault-Mascard et al., 2005).

One effector caspase, caspase-7, has also been shown to be modified by SUMO (Hayashi et al., 2006). While it is unclear if caspase-7 localises to PML NBs directly, it does co-localise with SUMO-1 (Hayashi et al., 2006). The results suggest that it is indeed PML NBs caspase-7 localises to but this requires further investigation. This is also the case with the role PML and PML NBs play in caspase-dependent apoptosis.

1.5.5 Tumor necrosis factor receptor (TNF-R)-associated factor (TRAF)

The TRAF family of proteins is involved in cell survival, proliferation, differentiation and apoptosis. The proteins were originally identified as signalling adaptors binding to the cytoplasmic region of of the receptor of the TNF-R family (Ha et al., 2009). TRAF proteins are characterised by the presence of a TRAF domain at the C-terminus. The TRAF domain consists of a coiled-coil domain followed by a conserved TRAF-C domain. The C-domain interacts with the TNF-R family whereas the coiled-coil domain allows for oligomerisation of TRAF proteins. The N-terminus of TRAF proteins, except for TRAF1, contains a RING finger and several zinc finger motifs that are important for signalling downstream events (Aggarwal, 2003; Arch et al., 1998; Bradley and Pober, 2001; Chung et al., 2002). All TRAFs, apart from TRAF4, have benn identified by yeast two-hybrid screening using a cytoplasmic domain of various members of the TNFR family. TRAFs can act as E3 ubiqutin ligases and are involved in the pathogenesis of human diseases such as cancers (reviewed in Xie, 2013).

1.6 Aims

Taken together, these results strongly suggest that PML acts as a cell growth regulator and is involved in apoptosis. The interplay between PML protein and PML NBs remains unresolved, as does the recruitment of PML NB components and cellular function. A small fraction of PML protein is soluble within the nucleoplasm (N. Boddy, PhD thesis, Univ. London, 1996), suggesting that PML could have a functional role separate from that of insoluble PML NBs.

The overall aims and objectives of this PhD project were to elucidate further functional data on PML in relation to its role in apoptosis, and more specifically to explore:

- **The role of PML and PML NBs in FADD-mediated apoptosis**
    - **Specific aims:**
        - **To identify new PML-interacting components**
        - **To explore the connection between PML NBs and DEFs**

- **To determine the role of PML in FADD phosphorylation**
- **To determine the role of PML NBs in regulating FADD phosphorylation**

2 Materials and methods

2.1 Materials

Table 2.1. Media for bacterial growth

LB broth	1% (w/v) bactotryptone, 1% (w/v) NaCl, 0.5% (w/v) bacto-yeast extract
SOC	20 mM glucose, 0.01 mM $MgCl_2$, 0.0025 mM KCl, 2% (w/v) bactotryptone, 0.05% (w/v) NaCl, 0.5% (w/v) bacto-yeast extract
LB-agar	LB broth, 1.2% (w/v) agar

Table 2.2. DNA electrophoresis

TAE	40 mM Tris-acetate, 1 mM EDTA
Gel loading buffer (6x)	10 mM EDTA, 50% Glycerin, 0.1% Bromphenolblue
Agarose gel	1% agarose in TAE, 0.0006% (v/v) GelRed

Table 2.3. Protein electrophoresis and detection

SDS-gel reducing buffer (2x)	100 mM Tris pH6.8, 200 mM DTT, 4% SDS, 0.2% Bromphenolblue, 20% Glycerol
SDS-gel running buffer	25 mM Tris, 192 mM Glycine, 0.2% (w/v) SDS, pH 8.3
Resolving buffer (4x)	1.5 M Tris, pH 8.8
Stacking buffer (4x)	0.5 M Tris, pH 6.8
Resolving gel	Acrylamide mix (8, 10, 12% (v/v)), 0.39 mM Tris (pH 8.8), 0.1% (w/v) SDS, 0.1% (w/v) Ammonium persulphate (APS), 0.04% (v/v) N,N,N',N'-Tetramethylethylenediamine (TEMED)
Stacking gel	4% (v/v) Acrylamide mix, 0.065 mM Tris (pH 6.8), 0.1% (w/v) SDS, 0.1% (w/v) APS, 0.04% (v/v) TEMED
Coomassie stain	0.05% (w/v) Coomassie Blue R-250, 30% (v/v) Ethanol, 10%

	(v/v) Acetic acid
Coomassie destain	30% (v/v) Ethanol, 10% (v/v) Acetic acid
Ponceau S	0.1% (w/v) Ponceau S, 5% (v/v) Acetic acid
Electroblotting transfer buffer	10mM 3-(cyclohexylamino)-1-propane sulfonic acid (CAPS), pH 11.0
Blocking solution	5% (w/v) skimmed milk powder in dH_2O
dPBS	138 mM NaCl, 2.7 mM KCl, 8.1 mM Na_2HPO_4-$7H_2O$, 1.47 mM KH_2PO_4, pH 7.4
dPBST	PBS, 0.1% (v/v) Polyoxyethylenesorbitanmonolaurate (Tween 20)

Table 2.4. Bacterial strains

Bacterial strain	**Genotype**	**Source**
XL1-Blue	*recA1 endA1 gyrA96 thi-1 hsdR17 supE44 relA1 lac* (F'*proAB lacIqZDM15* Tn10 (Tet^R)) Electrocompetent	Stratagene
One Shot™ TOP10	F- *mcrA D(mrr-hsdRMS-mcrBC) }80lacZΔM15 ΔlacX74 recA1 araD139 D(ara-leu)7697 galU galK rpsL* (Str^R) *endA1 nupG* Chemical competent	Life Technologies
LIBRARY EFFICIENCY® DH5α™	F- *}80lacZΔM15 Δ(lacZYA-argF)U169 recA1 endA1 hsdR17(r_k- , m_k+) phoA supE44 thi-1 gyrA96 relA1* Chemical competent	Life Technologies
BL21-GOLD(DE3)	*E.coli* B F- *ompT hsdS($r_β$- $m_β$-) dcm+ Tet^R galλ* (DE3) *endA Hte* Electrocompetent and chemical competent	Agilent
SoluBL21	F- *ompT hsdS($r_β$- $m_β$-) gal dcm* (DE3) (The SoluBL21 strain contains	Genlantis

	uncharacterised mutations obtained through special selection criteria. These mutations make the strain able to express insoluble proteins in soluble form, fully or partially, in most tests conducted). Electrocompetent.	
NEB 5-alpha	*fhuA2* Δ*(argF-LacZ)U169 phoA gln44* ϕ*88*Δ *(lacZ)M15 gyrA96 recA1 relA1 endA1 thi-1 hsdR17* Chemical competent	New England Biolabs

Table 2.5. Mammalian cell lines

Mammalian cell line	**Description**	**Source**
MEF	*Mus musculus* (mouse) adherent embryonic fibroblast (transfected with SV40 large T antigen)	Prof. Hugues de The, Paris
U2OS	*Homo sapiens* (human) adherent osteosarcoma epithelial	ICRF
HT1080	*Homo sapiens* (human) adherent fibrosarcoma epithelial	ICRF
Saos-2	*Homo sapiens* (human) adherent osteosarcoma epithelial	ICRF
NIH/3T3	*Mus musculus* (mouse) adherent fibroblast	ICRF

Table 2.6. Expression vectors

Name	Expression	Source
pSG5	Eukaryotic	Agilent
pSG5-FLAG	Eukaryotic	pSG5 modified with a FLAG tag (Sternsdorf et al., 1999).
pSG5-LINK	Eukaryotic	pSG5 modified with a SV40 NLS and a FLAG tag (Sternsdorf et al., 1999).
pSG5-LINK-EGFP	Eukaryotic	pSG5-LINK modified with EGFP
pcDNA3	Eukaryotic	Invitrogen
pEGFP-C1,2,3	Eukaryotic	Clontech
pDsRed-N1	Eukaryotic	Clontech
pDsRed-C1	Eukaryotic	Clontech
pDsRed2-C1	Eukaryotic	Clontech
pMLV-plink2T	Eukaryotic	
pET-28a/b	Prokaryotic	Novagen
pProEX HTa,b	Prokaryotic	Invitrogen
pGEX 6P-1	Prokaryotic	GE healthcare

Table 2.7. DNA Constructs

cDNA	Vector	Tag/ Fusion	Restriction sites used for cloning	Source/relevant information
FADD	pcDNA3	AU1	*Kpn*I/*Xho*I	A kind gift from T.G. Hofmann
FADD F25G	pcDNA3	AU1		
FADD K35R	pcDNA3	AU1		
FADD K33/35R	pcDNA3	AU1		
FADD K125R	pcDNA3	AU1		
FADD A174P	pcDNA3	AU1		
FADD S194A	pcDNA3	AU1		
FADD S194E	pCDNA3	AU1		

FADD S194D	pcDNA3	AU1		
FADD DED (aa 1-80)	pcDNA3	AU1	pcDNA3-AU1 FADD digested *Kpn*I/*Sal*I and cloned into pcDNA3-AU1 *Kpn*I/*Xho*I	
FADD DN (aa 80- 208)	pcDNA3	AU1		A kind gift from T.G. Hofmann
FADD	pEGFP	EGFP		A kind gift from T.G. Hofmann
Caspase-8	pEGFP	EGFP		A kind gift from T.G. Hofmann
Caspase-8 DED-AB	pEGFP	EGFP		A kind gift from T.G. Hofmann
CrmA	pcDNA3			A kind gift from T.G. Hofmann
Caspase-8 (FLICE)	pcDNA3	HA		A kind gift from T.G. Hofmann
CK1 alpha (isoform 1) or CK1 alpha LS	pSG5-FLAG	FLAG	*Hind*III/*Bam*HI	
CK1 alpha LS K46R	pSG5-FLAG	FLAG	*Hind*III/*Bam*HI	
CK1 alpha LS K138R	pSG5-FLAG	FLAG	*Hind*III/*Bam*HI	
CK1 alpha LS K46/138R	pSG5-FLAG	FLAG	*Hind*III/*Bam*HI	
CK1 alpha LS K22/46/138R	pSG5-FLAG	FLAG	*Hind*III/*Bam*HI	
CK1 alpha LS K46/257R	pSG5-FLAG	FLAG	*Hind*III/*Bam*HI	
CK1 alpha LS K46/260R	pSG5-FLAG	FLAG	*Hind*III/*Bam*HI	

CK1 alpha LS K46/257/260R	pSG5-FLAG	FLAG	*Hind*III/*Bam*HI	
CK1 alpha LS K46R/ V273A/E274A	pSG5-FLAG	FLAG	*Hind*III/*Bam*HI	
CK1 alpha LS V273A/ E274A	pSG5-FLAG	FLAG	*Hind*III/*Bam*HI	
CK1 alpha LS K22/46/138R, V273A/E274A	pSG5-FLAG	FLAG	*Hind*III/*Bam*HI	
CK1 alpha LS K46/257/260R, V273A/E274A	pSG5-FLAG	FLAG	*Hind*III/*Bam*HI	
E4 Orf3	pcDNA3	HA		A kind gift from H. Will
SUMO-1	pEGFP	EGFP		A kind gift from H. Will
SUMO-2	pEGFP	EGFP		A kind gift from H. Will
SUMO-3	pEGFP	EGFP		A kind gift from H. Will
SuPr-1	pEGFP	EGFP		A kind gift from H. Will
SuPr-1 C466S	pEGFP	EGFP		A kind gift from H. Will
SUMO-1	pSG5-LINK-EGFP	FLAG-EGFP	SUMO-1 *Xma*I/*Bam*HI and gSG5-LINK-EGPF *Xma*I. 5' ends filled in with Klenow.	
SUMO-1	pMLV-plink2T	MYC		(Duprez et al., 1999)
TFAF-1 (aa 79-316)	pSG5-	FLAG	*Eco*RI/*Bam*HI	

	FLAG			
TFAF-1 (aa 79-316)	pSG5-LINK	FLAG	*Eco*RI/*Bam*HI	
TFAF-1 (aa 79-316)	pEGFP	EGFP	*Eco*RI/*Bam*HI	
TFAF-1 (aa 79-316)	pDsRed-N1	DsRed	*Eco*RI/*Bam*HI	
TFAF-1 (aa 79-316)	pDsRed-C1	DsRed	*Eco*RI/*Bam*HI	
TFAF-1 full-length	DsRed-C1	DsRed	*Eco*RI/*Bam*HI	
TFAF-1 full-length	pDsRed-N1	DsRed	*Eco*RI/*Bam*HI	
TFAF-1 full-length	pSG5-FLAG	FLAG	*Eco*RI/*Bam*HI	
PML III	pSG5-LINK-EGFP	FLAG-EGFP	*Eco*RI/*Bam*HI	
PML IV	pSG5-LINK-EGFP	FLAG-EGFP	*Eco*RI	
PML IV	pSG5-FLAG	FLAG	*Eco*RI	
CK1 alpha (isoform 1) or CK1 alpha LS	pProEx HTb	His	*Bam*HI/*Xho*I	
CK1 alpha (isoform 1) or CK1 alpha LS	pGEX-6P-1	GST	*Bam*HI/*Xho*I	
CK1 alpha (isoform 1) or CK1 alpha LS	pET-28a	His	*Bam*HI/*Xho*I	
CK1 alpha (aa 1-301)	pProEx HTb	His	*Bam*HI/*Xho*I	Mr. Gene GmbH Codon optimised for expression in *E. coli*
CK1 alpha (aa 1-301)	pGEX-6P-	GST	*Bam*HI/*Xho*I	Mr. Gene

	1			GmbH Codon optimised for expression in *E. coli*
CK1 alpha (aa 1-301)	pET-28a	His	*Bam*HI/*Xho*I	Mr. Gene GmbH Codon optimised for expression in *E. coli*
CK1 alpha (aa 1-325)	pET-28a	His	*Bam*HI/*Xho*I	Mr. Gene GmbH Codon optimised for expression in *E. coli*
CK1 alpha (aa 1-325) (S313G)	pET-28a	His	*Bam*HI/*Xho*I	
CK1 delta (isoform 1)	pSG5-FLAG	FLAG	*Eco*RI/*Bam*HI	Imagenes GmbH. Clone name:IRQMp5018F077D
CK1 delta (isoform 1)	pEGFP-C2	EGFP	*Eco*RI/*Bam*HI	Imagenes GmbH. Clone name:IRQMp5018F077D
CK1 delta (aa 1-317)	pProEx HTb	His	*Bam*HI/*Xho*I	Mr. Gene GmbH Codon optimised for expression in *E. coli*
CK1 delta (aa 1-317)	pGEX-6P-1	GST	*Bam*HI/*Xho*I	Mr. Gene GmbH Codon optimised for expression in *E.*

				coli
CK1 delta (aa 1-317)	pET-28a	His	*Bam*HI/*Xho*I	Mr. Gene GmbH Codon optimised for expression in *E. coli*
CK1 delta (aa 1-317) ΔSTOP	pET-28a	N- and C-terminal His-tag	*Bam*HI/*Xho*I	
CK1 delta (aa 1-317) ΔSTOP K38R	pET-28a	N- and C-terminal His-tag	*Bam*HI/*Xho*I	
CK1 delta (aa 1-317) ΔSTOP K221,224,263,294R	pET-28a	N- and C-terminal His-tag	*Bam*HI/*Xho*I	G-Block from IDT
CK1 delta (aa 1-317) ΔSTOP K130,140,221,224,263,294R	pET-28a	N- and C-terminal His-tag	*Bam*HI/*Xho*I	G-Block from IDT
CK1 delta (aa 1-317) ΔSTOP K14,130,140,221,224,263,294R	pET-28a	N- and C-terminal His-tag	*Bam*HI/*Xho*I	G-Block from IDT
CK1 delta (aa 1-317) ΔSTOP K14,38,130,140,221,224,263,	pET-28a	N- and C-	*Bam*HI/*Xho*I	G-Block from IDT

294R		terminal His-tag		
CK1 delta (aa 1-317) ΔSTOP K38,130,154,155,171,217,221R	pET-28a	N- and C-terminal His-tag	*Bam*HI/*Xho*I	GeneArt String from GeneArt
CK1 delta (aa 1-317) ΔSTOP K14,130,140,154,217,221,224,263,294R	pET-28a	N- and C-terminal His-tag	*Bam*HI/*Xho*I	GeneArt String from GeneArt
CK1 delta (aa 1-317) ΔSTOP K14,38,130,140,154,217,221,224,263,294R	pET-28a	N- and C-terminal His-tag	*Bam*HI/*Xho*I	Synthesised by GeneArt
CK1 delta (aa 1-317) ΔSTOP K14,38,130,140,154,155,171,217,221,224,263,294R	pET-28a	N- and C-terminal His-tag	*Bam*HI/*Xho*I	GeneArt String from GeneArt
AU(E1),Ubc9(E2), SUMO-1/SUMO-3(S1/S3)	pT-Trx			A kind gift from Hisato Saitoh

Table 2.8. Oligonucleotides

(Oligonucleotides were ordered from Eurofins MWG Operon, Sigma-Aldrich, Integrated DNA Technologies (IDT) or Oligonucleotide Synthesis Service ICRF).

Constructs	**Sequence 5' – 3'**
pSG5-LINK-TFAF-1 (aa 79-316), pSG5-FLAG-TFAF-1 (aa 79-316) and pEGFP-C2-TFAF-1(aa 79-316)	Fwd: CCG **GAA TTC** ATG ACC AGT GTG GTT AAG
	Rev: CGC **GGA TCC** TTA CAT TTC TAA TAG CTG
pDsRed1-N1-TFAF-1 (aa 79-316)	Fwd: CC G**GA ATT C**AG ATG ACC AGT GTG GTT AAG
	Rev: CG C**GG ATC C**GC CAT TTC TAA TAG CTG CTC
pDsRed1-N1-TFAF-1 (full-length)	Fwd: CC G**GA ATT CAG** ATG GCG GCT CCC GAA G
	Rev: CG C**GG ATC C**GC CAT TTC TAA TAG CTG CTC
pDsRed1-C1-TFAF-1 (aa 79-316)	Fwd: C GG**G AAT TC**T ATG ACC AGT GTG GTT AAG
	Rev: CG C**GG ATC C**GC CAT TTC TAA TAG CTG CTC
pDsRed1-C1-TFAF-1 (full-length)	Fwd: C GG**G AAT TC**T ATG GCG GCT CCC GAA G
	Rev: CG C**GG ATC C**GC CAT TTC TAA TAG CTG CTC
pSG5-FLAG-TFAF 1 (full-length)	Fwd: CG **GAA TTC** ATG GCG GCT CCC GAA G
	Rev: CGC **GGA TCC** TTA CAT TTC TAA TAG CTG
pSG5-FLAG CK1 alpha isoform 1 or pSG5-FLAG CK1 alpha LS	Fwd: CCC **AAG CTT** ATG GCG AGT AGC AGC GGC
	Rev: CG **GGA TCC** TTA GAA ACC TTT CAT GTT ACT CTT GG
CK1 N-terminus	Fwd: CCC **AAG CTT** ATG GCG AGT AGC AGC GGC

	Rev: C TAG **CCA TGG** CAG GCT GGT TC
CK1 C-terminus	Fwd: C ATG **CCA TGG** CAA GGG CTA AAG
	Rev: CG **GGA TCC** TTA GAA ACC TTT CAT GTT ACT CTT GG
pSG5-FLAG CK1 alpha K22R	Fwd: GG AAA TAT AAA CTG GTA CGG A**G**G ATC GGG TCT GGC TCC
	Rev: GGA GCC AGA CCC GAT C**C**T CCG TAC CAG TTT ATA TTT CC
pSG5-FLAG CK1 alpha K46R	Fwd: C GAG GAA GTG GCA GTG A**G**G CTA GAA TCT CAG AAG G
	Rev: C CTT CTG AGA TTC TAG C**C**T CAC TGC CAC TTC CTC G
pSG5-FLAG CK1 alpha K138R	Fwd: G AAT TTT ATA CAC AGA GAC ATT A**G**A CCA GAT AAC TTC CTA ATG G
	Rev: C CAT TAG GAA GTT ATC TGG T**C**T AAT GTC TCT GTG TAT AAA ATT C
pSG5-FLAG CK1 alpha K257R	Fwd: GGG CTA AAG GCT GCA ACA A**G**G AAA CAA AAA TAT GAA AAG ATT AG
	Rev: CT AAT CTT TTC ATA TTT TTG TTT C**C**T TGT TGC AGC CTT TAG CCC
pSG5-FLAG CK1 alpha K260R	Fwd: G GCT GCA ACA AAG AAA CAA A**G**A TAT GAA AAG ATT AGT GAA AAG
	Rev: CTT TTC ACT AAT CTT TTC ATA T**C**T TTG TTT CTT TGT TGC AGC C
pSG5-FLAG CK1 alpha K257/260R	Fwd: GGG CTA AAG GCT GCA ACA A**G**G AAA CAA A**G**A TAT GAA AAG ATT AGT GAA AAG
	Rev: CTT TTC ACT AAT CTT TTC ATA T**C**T TTG TTT C**C**T TGT TGC AGC CTT TAG CCC
pSG5-FLAG CK1 alpha V273A/E274A	Fwd: GAA AAG AAG ATG TCC ACG CCT G**C**T G**C**A GTT TTA AAG GGG TTT CC
	Rev: GG AAA CCC CTT TAA AAC T**G**C A**G**C AGG CGT GGA CAT CTT CTT TTC

pSG5-FLAG CK1 delta, pEGFP-C2 CK1 delta	Fwd: CG **GAA TTC** ATG GAG CTG AGA GTC GG
	Rev: CG **GGA TCC** TCA TCG GTG CAC GAC AG
CK1 alpha (aa 1-325) (S313G)	Fwd: CAA CAG GCA GCG TCC TCT **G**GT GGA CAA GGT CAG CAA G
	Rev: C TTG CTG ACC TTG TCC AC**C** AGA GGA CGC TGC CTG TTG
CK1 delta ΔSTOP	Fwd: G GAA CGT CTG CGC CAT **GG**A CTC GAG CAC CAC CAC CAC CAC C
	Rev: G GTG GTG GTG GTG GTG CTC GAG T**CC** ATG GCG CAG ACG TTC C
CK1 delta K38R	Fwd: CT GGT GAG GAA GTC GCC ATT **CGT** CTG GAG TGT GTG AAA ACA AAA CAC
	Rev: GTG TTT TGT TTT CAC ACA CTC CAG **ACG** AAT GGC GAC TTC CTC ACC AG
pcDNA3-AU1 FADD F25G	Fwd: G CTG ACC GAG CTC AAG **GG**C CTA TGC CTC GGG CGC G
	Rev: C GCG CCC GAG GCA TAG G**CC** CTT GAG CTC GGT CAG C
pcDNA3-AU1 FADD K35R	Fwd: G CGC GTG GGC AAG CGC A**G**G CTG GAG CGC GTG CAG AG
	Rev: CT CTG CAC GCG CTC CAG C**C**T GCG CTT GCC CAC GCG C
pcDNA3-AU1 FADD K33/35R	Fwd: GC CTC GGG CGC GTG GGC A**G**G CGC A**G**G CTG GAG CGC G
	Rev: C GCG CTC CAG C**C**T GCG C**C**T GCC CAC GCG CCC GAG GC
pcDNA3-AU1 FADD K125R	Fwd: G CTC AAA GTC TCA GAC ACC A**G**G ATC GAC AGC ATC GAG GAC
	Rev: GTC CTC GAT GCT GTC GAT C**C**T GGT GTC TGA GAC TTT GAG C

pcDNA3-AU1 FADD A174P	Fwd: CAG ATG AAC CTG **C**CT GAC CTG GTA CAA GAG
	Rev: CTC TTG TAC CAG GTC AG**G** CAG GTT CAT CTG
pcDNA3-AU1 FADD S194A	Fwd: C AGG AGT GGG GCC ATG **G**CC CCG ATG TCA TGG AAC TC
	Rev: GA GTT CCA TGA CAT CGG GG**C** CAT GGC CCC ACT CCT G
pcDNA3-AU1 FADD S194E	Fwd: C AGG AGT GGG GCC ATG **GAA** CCG ATG TCA TGG AAC TC
	Rev: GA GTT CCA TGA CAT CGG **TTC** CAT GGC CCC ACT CCT G
pcDNA3-AU1 FADD S194D	Fwd: C AGG AGT GGG GCC ATG **GA**C CCG ATG TCA TGG AAC TC
	Rev: GA GTT CCA TGA CAT CGG G**TC** CAT GGC CCC ACT CCT G
pET-28b SENP2 (aa 366-588)	Fwd: GG GAA TTC **CAT ATG** GAA TTT ACA GAG GAC ATG G
	Rev: CCG **CTC GAG** CAG CAA CTG CTG GTG AAG

Table 2.9. G-Blocks/GeneArt® strings

Name	**Sequence**	**Company**
CK1 delta gBlock1 K14R (*Bam*HI/*Eco*RI)	CGC**GGATCC**ATGGAACTGCGTGTGGGTAA TCGCTATCGTCTGGGGCGTCGCATTGGTAG TGGCTCTTTCGGTGACATCTATCTGGGTAC TGACATTGCTGCTGGTGAGGAAGTCGCCA TTAAACTGGAGTGTGTGAAAACAAAACAC CCTCAGCTGCACATTGAATCCAAAATCTAT AAAATGATGCAAGGCGGTGTGG**GAATTC**C GG	IDT
CK1 delta gBlock1 K14,38R (*Bam*HI/*Eco*RI)	CGC**GGATCC**ATGGAACTGCGTGTGGGTAA TCGCTATCGTCTGGGGCGTCGCATTGGTAG TGGCTCTTTCGGTGACATCTATCTGGGTAC TGACATTGCTGCTGGTGAGGAAGTCGCCA TTCGTCTGGAGTGTGTGAAAACAAAACAC	IDT

	CCTCAGCTGCACATTGAATCCAAAATCTAT AAAATGATGCAAGGCGGTGTGG**GAATTC**C GG	
CK1 delta gBlock2 K130,140R (*Eco*RI/*Stu*I)	CCG**GAATTC**CGACAATTCGTTGGTGTGGT GCCGAAGGTGATTATAACGTCATGGTTAT GGAGCTGCTGGGTCCTTCTCTGGAAGATCT GTTCAACTTCTGTAGCCGTAAATTCAGCCT GAAAACCGTTCTGCTGCTGGCCGATCAGA TGATTTCCCGTATCGAGTATATCCACTCTA AAAACTTTATCCACCGTGATGTGCGTCCGG ACAACTTTCTGATGGGACTGGGCCGTAAA GGCAACCTGGTCTATATTATCGACTTCGGT CTGGCGAAAAAATATCGTGACGCCCGTAC TCATCAACACATCCCTTATCGTGAGAATAA AAACCTGACCGGTACAGCACGCTATGCCT CTATTAACACTCACCTGGGGATCGAACAA TCTCGTCGTGATGATCTGGAAAGCCTGGGT TATGTCCTGATGTATTTCAACCTGGGTTCT CTGCCGTGGCA**AGGCCT**TTC	IDT
CK1 delta gBlock3 K221,224,263,294R (*Stu*I/*Xho*I)	GAA**AGGCCT**GAAAGCTGCTACTCGCCGCC AACGTTATGAGCGTATCAGCGAGAAAAAA ATGAGCACCCCGATCGAGGTTCTGTGTAA AGGTTATCCGAGCGAGTTTGCCACATATCT GAACTTTTGCCGCTCACTGCGCTTTGACGA CCGTCCGGACTATTCCTATCTGCGCCAACT GTTTCGTAACCTGTTCCACCGTCAGGGA TTTTCGTATGACTATGTCTTTGACTGGAAT ATGCTGCGTTTCGGTGCCTCTCGTGCCGCC GATGATGCCGAACGTGAACGTCGTGACCG TGAGGAACGTCTGCGCCATGGA**CTCGAG**C GGC	IDT
GeneArt string CK1 delta K130,140,154,155,171R (*Eco*RI/*Stu*I)	CCG**GAATTC**CGACAATTCGTTGGTGTGGT GCCGAAGGTGATTATAACGTCATGGTTAT GGAGCTGCTGGGTCCTTCTCTGGAAGATCT GTTCAACTTCTGTAGCCGTAAATTCAGCCT GAAAACCGTTCTGCTGCTGGCCGATCAGA TGATTTCCCGTATCGAGTATATCCACTCTA AAAACTTTATCCACCGTGATGTGCGTCCGG ACAACTTTCTGATGGGACTGGGCCGTAAA GGCAACCTGGTCTATATTATCGACTTCGGT CTGGCGCGTCGTTATCGTGACGCCCGTACT CATCAACACATCCCTTATCGTGAGAATCGT AACCTGACCGGTACAGCACGCTATGCCTC TATTAACACTCACCTGGGGATCGAACAAT CTCGTCGTGATGATCTGGAAAGCCTGGGTT ATGTCCTGATGTATTTCAACCTGGGTTCTC TGCCGTGGCA**AGGCCT**TTC	GeneArt
GeneArt String CK1 delta K130,154,155,171,217,221R	CCG**GAATTC**CGACAATTCGTTGGTGTGGT GCCGAAGGTGATTATAACGTCATGGTTAT GGAGCTGCTGGGTCCTTCTCTGGAAGATCT	GeneArt

(*Eco*RI/*Xho*I)	GTTCAACTTCTGTAGCCGTAAATTCAGCCT GAAAACCGTTCTGCTGCTGGCCGATCAGA TGATTTCCCGTATCGAGTATATCCACTCTA AAAACTTTATCCACCGTGATGTGCGTCCGG ACAACTTTCTGATGGGACTGGGCAAAAAA GGCAACCTGGTCTATATTATCGACTTCGGT CTGGCGCGTCGTTATCGTGACGCCCGTACT CATCAACACATCCCTTATCGTGAGAATCGT AACCTGACCGGTACAGCACGCTATGCCTC TATTAACACTCACCTGGGGATCGAACAAT CTCGTCGTGATGATCTGGAAAGCCTGGGTT ATGTCCTGATGTATTTCAACCTGGGTTCTC TGCCGTGGCAAGGCCTGCGTGCTGCTACTC GTCGCCAAAAATATGAGCGTATCAGCGAG AAAAAAATGAGCACCCCGATCGAGGTTCT GTGTAAAGGTTATCCGAGCGAGTTTGCCA CATATCTGAACTTTTGCCGCTCACTGCGCT TTGACGACAAACCGGACTATTCCTATCTGC GCCAACTGTTTCGTAACCTGTTCCACCGTC AGGGATTTTCGTATGACTATGTCTTTGACT GGAATATGCTGAAATTCGGTGCCTCTCGTG CCGCCGATGATGCCGAACGTGAACGTCGT GACCGTGAGGAACGTCTGCGCCATGGA**CT CGAG**CGGC	

Table 2.10. Antibodies

Primary	**Immunogen**	**Species**	**Titer**	**Source**
FADD	aa 94-208	Mouse Monoclonal IgG1	1:50 IF	BD Transduction Laboratories Cat No. 610399
FADD	aa 28-209	Rabbit polyclonal IgG	1:100 IF 1:200 WB	Santa Cruz Biotechnology, Inc. (H-181): sc-5559
FADD	N-terminal peptide	Goat Polyclonal IgG	1:100 IF	Santa Cruz Biotechnology, Inc. (S-18): sc-6035
FADD	Full-length FADD	Rabbit polyclonal IgG	1:200 WB	Upstate Biotechnology Cat No. 06-711
Phospho-FADD	Synthetic	Rabbit	1:50 IF	Cell Signaling

(Ser 194) (Human Specific)	phosphopeptide corresponding to residues surrounding Ser 194 of human FADD	Polyclonal IgG		Technology Cat No. 2781
Phospho-FADD (Ser 191) (Mouse Specific)	Synthetic phosphopeptide corresponding to residues surrounding Ser 191 of mouse FADD	Rabbit Polyclonal IgG	1:200 IF	Cell Signaling Technology Cat No. 2785
CK1 alpha	C-terminus of human CK1 alpha	Goat Polyclonal IgG	1:25 IF	Santa Cruz Biotechnology, Inc. (C-19): sc-6477
SUMO		Rabbit polyclonal	1:200 IF	(Boddy et al., 1997)
SUMO-1	Full-length SUMO-1	Mouse Monoclonal IgG1 (Clone 21C7)	1:50 IF	Zymed laboratories Inc. Cat No. 33-2400 from Invitrogen
SUMO-1	Peptide specific for SUMO-1	Rabbit polyclonal	1:100 IF	Cell Signaling Technology Cat No. 4930
SUMO-2/3	C-terminal peptide of human SUMO2/3	Rabbit polyclonal IgG	1:100 IF	Abcam plc. Cat No. (ab3742)
PML		Rabbit polyclonal	1:200 IF	(Borden et al., 1995)
PML	aa37-51 of the human PML	Mouse Monoclonal	1:100 IF	Santa Cruz Biotechnology, Inc.

		IgG		(PG-M3): sc-966
PML	N-terminal peptide of human PML	Goat polyclonal IgG	1:200 IF	Santa Cruz Biotechnology, Inc. (N-19): sc-9862
Sp100		Rabbit polyclonal	1:200 IF	A kind gift from H. Will
Daxx	aa 727-739 of the mouse Daxx	Mouse Monoclonal IgG2a	1:100 IF	Santa Cruz Biotechnology, Inc. (H-7): sc-8043
Daxx	aa 627-739	Rabbit Polyclonal IgG	1:50 IF	Santa Cruz Biotechnology, Inc. (M-112): sc-7152
p53	aa 1-393	Rabbit Polyclonal IgG	1:50 IF	Santa Cruz Biotechnology, Inc. (FL-393):sc-6243
FLAG	FLAG peptide	Mouse Monoclonal IgG1	1:200 IF 1:2000 WB	Sigma-Aldrich Cat No. F 3165
FLAG	FLAG peptide	Rabbit polyclonal IgG	1:800 IF	Cell Signaling Technology Cat No. 2368
TFAF-1	Peptide 1 (aa 2-16)	Rabbit polyclonal	1:200 IF	Eurogentec
TFAF-1	Peptide 2 (aa 96-110)	Rabbit polyclonal	1:200 IF	Eurogentec
Keratin 18 (K18)	A-431 and MCF-7 cells	Mouse monoclonal IgG1	1:200 IF	Sigma-Aldrich Cat No. C8541
His	Synthetic peptide containing six His residues	Mouse monoclonal IgG1	1:1000 WB	Invitrogen Cat No. 37-2900
His	Recombinant poly-histidine	Mouse monoclonal	1:10000 WB	Sigma-Aldrich Cat No A7058

	tagged fusion protein	IgG2a		
HA	Internal peptide from the HA protein	Mouse Monoclonal IgG2a	1:50 IF	Santa Cruz Biotechnology, Inc. (F-7): sc7392
AU1	BPV-1. Detects epitope DTYRYI.	Mouse monoclonal IgG3	1:1000 IF	Covance
Caspase-8	C-terminal peptide of human Caspase-8	Mouse monoclonal IgG1	1:50 IF	Cell Signaling Technology Cat No. 9746
HIPK3	Synthetic peptide within aa100-200	Rabbit polyclonal IgG	1:100 IF	Abgent Cat No. AP7540c
Lamin B	C-terminal peptide of mouse Lamin B	Goat polyclonal IgG	1:100 IF	Santa Cruz Biotechnology, Inc. (M-20): sc-6217
Nucleolus	B23 purified from rat	Mouse monoclonal IgG1	1:50 IF	Zymed laboratories Inc. (Invitrogen) Cat No. 32-5200
Cajal bodies	aa 363-481 of human coilin	Mouse monoclonal IgG1	1:125 IF	Abcam plc. Cat No. (ab11822)

Table 2.11. Secondary Antibodies

Secondary	**Antigen**	**Titer**	**Source**
FITC-conjugated Donkey Anti-Rabbit	Rabbit IgG	1:100	Jackson ImmunoResearch Laboratories, Inc.
Cy3-conjugated Donkey Anti-Rabbit	Rabbit IgG	1:200	Jackson ImmunoResearch Laboratories, Inc.
FITC-conjugated Donkey	Mouse IgG	1:100	Jackson ImmunoResearch

Anti-Mouse			Laboratories, Inc.
Cy3-conjugated Donkey Anti-Mouse	Mouse IgG	1:200	Jackson ImmunoResearch Laboratories, Inc.
FITC-conjugated Donkey Anti-Goat	Goat IgG	1:100	Jackson ImmunoResearch Laboratories, Inc.
Cy3-conjugated Donkey Anti-Goat	Goat IgG	1:200	Jackson ImmunoResearch Laboratories, Inc.
Polyclonal Goat Anti-Rabbit HRP conjugated	Rabbit IgG	1:2000	Dako
Polyclonal Goat Anti-Mouse HRP conjugated	Mouse IgG	1:2000	Dako
Polyclonal Rabbit Anti-Goat HRP conjugated	Goat IgG	1:2000	Dako
Polyclonal Goat Anti-Rabbit HRP conjugated	Rabbit IgG	1:4000	Sigma-Aldrich

Table 2.12. Enzymes

Reagent	**Source**
*Bam*HI	New England Biolabs Inc.
*Dpn*I	New England Biolabs Inc.
*Eco*RI	New England Biolabs Inc.
*Hind*III	New England Biolabs Inc.
*Kpn*I	New England Biolabs Inc.
*Sal*I	New England Biolabs Inc.
*Stu*I	New England Biolabs Inc.
*Xba*I	New England Biolabs Inc.
*Xho*I	New England Biolabs Inc.
*Xma*I	New England Biolabs Inc.
T4 DNA Ligase	New England Biolabs Inc.
T4 Polynucleotide Kinase	New England Biolabs Inc.
Benzonase®	Merck

Pfu Ultra II DNA Polymerase	Agilent
PfuTurbo DNA Polymerase	Agilent
Shrimp Alkaline Phosphatase	Roche Diagnostics

Table 2.13. Kits

Reagent	**Source**
QIAprep Spin MiniPrep Kit	Qiagen
QIAfilter Plasmid Midi Kit	Qiagen
QIAquick Gel Extraction Kit	Qiagen
QIAquick PCR Purification Kit	Qiagen
RNeasy Mini Kit	Qiagen
Zero Blunt PCR Cloning Kit	Invitrogen
E.coli T7 S30 Extract System for Circular DNA	Promega
RTS 100 *E.coli* HY Kit	5 PRIME
ADP-Glo^{TM} Kinase Assay	Promega
Nuclear/Cytosol Fractionation Kit	BioVision

Table 2.14. Antibiotics

Reagent	**Source**
Ampicillin	Sigma-Aldrich
Kanamycin	Sigma-Aldrich
Chloramphenicol	Sigma-Aldrich
Tetracycline	Sigma-Aldrich

Table 2.15. DNA and protein ladders

Reagent	**Source**
1Kb Plus DNA Ladder	Invitrogen
PageRuler Prestained Protein ladder	Fermentas
Rainbow Molecular Weight Marker	GE Healthcare

Table 2.16. Miscellaneous reagents

Reagent	**Source**
Novex 4-20% Tris-Glycine Gels	Life Technologies
ECL detection reagent	Amersham/GE Healthcare
Whatman 3MM blotting paper	Whatman/GE Healthcare
dNTPs	Roche Diagnostics
Hybond ECL nitrocellulose membrane	Amersham/GE Healthcare
Amersham Hyperfilm ECL	Amersham/GE Healthcare
iBlot® Transfer Stack, nitrocellulose	Life Technologies
Tween 20	Sigma-Aldrich
SIGMA*FAST* Protease inhibitor cocktail tablets, EDTA-Free	Sigma-Aldrich

Table 2.17. Commonly used reagents in tissue culture

Reagent	**Source**
DMEM	Gibco®
Foetal Bovine Serum (FBS or FCS)	Gibco®
L-Glutamine 200 mM 100X	Gibco®
Penicillin (50 IU/ml)/streptomycin (50 µg/ml)	Gibco®
0.05%Trypsin-EDTA	Gibco®
dPBS	Gibco®
DMSO	Merck
16% Formaldehyde	TAAB laboratories
Triton X-100	Sigma-Aldrich
Citifluor	Citifluor Ltd
DAPI	Roche Diagnostics
Propidium Iodide	Roche Diagnostics
RNase A	Sigma-Aldrich

Chemicals and reagents

All chemicals and reagents were obtained from the following companies: Sigma-Aldrich, Roche Diagnostics, Merck, VWR and Fisher Scientific unless otherwise stated.

2.2 DNA and DNA manipulation methods

2.2.1 Amplification of full-length TFAF-1 and assembly of constructs

A human testis cDNA library (Origene Technologies Inc.) was screened by PCR and a full-length TFAF-1 clone was obtained. The following primers were used to screen the library: 5'-oligonucleotide CCA GAA GTT GAC TGA AAC TCA G and 3'-oligonucleotide ACT GTA GAA ATT GTT TTC ATT CTG G.

Subfragments of TFAF-1 were also generated by polymerase chain reaction amplification with specific oligonucleotides, which contained *Eco*RI (5'-oligonucleotides) and *Bam*HI (3'-oligonucleotides) restriction sites at their respective 5'- or 3'-ends. Fragments were inserted into plasmids pSG5-LINK, pSG5-FLAG, pEGFP-C2, pDsRed1-N1, pDsRed1-C1 or pDsRed2-C1 (Clontech) for localisation studies.

2.2.2 Amplification of full-length CK1 alpha isoform 1 (CK1 alpha LS)

Full-length CK1 alpha LS was not available from RZPD/Imagenes so the full-length clone was constructed using PCR fragments from two different clones: one clone containing the N-terminus of CK1 alpha and the other containing the C-terminus of CK1 alpha. The N-terminus (aa 1-249) was amplified from clone IRALp962M1925Q2 (RZPD/Imagenes) using primers with the restriction sites *Hind*III and *Nco*I at the 5' and the 3' end respectively. The C-terminus (aa 248-365) was amplified from IMAGp998A2212114Q1 (RZPD/Imagenes) using primers with the restriction sites *Nco*I and *Bam*HI at the 5' and the 3' end respectively. The PCR fragment containing the N-terminus of CK1 alpha was digested with *Hind*III and *Nco*I and the PCR fragment containing the C-terminus of CK1 alpha was digested with *Nco*I and *Bam*HI. Both fragments were PCR-purified and ligated in the NcoI site. The ligation products were used as a template and a further PCR was performed to obtain the full-length clone using the 5' *Hind*III primer and the 3' *Bam*HI primer. Full-length CK1 alpha LS was cloned into pSG5-FLAG.

2.2.3 Amplification of the SUMO-specific protease SENP2

The active domain of SENP2 (aa 366-588) was amplified from the I.M.A.G.E full-length cDNA clone IRAVp968H0878D (RZPD/Imagenes) using primers with the restriction sites *Nde*I and *Xho*I at the 5' and the 3' end respectively. The protease was cloned into pET-28b (Novagen) containing a N- and C-terminal 6xHis-tag.

2.2.4 Polymerase chain reaction (PCR)

For PCR, a single block (OmniGene (Hybaid)) or RoboCycler Gradient 40 (Stratagene) PCR machine was used. The PCR was performed in 25 µl reactions consisting of: 1 x *Pfu Turbo* reaction buffer, 100 ng each of forward and reverse primer, 2% (vol/vol) DMSO, 0.2 mM dNTPs, 1.25 units *Pfu Turbo* DNA polymerase, 10-30 ng DNA.

The following program was used if the primers had restriction sites at the 5' end for cloning purposes: 1 cycle at 95 ˚C for 30 sec, 10 cycles at 95 ˚C for 30 sec, 50-68 ˚C for 45 sec, 68 ˚C for x min (1 min/kb), 20 cycles at 95 ˚C for 30 sec, 50-68 ˚C for 45 sec, 68 ˚C for x min (1 min/kb), 1 cycle at 68 ˚C for 5 min.

After the PCR, samples were analysed by agarose gel electrophoresis.

PCR products were purified for primers, nucleotides and polymerases using the QIAquick PCR Purification kit according to manufacturer's protocol.

2.2.5 Site-directed mutagenesis

The protocol for site-directed mutagenesis was based on the Stratagene QuikChange protocol. Primers used for site-directed mutagenesis were designed taking the following into consideration:

1. Both primers must contain the mutation.
2. The primers should be around 35-40 nucleotides long with the mutation in the middle.
3. The melting temperature of each site of the mutation (around 15-18 nucleotides) should be adjusted to the same temperature (usually around 50-55 ˚C).
4. The nucleotide at the 3' end of the primer should be a C or a G.

The following protocol was used for site-directed mutagenesis (25 µl reactions): 1 x *Pfu Turbo* reaction buffer, 100 ng each of forward and reverse primer, 2% (vol/vol) DMSO, 0.2 mM dNTPs, 1.25 units *Pfu Turbo* DNA polymerase, 10-30 ng DNA.
A negative control without primers was always included. It was used to check the efficiency of the *Dpn*I digest of the methylated non-mutated parental DNA.
The following program was used on the RoboCycler Gradient 40 (Stratagene) PCR machine: 1 cycle at 95 ˚C for 30 sec, 16 cycles at 95 ˚C for 30 sec, 48-54 ˚C for 45 sec, 68 ˚C for x min (1 min/kb).
After the PCR, samples were analysed by agarose gel electrophoresis. If there was a visible band on the DNA gel, *Dpn*I was added to the PCR to digest the methylated, non-mutated, parental DNA at 37 ˚C for 1-2 hours.
DNA was transformed into competent cells where the nicks in the mutated plasmid were repaired.

2.2.6 Agarose gel electrophoresis

Agarose gels (0.6% to 1.2% w/v in TAE) with addition of GelRed (10,000X) were prepared, and run in TAE buffer. Resolved DNA fragments were visualised by using a UV transilluminator, or Gene Genius (Syngene).

2.2.7 Restriction enzyme digestion of plasmid DNA and PCR products

Plasmid DNA or PCR products were digested with ~5 units of restriction enzyme/mg of DNA for 1-2 hrs. The enzyme concentration did not exceed 10% v/v and glycerol was kept below 5% v/v. Restriction enzymes were obtained from New England Biolabs (NEB) and addition of BSA and choice of buffer were in accordance to the manufacturer's protocol. Digests were analysed by agarose gel electrophoresis.

2.2.8 PCR purification of DNA

PCR products and PCR products digested with restriction enzymes were purified from primers, nucleotides, salt, polymerases and restriction enzymes using the QIAquick PCR Purification kit according to the manufacturer's protocol.

2.2.9 Extraction of DNA fragments from agarose gels

DNA was extracted from gel slices, following the agarose gel electrophoresis purification of restriction fragments and excision under long wave UV (~360nm).

Isolation of DNA from gel slices was performed using QIAquick Gel Extraction Kit (Qiagen) according to the manufacturer's protocol.

2.2.10 Dephosphorylation of DNA

To prevent self-ligation of the vector DNA, dephosphorylation of 5' phosphates from DNA was carried out using the Shrimp alkaline phosphatase (Roche Diagnostics) according to the manufacturer's protocol.

2.2.11 Phosphorylation of DNA

T4 polynucleotide kinase (NEB) was used according to the manufaturer's protocol to phosphorylate 5' hydroxyl end of double-stranded DNA prior to ligation.

2.2.12 Ligation of DNA

Ligations were carried out in 10 µl volumes using T4 DNA ligase (NEB). The DNA ligase forms a phosphodiester bond between 5' phosphate and the 3' hydroxyl end of DNA. For cohesive end ligation a ratio of 1:3 pmol vector to insert was used and for blunt end ligation a ratio of 1:6 pmol vector to insert was used. The concentration of the DNA was estimated on an agarose gel. 25 ng of the vector was always used for ligations and the concentration of the insert adjusted accordingly.

2.2.13 Transformation of *E.coli*

Electroporation of electrocompetent cells was routinely used for the transformation of *E.coli* with plasmid DNA. *E.coli* (XL1-BLUE and BL21-GOLD(DE3)) were prepared for electroporation using the following protocol: cells were grown to mid-log phase (A_{600} = 0.4-0.6) in LB broth with 20 µg/ml tetracycline at 37 ^{o}C, pelleted (4000 rpm, 15 minutes at 4 ^{o}C), and washed with chilled dH_2O, repelleted, and then resuspended in 10% (v/v) glycerol in dH_2O. Finally cells were resuspended in 1/400 volume of 10% (v/v) glycerol in dH_2O, and stored in single use aliquots of 50 µl at -80 ^{o}C.

Cells were transformed in a 0.1cm electrode gap cuvette using a BioRad Gene Pulsar (settings: 1.67 kV, 25 mF, 200 Ω). Post-electroporation, cells were suspended in 450 µl LB or SOC media and incubated at 37 ^{o}C for 30-45 minutes, before they were plated on LB-agar (LB with 1.2% w/v agar) containing appropriate antibiotic. Plates

were incubated at 37 ^{o}C overnight. SoluBL21 were transformed according to the manufacturer's protocol.

Bacterial cells (TOP10, LIBRARY EFFICIENCY® DH5a™, BL21-GOLD(DE3) and NEB 5-alpha) were chemically transformed. Cells were incubated with plasmid DNA on ice for 30 minutes, transformed by incubation at 42 ^{o}C for 45 seconds and on ice for 2 minutes. Cells were resuspended in 450 µl SOC, and incubated at 37 ^{o}C for 30-45 minutes, then plated on LB-agar plates containing appropriate antibiotic, and incubated at 37 ^{o}C overnight.

2.2.14 Isolation of plasmid DNA

Isolation of plasmid DNA from varying amounts of bacteria-inoculated media was performed using a modified alkaline lysis method (Birnboim and Doly, 1979). Small-scale plasmid purification followed the QIAprep Miniprep protocol (Qiagen). For larger scale isolations the QIAfilter plasmid Midi/Maxi Kit (Qiagen) was used according to the manufacturer's protocol.

2.2.15 Quantification of plasmid DNA

Concentration of plasmid DNA was determined by using one of the following methods:

A. DNA concentration was determined using 1:100 dilutions of stock plasmid DNA according to the formula: absorbance of one A_{260} unit approximately equates to 50 ng/µl of double-stranded DNA.

B. DNA concentration was determined using the Thermo Scientific NanoDrop™ 1000 Spectrophotometer according to the manufacturer's protocol.

C. DNA concentration was determined using the NanoPhotometer® P-Class from IMPLEN GmbH according to the manufacturer's protocol.

2.2.16 Sequencing of plasmid DNA

1 µg of purified DNA was prepared in a 1.5 ml tube in either dH_20 or 5 mM Tris-HCL (pH 8-9) to a total volume of 15 µl including 15 pmol of sequencing primer. Samples were sent to Eurofins MWG Operon for sequencing.

2.3 Tissue culture

2.3.1 Mammalian cell lines

MEFs, U2O-S, Saos-2 and HT1080 cells were grown in T25 or T75 flasks in Dulbecco's Modified Eagle Medium (DMEM) supplemented with 10% FCS (foetal calf serum), 2 mM glutamine, 50 IU/ml penicillin and 50 mg/ml streptomycin (Life Technologies). Cells were passaged by removing media, washed with PBS and incubated with Trypsin-EDTA (0.05% Trypsin, 0.5 mM EDTA) for ~2 minutes, adding 5X of complete growth media to neutralise the trypsin and replated at a dilution of 1:5-1:20.

2.3.2 Freezing of cell lines

Cells were grown in a T75 flask until they were 80-90% confluent. Media was removed from the cells, washed with PBS and incubated with trypsin-EDTA (0.05% Trypsin, 0.5 mM EDTA) for ~2 minutes, then 5X of complete growth media was added to neutralise the trypsin. Cells were spun down for 5 minutes at 1000 rpm. Cells were resuspended in 5 ml of supplemented DMEM containing 10% DMSO and divided into 5 cryo tubes (Nunc). Tubes were wrapped in paper towels and put in a small styrofoam box and stored at -80 ˚C for 2 days. This was to allow slow cooling. Vials were then transferred to liquid nitrogen for long-term storage.

2.3.3 Thawing of cell lines

Vials containing the cells were removed from liquid nitrogen and immediately put into a 37 ˚C waterbath. This was to ensure fast thawing of the cells. Cells were added into pre-warmed media and spun down for 5 minutes at 1000 rpm. Media containing the DMSO was removed and cells were resuspended in supplemented DMEM and grown in a T25 flask.

2.3.4 Transient transfection of mammalian cells

U2OS or HT1080 cells were transiently transfected using SUPERFECT (Qiagen) or FuGENE 6 (Roche Diagnostics) according to the manufacturer's protocol.

U2OS or HT1080 cells were plated out (~$3x10^5$ cells/well) and grown overnight in a 6-well plate (FALCON) containing a glass coverslip (22mm x 22mm). When

SUPERFECT was used for the transfection, a mix of DNA (2 μg), DMEM (700 μl) and Superfect (10 μl) was applied to every well and incubated for 3 hours at 37 ^{o}C. After 3 hours, cells were washed with PBS, and then 2ml DMEM containing supplements was added. Cells were incubated for 24-40 hours.

When FuGENE 6 was used for the transfection a mix of DNA (2 μg), DMEM (94 μl) and FuGENE 6 (6 μl) was applied to every well and incubated for 18 hours. Then the media was removed and replaced with fresh media. Cells were incubated another 6-24 hours.

2.3.5 Fixation and permeabilisation of mammalian cells

After incubation, media was removed from the cells. Cells were washed with PBS then fixed in 4% parafomaldehyde in PBS for 10 minutes. Paraformaldehyde was removed and cells were washed again with PBS, then permeabilised in 0.5% Triton X-100 in PBS for 20 minutes. Triton X-100 was removed and cells were washed twice with PBS. Fixed cells were stored at 4 ˚C until required.

2.3.6 Immunofluorescence studies

Primary antibodies in PBS at an appropriate dilution were added to cells fixed on coverslips and incubated for 30-60 minutes. Coverslips were then washed in PBS, (3 x 10 minutes). Secondary antibodies (50 μl) in PBS at an appropriate dilution were added to the coverslips and incubated in the dark for 30-60 minutes. Coverslips were washed in the dark in PBS, (3 x 10 minutes). DNA was stained with propidium iodide (0.5 μg/ml (Roche)) or DAPI (0.25 μg/ml (Roche)) and cells were viewed on a confocal microscope (Zeiss LSCM 510) with a Zeiss objective Plan-Apochromat 63x/1.40 oil DIC.

2.3.7 Propidium iodide staining

To outline the nuclear volume only, cells were washed with PBS, treated with Ribonuclease (100 μg/ml RNase (Roche)) for 20 minutes at 37 ^{o}C and DNA was stained with propidium iodide (0.5 μg/ml).

2.3.8 Preparation of total cellular protein extracts

After incubation, media was removed from the cells. Cells were washed with PBS and then lysed directly in the plate with 150 µl 2 x SDS sample buffer containing 0.75µl Benzonase® (100U/µl) for 5-10 minutes on ice. Cell extracts were incubated 5 minutes at 95 ˚C, then centrifuged for 5 minutes at 13000 rpm and stored at -20 ˚C until required.

2.3.9 Nuclear/cytoplasmic fractionations

Nuclear and cytoplasmic fractionations were isolated from mammalian cells according to the manufacturer's protocol (BioVision). The fractionation was performed using untransfected or transfected mammalian cells.

2.3.10 SDS polyacrylamide gel electrophoresis (SDS-PAGE), western blotting and chemiluminescent detection of proteins

Preparation of total cellular protein extracts and SDS-polyacrylamide electrophoresis was carried out according to standard protocols (Sambrook, 1989). Gels used were either commercially available or made. Samples were lysed in SDS gel-reducing buffer, boiled and loaded onto an appropriate % Tris-Glycine polyacrylamide gel. Proteins were then transferred to Hybond ECL nitrocellulose membrane (Amersham Pharmacia) using the Hoefer Semiphor semi-dry transfer procedure or the iBlot® gel transfer device (Life Technologies) and then blocked overnight in 5% (w/v) skimmed milk powder in dH_20.

Blocked membranes were probed with an antibody diluted appropriately in blocking solution. Membranes were washed twice with PBST and once with PBS. Membranes were then incubated with horseradish peroxidase conjugated IgG antibody (Dako) diluted in blocking solution. Membranes were again washed twice with PBST and once with PBS. Binding of secondary antibodies was detected using ECL (Amersham Pharmacia).

2.3.11 Production of polyclonal antisera against the TFAF-1 protein

Two polyclonal antibodies 822 and 823 against the TFAF-1 protein were made by immunizing rabbits with two synthetic TFAF-1 peptides (residues 2-16 and 96-110) coupled to the carrier protein Hemocyanin (Eurogentec). Both antibodies detected exogenous TFAF-1 protein as described in Results.

2.4 Protein expression and purification methods

2.4.1 Cell-free protein expression

Cell-free protein expression is used for fast protein synthesis. It can be used for toxic gene products and can be a rapid way of mapping PCR-generated mutations. It can be used with PCR-generated templates or used with circular plasmids depending on the kit. The cell-free protein expression kits use coupled transcription/translation for *in vitro* protein synthesis.

2.4.2 RTS 100 *E.coli* HY Kit

The RTS kit (5 PRIME) requires a DNA template where the gene is under control of a T7 promoter. The DNA is transcribed into mRNA by the T7 polymerase followed by translation into protein by the ribosomal machinery.

The manufacturer's protocol was amended slightly. Instead of running the experiment in 50 µl reactions it was scaled down to 20 µl.

The following protocol was used and the expression was tested at 16 ˚C, at room temperature and at 28 ˚C.

4.8 µl *E.coli* lysate
4.0 µl Reaction mix
4.8 µl Amino acids
0.4 µl Methionine
2.0 µl Reconstitution buffer
4.0 µl DNA (0.4 µg) in water

Reactions were left overnight. Proteins were precipitated prior to SDS-PAGE using the following protocol:

10 µl sample and 100 µl ice cold acetone was mixed and left on ice for 5 minutes. Samples were then centrifuged for 5 minutes at 13000 rpm. Supernatants were discarded and pellets air-dried for 10 minutes. The pellets were then dissolved in 20 µl of SDS sample buffer, heated to 95 ˚C for 5 minutes and 15 µl was loaded onto a SDS gel. SDS page was followed by western blotting and chemiluminescent detection of the synthesised proteins.

2.4.3 *E.coli* T7 S30 Extract System for Circular DNA

The T7 S30 Extract System for Circular DNA requires a circular DNA template where the gene is under control of a T7 promoter or an efficient *E.coli* promoter.
Again the protocol was amended slightly. The reactions were scaled down to 25 µl instead of 50 µl. The following protocol was used and the expression was tested at 16 ˚C, at room temperature and at 28 ˚C.

1.25 µl Amino acid mixture minus methionine
1.25 µl Amino acid mixture minus cysteine
10.0 µl S30 Premix without amino acids
7.5 µl T7 S30 Extract, Circular
5.0 µl DNA template (1 µg) in water

Reactions were left overnight. 10 µl was mixed with SDS sample buffer, heated up to 95 ˚C for 5 minutes and 15 µl loaded on a gel. SDS page was followed by western blotting and chemiluminescent detection of the synthesised proteins.

2.4.4 Test expression of recombinant proteins

The plasmid containing the sequence with the protein of interest was transformed into BL21-GOLD(DE3) or SoluBL21. Cells were plated on LB-agar containing the appropriate antibiotic and incubated overnight. One colony was picked and added to 5 ml of media containing antibiotics and grown overnight. The overnight culture was diluted 1:20 (500 µl + 9.5 ml) and grown for around 2 hours to an OD_{600} of 0.6. The culture was divided: 1 ml was left uninduced and IPTG was added to the remaining 9 ml to induce expression of the protein of interest. Both cultures were left for 6 hours to grow. Samples were centrifuged for 10 minutes at 4000 rpm. Pellets were resuspended in lysis buffer (8 M Urea, 100 mM NaH_2PO_4, 10 mM Tris pH 8.0, (50 µl/1 ml culture)) and left for 20 minutes at room temperature. Samples were mixed with SDS sample buffer and expression of the protein was checked on a Coomassie gel or by western blotting.

2.4.5 SUMO-modification in *E. coli*

This method was first described by Uchimura et al., 2004. The authors developed a binary vector system where a synthetic SUMO conjugation pathway is introduced in *E.coli*. They made a tri-cistronic plasmid for over-expression of SUMO-E1 activating enzyme and -E2 conjugating enzyme and either SUMO-1 or SUMO-3 (pE1E2S1/3). This vector was used for expression of E1, E2 and either SUMO-1 or SUMO-3 and a protein of interest leading to efficient SUMO modification of the protein in *E.coli*.

The following protocol was used for modification of our protein of interest.

pE1E2S1/3 and pET-28 CK1 alpha LS, CK1 alpha 325 or CK1 alpha 301 or pET-28 CK1 delta 317 were co-transformed into BL21-GOLD(DE3) or SoluBL21. Cells were plated on LB with the appropriate antibiotics and incubated overnight. One colony was picked and added to 10 ml of media containing antibiotics and grown overnight. The overnight culture was added to 500 ml of media containing antibiotics and grown to an OD_{600} of 1.0. The 500 ml culture was cooled to 15 ˚C for expression of CK1 alpha protein or to 22 ˚C for expression of CK1 delta and IPTG was added to a final concentration of 0.2 mM. The culture was left to grow overnight or for 5 or 6 hours at the appropriate temperature and spun down for 15 minutes at 4500 rpm. The pellets were stored at -80 ˚C until required.

2.4.6 Protein purification

Protein purification of the casein kinases was done using a protocol from (Burzio et al., 2002) that was subsequently modified.

Bacterial pellets were re-suspended in buffer A (50 mM HEPES pH 8.0, 500 mM NaCl, 10 mM Imidazole, 1% Triton X-100) containing a SIGMA*FAST* inhibitor protease cocktail and Lysozyme (1 mg/ml) and lysed on ice for 1 hour. Lysates were sonicated on ice for 4 minutes (2 seconds on, 2 seconds off, 50% amplitude) and centrifuged at 15000 rpm at 4 ˚C for 45 minutes. Lysates were loaded onto a 1 ml Nickel-affinity column or a 1 ml HIS-Select Cobalt Affinity Gel using an AKTA system at 4 ˚C at a flowrate of 0.5 ml/min and UV detection at 280 nm. The column was washed with 12 volumes buffer A without Triton X-100, then washed with 12 volumes 15% buffer B (50 mM HEPES pH 7.5, 200 mM NaCl, 250 mM Imidazole) and eluted with 50% buffer B. The column was finally washed with 6 volumes 100% buffer B to clean the resin.

After visualizing on an SDS gel the eluted protein was concentrated and buffer exchanged using an Amicon Ultra centrifugal filter with a 10K MW cut-off using buffer (40 mM Tris pH 7.5, 20 mM $MgCl_2$, 150 mM NaCl). 2 ml purifed protein was concentrated to 0.5-1.0 ml. The protein concentration was determined using the NanoPhotometer® P-Class from IMPLEN GmbH according to the manufacturer's protocol.

2.4.7 Expression and purification of SUMO-specific protease

pET-28b SENP2 (aa 366-588) was transformed into BL21-GOLD(DE3). Cells were plated on LB-agar containing Kanamycin and incubated overnight. One colony was picked and added to 10 ml of media containing antibiotics and grown overnight. The overnight culture was added to 500 ml of media containing antibiotics and grown to an OD_{600} of 0.6. The 500 ml culture was cooled down to 22 ˚C and IPTG was added to a final concentration of 0.5 mM for induction of expression of the SUMO-protease. The culture was left to grow overnight at 22 ˚C and spun down for 15 minutes at 4500 rpm. Pellets from a 500 ml culture were resuspended in 15 ml of buffer A (10 mM Tris pH 7.6, 0.5 M NaCl and 5 mM Imidazole), then sonicated on ice for 4 minutes (2 seconds on, 2 seconds off, 50% amplitude) and centrifuged at 15000 rpm at 4 ˚C for 45 minutes. Supernatant was loaded onto a 5 ml Nickel-affinity column using an AKTA system at 4 ˚C with a flowrate of 0.5 ml/min and UV detection at 280 nm. Column was washed with 10 volumes buffer A. Then washed with 10 volumes 10% buffer B (10 mM Tris pH 7.6, 0.5 M NaCl and 0.5 M Imidazole) and eluted with 100% buffer B. The protein was concentrated and buffer-exchanged using an Amicon Ultra centrifugal filter with a 10K MW cut-off in 2 x storage buffer (1 x storage buffer: 25 mM Tris pH 8.0, 250 mM NaCl and 0.5 mM DTT). 7 ml of purified protein was concentrated to 3 ml. The concentrated SUMO protease was diluted in glycerol (50% final concentration) and stored at -20 ˚C.

2.4.8 De-modification of CK1 delta 317/SUMO-1

The concentrated purified proteins CK1 delta 1-317 and CK1 delta 1-317/SUMO modified were diluted to a concentration of 5 µg/100 µl in 1 x kinase buffer (40 mM Tris pH 7.5, 20 mM $MgCl_2$) and 10 µl SUMO-specific protease (3 µg/µl) was added, mixed well and incubated at room temperature. The de-modified CK1 protein was used in the kinase assay to check the activity after protease treatment.

2.4.9 ADP-Glo™ Kinase Assay

The kinase assay was performed according to the manufacturer's protocol with slight modifications.

Kinase reaction buffer (5 ml 40 mM Tris pH 7.5, 20 mM $MgCl_2$ + 50 µl BSA (10 mg/ml)) was prepared and the following protocol used for the assay:

2.6 µl CK1 (5 ng purified protein/µl)

5 µl substrate CK1 peptide (pS7) 600 µM

3.75 µl ATP 500 µM

1.25 µl Kinase reaction buffer

Incubated 10-30 minutes at room temperature

Added 12.5 µl ADP-Glo reagent

Incubated 40 minutes at room temperature

Added 25 µl kinase detection reagent

Luminescence measured on the POLARstar Omega (BMG LABTECH GmbH)

Instrument settings:

Measurement time 1 second

Cycle time 60 seconds

Cycles 40 minutes

Gain Dependent on ADP concentration

2.5 Prediction servers

2.5.1 SUMO prediction server

To predict where our protein of interest could be covalently modified by SUMO the following servers were used.

SUMOplot: http://www.abgent.com/tools/sumoplot

SUMOsp: http://sumosp.biocuckoo.org/

seeSUMO: http://bioinfo.ggc.org/seesumo/

PCI-SUMO: http://bioinf.sce.carleton.ca/SUMO/start.php

The following server was used to predict if our protein of interest contains a SUMO-interacting motif (SIM), also called the SUMO-binding motif (SBM).
GPS-SBM 1.0: **http://sumosp.biocuckoo.org/**

2.5.2 PSIPRED secondary structure prediction server

To predict the secondary structure of the TFAF-1 protein the following server was used.
http://bioinf.cs.ucl.ac.uk/psipred/

3 Results

3.1 Signal transduction pathways as part of a PML regulatory cascade

3.1.1 Introduction

In order to gain a better understanding of PML and PML NBs a yeast two-hybrid assay was previously carried out (Boddy et al., 1996). This is a well-established method for screening a large number of independent cDNAs encoding proteins, which might interact with a target protein. The isoform PMLVI was used as bait and preliminary data indicated that PMLVI interacted with TRAF4-associated factor 1 (TFAF-1). This clone was of particular interest because the TRAF family of proteins is involved in cell survival, proliferation, differentiation and apoptosis.

As discussed earlier TRAF proteins are characterised by the presence of a TRAF domain at the C- terminus. The TRAF domain consists of a coiled-coil domain followed by a conserved TRAF-C domain. The N-terminus of TRAF proteins, except for TRAF1, contains a RING finger and several zinc finger motifs that are important for signalling downstream events (Aggarwal, 2003; Arch et al., 1998; Bradley and Pober, 2001; Chung et al., 2002). All TRAFs, apart from TRAF4, were identified by yeast two-hybrid screening using a cytoplasmic domain of various members of the TNFR family. Even though TRAF4 has no known function in the signalling of TNF it was still worth investigating. One observation worth pointing out is that TRAF proteins share structural features with the PML protein (Arch et al., 1998).

This interaction between PML and TFAF-1 was investigated further using colocalisation studies.

3.1.2 Amplification of full-length TFAF-1

A human testis cDNA library was screened by PCR and two TFAF-1 clones were obtained. TFAF-1 specific primers were used for the screening. Truncated TFAF-1 constructs were used in some of the experiments as this was the only partial coding sequence known when the studies commenced.

In Figure 3.1 an overview can be seen of the TFAF-1 clones used in this study. Predicted functional domains are also shown.

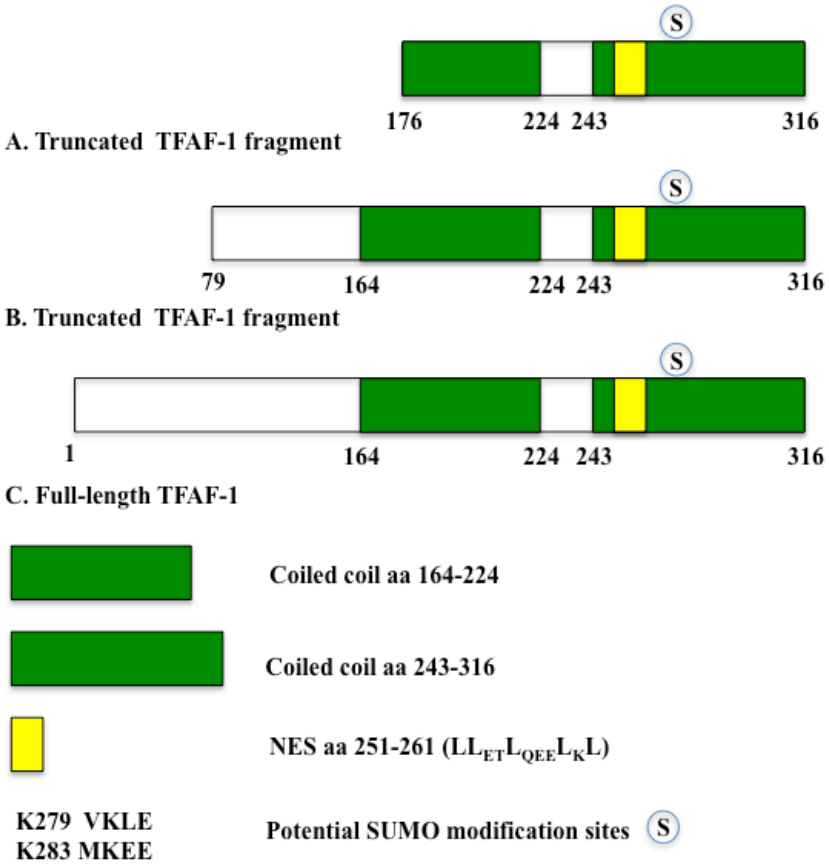

Figure 3.1. Schematic representation of the TFAF-1/SKAP constructs and predicted functional domains

A: The TRAF-1 clone pulled out in the yeast-two hydrid screen (TFAF-1 aa 176-316).
B: The truncated TFAF-1 aa 79-316 was used in some of the experiments as this was the only partial coding sequence known when the studies commenced.
C: Full-length TFAF-1 construct.

3.1.3 Subcellular localisation studies of TFAF-1

To study the subcellular localisation of TFAF-1, U2OS cells were transfected with a plasmid encoding the enhanced green fluorescent protein (EGFP), resulting in a EGFP-TFAF-1 fusion protein (pEGFP-TFAF-1 (aa 79-316)). TFAF-1 was excluded from the nucleus and showed a speckled distribution in the cytoplasm (Figure 3.2, A-C). When TFAF-1 (aa 79-316) was expressed with a FLAG- tag it had a diffuse nuclear and cytoplasmic distribution (Figure 3.2, E-F). Expression of a FLAG-TFAF-1 (aa 79-316) construct with an exogenous SV40-nuclear localisation signal (NLS) changed the cytoplasmic distribution. The FLAG-NLS-TFAF-1 (aa 79-316) protein showed a diffuse distribution in the nucleus (Figure 3.2, H-I). A red fluorescent TFAF-1 fusion protein expressed in U2OS cells resulted in a very distinctive cytoplasmic network (Figure 3.2, K-L). The TFAF-1 filaments appeared to link PML NBs (Figure 3.2L). The pDsRed-N1-TFAF-1 full-length protein showed a similar filamentous pattern in many of the transfected cells (Figure 3.3B). In some cells, the TFAF-1 full-length showed a speckled distribution that did not colocalise with PML NBs (Figure 3.3F). The vector pDsRed-N1 was used as a control and did not form filaments in transfected cells.

3.1.4 Generation of an anti-peptide antibody against the TFAF-1 protein

To characterise the subcellular localisation of endogenous TFAF-1 protein, two polyclonal antisera against two 15-residue synthetic peptides were made (residues 2-16 and 96-110). In Figure 3.4 the predicted secondary structure of the TFAF-1 protein is presented. The secondary structure was used to choose the most promising peptides of the TFAF-1 protein sequence against which to raise an antiserum.

Neither preimmune sera recognised exogenous TFAF-1 protein. Only the two polyclonal antisera detected exogenous TFAF-1 protein (Figure 3.5). In non-transfected cells a diffuse pattern throughout the cytoplasm and the nucleus was seen using the rabbit polyclonal anti-TFAF-1 antisera.

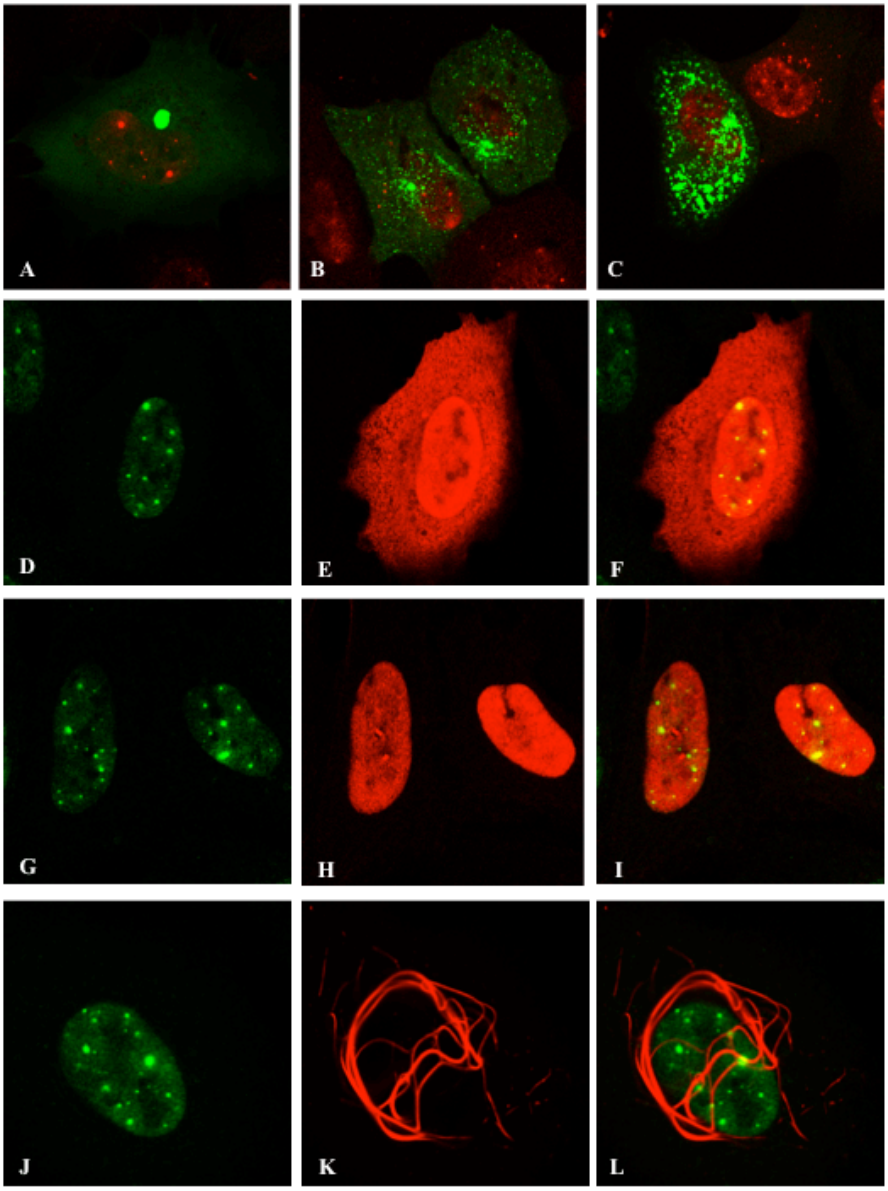

Figure 3.2. Subcellular localisation studies of the TFAF-1 protein

A-C: A green fluorescent protein (GFP)-TFAF-1 fusion protein localised to the cytoplasm in U2OS cells and showed a speckled distribution. Cells were stained with polyclonal rabbit anti-PML antibodies (red fluorescence). **D-F**: An N-terminal FLAG-tagged TFAF-1 protein showed a diffuse nuclear and cytoplasmic distribution in U2OS cells. Cells were stained with anti-FLAG mAb (red fluorescence) and with polyclonal rabbit anti-PML antibodies (green fluorescence). **G-I**: The FLAG-TFAF-1 protein was redistributed to the nucleus in U2OS cells when it was expressed with an exogenous SV40-nuclear localisation signal (NLS). Cells were stained with an anti-FLAG mAb (red fluorescence) and with polyclonal rabbit anti-PML antibodies (green fluorescence). **J-L**: A red fluorescent TFAF-1 fusion protein showed a filamentous structure in U2OS cells. Cells were stained with polyclonal rabbit anti-PML antibodies (green fluorescence).

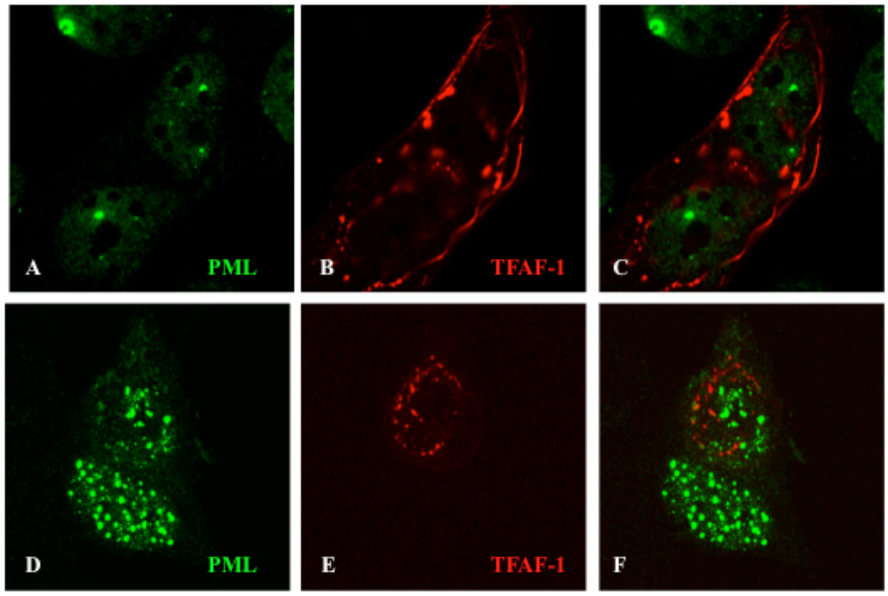

Figure 3.3. Localisation of red fluorescent TFAF-1 full-length fusion protein

A-C: DsRed-TFAF-1 full-length fusion protein formed filaments in some of the transfected cells.
D-F: In other cells it formed some kind of bodies that did not colocalise with PML NBs.
U2OS cells transiently transfected with pDsRed-N1-TFAF-1 (full-length). Cells were stained with polyclonal rabbit anti-PML antibodies (green fluorescence).

Figure 3.4. Predicted secondary structure of the TFAF-1 protein using the PSIPRED protein structure prediction server

References:
The PSIPRED server:
McGuffin LJ, Bryson K, Jones, D.T. (2000) The PSIPRED protein structure prediction server. Bioinformatics. 16, 404-405.
PSIPRED:
Jones, D.T. (1999) Protein secondary structure prediction based on position-specific scoring matrices. J. Mol. Biol. 292, 195-202.

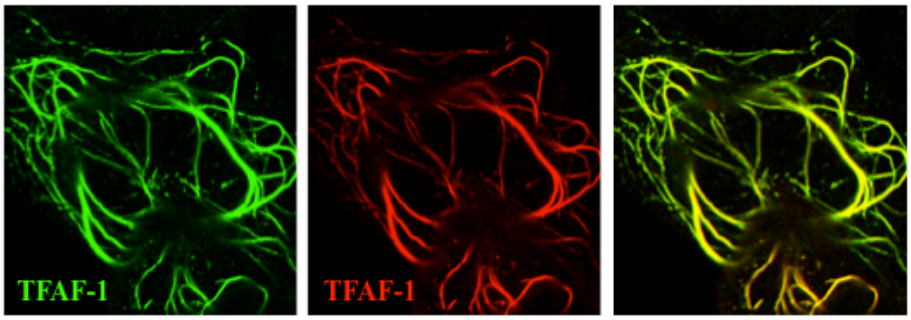

Figure 3.5. Anti-peptide antibody against the TFAF-1 protein

The anti-peptide antibody recognised TFAF-1.
U2OS cells transiently transfected with pDsRed-N1-TFAF-1 (aa 79-316). Cells were stained with polyclonal rabbit anti-TFAF-1 antibodies (green fluorescence).

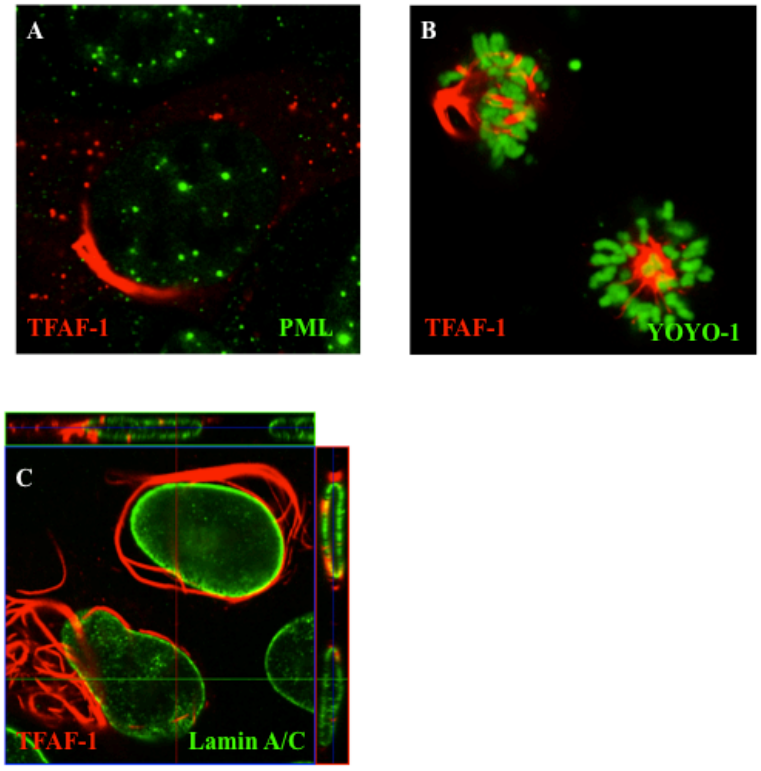

Figure 3.6. TFAF-1 filaments are cytoplasmic filaments, part of the microtubule cytoskeleton

A-C: U2OS cells transiently transfected with pDsRed-N1-TFAF-1 (aa 79-316).
A: 20 hours after transfection cells were treated with Nocodazole (20 µM 2.5 hrs). Cells were stained with polyclonal rabbit anti-PML antibodies (green fluorescence).
B: YOYO-1 dye-stained chromosomes (green fluorescence).
C: Cells were stained with mouse monoclonal anti-Lamin A/C antibodies (green fluorescence).

3.1.5 TFAF-1 filaments are a part of the microtubule cytoskeleton

To find out more about the TFAF-1 filaments, U2OS cells were transfected with pDSRed-N1-TFAF-1 (aa 79-316) and treated with Nocodazole (Figure 3.6A). Nocodazole induces microtubule depolymerization by inhibiting addition of tubulin monomers. In Figure 3.6A it can be seen that TFAF-1 filaments were disrupted after Nocodazole treatment. This means that TFAF-1 filaments are associated with the microtubule cytoskeleton. TFAF-1 filaments did not break down during mitosis (Figure 3.6B). In figure 3.6C it is very clear that TFAF-1 filaments are cytoplasmic filaments. Cells were stained with LaminA/C and captured as a z-stack. Some of the filaments might just touch the nucleus but they do not appear to go through it.

3.1.6 Colocalisation studies of TFAF-1 and known cytoskeletal filaments

To test whether TFAF-1 filaments colocalised with other known cytoskeletal filaments, double immunofluorescent studies were performed. Because it had been reported that TNFR-associated death domain (TRADD) could be found in the PML NBs in the absence of export (Morgan et al., 2002), and that overexpressed TRADD localised in K18 filaments (Inada et al., 2001), a subcellular distribution of TFAF-1 and K18 was carried out (Figure 3.7, A-C). Overexpressed TFAF-1 did not colocalise with K18.

The TFAF-1 protein contains a predicted coiled-coil domain. Coiled coils mediate both homo- and heterodimeric interactions. Another protein, TRIM 29, which also contains a coiled-coil domain and localises in cytoplasmic filaments (Reymond et al., 2001), was tested for colocalisation with TFAF-1 (Figure 3.7, D-F). No colocalisation of TFAF-1 and TRIM 29 was found here either.

A third structure, named death-effector filaments (DEFs), resembles cytoskeleton filaments although microtubule and microfilament proteins are not involved. DEFs are formed by overexpression of the Fas-associated death domain (FADD) or the prodomain of caspase-8 and usually assemble into structures orbiting around the nucleus (Siegel et al., 1998). Figure 3.7, G-I shows a partial colocalisation of DEFs and TFAF-1 filaments. These results suggested that the TFAF-1 protein might play a role in the Fas death-signalling pathway.

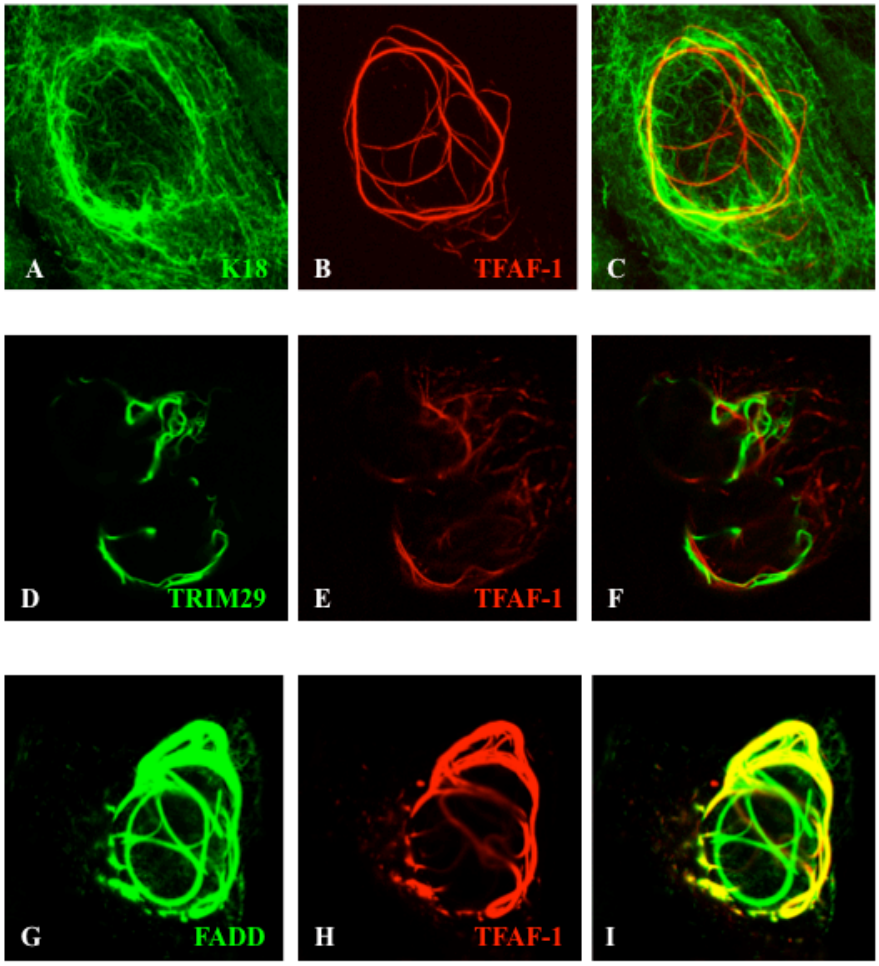

Figure 3.7. Colocalisation studies of TFAF-1

TFAF-1 colocalised partially with death-effector filaments formed by FADD.
A-C: The red fluorescent-TFAF-1 fusion protein did not colocalise with K18 in U2OS cells. Cells were stained with an anti-cytokeratin peptide 18 mAb (green fluorescence).
D-F: The red fluorescent-TFAF-1 fusion protein did not colocalise with the green fluorescent protein (GFP)-TRIM29 in U2OS cells.
G-I: The red fluorescent-TFAF-1 fusion protein partially colocalised with death-effector filaments in U2OS cells. Cells were stained with an anti-Fadd mAb (green fluorescence).

3.1.7 Summary

- **TFAF-1 interacted with PMLVI in a yeast two-hybrid assay**
- **TFAF-1 did not colocalise to PML NBs but showed a diffuse distribution throughout the cell**
- **TFAF-1 formed cytoplasmic filaments when expressed as a fusion protein with DsRed**
- **The TFAF-1/DsRed filaments were a part of the cytoplasmic cytoskeleton**
- **TFAF-1/DsRed filaments partially colocalised with DEFs formed by FADD**

3.1.8 Conclusion and hypothesis

These results suggested that TFAF-1 might interact with a soluble fraction of PML outside PML NBs. TFAF-1/DsRed colocalised with DEFs in the cytoplasm and could be involved in Fas-mediated apoptosis. This association was investigated further using colocalisation studies with DEFs and PML NB components.

Interaction studies between PML VI and TFAF-1 were repeated in a mammalian two-hybrid system and in co-immunopreciptation experiments. However, it was not possible to reproduce the results from the yeast two-hybrid system. It was therefore speculated that it was possibly not a specific interaction between PML and TFAF-1 but an unspecific interaction between the two coiled-coil domains in the corresponding proteins.

3.2 PML nuclear bodies and death-effector filaments

3.2.1 Introduction

Studies in PML -/- cells show that PML might be involved in Fas-mediated apoptosis. PML -/- cells are less responsive to apoptotic inducers such as Fas and TNF ligands and PML plays a role in the response of caspase-1 and caspase-3 upon treatment with these ligands (Wang et al., 1998b). Another protein called TRADD, which shuttles between the cytoplasm and the nucleus where it localizes to PML NBs, links PML to death receptor-mediated apoptosis (Morgan et al., 2002). Furthermore the Daxx

protein, which interacts with SUMO-modified PML and localizes to PML NBs. was originally found as an interacting partner with the Fas receptor.
FADD, which forms death-effector filaments, is also involved in death receptor-mediated apoptosis and a working hypothesis could suggest that FADD is part of PML NBs and Fas-mediated apoptosis.

3.2.2 Death-effector filaments modify the distribution of PML

It was observed that in some of the U2OS cells expressing the DsRed-TFAF-1 fusion protein the pattern of endogenous PML was rearranged into fewer bodies (Figure 3.8). To find out if this was specific for the TFAF-1 filaments and to investigate the connection between DEFs and TFAF-1 filaments further, U2OS cells were transfected with a plasmid expressing the FADD protein. Interestingly, the distribution of PML NBs was also rearranged in some of the cells expressing the FADD protein (Figure 3.9A). The bodies appeared to become elongated and formed tracks while in other cells PML NBs were associated with the DEFs (Figure 3.9B). DEFs are described as cytoplasmic structures (Siegel et al., 1998) and PML NBs are localised in the nucleus. To show that there was a physical connection between the DEFs and PML NBs, U2OS cells were transfected with FADD (Figure 3.9C and D). Figure 3.9C shows that the PML protein stays in the nucleus in smaller filaments or tracks after disruption. Figure 3.9D shows that DEFs are not only cytoplasmic structures but also travel through the nuclear envelope into the nucleus. This result was also confirmed by a 3D reconstruction of U2OS cells transiently transfected with FADD (Figure 3.10: 3D reconstruction with kind help from Dr Suhail Islam). In figure 3.10 it was very clear that the DEFs were not only cytoplasmic filaments but also nuclear and that PML was forming tracks on the filaments.

3.2.3 Electron microscopy analysis of FADD death-effector filaments in the nucleus

Electron microscopy was also used to confirm that the DEFs are nuclear as well as cytoplasmic filaments. U2OS cells were transfected with FADD and analysed by electron microscopy and immunogold labeling (Figure 3.11: Electron microscopy analysis with kind help from Dr Fabienne Beuron). The filaments seemed to penetrate the nuclear envelope (Figure 3.11B).

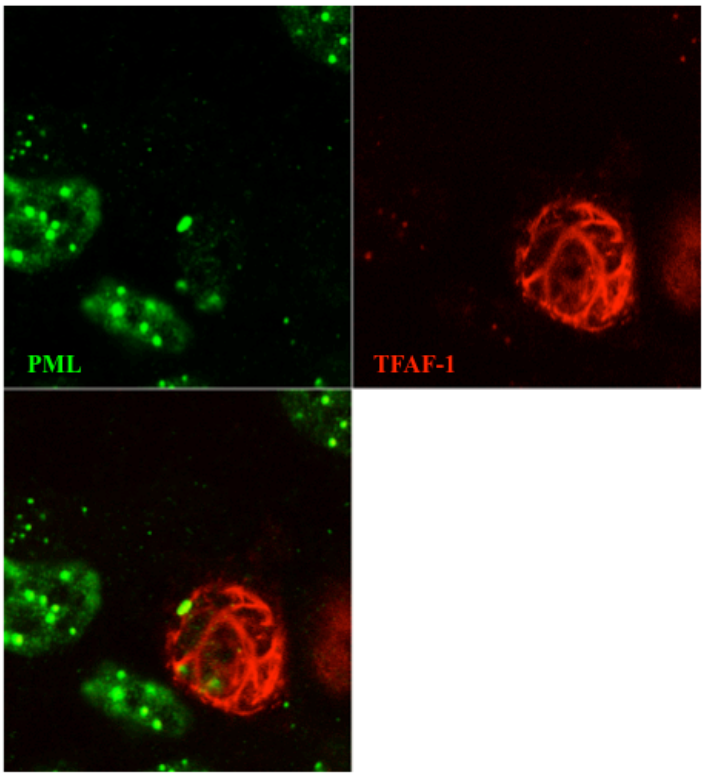

Figure 3.8. TFAF-1 changes the pattern of PML nuclear bodies

The red fluorescent-TFAF-1 fusion protein changed the distribution of the PML nuclear bodies in some of the transfected U2OS cells. Cells were stained with polyclonal rabbit anti-PML antibodies (green fluorescence).

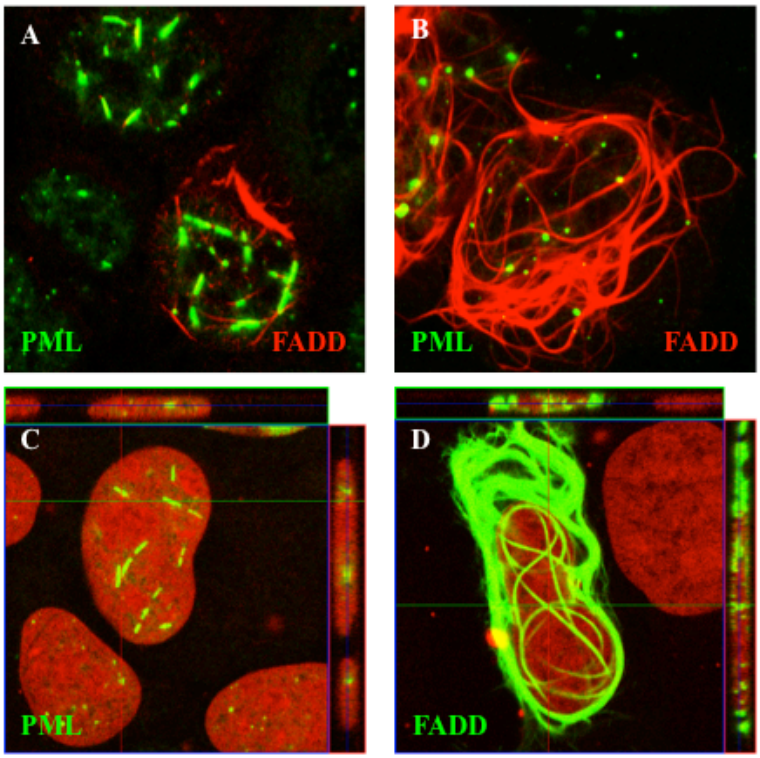

Figure 3.9. Death-effector filaments change the distribution of PML nuclear bodies

A: The death-effector filaments disrupted PML 24 hours after transfection of pcDNA3-AU1 FADD. **B**: PML colocalised with the death-effector filaments. U2OS cells were stained with polyclonal rabbit anti-PML antibodies (green fluorescence) and with an anti-FADD mAb (red fluorescence). **C:** PML stayed in the nucleus after transfection of pcDNA3-AU1 FADD. U2OS cells were stained with polyclonal rabbit anti-PML antibodies (green fluorescence) and propidium iodide. **D:** Death-effector filaments were not only cytoplasmic structures but also nuclear. U2OS cells were stained with an anti-FADD mAb (green fluorescence) and propidium iodide.

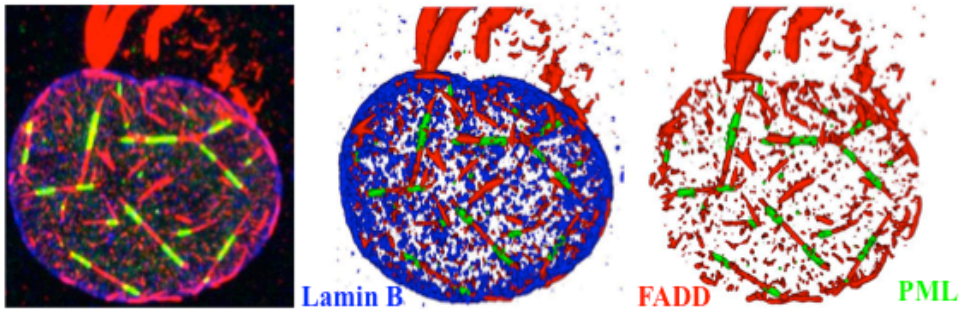

Figure 3.10. Death-effector filaments are nuclear and change the distribution of PML nuclear bodies

The death-effector filaments disrupted PML 24 hours after transfection of pcDNA3-AU1 FADD. PML colocalised with death-effector filaments. U2OS cells were stained with polyclonal rabbit anti-PML antibodies (green fluorescence) and with an anti-FADD mAb (red fluorescence). Lamin B was used to outline the nucleus and stained with goat anti-Lamin B antibodies (blue fluorescence).

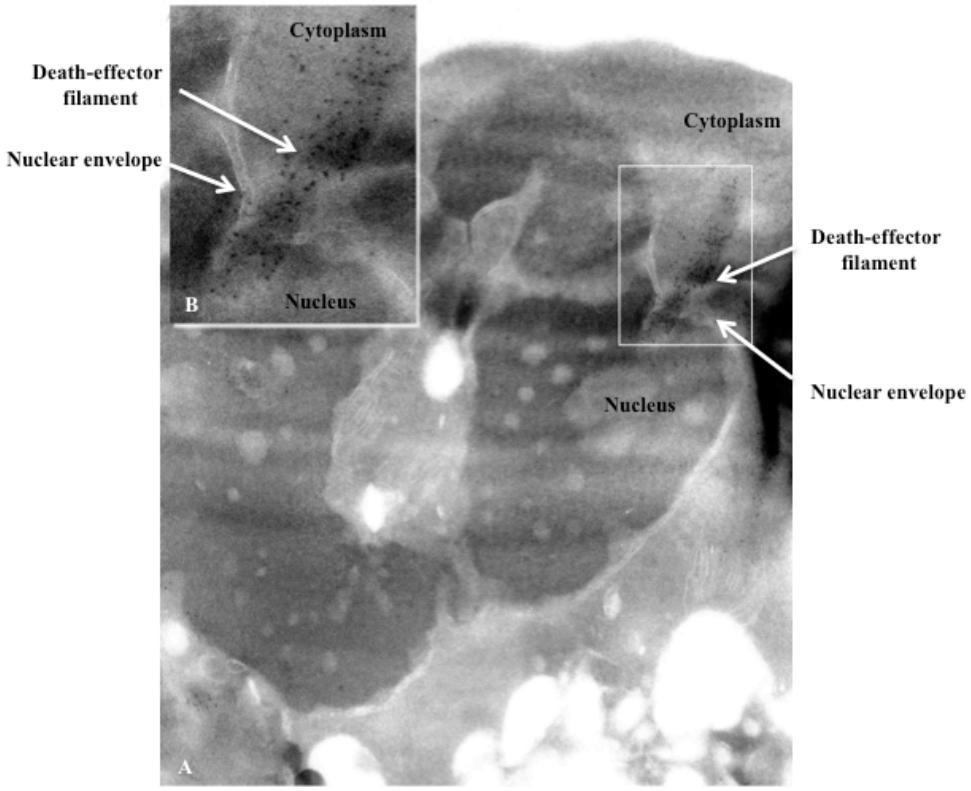

Figure 3.11. Preliminary electron microscope analysis of FADD death-effector filaments in the nucleus

A: U2OS cells were tranfected with pCDNA3-AU1 FADD, analysed by electron microscopy and immunogold labelling. Death-effector filaments were localised in the cytoplasm and in the nucleus (see arrows) and the filaments penetrated the nuclear envelope. Higher magnification of a part of the cell is shown as **B**.
Specimen preparation: sample high pressure frozen, embedded in resin and sectioned, followed by immunogold labelling.

3.2.4 Death-effector filaments modify other PML nuclear body components

To see if the modification of the PML NBs by DEFs was specific for the PML protein, the patterns of three other PML nuclear body components, Sp100, SUMO-1 and Daxx, were tested in cells expressing DEFs. Interestingly, the pattern of Sp100 did not change until ~48 hours after transfection of FADD (Figure 3.12A), whereas the pattern of PML already changed ~24 hours after transfection. Sp100, like PML, also associated with the DEFs before becoming disrupted (Figure 3.12B). The SUMO-1 protein colocalised 24 hours after transfection (Figure 3.12C) although 48 hours after FADD transfection the SUMO-1 protein completely overlaid the nuclear DEFs (Figure 3.12D), unlike PML and Sp100. A third nuclear body protein, Daxx, also showed association with the DEFs ~48 hours after transfection of FADD (Figure 3.12, E-F). Figure 3.12G shows that the PML filaments/tracks colocalised with the SUMO-1 filaments. This result suggested that all disrupted PML nuclear body components localised to the same filamentous structure in the nucleus.

Given that PML and PML NBs play an important role in apoptosis by regulating the activity of tumour suppressor p53, the localisation of p53 after FADD transfection was tested. The pattern of p53, however, did not change in cells transfected with FADD. Taken together these preliminary results showed that PML, SUMO-1, Sp100 and Daxx formed part of nuclear DEFs or were recruited to these filaments after being formed.

3.2.5 Death effector filaments do not modify other nuclear compartments

To ensure that the disruption of the PML bodies was specific, three other nuclear compartments were stained after tranfection of FADD. HIPK2, Cajal bodies and nucleoli (Figure 3.13) were tested and none of the compartments was modified by DEF. This suggested that the disruption of the PML bodies might be specific and not just an event where the filaments randomly penetrated the nucleus and disrupted nuclear compartments.

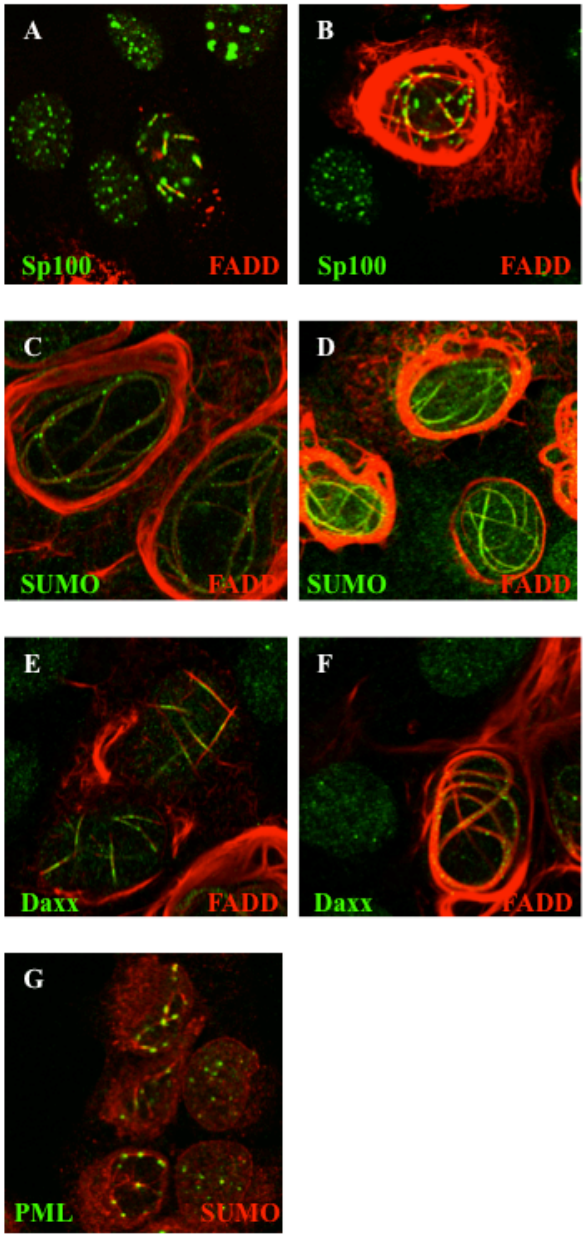

Figure 3.12. Death-effector filaments change the distribution of other PML nuclear body components

A: Death-effector filaments disrupted Sp100 in some of the U2OS cells 48 hours after transfection of pcDNA3-AU1 FADD and CrmA. **B:** Sp100 colocalised with the death-effector filaments. Cells were stained with polyclonal rabbit anti-Sp100 antibodies (green fluorescence) and with an anti-FADD mAb (red fluorescence). **C:** Death-effector filaments changed the pattern of SUMO-1 24 hours after transfection. **D:** The death-effector filaments recruited SUMO-1 into the filaments 48 hours after transfection of pcDNA3-AU1 FADD and CrmA. Cells were stained with polyclonal rabbit anti-SUMO antibodies (green fluorescence) and with an anti-FADD mAb (red fluorescence). **E-F:** The death-effector filaments recruited Daxx into the filaments 48 hours after transfection of pcDNA3-AU1 FADD and CrmA. Cells were stained with polyclonal rabbit anti-Daxx antibodies (green fluorescence) and with an anti-FADD mAb (red fluorescence). **G:** PML filaments (green fluorescence) colocalised with SUMO-1 filaments (red fluorescence) 48 hours after transfection of pcDNA3-AU1 FADD and CrmA.

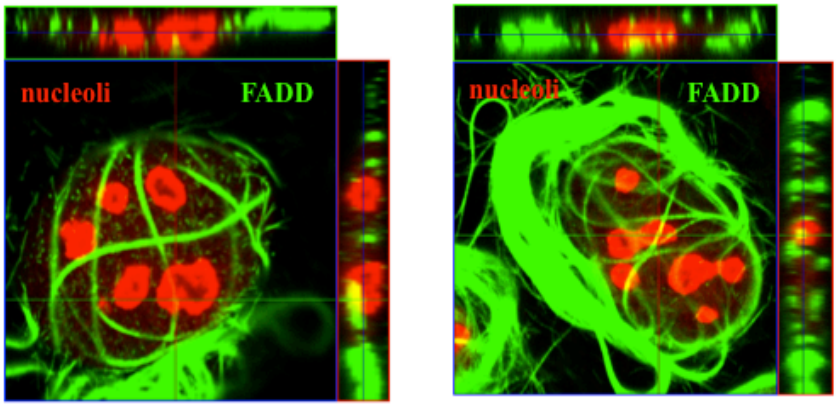

Figure 3.13. Death-effector filaments do not disrupt other nuclear substructures

The DEFs did not disrupt nucleoli after transfection of pcDNA3-AU1 FADD. U2OS cells were stained with polyclonal goat anti-FADD antibodies (green fluorescence) and with an anti-nucleophosmin mAb (red fluorescence).

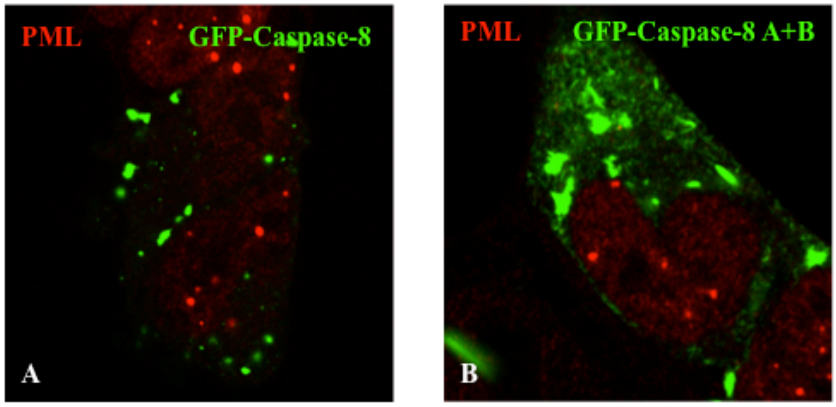

Figure 3.14. Caspase-8 and death-effector filaments formed by the DED domains of Caspase-8 do not disrupt PML nuclear bodies

A: U2OS cells transiently transfected with pEGFP-Caspase-8. Cells were stained with polyclonal rabbit anti-PML antibodies (red fluorescence).
B: U2OS cells transiently transfected with pEGFP-Caspase-8 DED-AB. Cells were stained with polyclonal rabbit anti-PML antibodies (red fluorescence).

3.2.6 Relocalisation of PML nuclear bodies is independent of recruitment of caspases

To see if filament formation and PML NB disruption were dependent on caspase-recruitment the following experiments were performed.

It has been reported that endogenous caspase-8 is recruited to DEFs (Siegel et al., 1998). Overexpression of full-length caspase-8 did not lead to formation of DEFs (Figure 3.14A); only caspase-8 DED-AB and caspase-8 DED-B were able to form DEFs (Siegel et al., 1998). Full-length caspase-8 did not relocalise PML (Figure 3.14A) neither did caspase-8 DED-AB (Figure 3.14B).

Filament formation of PML and SUMO was still observed in U2OS cells treated with the caspase inhibitor z-VAD-fmk. 100 μM caspase inhibitor z-VAD-fmk was added 1 hour before transfection and left on the cells 23 hours after transfection of FADD. The same result was obtained by co-transfection of FADD and the cowpox serpin cytokine response modifier A (CrmA). CrmA is a serpin-like protease inhibitor and blocks the activities of many caspases (group I caspases: caspase-1, 4 and 5 and group III caspases: caspase-8, 9 and 10).

These results suggested that the disruption of the PML NBs by FADD was independent of caspase recruitment.

3.2.7 Death-effector filaments and Ad5 E4 Orf3

PML NBs are disrupted or targeted by many different viral proteins (Geoffroy and Chelbi-Alix, 2011). One of them, Ad5 E4 Orf3, is able to self-associate and form filaments/tracks (Hoppe et al., 2006) that disrupt PML NBs and also make PML form small tracks (Figure 3.15). The PML tracks formed by Ad5 E4 Orf3 appear similar to the PML tracks formed by death-effector filaments and it was tempting to think that they might be the same. In figure 3.16 it can be seen that the filaments formed by FADD showed a partial colocalisation with Ad5 E4 Orf3. These results suggested that track formation of PML NBs could be the same.

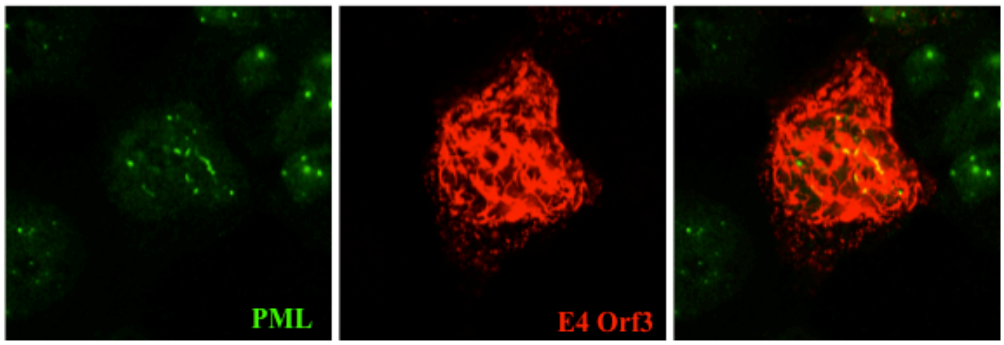

Figure 3.15. Adenovirus Type 5 E4 Orf3 rearrange PML NBs into tracks

U2OS cells transiently transfected with pcDNA3-HA E4 Orf3. Cells were stained with polyclonal rabbit anti-PML antibodies (green fluorescence) and an anti-HA mAb (red fluorescence).

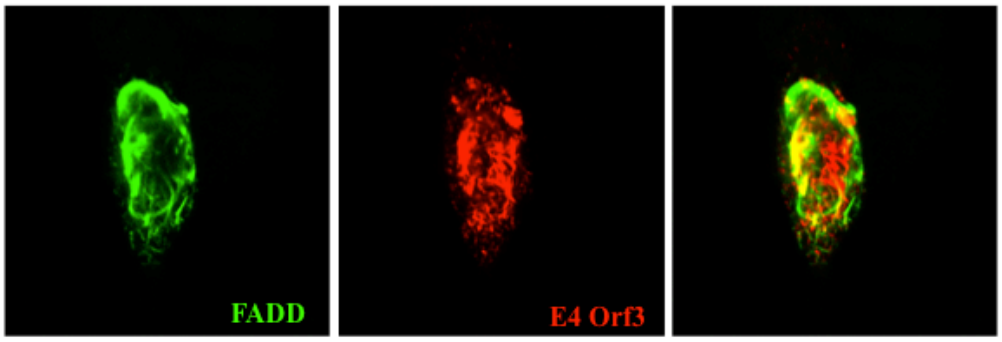

Figure 3.16. Death-effector filaments and filaments formed by Adenovirus Type 5 E4 Orf3 show a partial colocalisation

U2OS cells transiently transfected with pcDNA3-AU1 FADD and pcDNA3-HA E4 Orf3. Cells were stained with polyclonal rabbit anti-FADD antibodies (green fluorescence) and an anti-HA mAb (red fluorescence).

3.2.8 Death effector filaments colocalise with NLS/Vimentin

DEFs were originally discovered by Siegel et al., 1998. In that paper the authors mention some resemblance to the Vimentin network. Vimentin is type III intermediate filament. NLS-Vimentin is engineered to translocate into the nucleus and outline the ICD compartment, which lies outside of the chromosome territories (Bridger et al., 1998). PML has been shown to localise to the interchromosomal domain compartment (ICD) (Bridger et al., 1998). To see if the DEFs localises to ICD, cells were co-transfected with human NLS-/YFP-Vimentin (9:1) and pcDNA3-AU1 FADD (Figure 3.17: Data kindly provided by Hannah Stage and Hans Will, Hamburg). DEFs and NLS Vimentin showed a partial colocalisation in the nucleus. This result suggested that PML and DEFs were to be found in the same compartment in the cell nucleus in the ICD.

3.2.9 Treatments of cells with apoptotic inducers

It was important to see if DEFs could be found in cells without over-expression of the FADD protein. Apoptotic inducers were used to treat cells to induce the formation of the DEFs.

It has previously been shown that endogenous FADD can form DEFs in Jurkat cells when treated with cyclohexamide (CHX) (Tang et al., 1999). Treatment with CHX (2.5 μg/ml 20 hours) took endogenous FADD into DEFs in HT1080 cells (Figure 3.18B) and U20S cells (Figure 3.18D). In untreated HT1080 cells FADD localised to the nucleus and in small filaments, which could be DEFs (Figure 3.18A) and in untreated U2OS cells endogenous FADD localised mainly to the nucleus (Figure 3.18C). Treatment with CHX did not change the PML bodies, although there might have been a slight decrease in PML bodies as CHX inhibits protein synthesis.

Treatment with TNF (100 pg/ml for HT1080 and 1 ng/ml for U2OS 20 hours) and treatment with FasL (50 ng/ml for 20 hours HT1080 and U2OS cells or 100 ng/ml FasL + z-VAD-fmk 100 μM 6 hours or 24 hours for HT1080 cells) did not relocalise PML.

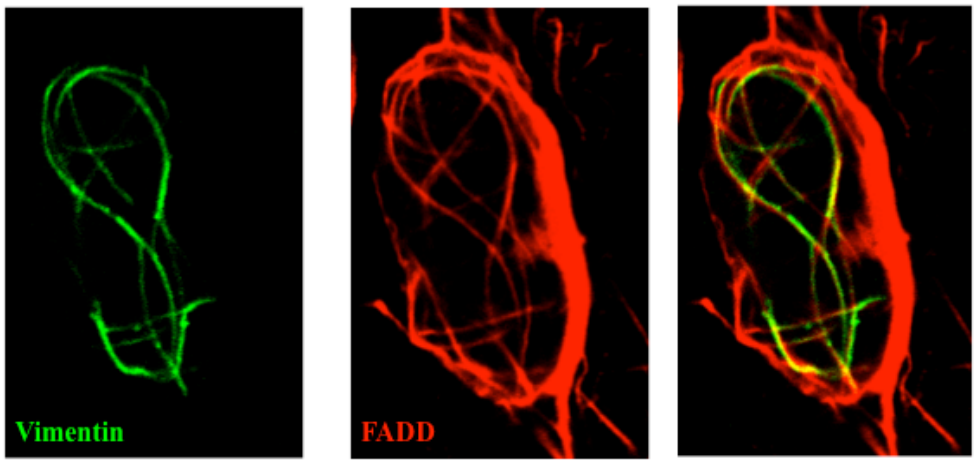

Figure 3.17. NLS-Vimentin and death-effector filaments localise (partially) in the same interchromosomal spaces

HeLa cells transiently transfected with human NLS-/YFP-Vimentin (9:1) and pcDNA3-AU1 FADD. Cells were stained with an anti-FADD mAb (red flourescence).

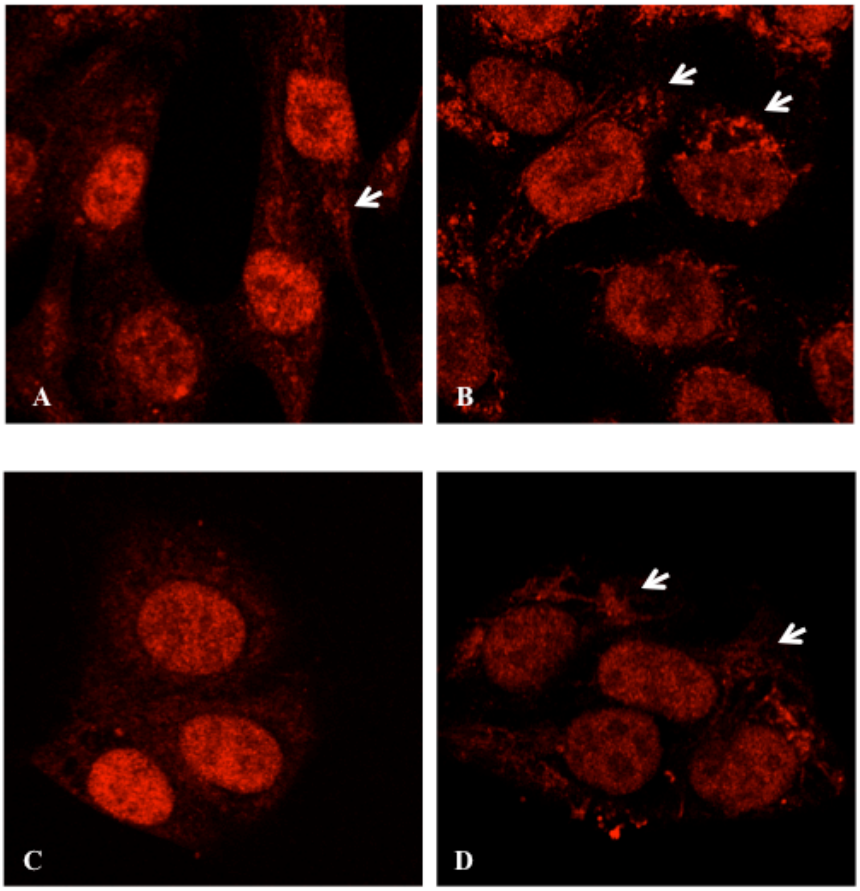

Figure 3.18. HT1080 cells and U2OS cells treated with apoptotic inducers

Endogenous FADD localised to small filaments (indicated by white arrows) in untreated HT1080 cells (A), treated HT1080 (B) and U2OS cells (A) which could be DEFs.
A: HT1080 cells untreated.
B: HT1080 cells treated with CHX (2.5 µg/ml 20 hours).
C: U2OS cells untreated.
D: U2OS cells treated with CHX (2.5 µg/ml 20 hours).
Cells were stained with an anti-FADD mAb (red fluorescence).

3.2.10 Death effector filaments in PML -/- KO mice.

To check whether PML and PML NBs are necessary for the formation of DEFs, PML -/- cells were transfected with pcDNA3-AU1 FADD and pEGFP-FADD. In Figures 3.19 and 3.20 the various distributions of AU-FADD are shown. In Figure 3.21 the pattern of GFP-FADD in PML -/- cells is shown. There was a discontinuous formation of DEFs in PML -/- cells. These results suggested that PML NBs might be needed for the formation of DEFs.

PML nuclear body components such as Sp100, Daxx and SUMO-1 fail to accumulate in the PML bodies in the absence of PML (Zhong et al., 2000). It is also known that SUMO-modification of PML is needed for the formation of mature PML NBs (Lallemand-Breitenbach et al., 2001). It was therefore interesting to see whether SUMO was necessary for a proper formation of DEFs by co-transfection of pEGFP-FADD and pSG5-LINK-EGFP SUMO-1 in PML -/- cells. Co-expression of SUMO did not change the formation of DEFs in PML -/- cells.

PML -/- KO mice and cells are protected from apoptosis induced by Fas and TNF (Wang et al., 1998b) and it is well known that FADD is important for signalling from the Fas and other TNF receptor family members (Chinnaiyan et al., 1996). Phosphorylation of FADD has been speculated to regulate its apoptotic properties by interfering with cell cycle progression (Alappat et al., 2003). To see whether there was a difference in phosphorylation of FADD in PML -/- cells and NIH/3T3 cells, cells were transfected with FADD and CrmA or FADD alone and western blotting was performed. More phosphorylated FADD was found in NIH/3T3 after co-transfection of CrmA (Figure 3.22). This experiment was done using two different mouse cell lines as the corresponding PML wild type cells were not available to us and therefore the results might not be conclusive.

This experiment was repeated in the PML-inducible cell line PML III cl.19 but no difference in the phosphorylation of transfected FADD before and after induction of PML III was observed. This might have been because it was only one PML isoform being expressed in the inducible cell line: a better experiment would have been depletion of PML. PML depletion using siRNA was attempted but at the time it was not possible to produce a stable cell line without PML.

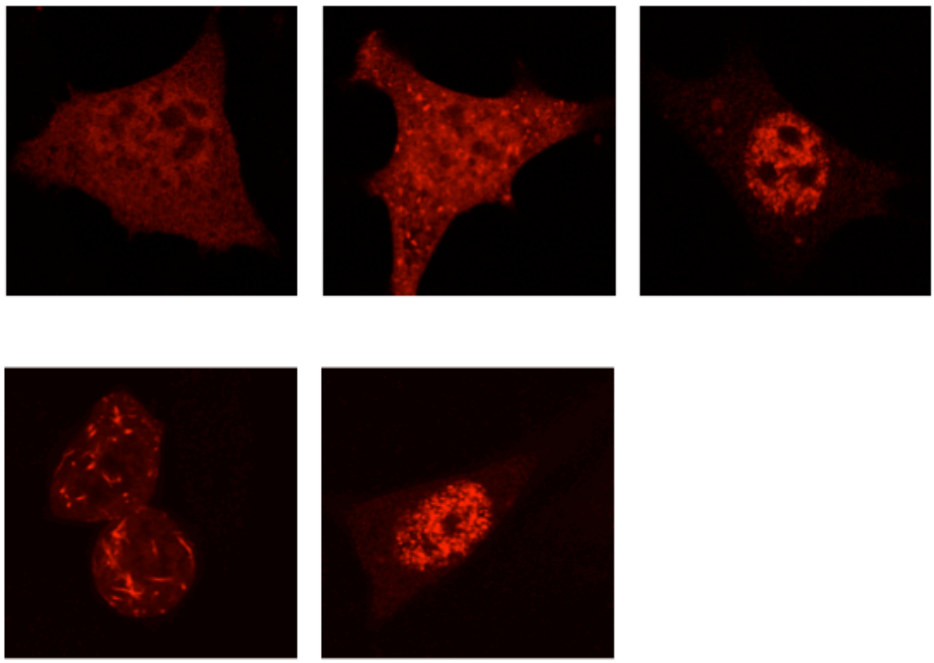

Figure 3.19. Death-effector filaments in PML -/- cells

There was no proper death-effector filament formation in PML -/- cells. PML -/- cells transfected with pcDNA3-AU1 FADD. Cells were stained an anti-FADD mAb.

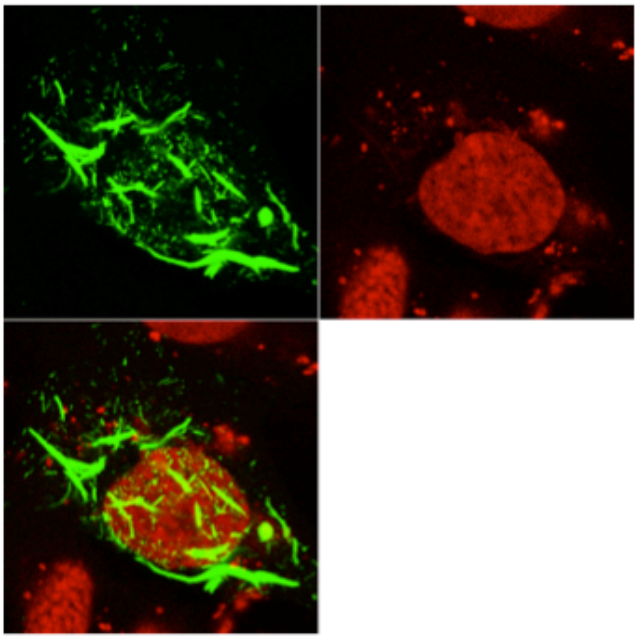

Figure 3.20. Death-effector filaments in PML -/- cells

PML -/- cells transfected with pcDNA3-AU1 FADD and pcDNA3-CrmA. Cells were stained anti-FADD mAb antibodies (green fluorescence) and with propidium iodide.

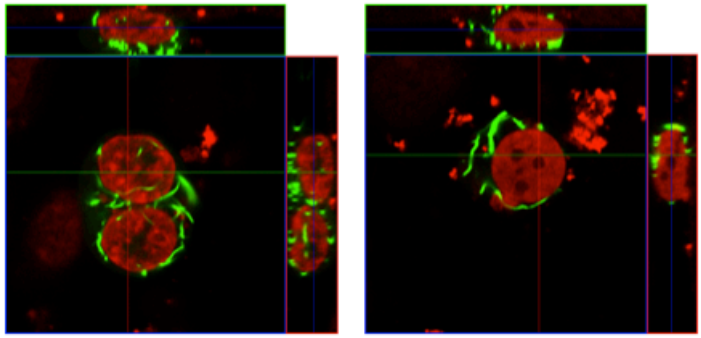

Figure 3.21. Death-effector filaments in PML -/- cells

Death-effector filaments formed by the fusion protein EGFP-FADD were slighter shorter in PML -/- cells. PML -/- cells transfected with pEGFP-FADD and stained with propidium iodide.

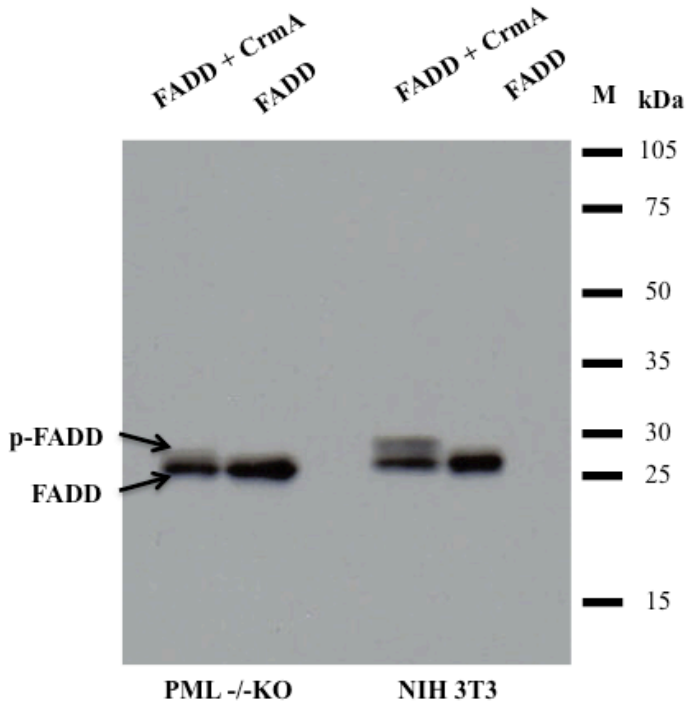

Figure 3.22. FADD phosphorylation in PML -/- cells

FADD seemed less efficiently phosphorylated in PML -/- cells.
PML -/- cells and NIH/3T3 cells transfected with pcDNA3-AU1 FADD and pcDNA3-CrmA and pcDNA3-AU1 FADD alone and analysed by immunoblotting using anti-FADD antibodies.

3.2.11 Summary

- **SUMO and PML formed filaments/tracks which colocalised with DEFs 24 hours after transfection of FADD**
- **Sp100 and Daxx formed filaments/tracks which colocalised with DEFs 48 hours after transfection of FADD**
- **DEFs were not only cytoplasmic filaments but also went through the nucleus where they localised to the ICD**
- **DEFs disrupted PML NBs when FADD was overexpressed**
- **DEFs formed by endogenous FADD formed small filaments in the cytoplasm and these filaments did not disrupt the PML NBs**
- **The disruption of the PML NBs by DEFs was independent of caspase recruitment**
- **DEFs showed a partial colocalisation with filaments/tracks formed by Ad5 E4 Orf3**
- **DEFs formed in PML -/- cells were non-continuous and appeared shard-like**
- **FADD appeared to be less efficiently phosphorylated in PML -/- cells compared to NIH/3T3 cells. This result may be inconclusive as two cell lines from two different mouse strains were used**

3.2.12 Conclusion and hypothesis

DEFs formed by FADD disrupted the PML NBs. The NBs associated with DEFs before forming filament/tracks colocalising with the DEFs. SUMO was the first protein to form filaments colocalising with the DEFs and PML then followed, forming tracks. Later, Sp100 and Daxx left the PML NBs, colocalising with the DEFs. PML might be necessary for the formations of DEFs and phosphorylation of FADD seemed to be altered in PML -/- cells. FADD is involved in death receptor-mediated apoptosis and the hypothesis is that it could be a part of PML NBs and Fas-mediated apoptosis. This led to the next set of experiments where the FADD domains, which are necessary for the disruption of PML NBs, were mapped.

During my studies several different cell lines such as U2OS, SAOS-2 and HT1080 were tested after tranfection of FADD and there was no difference in the track/filament formation of PML NBs observed. The track/filament formation was not

cell-type specific and all images shown here are representative of what was observed in the transfected cells.

3.3 PML nuclear bodies and FADD

3.3.1 Introduction

FADD was originally discovered as an interacting partner with the Fas receptor in a yeast two-hydrid screen (Chinnaiyan et al., 1995). It contains an N-terminal death-effector domain (DED) and a C-terminal death domain (DD). It interacts with the Fas-receptor through the DD and with caspase-8 through the DED, forming the death-inducing signalling complex (DISC). FADD is phosphorylated by casein kinase 1 (CK1) alpha at a single residue serine 194 at the C-terminus. Phosphorylation af FADD and therefore the C-terminus of the FADD protein affects apoptosis not only binding to the death receptors but also by playing an important role in cell cycle progression (Alappat et al., 2003). As mentioned earlier, one of the main interests of this study is to try to find and explain the connection between Fas-mediated apoptosis and PML and PML NBs and thus explain the altered response to death receptor ligands in PML -/- KO mice and cells. This was tested by mapping the domains in the FADD protein, which are necessary for the disruption of PML NBs.

3.3.2 Mapping of the FADD domain that modifies PML nuclear bodies

Truncated FADD constructs and FADD mutants were made to test which domain was necessary for the disruption of the PML NBs (Figure 3.23).

FADD DED, which is necessary for homo- and hetero-oligomerisation of DED-containing proteins, is known to induce apoptosis and form smaller, more numerous filaments (Siegel et al., 1998). As seen in Figure 3.24, this domain is sufficient to change the localisation of PML and Sp100. PML and Sp100 both formed tracks after transfection of FADD DED.

The FADD protein contains two different domains: the death-effector domain (aa 3-81) and the death domain (aa 97-181). The FADD DN protein encodes for the C-terminus of FADD aa 80-208 and binds to the DD of the Fas receptor, but is unable to bind to the DED in caspase-8 because of the missing FADD DED. Furthermore, the FADD DN does not form DEFs (Siegel et al., 1998). FADD DN showed a diffuse

localisation and changed neither PML (Figure 3.25A) nor Sp100 (Figure 3.25B). These results showed that DEFs and therefore the DED was necessary for the relocalisation of PML NBs.

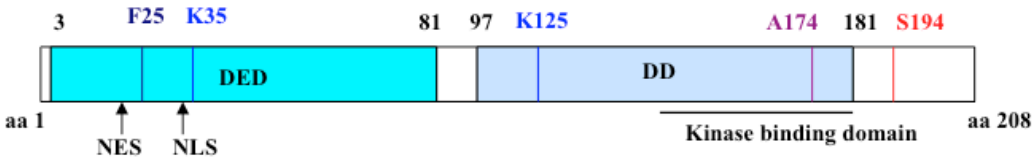

	Filament formation	PML NB disruption
FADD full-length	+	+
FADD DED (aa 1-80)	+(very short filaments)	+
FADD DN (aa 80-208)	-	-
FADD F25G	+/diffuse	+/-
FADD K35R	+	+
FADD K125R	+	+
FADD A174P	+/dots	+/-
FADD S194A	+	-
FADD S194E	+	-
FADD S194D	+	-

Figure 3.23. Structure and function of wildtype FADD and FADD mutants

All the single residues were changed using site-directed mutagenesis. FADD DED was sufficient to disrupt PML NBs and FADD had to be phosphorylated to disrupt PML NBs.

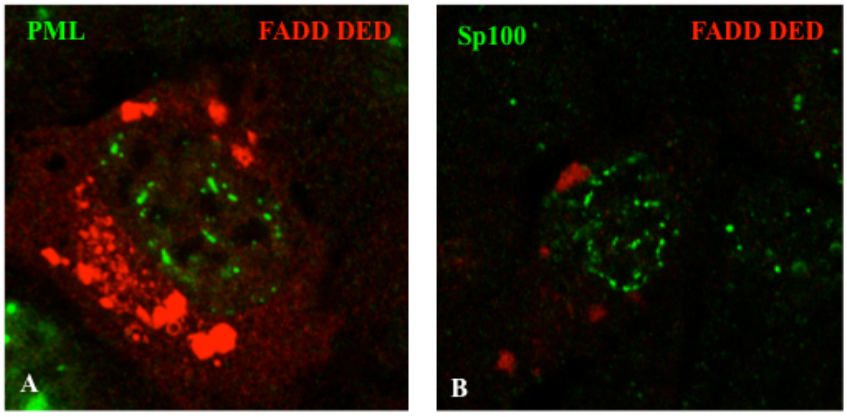

Figure 3.24. The nuclear localisations of PML and Sp100 are modified by the FADD death-effector domain

The FADD DED was able to disrupt PML NBs.
A: U2OS cells transfected with pcDNA3-AU1 FADD DED and stained with an anti-FADD mAb (red fluorescence) and polyclonal rabbit anti-PML antibodies (green fluorescence).
B: U2OS cells transfected with pcDNA3-AU1 FADD DED and stained with an anti-FADD mAb (red fluorescence) and polyclonal rabbit anti-Sp100 antibodies (green fluorescence).

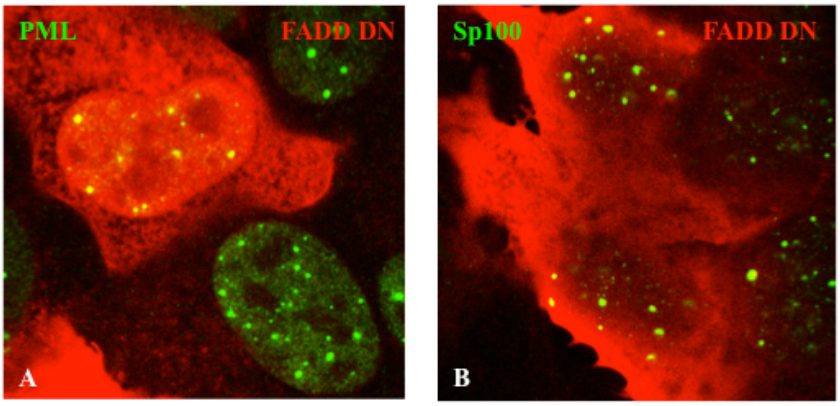

Figure 3.25. The death domain is not sufficient to disrupt the PML bodies

U2OS cells transiently transfected with pcDNA3-AU1 FADD DN.
A: Cells were stained with polyclonal rabbit anti-PML antibodies (green fluorescence) and with an anti-FADD mAb (red fluorescence).
B: Cells were stained with polyclonal rabbit anti-Sp100 antibodies (green fluorescence) and an anti-FADD mAb (red fluorescence).

The FADD F25G mutant when expressed in cells induces low levels of caspase-3 activity and reduced binding to caspase-8 (Kaufmann et al., 2002). F25 is in a hydrophobic region of FADD important for protein-protein interactions (Eberstadt et al., 1998). The FADD F25G mutant was able to form DEFs in some of the transfected cells and here SUMO was associated with the DEFs (Figure 3.26, A-C). In other cells the mutant showed a diffuse pattern and there was no PML NB disruption (Figure 3.26, D-F). These results suggested that caspase activation was probably not necessary for the PML NB disruption.

It could be SUMO-modified FADD that was detected in the immunofluorescence when SUMO colocalised with the DEFs. The FADD sequence contains two potential SUMO-modification sites, K35 and K125, where K35 is a part of a potential nuclear localisation signal. The mutants FADD K35R and FADD K125R still formed DEFs and SUMO was still associated with the filaments. This result suggested that it was probably not SUMO-modified FADD that was detected but another protein recruited to the filaments that was being modified by SUMO, or that FADD was being modified at a different lysine. To test if it was perhaps only nuclear FADD that was SUMO-modified, a western blot was prepared with nuclear and cytoplasmic fractions of cells (Figure 3.27). There was no higher migrating band detected in the nuclear fraction of FADD-transfected cells, which suggested that FADD was not SUMO-modified. This is confirmed by the absence of any literature attesting to the fact.

FADD DN A174P mutant has been shown not to bind to Fas and does not induce apoptosis (Morgan et al., 2001) although it can still bind to TRADD (Morgan et al., 2001). The A174 is located in the kinase-binding domain of FADD and this mutant has been shown to be less phosphorylated than wild type (Alappat et al., 2005). The interesting thing about this mutant was that it showed a partial colocalisation with PML NBs (Figure 3.28, A-C). It was also able to form DEFs in a minority of the cells (Figure 3.28, D-F).

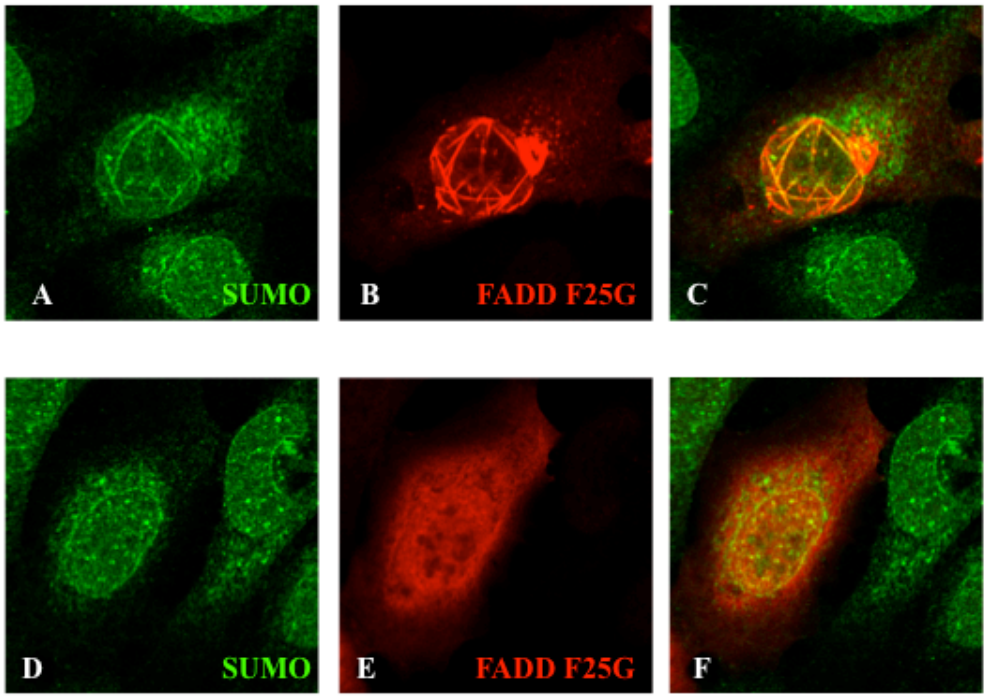

Figure 3.26. **SUMO forms filaments in some of the cells tranfected with FADD F25G**

A-F: U2OS cells transiently transfected with pcDNA3-AU1 FADD F25G and CrmA. Cells were stained with polyclonal rabbit anti-SUMO antibodies (green fluorescence) and an anti-FADD mAb (red fluorescence).

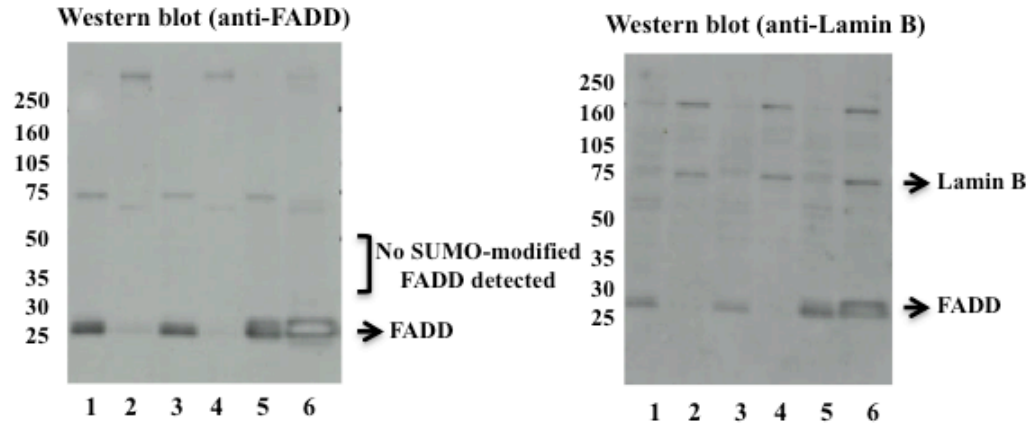

Figure 3.27. Cytoplasmic and nuclear FADD

There were no higher migrating bands detected after transfection of FADD.
Lanes 1 and 2: Untransfected HT1080 cells. Lanes 3 and 4: HT1080 cells transfected with pSG5-FLAG- CK1 alpha LS. Lanes 5 and 6: HT1080 cells transfected pcDNA3-AU1 FADD.
Cytoplasmic and nuclear extracts were loaded onto a 4-20% polyacrylaminde gradient gel, transferred onto nitrocellulose stained with anti-FADD mAb antibodies to check for SUMO modification of FADD and with polyclonal anti-Lamin B antibodies as a control for the nuclear fraction.

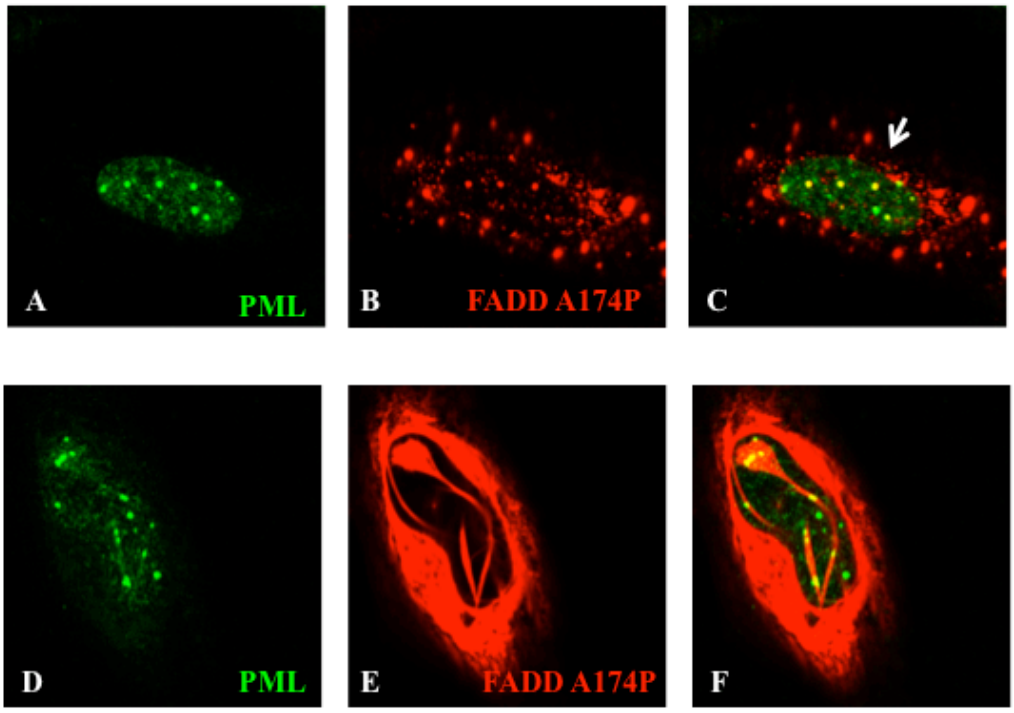

Figure 3.28. The FADD A174P mutant shows a partial colocalisation with PML NBs

A-F: SAOS-2 cells transfected with pcDNA3-AU1 FADD A174P and stained with polyclonal rabbit anti-PML antibodies (green fluorescence) and with an anti-FADD mAb (red fluorescence).

It has previously been shown that FADD is phosphorylated in the G2/M phase of the cell cycle and only non-phosphorylated FADD is found in G1/S phase (Scaffidi et al., 2000; Alappat et al., 2005). The phosphorylation site has been mapped to S194 (Scaffidi et al., 2000), and shown to be necessary for cell cycle arrest in G_2/M in a non-tumour cell line (Alappat et al., 2005). For further experiments, the serine was mutated to alanine to have a phospho-dead mutant and to glutamic acid and aspartic acid to mimic phosphorylation as these mutations are chemically similar to a phosphorylated serine.

U2OS cells transfected with pcDNA3-AU1 FADD S194A and pcDNA3-AU1 FADD S194E (Figure 3.29), showed no disruption of the PML bodies 24 hours after transfection. The DEFs formed by the phosphorylation mutants were not phosphorylated (Figure 3.30). Endogenous phosphorylated FADD was not recruited to the filaments 24 hours after transfection but it was possible to detect phosphorylated FADD in some of the transfected cells after 48 hours. Different results were obtained in HT1080 cells, where it was already possible to detect endogenous phosphorylated FADD in the DEFs 24 hours after transfection, which resulted in a disruption of the PML NBs.

These results showed that FADD had to be phosphorylated to disrupt the bodies and this raised the following question: were non-phosphorylated DEFs nuclear or only cytoplasmic filaments? In a 3D reconstruction (Figure 3.31: 3D reconstruction with kind help from Dr Suhail Islam) of FADD S194A it was possible to see that the non-phosphorylated filaments went through the nucleus. This result was confirmed using another FADD mutant, FADD S194D as well as FADD S194A, in confocal microscopy (Figure 3.32). When comparing the DEFs, non-phosphorylated and phosphorylated, from transfected cells there was no obvious difference in the appearance of the filaments (Figure 3.33). The phosphorylation of the FADD protein appeared to be necessary for the observed disruption of PML NBs.

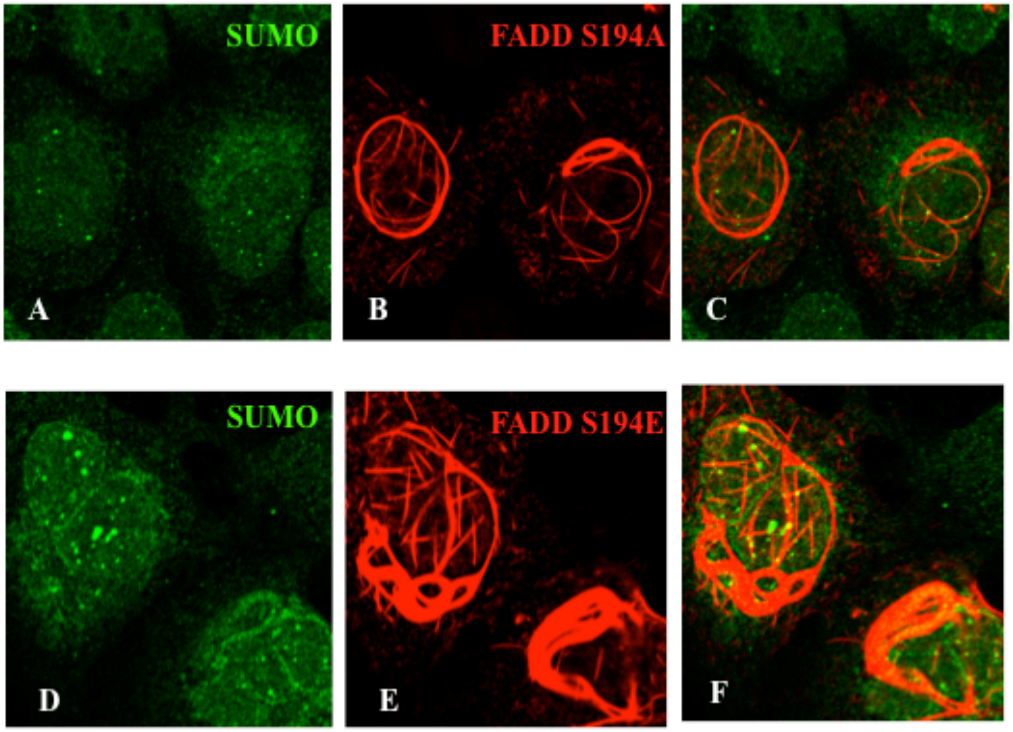

Figure 3.29. **SUMO is not disrupted in cells transfected with FADD phosphorylation mutants**

A-C: U2OS cells transiently transfected with the FADD mutant pcDNA3-AU1 FADD S194A.
D-F: U2OS cells transiently transfected with the FADD mutant pcDNA3-AU1 FADD S194E. Cells were stained with polyclonal rabbit anti-SUMO antibodies (green fliorescence) and with an anti-FADD mAb (red fluorescence).

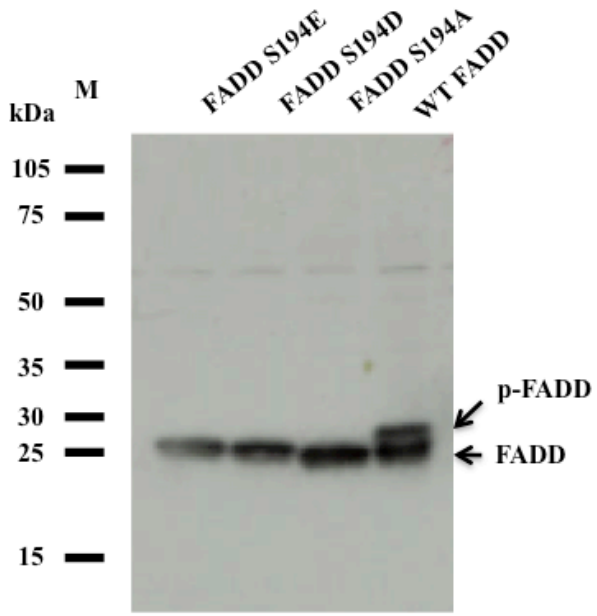

Figure 3.30. FADD phosphorylation mutants are unable to be phosphorylated

NIH/3T3 cells transfected with pcDNA3-AU1 FADD and FADD phosphorylation mutants pcDNA3-AU1 FADD S194A/D/E. Whole cell extracts were loaded onto a 4-20% polyacrylamide gradient gel, transferred onto nitrocellulose and analysed by immunoblotting using anti-FADD antibodies.

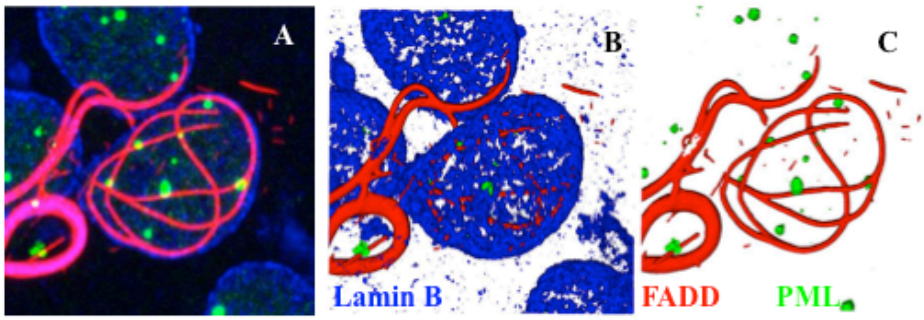

Figure 3.31. DEFs formed by FADD S194A are nuclear as well as cytoplasmic

Saos-2 cells transiently transfected with pcDNA3-AU1 FADD S194A.
A: The non-phosphorylated death-effector filaments did not disrupt PML 24 hours after transfection.
A-C: PML colocalised with the death-effector filaments.
Cells were stained with polyclonal rabbit anti-PML antibodies (green fluorescence) and with an anti-FADD mAb (red fluorescence). Lamin B was used to outline the nucleus and stained with goat anti-Lamin B antibodies (blue fluorescence).

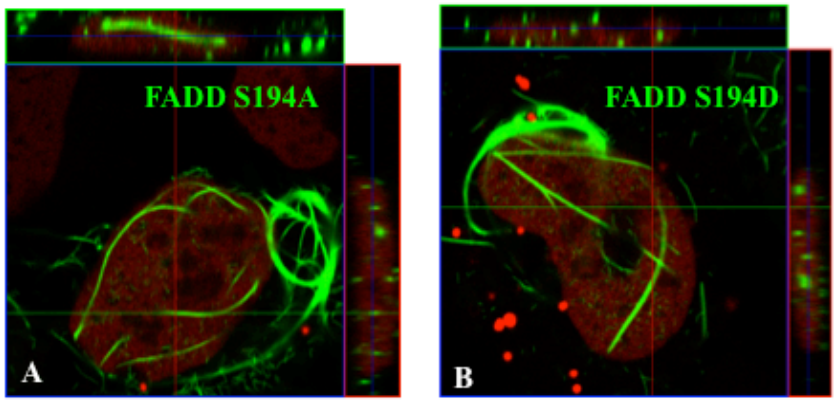

Figure 3.32. Non-phosphosphorylated filaments do penetrate the nucleus

A: U2OS cells transiently transfected with pcDNA3-AU1-FADD S194A. Cells were stained with an anti-FADD mAb (green fluorescence) and with propidium iodide.
B: U2OS cells transiently transfected with pcDNA3-AU1-FADD S194D.
Cells were stained with an anti-FADD mAb (green fluorescence) and with propidium iodide.

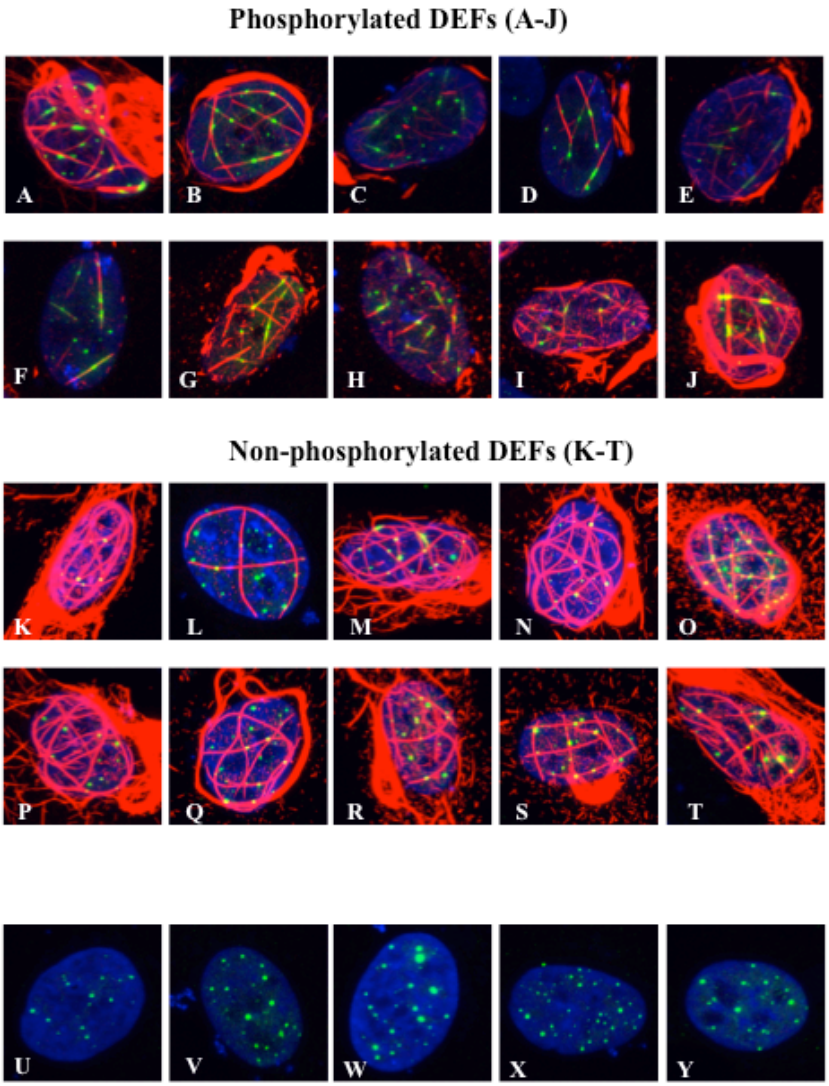

Figure 3.33. No obvious difference in phosphorylated and non-phosphorylated DEFs

A-J: U2OS cells transiently transfected with pcDNA3-AU1 FADD.
K-T: U2OS cells transiently transfected with pcDNA3-AU1 FADD S194A.
U-Y: PML NBs were not disrupted in untransfected cells.
Cells were stained with polyclonal rabbit anti-PML antibodies (green fluorescence), and with an anti-FADD mAb (red fluorescence).

3.3.3 Summary

- **The DED in FADD was sufficient for the disruption of PML NBs**
- **Again, caspase activity did not seem to be necessary for the PML NB alteration**
- **FADD was not modified by SUMO**
- **FADD needed to be phosphorylated to disrupt PML NBs**
- **DEFs formed by FADD phosphorylation mutants were cytoplasmic as well as nuclear**
- **There was no obvious difference between DEFs formed by FADD and the FADD phosphorylation mutants**

3.3.4 Conclusion and hypothesis

The DED domain and therefore filament formation appeared to be necessary for PML NB disruption and so did phosphorylation of FADD. The DEFs needed to be phosphorylated to disrupt the PML NBs. This suggested that the kinase phosphorylating FADD could be involved in the disruption of the PML NBs and this was investigated further.

Again, different cell lines were tested after transfection of truncated FADD contructs. The track/filament formation of PML NBs was only observed when the constructs contained the DED domain and was able to be phosphorylated. This suggested the PML NB disruption was caused by the FADD domains and not by the transfection of the vector used in these experiments. Again all images shown here are representative of what was observed in the transfected cells.

3.4 The role of PML in FADD phosphorylation

3.4.1 Introduction

Many research groups have failed to identity the kinase that phosphorylates FADD. First it was reported to be 70 kDa cell cycle-regulated kinase phosphorylating FADD at S194 (Scaffidi et al., 2000). Then almost in parallel a very interesting publication appeared which fitted well with the connection to PML NBs (Rochat-Steiner et al.,

2000). In the paper, FADD was described as phosphorylated by HIPK3, which shows a partial colocalisation to PML NBs (Rochat-Steiner et al., 2000). Later, it was reported be to casein kinase 1 alpha phosphorylating FADD and thereby regulating non-apoptotic activities of FADD (Alappat et al., 2005).

3.4.2 Phosphorylation of the FADD protein by HIPK3

It has previously been shown that homeodomain-interacting protein kinase 3 (HIPK3) colocalises partially with PML NBs and is able to induce phosphorylation of FADD (Rochat-Steiner et al., 2000). Colocalisation studies with PML, HIPK3 and phosphorylated FADD are shown in Figure 3.34. Endogenous FADD showed a diffuse nuclear and cytoplasmic staining (Figure 3.34A). In contrast, endogenous phosphorylated FADD (phospho-FADD) showed a striking nuclear speckled pattern (Figure 3.33B) very similar to the pattern of HIPK3 (Figure 3.34C).

Both endogenous HIPK3 and endogenous phosphorylated FADD showed a partial colocalisation with PML NBs (Figures 3.34D and E).

These results suggested that FADD is phosphorylated in HIPK domains that colocalise with PML NBs.

To try to confirm that FADD was phosphorylated by HIPK3 (Rochat-Steiner et al., 2000) experiments were repeated by transfecting U2OS or HT1080 cells with HIPK3 alone or FADD and HIPK3. No difference in phosphorylation of FADD was seen after co-transfection of HIPK3. Other groups like (Alappat et al., 2005) also tried and failed to reproduce the results from Rochat-Steiner et al., 2000.

3.4.3 Phosphorylation of FADD by casein kinase 1 alpha

Later casein kinase 1 (CK1) alpha was shown to phosphorylate FADD at S194 *in vivo* and *in vitro* (Alappat et al., 2005). It was shown that phosphorylated FADD colocalises with CK1 alpha at the spindle poles in metaphase (Alappat et al., 2005). CK1 alpha is expressed as four different splice variants, CK1 alpha, CK1 alpha L, CK1 alpha S and CK1 alpha LS (Fu et al., 2001; Burzio et al., 2002). All four splice variants are able to phosphorylate FADD (Alappat et al., 2005). CK1 alpha LS contains an L insert in the catalytic domain and an S insert at the C-terminus (Figure 3.35). The alternative splicing results in different kinase activity and localisation of the four splice variants (Burzio et al., 2002).

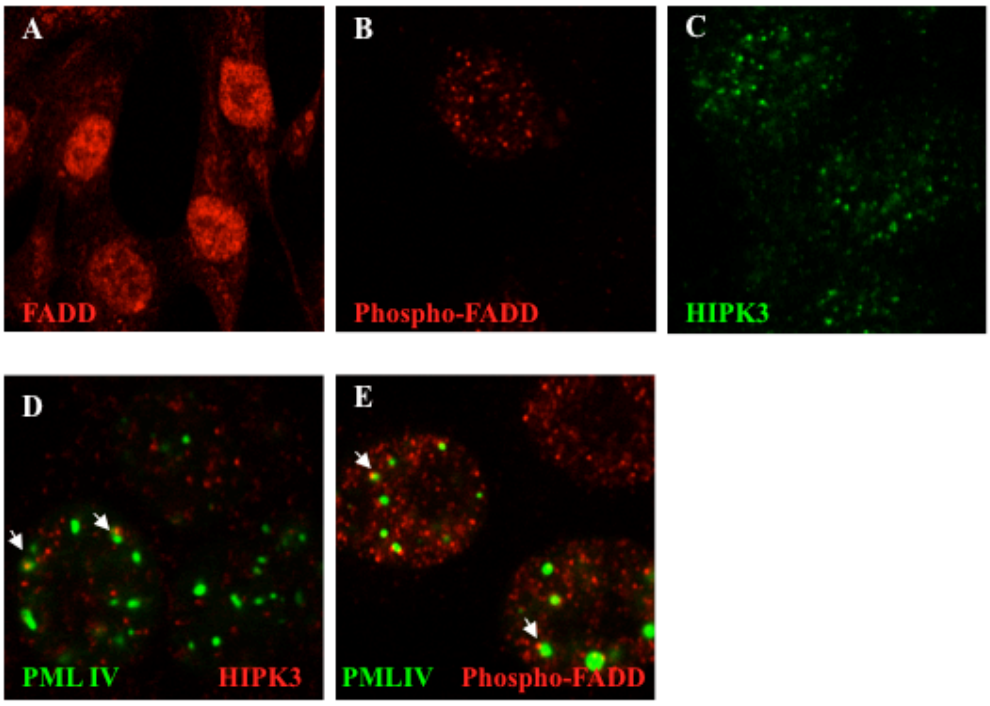

Figure 3.34. PML, phospho-FADD and HIPK3 show a partial colocalisation

A: Endogenous FADD in HT1080 cells. Cells were stained with an anti-FADD mAb (red fluorescence).
B: Endogenous phosphorylated FADD in HT1080 cells. Cells were stained with polyclonal rabbit anti-phospho-FADD antibodies (red fluorescence).
C: Endogenous HIPK3 in HT1080 cells. Cells were stained with polyclonal rabbit anti-HIPK3 antibodies (green fluorescence).
D: HT1080 cells transfected with pSG5-LINK-EGFP PML IV and stained with polyclonal rabbit anti-HIPK3 antibodies (red fluorescence).
E: HT1080 cells transfected with pSG5-LINK-EGFP PML IV and stained with polyclonal rabbit anti-phospho-FADD antibodies (red fluorescence).

MASSSGSKAEFIVGGKYKLVRKIGSGSFGDIYLAINITNGEEVAVKLESQKAR
HPQLLYESKLYKILQGGVGIPHIRWYGQEKDYNVLVMDLLGPSLEDLFNFCS
RRFTMKTVLMLADQMISRIEYVHTKNFIHRDIKPDNFLMGIGRHCNKCLESP
VGKRKRSMTVSTSQDPSFSGLNQLFLIDFGLAKKYRDNRTRQHIPYREDKN
LTGTARYASINAHLGIEQSRRDDMESLGYVLMYFNRTSLPWQGLKAATKKQ
KYEKISEKKMSTPVEVLCKGFPAEFAMYLNYCRGLRFEEAPDYMYLRQLFR
ILFRTLNHQYDYTFDWTMLKQKAAQQAASSSGQGQQAQTPTGKQTDKTKS
NMKGF

Figure 3.35. Casein kinase 1 alpha (isoform 1)/ CK1 alpha LS

L insert (shown in light blue): contains an contains a potential NLS
S insert (in green)
The splice variants containing the L and the LS inserts are targeted to the nucleus.

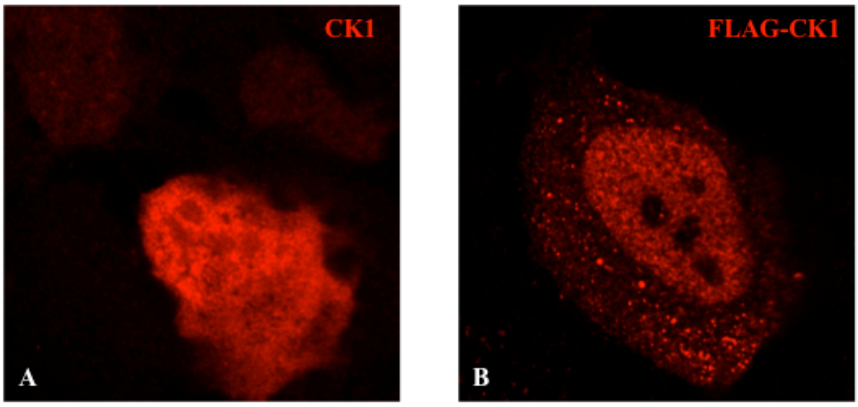

Figure 3.36. Localisation of CK1 alpha LS in U2OS cells

U2OS cells transiently transfected with pSG5-FLAG CK1 alpha LS.
A: Endogenous and transfected CK1 alpha. Cells were stained with goat polyclonal anti-CK1 alpha antibodies.
B: Transfected CK1 alpha cells were stained with an anti-FLAG mAb.

Full-length CK1 alpha LS was made from two I.M.A.G.E. (Integrated Molecular Analysis of Genomes and their Expression) clones using PCR and cloning methods. U2OS cells were transfected with FLAG-tagged full-length CK1 alpha and stained using immunofluorescence (Figure 3.36). When cells were stained with goat polyclonal anti-CK1 alpha antibodies, which stained endogenous and transfected CK1, CK1 alpha showed a diffuse localisation throughout the cell, whereas FLAG-CK1 alpha LS showed a more speckled pattern. This has also been described earlier in the literature and the speckles are thought to be splicing speckles (Gross et al., 1999).

To determine whether CK1 alpha was recruited to the DEFs, colocalisation studies were performed by co-transfecting pcDNA3-AU1 FADD and pSG5-FLAG CK1 alpha LS into U2OS cells. Figure 3.37 shows a colocalisation of FADD and CK1 alpha in the nucleus. A very interesting result is shown in Figure 3.38 where CK1 alpha does not colocalise with FADD S194A. This experiment was repeated with pcDNA3-AU1 FADD S194D/E and pSG5-FLAG CK1 alpha LS and also here there was no colocalisation. This suggested that CK1 was only recruited to DEFs when FADD was able to be phosphorylated. It was also tested to determine if not only transfected but also endogenous CK1 alpha was recruited to the DEFs (Figure 3.39) and whether CK1 alpha colocalised with SUMO in the DEFs (Figure 3.39). SAOS-2 cells were transfected with pcDNA3-AU1 FADD and stained for CK1 alpha and SUMO. Figure 3.39, A-C shows a colocalisation in the nucleus of CK1 alpha and SUMO. It was not always the case, as can be seen in Figure 3.39, D-F, where one of the transfected cells did not have SUMO localising to the DEFs. This suggested that it could be a cell cycle-dependent phenomenon or that CK1 alpha was SUMO-modified after phosphorylating the FADD protein.

Earlier results showed that phosphorylation of FADD was necessary for the disruption of the PML NBs and SUMO filament formation. The next question was whether CK1 alpha was the SUMO-modified protein detected on the DEFs. Using SUMO prediction servers, several potential SUMO-modification sites were identified in the CK1 sequence (Figure 3.40).

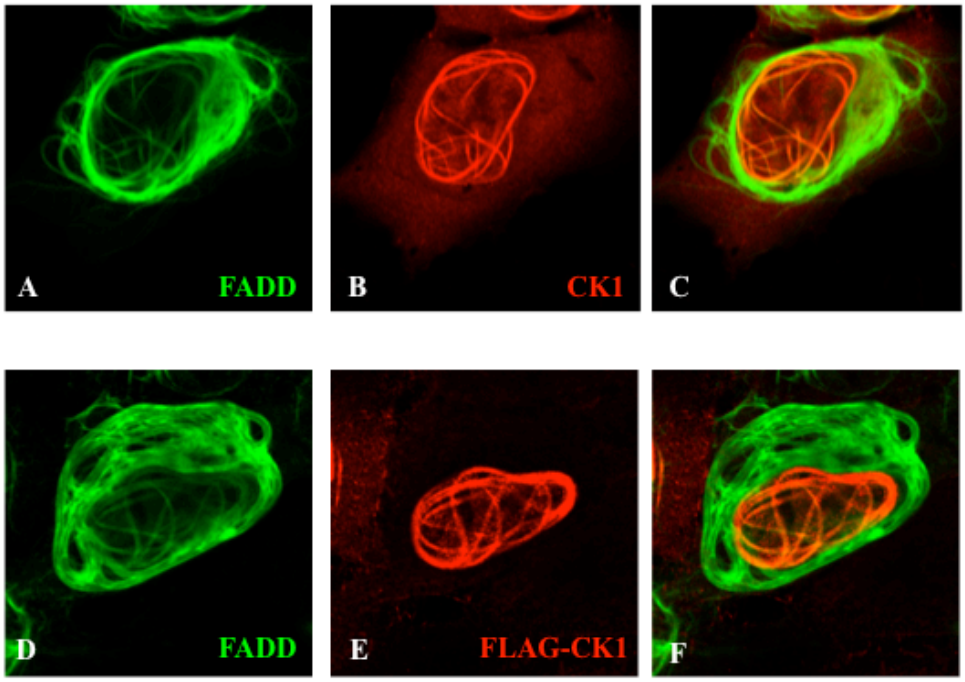

Figure 3.37. CK1 alpha LS colocalises with FADD in the nucleus

U2OS cells transfected with pcDNA3-AU1 FADD and pSG5-FLAG CK1 alpha LS.
A-C: Cells were stained with an anti-FADD mAb (green fluorescence) and with a polyclonal goat anti-CK1 alpha (red fluorescence).
D-F: Cells were stained a polyclonal rabbit anti-FADD antibody (green fluorescence) and with an anti-Flag mAb (red fluorescence).

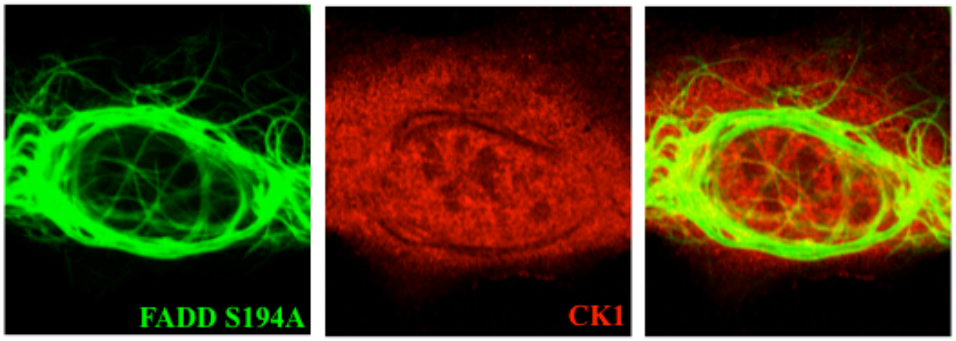

Figure 3.38. CK1 alpha LS does not colocalise with FADD S194A in the nucleus

U2OS cells transfected with pcDNA3-AU FADD S194A and pSG5-FLAG CK1 alpha LS. Cells were stained with an anti-FADD mAb (green fluorescence) and with a polyclonal goat anti-CK1 alpha antibody (red fluorescence).

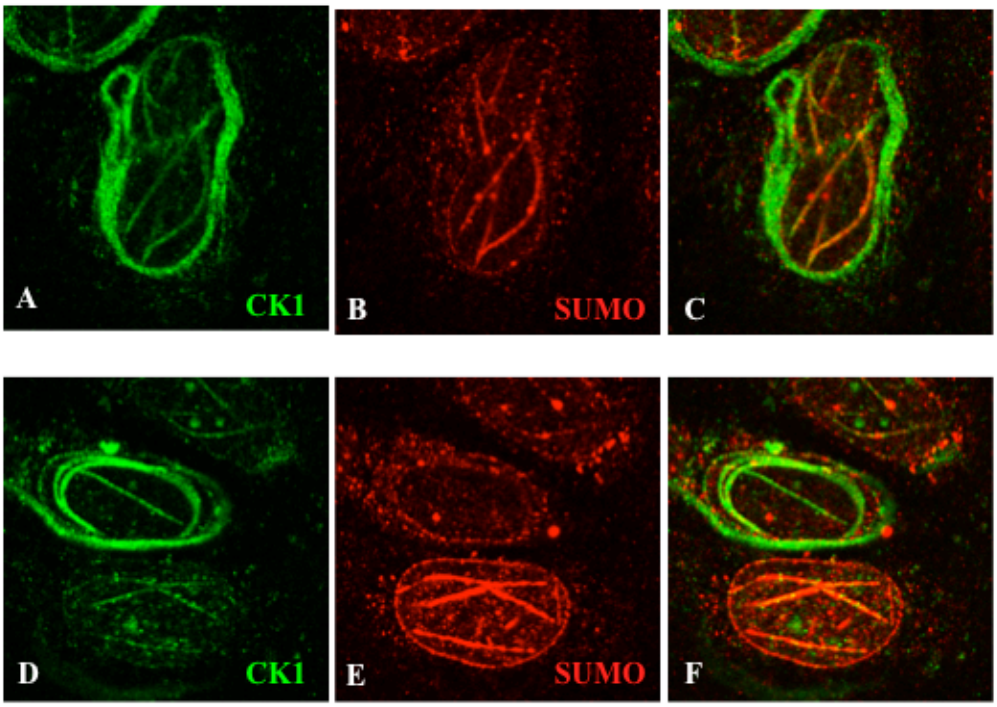

Figure 3.39. Endogenous CK1 alpha colocalises with endogenous SUMO in the nucleus in the presence of DEFs formed by FADD

SAOS-2 cells transiently transfected with pcDNA3-AU1 FADD and stained with polyclonal goat anti-CK1 alpha antibodies (green fluorescence) and polyclonal rabbit anti-SUMO antibodies (red fluorescence).

SUMO site prediction of CK1 alpha LS

MASSSGSKAEFIVGGKYKLVRKIGSGSFGDIYLAINITNGEEVAVKLESQK
ARHPQLLYESKLYKILQGGVGIPHIRWYGQEKDYNVLVMDLLGPSLEDLF
NFCSRRFTMKTVLMLADQMISRIEYVHTKNFIHRDIKPDNFLMGIGRHCN
KCLESPVGKRKRSMTVSTSQDPSFSGLNQLFLIDFGLAKKYRDNRTRQHI
PYREDKNLTGTARYASINAHLGIEQSRRDDMESLGYVLMYFNRTSLPWQ
GLKAATKKQKYEKISEKKMSTPVEVLCKGFPAEFAMYLNYCRGLRFEEA
PDYMYLRQLFRILFRTLNHQYDYTFDWTMLKQKAAQQAASSSGQGQQA
QTPTGKQTDKTKSNMKGF

Near-consensus SV40 T antigen putative nuclear localisation sequence underlined
VLVM and VEVL: potential SUMO-interacting motif (SIM)

Potential SUMO site	Sequence	
K22	RKIG	
K46	VKLE	SUMO consensus sequence
K138	IKPD	
K257	TKKQ	
K260	QKYE	
K363	MKGF	

Figure 3.40. SUMO site prediction of CK1 alpha LS

Several SUMO prediction servers were used to predict potential SUMO modification sites in CK1 alpha LS.
SUMOplot: http://www.abgent.com/tools/sumoplot
SUMOsp 2.0: http://sumosp.biocuckoo.org/
seeSUMO: http://bioinfo.ggc.org/seesumo/
GPS-SBM 1.0: http://sbm.biocuckoo.org/

3.4.4 Summary

- **PML and endogenous phosphorylated FADD showed a partial colacalisation**
- **Both endogenous and overexpressed CK1 alpha was recruited to the phosphoryalted DEFs**
- **CK1 alpha was not recruited to the DEFs formed by the FADD phosphorylation mutants**
- **SUMO colocalised with CK1 alpha in DEFs in many of the transfected cells 24 hours after transfection. This colocalisation increased over time and could be a cell cycle-dependent phenomenon**

3.4.5 Conclusion and hypothesis

The results involving HIPK3 phosphorylation of FADD could not be reproduced. Instead the interaction with CK1 alpha was investigated further. FADD had to be phosphorylated to recruit CK1 alpha. CK1 alpha colocalised with SUMO in DEFs and this led to the next question: could CK1 alpha be the SUMO-modified protein observed in DEFs?

3.5 The role of PML nuclear bodies in regulating FADD phosphorylation

3.5.1 Introduction

It has been speculated that SUMO-modification of proteins occurs at PML NBs. Could it be that CK1 alpha is SUMO-modified in order to regulate the activity of the kinase and its localisation? SUMO-modification can change protein-protein interactions. There have only been a few publications which show a regulation of SUMO-modification and kinase activity. One of them demonstrates that Glycogen Synthase Kinase 3ß is SUMO-modifed: SUMO-modification promotes nuclear localisation of GSK 3ß and is required for kinase activation (Eun Jeoung et al., 2008). In addition, SUMO-modified GSK 3ß regulates protein stability and apoptosis (Eun Jeoung et al., 2008). Another publication shows that Aurora B contains a SUMO-

modification motif in the kinase domain and that mutating the lysine to an arginine increases the activity of the kinase slightly (Fernandez-Miranda et al., 2010). The authors speculate that SUMO-modification changes the activity and the localisation of the Aurora B. Recently it was shown that the yeast kinase SNF1 is not only SUMO-modified but also contains a SUMO-interacting motif (SIM) near the active site (Simpson-Lavy and Johnston, 2013). The kinase activity of SNF1 is decreased upon SUMO-modification, perhaps by interacting with the SIM in the kinase domain and thereby stabilising the inactive form of the kinase. An SNF1 SUMO-interacting mutant is less stable and targeted for degradation by the SUMO-targeted ubiquitin ligase Slx8.

The hypothesis here was that CK1 alpha is SUMO-modified and the modification takes place at the PML NBs, and that it regulates the activity and localisation of the kinase, thereby regulating the phosphorylation and the apoptotic activity of FADD.

3.5.2 SUMO modification of CK1 alpha LS

To see if a SUMO-specific protease could be recruited to the SUMO filaments and hydrolyse SUMO from them, cells were co-transfected with FADD and a SUMO-specific protease called SuPr-1 (Best et al., 2002). This was done to find out if SUMO was necessary for the track/filament formation of PML NB components after transfection of FADD. EGFP-SuPr-1 seemed to associate with DEFs, as both wild type SuPr-1 and the inactive mutant SuPr-1 C466S colocalised to the death effector filaments (Figure 3.41). Interestingly but as expected, neither the wild-type SUMO protease nor the mutant SUMO protease colocalised with phosphorylation mutant FADD S194A (Figure 3.42). When EGFP-SuPr-1 colocalised with DEFs there was no track/filament formation of PML NBs. This means that SuPr-1 hydrolyses SUMO from the filaments and that SUMO is necessary for the track/filament formation. A summary for the many colocalisations studies is seen in Table 3.1.

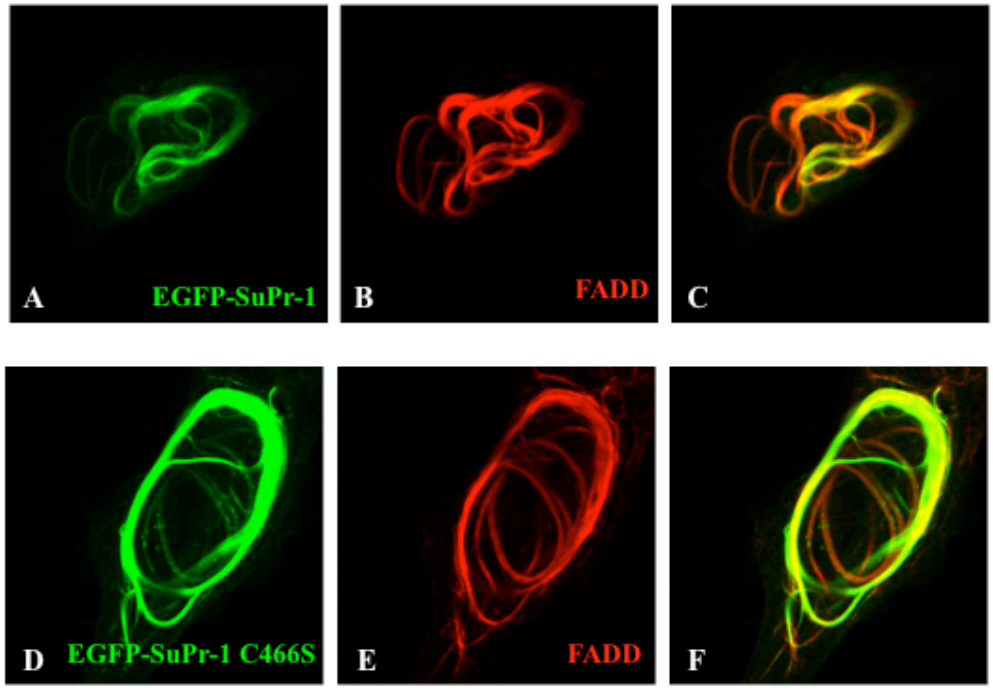

Figure 3.41. Colocalisation studies of FADD and SuPr-1

The SUMO specific protease SuPr-1 was recruited to the DEFS and hydrolysed SUMO from them. The mutant SuPr-1 C466S was also recruited to the DEFs.
A-C: U2OS cells transiently transfected with pcDNA3-AU1 FADD and EGFP-SuPr-1. Cells were stained with an anti-FADD mAb (red fluorescence).
D-F: U2OS cells transiently transfected with pcDNA3-AU1 FADD and EGFP-SuPr-1 C466S. Cells were stained with an anti-FADD mAb (red fluorescence).

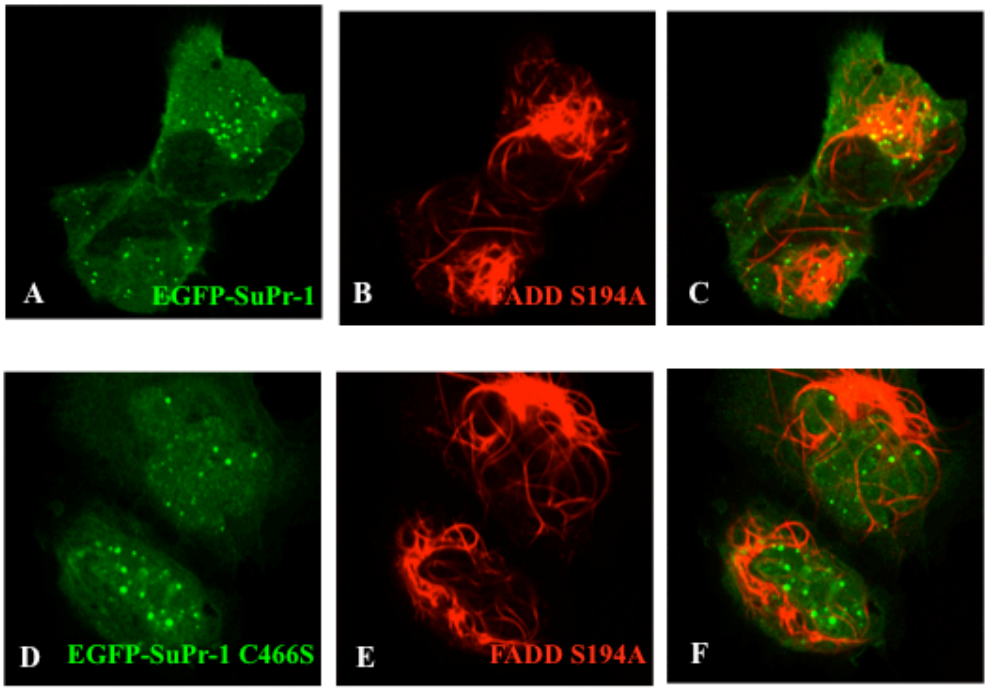

Figure 3.42. No cocalisation of FADD S194A and SuPr-1/SuPr-1 C466S

The SUMO specific protease SuPr-1 and the SuPr-1 mutant are not recruited to the non-phosphorylated DEFs.
A-C: U2OS cells transiently transfected with pcDNA3-AU1 FADD S194A and pEGFP-SuPr-1. Cells were stained with an anti-FADD mAb (red fluorescence).
D-F: U2OS cells transiently transfected with pcDNA3-AU1 FADD S194A and pEGFP-SuPr-1 C466S. Cells were stained with an anti-FADD mAb (red fluorescence).

Table 3.1. Colocalisation studies after transfection of FADD

	PML	CK1 alpha	SUMO-1	SUMO-2/3	Sp100	Daxx	SuPr-1	SuPr-1 C466S
FADD	Partial[92, 93, 119]	Partial[125]	partial	partial	Partial[96]	Partial[96]	Full[130]	Full[130]
FADD S194A	None[118, 119]	None[125]	none	none	none	none	None[131]	None[131]
PML	------	partial (1)	partial	occasionally	partial	partial	none	partial (2)
CK1	------	-------	Almost full (3)	almost none	n/a	n/a	partial	partial
SUMO-1	-------	-------	-------	partial	n/a	n/a	none	partial
SUMO-2/3	-------	-------	--------	-------	n/a	n/a	none	partial
Sp100	-------	-------	--------	---------	-------	n/a	none	few (4)
Daxx	-------	-------	-------	---------	-------	-------	none	few (4)

Table 3.1. Colocalisation studies of endogenous PML, CK1 alpha, SUMO-1, SUMO-2/3, Sp100 and Daxx after transfection of FADD and cotransfection of FADD and SuPr-1/SuPr-1 C466S

1. PML was not yet disrupted but colocalised with CK1 filaments.
2. Some PML formed tracks, which indicated that SUMO is needed for the disruption of the PML NBs.
3. Almost 100 % colocalisation observed, but difficult to judge because many PML NB components are SUMO-modified, such as PML, Sp100 and Daxx. Colocalisation increased over time.
4. Sp100 and Daxx disrupt later after transfection of FADD.

Partial colocalisation implies that in some of the transfected cells PML colocalised with DEFs and was not yet disrupted. In other cells, PML was disrupted and had formed tracks. This disruption increased over time. Or CK1 colocalised with SUMO in some of the cells but not in all. This colocalisation also increased over time.

The SUMO antibody used in the colocalisation experiments shown in my thesis detected SUMO-1/2/3. Only later during my studies were antibodies against SUMO-1 and SUMO-2/3 obtained and those results are shown in the above table.

Numbers shown in superscript refer to page numbers.

Mammalian cells were transiently transfected with CK1 alpha LS and CK1 alpha LS with SUMO-1 to try to detect SUMO-modified CK1 alpha. Cells were lysed 24 hours after transfection and cell extracts were loaded onto a polyacrylamide gradient gel. In Figures 3.43 and 3.44 it is possible to see some higher migrating bands, which could potentially be SUMO-1-modified CK1 alpha.

Another experiment was performed where U2OS cells were transiently transfected with CK1 alpha and CK1 alpha with pEGFP-SUMO-1,2,3 to see which SUMO-modification it was. Often a SUMO-modified protein can be modified by any of the three SUMOs but often there is a preference (Figure 3.45). It was very difficult to detect a difference in SUMO-modification in western blot, and in parallel, several CK1 alpha LS mutants were made using site-directed mutagenesis (Figure 3.46) and transfected into U2OS and HT1080 cells. There was no major difference in the pattern detected by immunofluorescence. The only mutant that seemed to change was CK1 alpha LS K138R, where more SUMO filaments were detected when co-transfected with FADD. It was very difficult to detect any changes in SUMO-modification of CK1 alpha LS and CK1 alpha LS mutants in western blot. The reason for this could be that the CK1 alpha isoform used here contained the L insert, which has been shown to degrade more rapidly than the shorter isoform CK1 alpha (Burzio et al., 2002). CK1 alpha LS has a half life of 100 minutes compared to 400 minutes for the shorter isoform CK1 alpha.

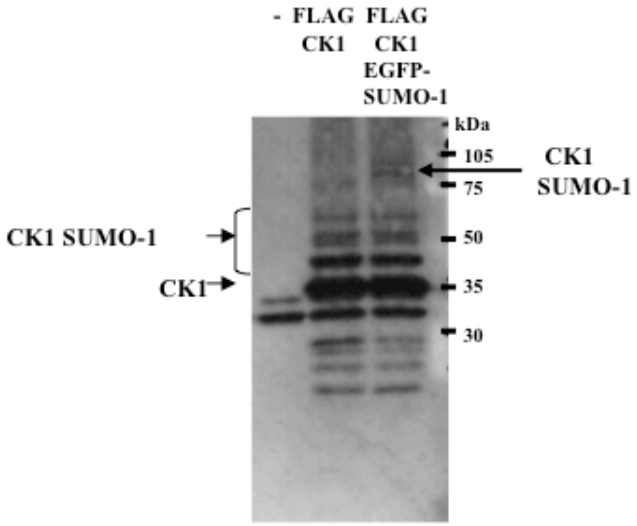

Figure 3.43. CK1 alpha LS might be modified by SUMO-1

Immunoblot analysis of U2OS cells transfected with pSG5-FLAG CK1 alpha LS +/- pEGFP-SUMO-1. Cell extracts were loaded onto a 4-20% polyacrylamide gradient gel. Proteins were transferred onto nitrocellulose membrane and the CK1 alpha protein was detected with polyclonal goat anti-CK1 alpha antibodies.

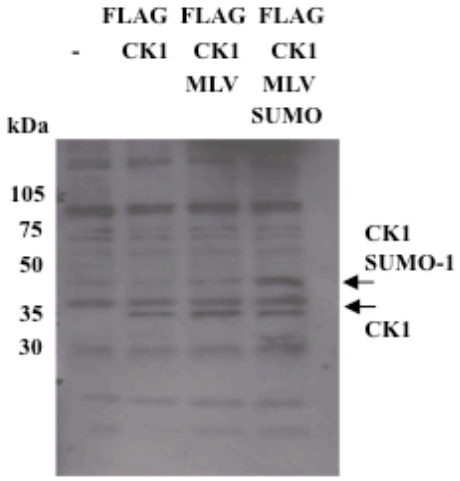

Figure 3.44. CK1 alpha LS might be modified by SUMO-1

Immunoblot analysis of HT1080 cells transfected with pSG5-FLAG CK1 alpha LS, +/- MLV-SUMO-1. Cell extracts were loaded onto a 4-20% polyacrylamide gradient gel. Proteins were transferred onto nitrocellulose membrane and the CK1 protein was detected with anti-FLAG mAbs.

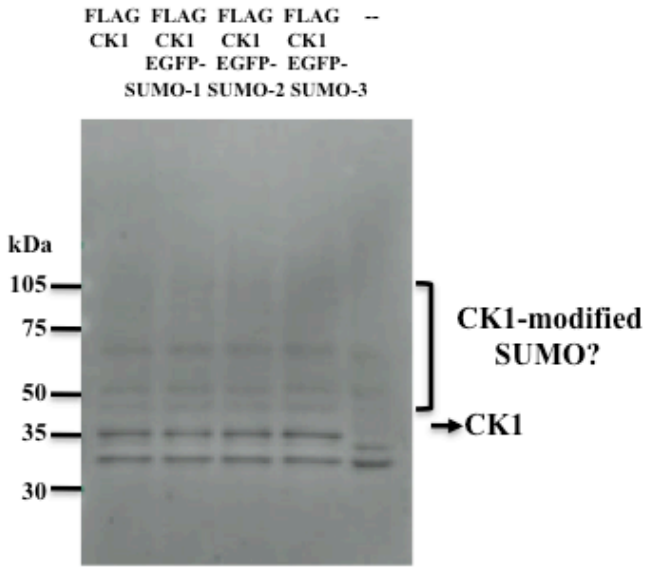

Figure 3.45. Test expression of CK1 alpha LS and SUMO-1/2/3

Immunoblot analysis of U2OS cells transfected with pSG5-FLAG CK1 alpha LS +/- pEGFP-SUMO-1/2/3. Cell extracts were loaded onto a 4-20% polyacrylamide gradient gel. Proteins were transferred onto nitrocellulose membrane and the CK1 protein was detected with polyclonal goat anti-CK1 alpha antibodies.

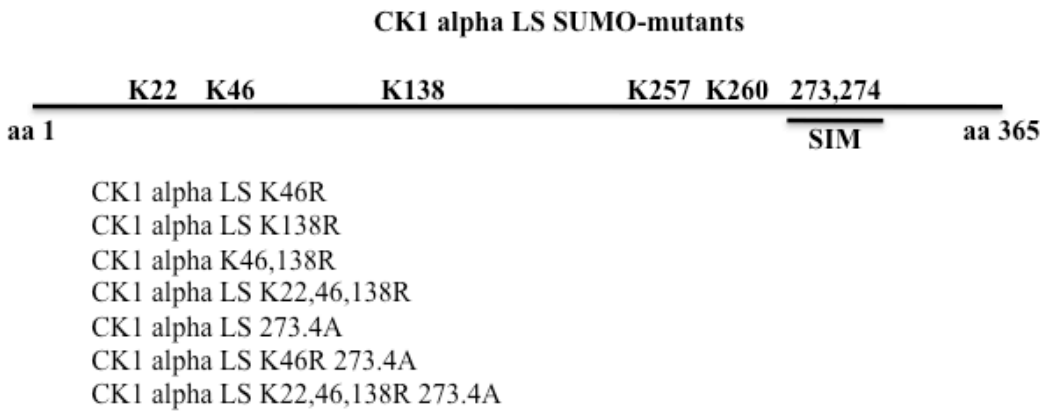

Figure 3.46. CK1 alpha LS SUMO mutants

All mutants were made using site-directed mutagenesis and transfected into HT1080 and U2OS cells. SUMO modification was detected in western blot and immunofluorescence. CK1 K46R was still recruited to the DEFs, although the mutant was not active. CK1 alpha LS K138R results in more SUMO filaments localising to the DEFs.

3.5.3 SUMO-modification of CK1 alpha LS in *E. coli*

It was decided to try to map the SUMO-modification sites in CK1 alpha LS in a system developed by Uchimura et al., 2004 (overview in Figure 3.47). CK1 alpha LS was cloned into several prokaryotic expression vectors either containing a His- or a GST-tag. BL21-Gold(DE3) were co-transformed with the plasmid expressing CK1 alpha LS and the SUMO-modification machinery – Aos1 and Uba2 (AU) and Ubc9 – and SUMO-1 or SUMO-3. Various conditions were tested but it was not possible to detect any GST-tagged CK1 alpha LS expressed even with different conditions of IPTG and at different temperatures. The only test expression that showed any result was of His-tagged CK1 alpha LS induced with 0.5 mM IPTG for 6 hours at 37 ˚C (Figure 3.48). The expression was still very poor and the CK1 alpha LS protein was degraded.

It was then decided to try *in vitro* protein synthesis using cell-free extract to express CK1 alpha LS to avoid the degradation and possible toxicity issues. No SUMO modification of CK1 alpha LS was observed when it was expressed together with SUMO-1 or SUMO-3 in the cell-free extract (Figure 3.49). RanGAP1, which has been shown to be SUMO-modified (Matunis et al., 1996) was used as a positive control. Two different cell-free extract kits were tested but neither gave a positive result when used for SUMO modification of CK1 alpha. This suggested that CK1 alpha LS was insoluble and two new DNA constructs were ordered and synthesised by Mr Gene. The sequences chosen were based on past publications. A truncated variant of CK1 (Cki1Δ298) from *Schizisaccharomyces pombe* has been successfully used in crystallisation studies (Xu et al., 1995). CK1 alpha S was aligned with Cki using the Clustal 2.1 multiple sequence alignment programme (Figure 3.50) and the construct CK1 alpha (aa 1-301) was chosen for expression experiments. Another CK1 isoform lacking the C-terminal autoinhibitory region, CK1 delta (aa 1-317), has also been used in crystallisation studies earlier (Longenecker et al., 1996). This isoform was chosen for the expression studies as well.

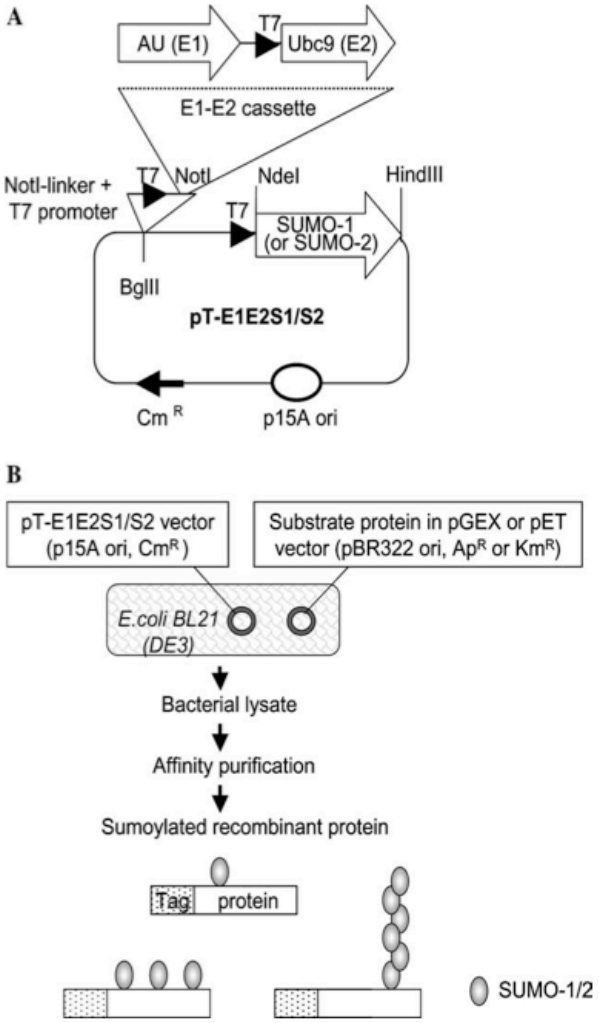

Figure 3.47. Overproduction of eukaryotic SUMO-1- and SUMO-2/3-conjugated proteins in *Escherichia coli*

A: One vector expresses the SUMO-modification machinery E1 and E2 + SUMO.
B: Cotransformation of the vector expressing the SUMO modification machinery and a second vector that expresses the protein of interest. (Figure taken from Uchimura et al., 2004).

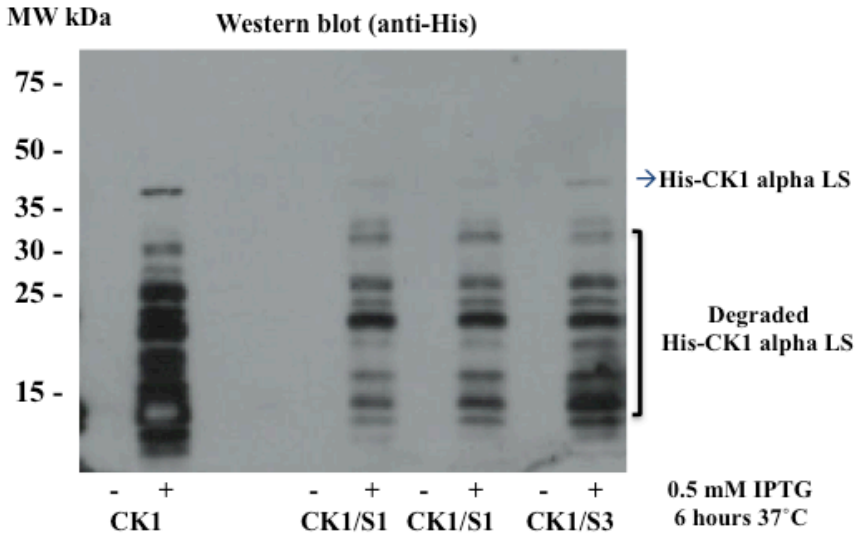

Figure 3.48. **Test expression of CK1 alpha LS**

Immunoblot analysis of lysates from BL21-Gold(DE3) cells transformed with pProEx HTb CK1 alpha LS and pT-Trx-AU(E1)-Ubc9(E2)-SUMO-1/3, induced with 0.5 mM IPTG and left to grow 6 hours at 37 ˚C. Lysates were loaded onto a 4-20% polyacrylamide gradient gel. Proteins were transferred onto a nitrocellulose membrane and the expressed CK1 protein was detected using an anti-His mAb.

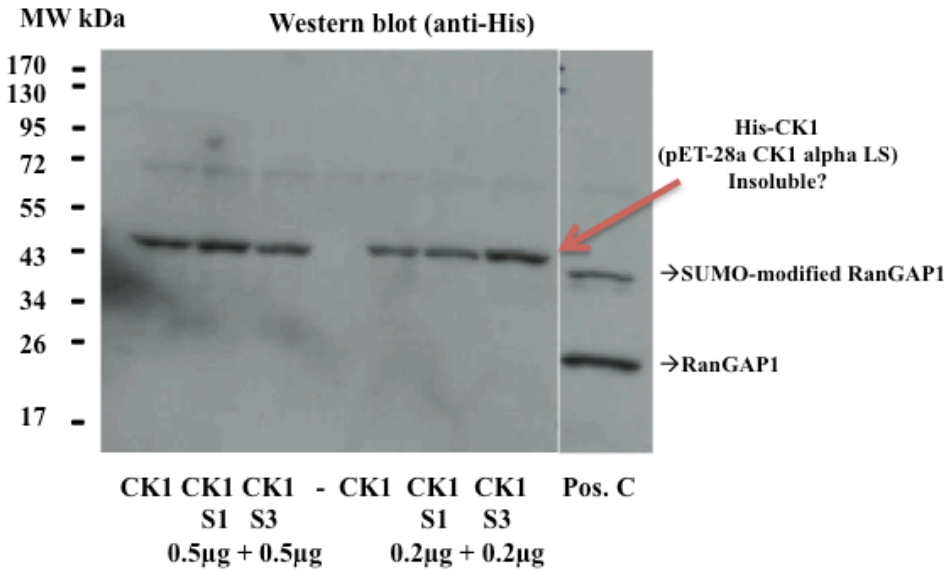

Figure 3.49. Cell-free test expression of CK1 alpha LS with and without SUMO-1 and SUMO-3

Immunoblot analysis from cell-free expression of CK1 alpha LS (CK1) with or without SUMO-1(S1) or SUMO-3(S3). SUMO-modified RanGAP1 was used as a positive control. Lysates were loaded onto a 4-20% polyacrylamide gradient gel. Proteins were transferred onto nitrocellulose membrane and the expressed proteins were detected using an anti-His mAb.

Figure 3.50. Alignment of CK1 sequences using Clustal 2.1 multiple sequence alignment

A truncated variant of CK1 (Cki1Δ298) from *Schizisaccharomyces pombe* has been successfully used in crystallisation studies (Xu *et al*., 1996). Based on the alignment above, the construct CK1 alpha aa 1-301 was chosen for expression experiments (see arrow).

3.5.4 Expression of CK1 alpha 1-301 and CK1 delta 1-317 in *E. coli*

CK1 alpha 1-301 and CK1 delta 1-317 were cloned into several different prokaryotic expression vectors with either a His- or a GST-tag. BL21-Gold(DE3) cells were transformed with the plasmids and test expression experiments were performed with 0.2 mM IPTG for 6 hours at 25 ˚C. The temperature was lowered from 37 ˚C to 25 ˚C to help protein folding and solubility. The expression was still poor for most constructs (Figure 3.51) but pET-28a seemed to give the best expression of CK1 alpha 1-301. To check for protein solubility, another test expression experiment with pET-28a CK1 alpha 1-301 and pET-28a CK1 delta 1-317 was performed. This time the cells were grown to an OD_{600} of 1.0 at 37 ˚C, induced with 0.2 mM IPTG and left for expression overnight at 15 ˚C (Burzio et al., 2002). Only CK1 delta 1-317 was soluble under these conditions (Figure 3.52). Another test expression was done with pET-28a CK1 alpha 1-301 and as seen in Figure 3.53, CK1 alpha 1-301 was found in the pellet and was insoluble. The shortest CK1 alpha isoform has been used previously in biochemical studies (Burzio et al., 2002) and in autophosphorylation studies (Budini et al., 2009). This isoform (Figure 3.54) was now ordered and synthesised by Mr Gene. It was cloned into pET-28a and a test expression was performed; but again CK1 alpha was insoluble. This was the smallest human CK1 alpha isoform, CK1 alpha 1-325 without the L and S insert. The only difference in the sequence when compared to the clones used in the studies from Burzio et al., 2002 and Budini et al., 2009, was the serine at position 313 (shown in red in Figure 3.54) which is a glycine in the CK1 alpha variants used in Burzio et al., 2002 and Budini et al., 2009. Serine 313 in CK1 alpha was mutated to glycine using site-directed mutagenesis and again test expression was repeated, but this time together with SUMO-1 (Figure 3.55) in the hope that SUMO-1 might make the CK1 alpha protein more soluble. Also under the new conditions the CK1 alpha protein was mainly found in the pellet and the small soluble portion detected was not SUMO-modified (Figure 3.55).

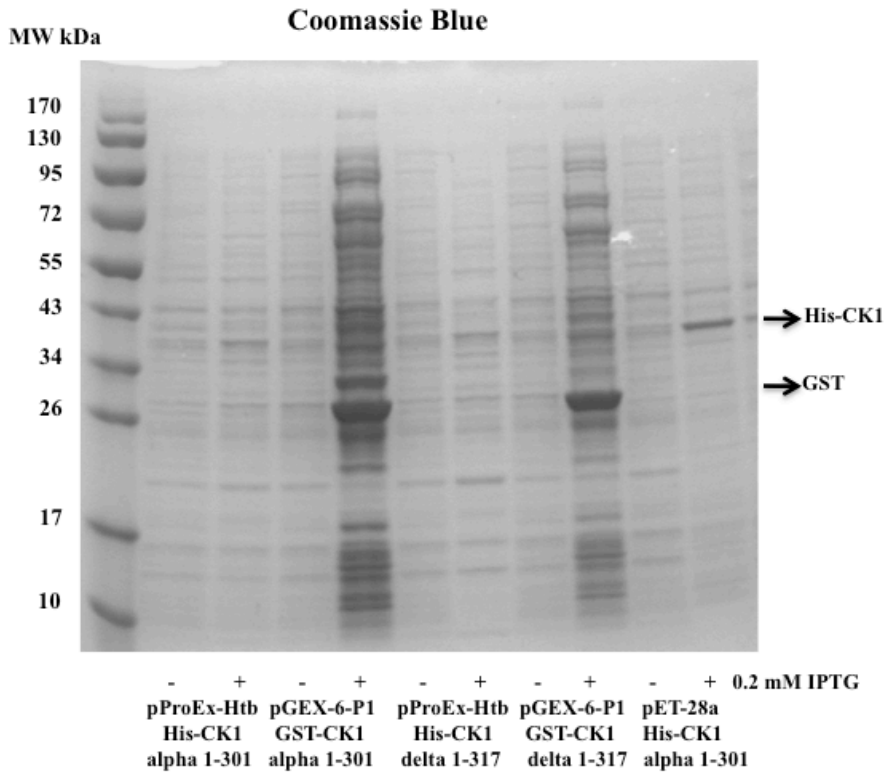

Figure 3.51. Test expression of CK1 alpha 1-301 and CK1 delta 1-317

Transformed BL21-Gold(DE3) cells were induced with 0.2 mM IPTG and left to grow for 6 hours at 25 ˚C. Cells were lysed and loaded onto a 4-20% polyacrylamide gradient gel and stained with Coomassie Blue.

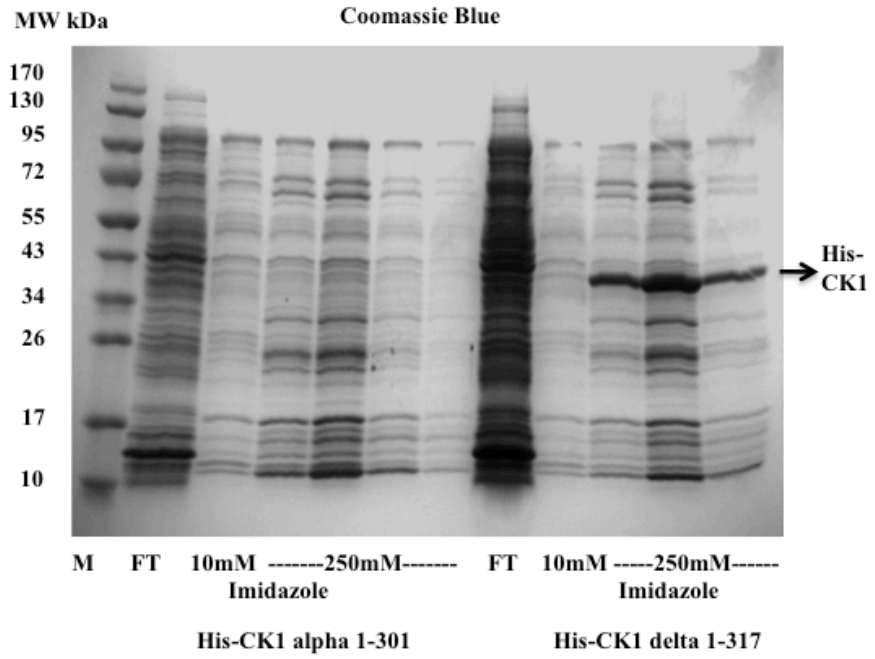

Figure 3.52. Test expression of CK1 alpha 1-301 and CK1 delta 1-317

Transformed BL21-Gold(DE3) cells were induced with 0.2 mM IPTG and left to grow overnight at 15 ˚C. Proteins were purified and several fractions were loaded onto a 4-20% polyacrylamide gradient gel and stained with Coomassie Blue. Marker (M), Flow through (FT).

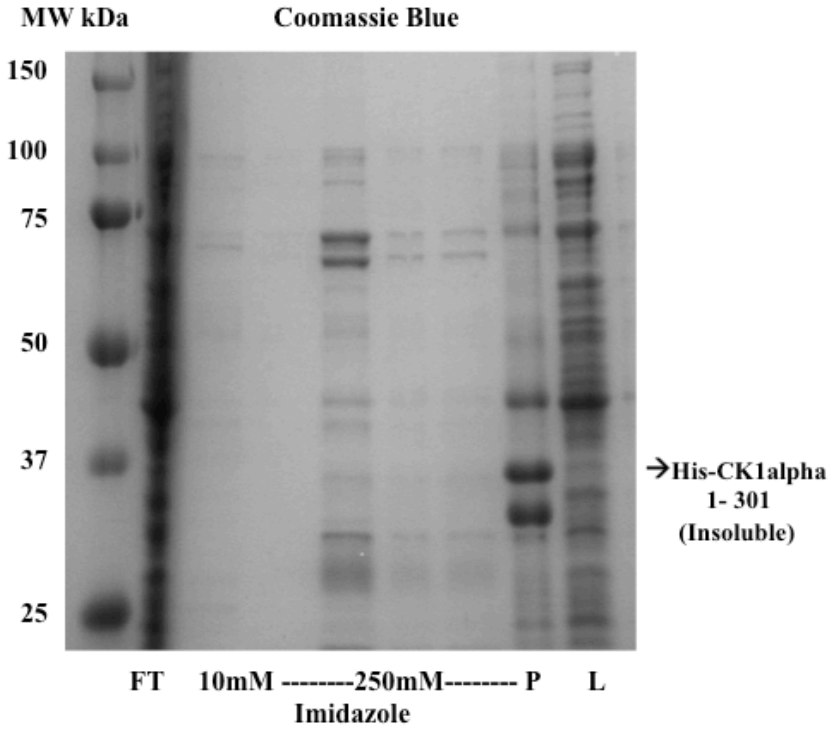

Figure 3.53. Solubility test of pET-28a CK1 alpha 1-301

Transformed BL21-Gold(DE3) cells were induced with 0.2 mM IPTG and left to grow overnight at 15 ˚C. Protein was purified and several fractions were loaded onto a 4-20% gradient gel and stained with Coomassie Blue. Flow through (FT), Pellet (P), Load (L).

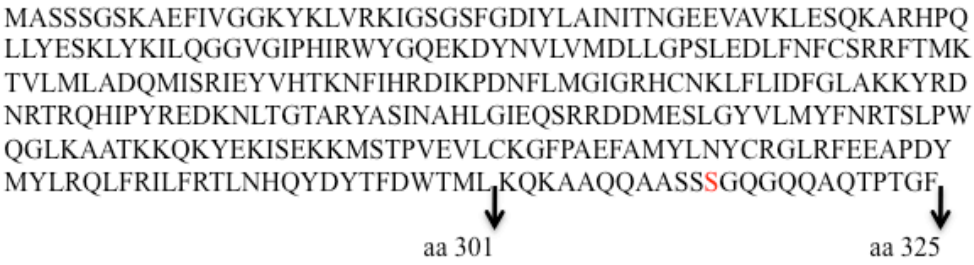

Figure 3.54. Shortest CK1 alpha isoform

The shortest CK1 alpha isoform has been used in biochemical studies (CK1 alpha 1-325 (S313G) (Burzio *et al*. 2002) and in auto-phosphorylation studies (Budini *et al*. 2009). The only difference is the serine at position 313 (in red) which is a glycine in the CK1 alpha variants mentioned in the studies above.

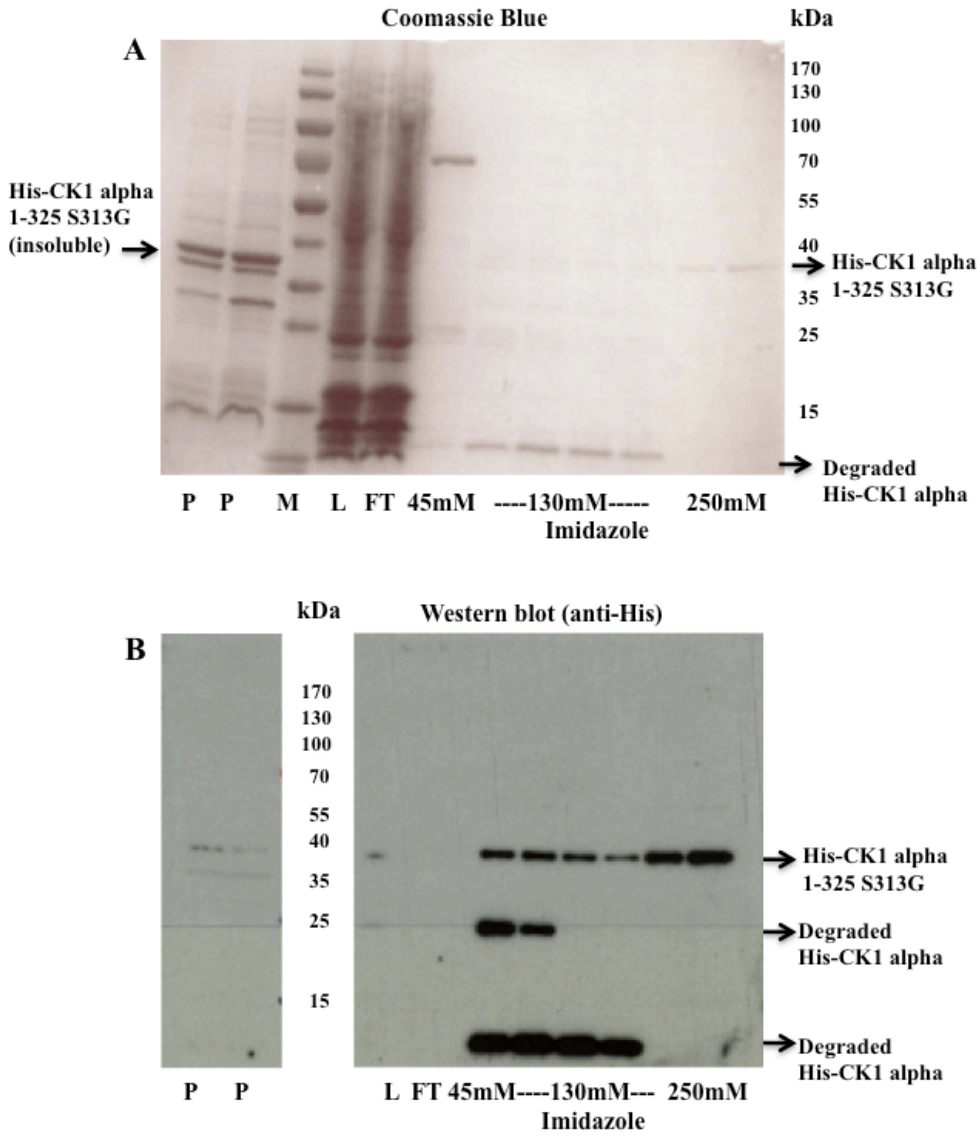

Figure 3.55. CK1 alpha 1-325 S313G is still insoluble

BL21-Gold(DE3) cells co-transformed with pET-28a CK1 alpha 1-325 S313G and pT-Trx-AU(E1)-Ubc9(E2)-SUMO-1 were induced with 0.2 mM IPTG and left to grow overnight at 15 ˚C. Protein was purified and several fractions were loaded onto a 4-20 % polyacrylamide gradient gel and stained with either (A) Coomassie Blue or (B). Proteins were transferred to a nitrocellulose membrane and the expressed proteins were detected using an anti-His mAb. Load (L), Flow through (FT), Pellet (P), Marker (M).

Further test expression experiments with the various CK1 alpha constructs were also carried out in SoluBL21. SoluBL21 is a mutant strain of BL21(DE3) which has been optimised for expressing insoluble proteins in a soluble form, but here also CK1 alpha remained insoluble. It was then decided to continue mapping the SUMO-modification sites in the CK1 delta isoform. CK1 alpha is 76% identical to the amino acid level of CK1 delta (Gross and Anderson, 1998).

3.5.5 Expression and SUMO modification of CK1 delta 1-317 in *E. coli*

CK1 alpha LS and full-length CK1 delta were aligned using the Clustal 2.1 multiple sequence alignment programme. As can be seen in Figure 3.56, all of the predicted SUMO-modification sites in CK1 alpha LS are conserved in CK1 delta except for K363. To examine SUMO-modification of CK1 delta 1-317 in *E. coli*, BL21-Gold(DE3) cells were transformed with pET-28a CK1 delta 1-317 with or without the SUMO-1/3 expressing plasmids. Again cells were grown to an OD_{600} of 1.0 at 37 ˚C, induced with 0.2 mM IPTG and left for expression overnight at 15 ˚C (Burzio et al., 2002). Proteins were purified and loaded onto a 4-20% polyacrylamide gradient gel and stained with Coomassie Blue (Figure 3.57). Unfortunately, the SUMO-modified CK1 delta 1-317 was too weak to see properly in the Coomassie Blue-stained gel and a western blot was performed using an anti-His mAb and a polyclonal rabbit anti-SUMO-2/3 antibody (Figure 3.58). CK1 delta 1-317 is SUMO-modified in *E.coli*. There are three very strong SUMO-modified bands and one weaker band detected with the SUMO-2/3 antibody. There is a weak band showing underneath the SUMO-modified CK1 delta band in the western blot stained with the SUMO-2/3 antibody. This is contamination from the first detection with the His antibody. Preliminary data show that CK1 delta 1-317 can be modified by SUMO-1 and SUMO-3.

It was decided to use SUMO-1 for future modification experiments. This would make it easier to interpret the results as the SUMO-1 protein does not contain the lysine residue that corresponds to lysine 48 in ubiquitin and therefore cannot make SUMO-chains (Bayer et al., 1998). The CK1/SUMO higher molecular weight bands should each count for one SUMO-attachment.

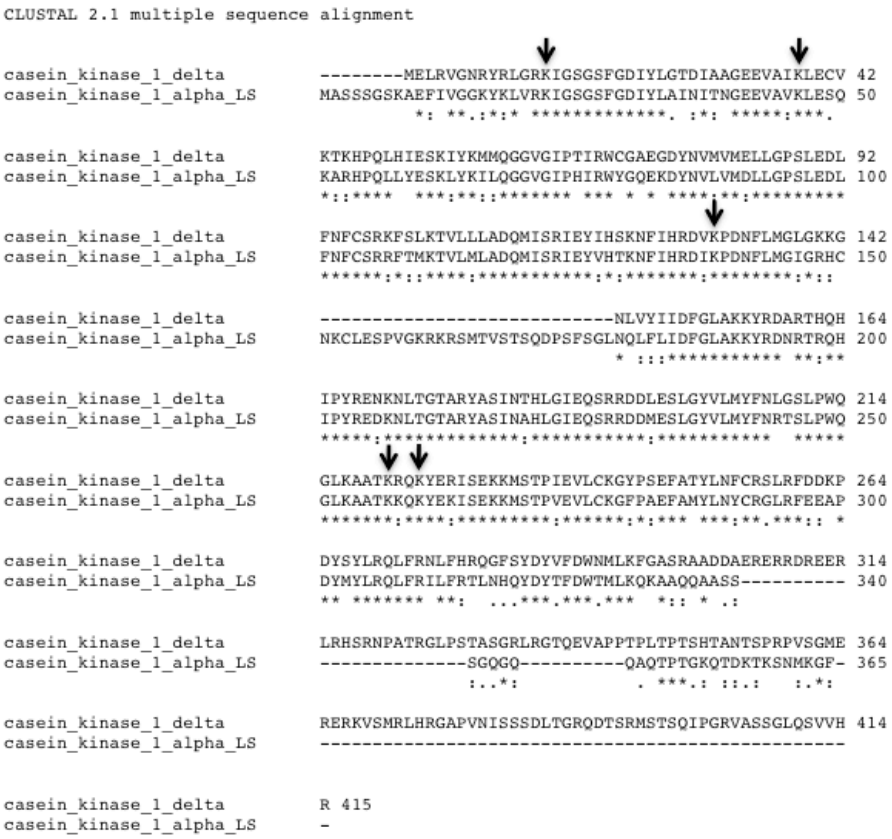

Figure 3.56. Alignment of CK1 sequences using Clustal 2.1 multiple sequence alignment

All the lysines predicted to be SUMO-modified in CK1 alpha LS are conserved in CK1 delta – K22/14, K46/38, K138/130, K257/221, K260/224 – except for K363. Conserved lysine positions are marked with an arrow.

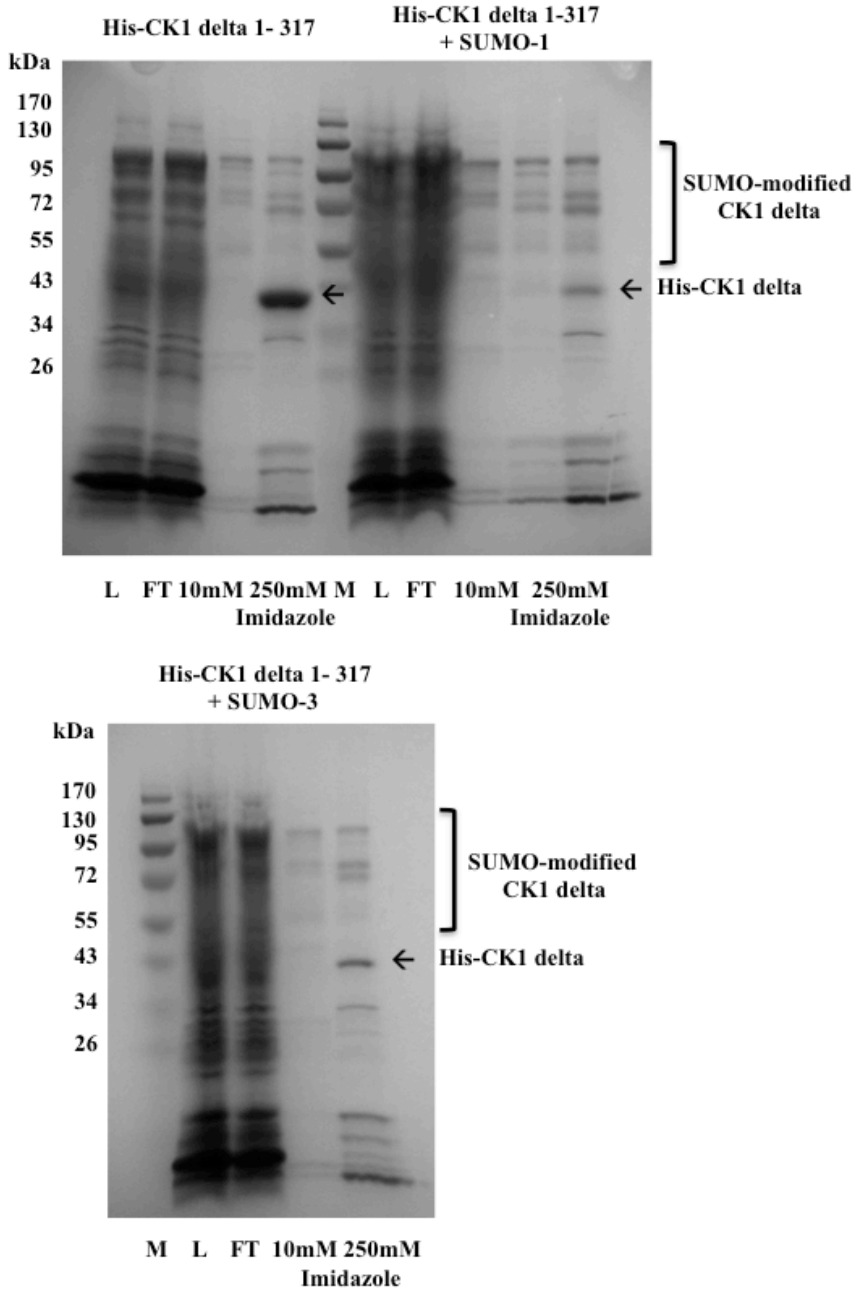

Figure 3.57. Expression and SUMO-modification of CK1 delta 1-317

BL21-Gold(DE3) cells transformed with pET-28a-CK1 delta 1-317 with or without pT-Trx-AU(E1)-Ubc9(E2)-SUMO-1 were induced with 0.2 mM IPTG and left to grow overnight at 15 ˚C. Protein was purified and several fractions were loaded onto a 4-20% polyacrylamide gradient gel and stained with Coomassie Blue. Load (L), Flow through (FT), Marker (M).

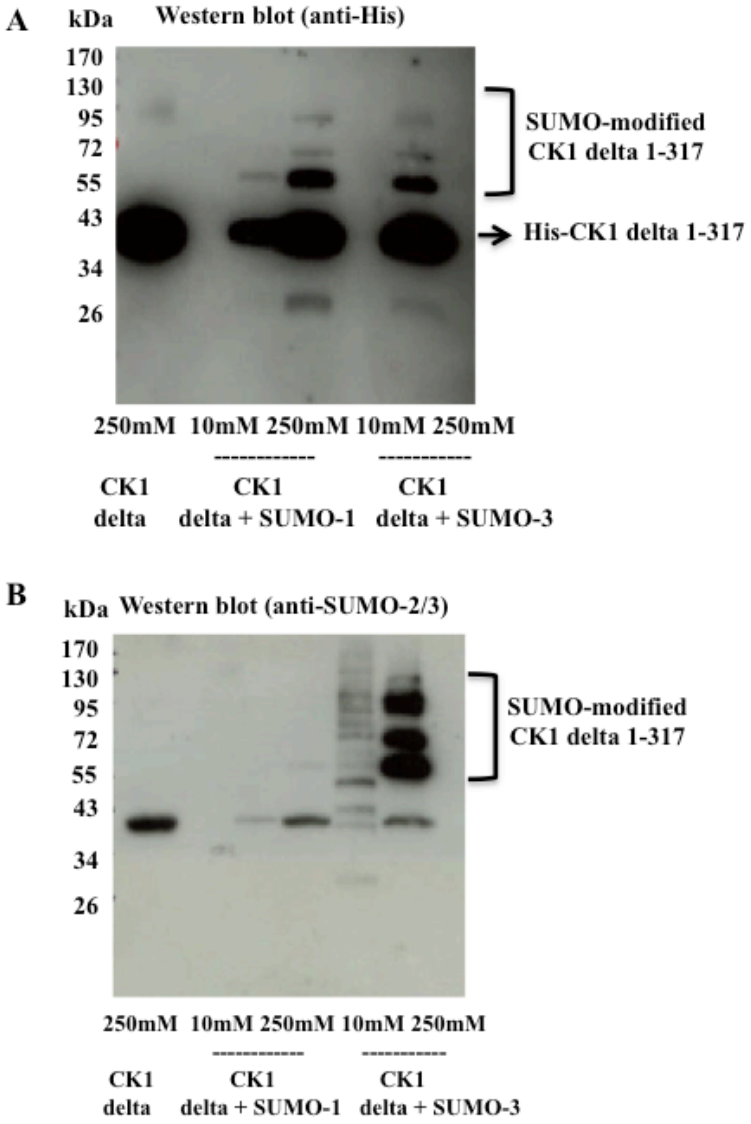

Figure 3.58. SUMO-modification of CK1 delta 1-317 in *E.coli*

BL21-Gold(DE3) cells transformed with pET-28a-CK1 delta 1-317 with or without pT-Trx-AU(E1)-Ubc9(E2)-SUMO-1/3 and induced with 0.2 mM IPTG and left to grow overnight at 15 ˚C. Protein was purified and several fractions were loaded onto a 4-20% polyacrylamide gradient gel and proteins were transferred onto a nitrocellulose membrane and the expressed proteins were detected using an anti-His mAb (A) and polyclonal rabbit anti-SUMO-2/3 antibodies (B).

3.5.6 Optimisation of expression and SUMO modification of CK1 delta 1-317 in *E. coli*

To optimise the expression and SUMO modification of CK1 delta 1-317 a few changes to plasmids and protocols were made. The vector pET-28a contains a potential N- and C-terminal His-tag. All constructs used in the preliminary experiments contained a STOP codon before the C-terminal His-tag. This was changed in pET-28a CK1 delta 1-317 using site-directed mutagenesis. The protein expressed using the new pET-28a CK1 delta 1-317 construct contained an N- and a C-terminal His-tag and had a much better affinity to the column during protein purification. This was not the only change made to the purification protocol. Instead of using a nickel-affinity column it was decided to try and use a cobalt-affinity column, which has very low non-specific binding. It was also noticed when using Triton X-100 in the elution buffer, as done by (Burzio et al., 2002), that a more indistinct band pattern was observed in western blot (Figure 3.59). Triton X-100 was therefore excluded from the elution buffer. To reduce unspecific background even further washing and elution conditions were tested (Supplementary Figure 6.1). When 30 mM Imidazole was used in the wash buffer and 130 mM for elution there were still some contaminants in the elution. When 60 mM Imidazole was used in the wash buffer and 130 mM in the elution a part of the SUMO-modified CK1 was lost. It was decided to use 45 mM Imidazole in the wash buffer and 130 mM in the elution buffer. The temperature the cells were grown at overnight after induction was also changed from 15 ˚C to 22 ˚C for CK1 delta 1-317. A typical trace for the protein purification can be seen in Figure 3.60.

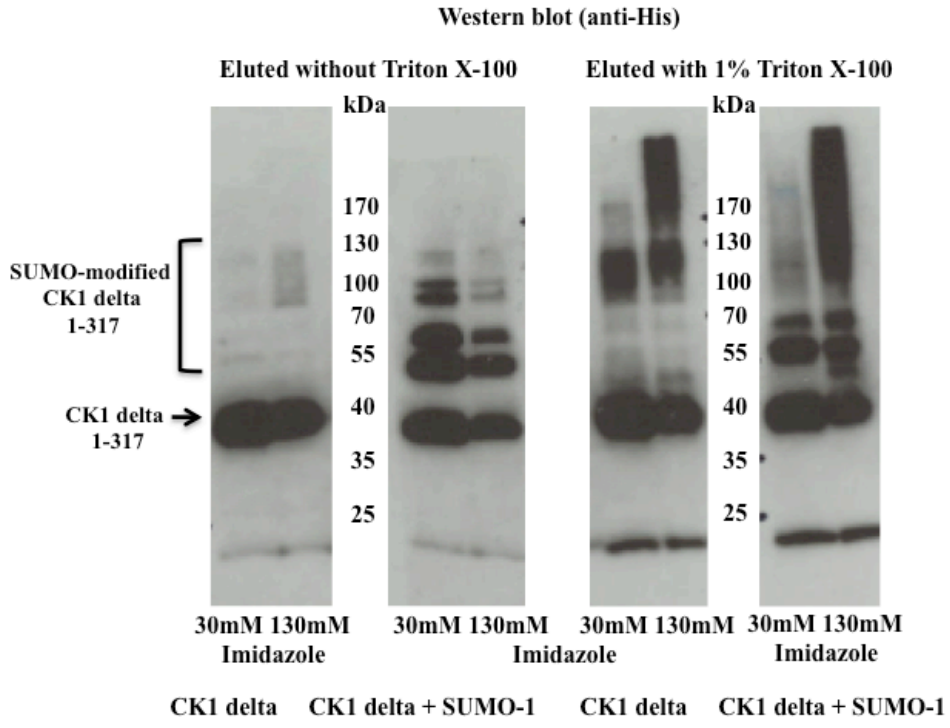

Figure 3.59. Testing elution buffer for SUMO-modified CK1 delta 1-317

BL21-Gold(DE3) cells transformed with pET-28a CK1 delta 1-317 with or without pT-Trx-AU(E1)-Ubc9(E2)-SUMO-1, induced with 0.2 mM IPTG and left to grow overnight at 15 ˚C. Protein was purified and several fractions were loaded onto a 4-20% polyacrylamide gradient gel, transferred onto a nitrocellulose membrane, detected using an anti-His mAb. Please note that there seems to be a minor contamination of SUMO-modified CK1 in the lane on the left with CK1 eluted with Triton X-100, which could be a loading issue.

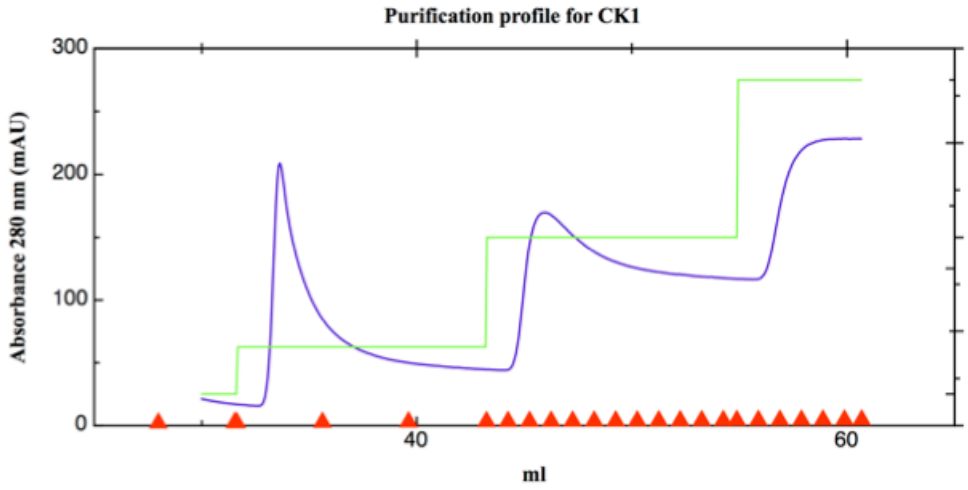

Figure 3.60. Typical purification profile for CK1 or SUMO-modified CK1

Blue line: The first peak is the 15% wash, the second peak is the 50% elution and the third peak is the 100% Imidazole wash. The green line shows the Imidazole concentrations 15%, 50% and 100%. The red triangles illustrate the fractions.

3.5.7 Mapping of the SUMO modification of CK1 delta 1-317 in *E. coli*

Several different SUMO prediction servers were used to find potential SUMO-modifications sites in CK1 delta 1-317 (Figure 3.61). Earlier during this study an alignment with CK1 alpha LS and CK1 delta was done to see if the predicted SUMO-modification sites in CK1 alpha LS were conserved in CK1 delta (Figure 3.56). Now the predicted SUMO-modification sites from CK1 delta were compared to CK1 alpha. Most of the predicted sites in CK1 delta were conserved in CK1 alpha (Figure 3.62). The predicted lysines were mutated to arginines for mapping experiments of the potential SUMO sites in CK1 delta 1-317. Mutating lysines to arginines should keep the structure and charge balance of the CK1 mutants suited to the wild-type CK1. The CK1 delta 1-317 SUMO mutants were either made using site-directed mutagenesis, by cloning G-blocks/GeneArt strings in different combinations or by gene synthesis (Figure 3.63). All CK1 delta SUMO mutants were co-transformed into BL21-Gold(DE3) cells together with the pT-Trx-AU(E1)-Ubc9(E2)-SUMO-1 plasmid, grown to an OD_{600} of 1.0, induced with 0.2 mM IPTG and left to grow overnight at 22 ˚C. The proteins were purified and detected in western blots using an anti-His mAb (Figures 3.64 and 3.65). It soon became clear that the SUMO-modification of CK1 delta 1-317 was difficult to map using the system in *E.coli* because SUMO seemed to modify other lysines in the SUMO mutants. It was only when CK1 was mutated that SUMO modified unspecific lysines. It was always the same pattern detected in SUMO-modified wild-type CK1 delta 1-317 when expressed overnight. The only mutation that often showed a change in the band pattern was K38 (Figure 3.64). K38 is the active site of CK1 delta and when mutated to arginine it results in a kinase dead mutant. It was decided to try and map the modified lysines in CK1 delta 1-317 using mass spectrometry. In parallel *E.coli* modification studies were continued with slight changes. The transformed cells were only grown to an OD_{600} of 0.6, induced with 0.2 mM IPTG and left to grow at 22 ˚C but only for 5-6 hours. That improved the assay and the results were easier to interpret (Figures 3.66 and 3.67) but it was still not clear which lysines were SUMO-modified until the data was compared with the mass spectrometry analysis.

SUMO site prediction of CK1 delta

MELRVGNRYRLGRKIGSGSFGDIYLGTDIAAGEEVAIKLECVKTKHPQLHIE
SKIYKMMQGGVGIPTIRWCGAEGDYNVMVMELLGPSLEDLFNFCSRKFSL
KTVLLLADQMISRIEYIHSKNFIHRDVKPDNFLMGLGKKGNLVYIIDFGLA
KKYRDARTHQHIPYRENKNLTGTARYASINTHLGIEQSRRDDLESLGYVLM
YFNLGSLPWQGLKAATKRQKYERISEKKMSTPIEVLCKGYPSEFATYLNFC
RSLRFDDKPDYSYLRQLFRNLFHRQGFSYDYVFDWNMLKFGASRAADDA
ERERRDREERLRH

Near-consensus SV40 T antigen putative nuclear localisation sequence underlined

Potential SUMO-interacting motif (low probability) using the program GPS-SBM 1.0: VLLL, LVYI and VYII

Potential SUMO site	Sequence	
K14	RKIG	
K38	IKLE	SUMO consensus sequence
K130	VKPD	
K140	GKKG	
K154	AKKY	
K155	KKYR	
K217	LKAA	
K221	TKRQ	
K224	QKYE	
K263	DKPD	
K294	LKFG	

Figure 3.61. SUMO site prediction of CK1 delta

Several SUMO prediction servers were used to predict potential SUMO-modification sites in CK1 delta.
SUMOplot: http://www.abgent.com/tools/sumoplot
SUMOsp 2.0: http://sumosp.biocuckoo.org/
seeSUMO: http://bioinfo.ggc.org/seesumo/
GPS-SBM 1.0: http://sbm.biocuckoo.org/
PCI-Based Sumo Site Prediction Server: http://bioinf.sce.carleton.ca/SUMO/start.php

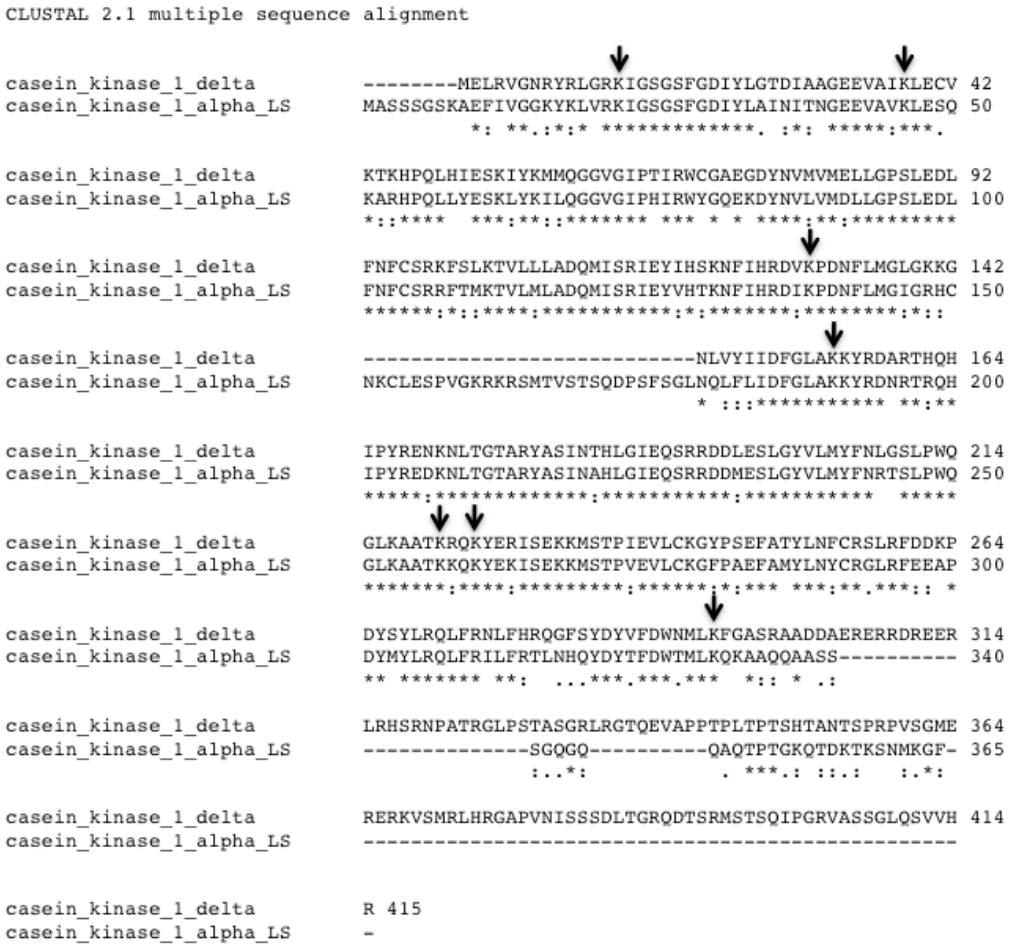

Figure 3.62. Alignment of CK1 sequences using Clustal 2.1 multiple sequence alignment

The following predicted lysines from CK1 delta are conserved in CK1 alpha LS: K14/22, K38/46 K130/138, K154/190, K155/191, K221/257, K224/260, K294/330.

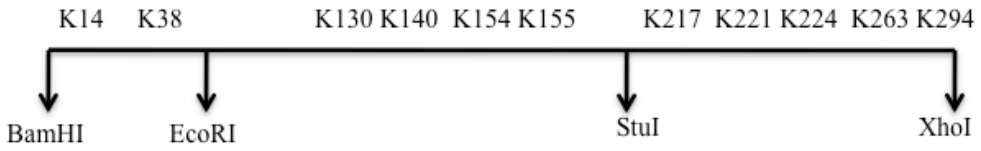

- CK1 delta (aa1-317) ΔSTOP K38R
- CK1 delta (aa1-317) ΔSTOP K221,K224,K263,K294R
- CK1 delta (aa1-317) ΔSTOP K130,K140,K221,K224,K263,K294R
- CK1 delta (aa1-317) ΔSTOP K14,K130,K140,K221,K224,K263,K294R
- CK1 delta (aa1-317) ΔSTOP K14,K38,K130,K140,K221,K224,K263,K294R

- CK1 delta (aa1-317) ΔSTOP K38,K130,K154,K155,K171,K217,K221R
- CK1 delta (aa1-317) ΔSTOP K14,K130,K140,K154,K217,K221,K224,K263,K294R
- CK1 delta (aa1-317) ΔSTOP K14,K38,K130,K140,K154,K217,K221,K224,K263,K294R
- CK1 delta (aa1-317) ΔSTOP K14,K38,K130,K140,K154,K155,K171,K217,K221,K224,K263,K294R

Figure 3.63. Overview of CK1 delta SUMO mutants

The CK1 delta 1-317 SUMO mutants were made by using either site-directed mutagenesis, cloning G-blocks/GeneArt strings in different combinations or by gene synthesis.

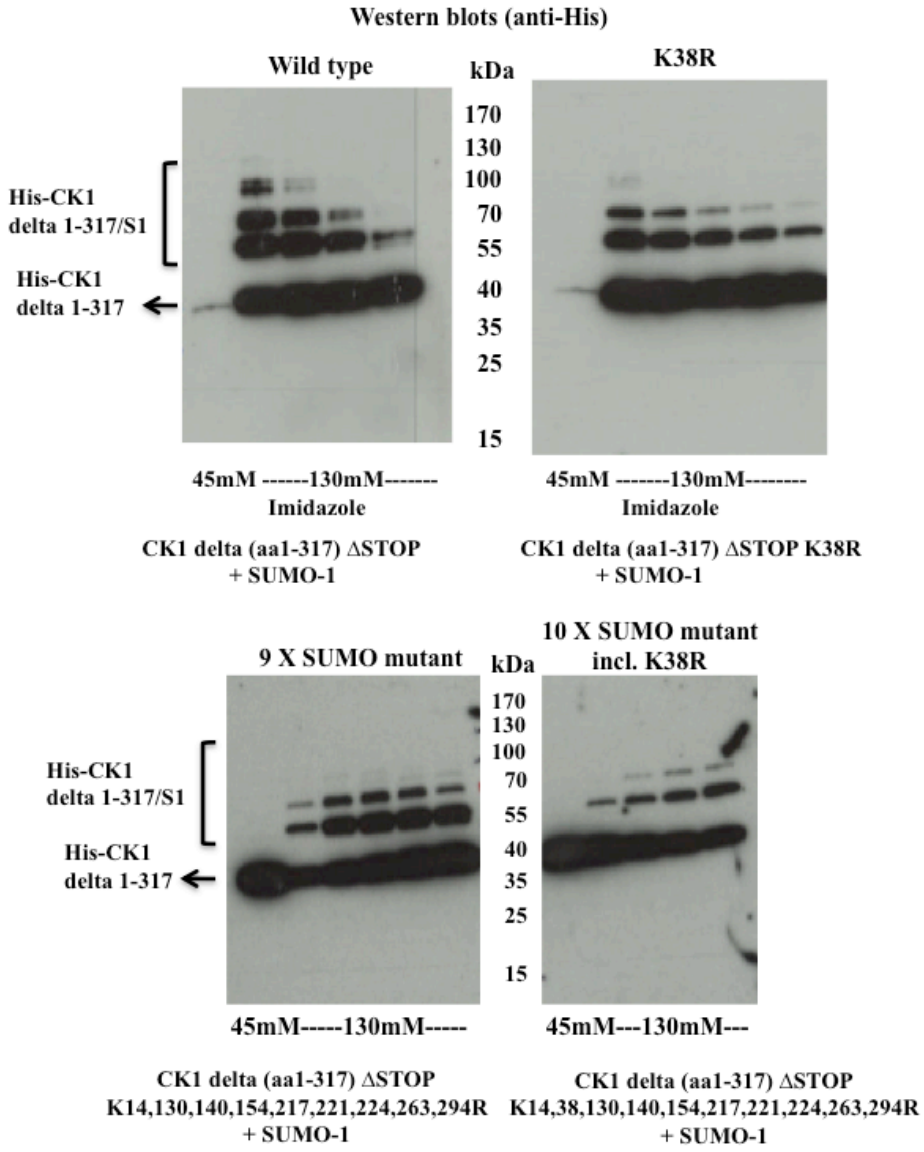

Figure 3.64. SUMO modification of CK1 delta 1-317 SUMO mutants

BL21-Gold(DE3) cells co-transformed with pET-28a CK1 delta 1-317 SUMO mutants and pT-Trx-AU(E1)-Ubc9(E2)-SUMO-1 were induced with 0.2 mM IPTG and left to grow overnight at 22 ˚C. Proteins were purified and several fractions were loaded onto a 4-20% polyacrylamide gradient gel, transferred onto a nitrocellulose membrane and the expressed proteins were detected using an anti-His mAb.

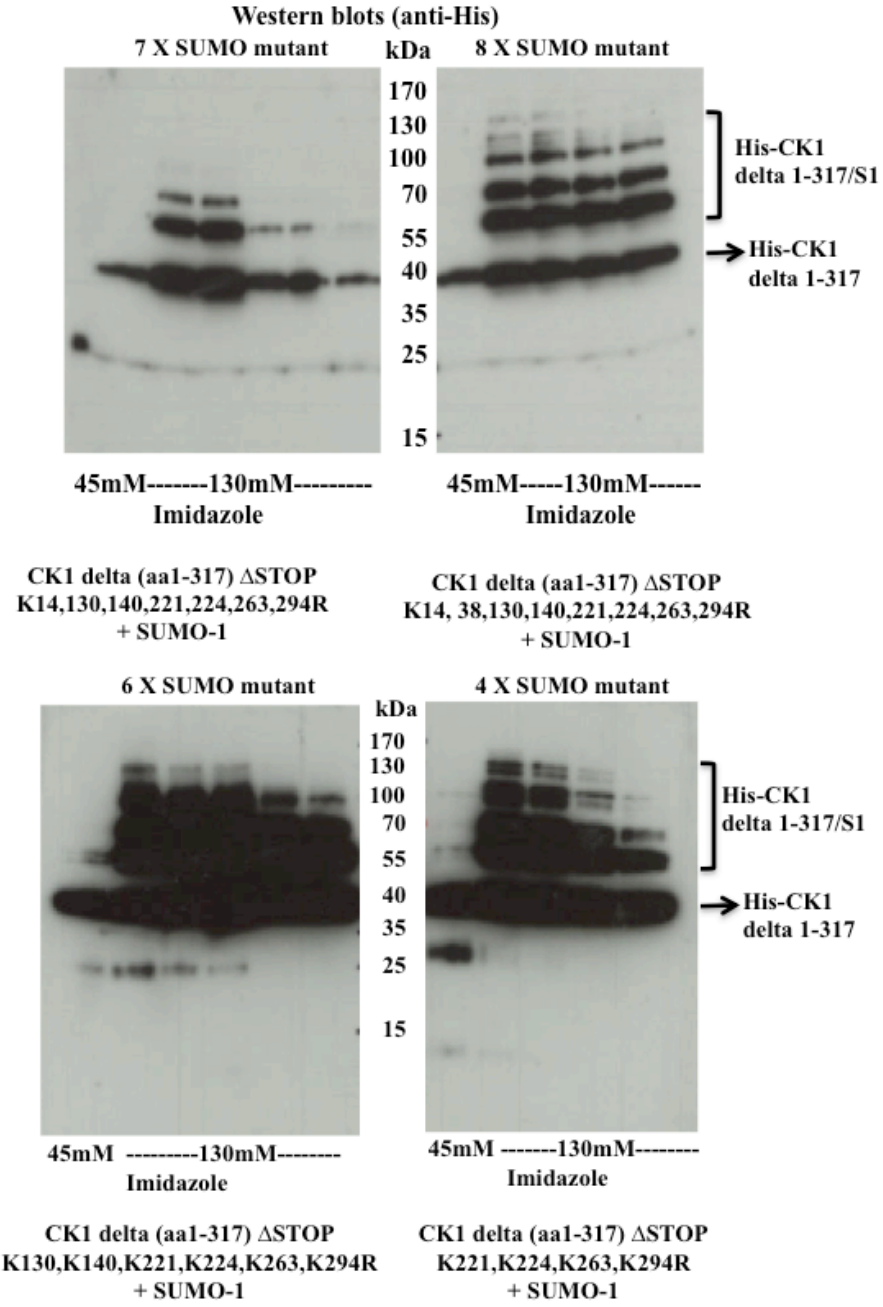

Figure 3.65. SUMO modification of CK1 delta 1-317 SUMO mutants

BL21-Gold(DE3) cells co-transformed with pET-28a-CK1 delta 1-317 SUMO mutants and pT-Trx-AU(E1)-Ubc9(E2)-SUMO-1 were induced with 0.2 mM IPTG and left to grow overnight at 22 ˚C. Proteins were purified and several fractions were loaded onto a 4-20% polyacrylamide gradient gel, transferred onto a nitrocellulose membrane and the expressed proteins were detected using an anti-His mAb.

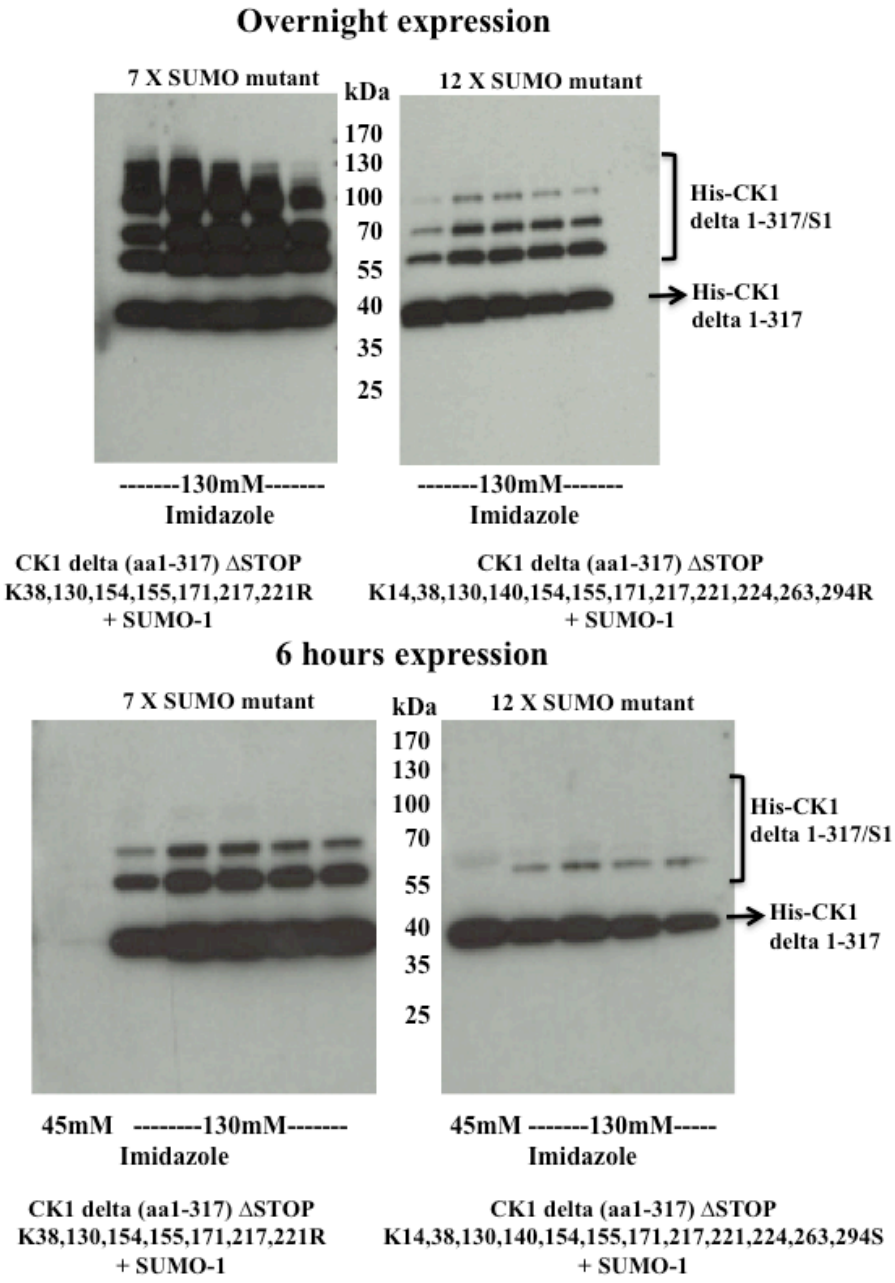

Figure 3.66. Comparison of efficiency of SUMO-1 modification machinery in *E.coli*

BL21-Gold(DE3) cells co-transformed with pET-28a CK1 delta 1-317 SUMO mutants and pT-Trx-AU(E1)-Ubc9(E2)-SUMO-1 were induced with 0.2 mM IPTG and left to grow overnight or for 6 hours at 22 ˚C. Proteins were purified and several fractions were loaded onto a 4-20% polyacrylamide gradient gel, transferred onto a nitrocellulose membrane and the expressed proteins were detected using an anti-His mAb.

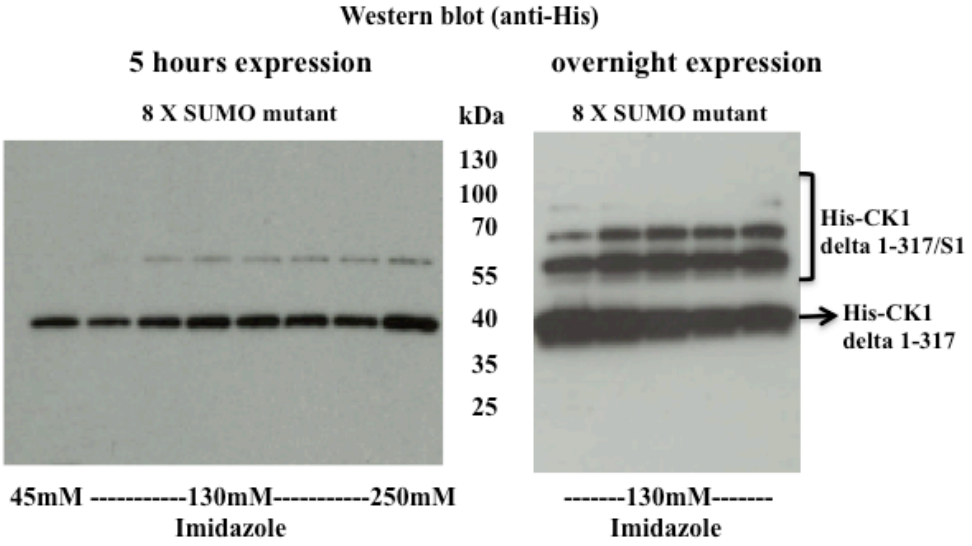

Figure 3.67. Comparison of efficiency of SUMO-1 modification machinery in *E.coli*

BL21-Gold(DE3) cells co-transformed with pET-28a CK1 delta 1-317 SUMO mutant and pT-Trx-AU(E1)-Ubc9(E2)-SUMO-1 were induced with 0.2 mM IPTG and left to grow overnight or for 5 hours at 22 ˚C. Protein was purified and several fractions were loaded onto a 4-20% polyacrylamide gradient gel, transferred onto a nitrocellulose membrane and the expressed proteins were detected using an anti-His mAb.

3.5.8 Mass spectrometry of SUMO-modifed CK1 delta 1-317 from *E. coli*

Mass spectrometry analysis was performed by Dr Paul Hitchen in the CISBIO Mass Spectrometry Core facility at Imperial College London. Samples for mass spectrometry were prepared by co-transforming BL21-Gold(DE3) cells with pET-28a CK1 delta 1-317 ΔSTOP and pT-Trx-AU(E1)-Ubc9(E2)-SUMO-1 plasmids. Transformed cells were grown to an OD_{600} of 1.0, induced with 0.2 mM IPTG and left to grow overnight at 22 ˚C. Protein was purified and loaded onto a 4-20% polyacrylamide gradient gel and stained with Coomassie Blue (Figure 3.68). Two bands (Figure 3.68, marked with arrows) were cut out for mass spectrometry analysis, the lower unmodified band to check it is the right protein expressed and the higher migrating band where one SUMO should be covalently attached to CK1 delta. Under normal conditions in the mammalian cells there would probably be a preferential lysine in the protein but under the conditions in the *E.coli* the hope was to see a mixture of SUMO-modified bands. The protein was digested into peptides using trypsin, which cleaves at the carboxyl side of a lysine or an arginine except for when there is a proline present as the following amino acid. The expected CK1 delta and SUMO-1 peptides used in the analysis are shown in Tables 3.2 and 3.3. The peptide mass of CK1 delta and SUMO-1 were estimated using PeptideMass on the ExPASy server.

The mass spectrometry peptide dataset was first used to search for the potential SUMO-modified CK1 sequences and if the peptide sequence was absent, then it was a good indication for it being potentially modified. When the mass spectrometer checks the peptide sequence and the mass of the peptide, it realises that there is too much mass for that peptide and the data is automatically discarded.

All the potential charges and masses of the SUMO-modified CK1 delta peptides were calculated (Table 3.4) and checked in the mass spectrometry dataset. The following CK1 peptides were found to be modified by SUMO-1: K38, K130, K140, K224 and K294 (shown in bold in Table 3.4).

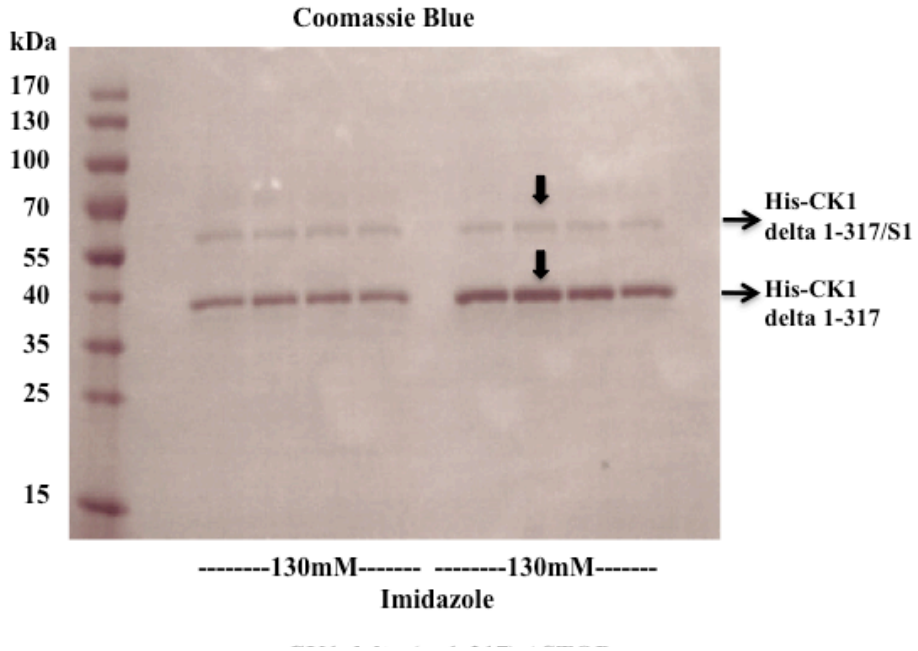

Figure 3.68. Expression of SUMO-modified CK1 delta 1-317 for mass spectrometry analysis

BL21-Gold(DE3) cells transformed with pET-28a CK1 delta 1-317 and pT-Trx-AU(E1)-Ubc9(E2)-SUMO-1, induced with 0.2 mM IPTG and left to grow overnight at 22 ˚C. Protein was purified and two fractions were loaded onto a 4-20% polyacrylamide gradient gel and stained with Coomassie Blue. Bands marked with an arrow were cut out for mass spectrometry analysis.

Table 3.2. Peptide mass of CK1 delta

SUMO site in CK1 delta 1-317	Peptide sequence	Theoretical Mass (monoisotopic mass)
K14	LGRKIGSGSFGDIYLGTDIAAGEEVAIK	2837.5043
K38	IGSGSFGDIYLGTDIAAGEEVAIKLECVK	3012.5233
K130	DVKPDNFLMGLGK	1433.7457
K140	DVKPDNFLMGLGKK	1561.8406
K154	GLNVYIIDFGLAKK	1550.8940
K155	GNLVYIIDFGLAKKYR	1870.0585
K217	DDLESLGYVLMYFNLGSLPWQGLKAATK	3129.5965
K221	AATKR	546.3358
K224	QKYER	723.3784
K263	FDDKPDYSYLR	1418.6586
K294	QGFSYDYVFDWNMLKFGASR	2431.1175

Table 3.2. The peptide mass of CK1 delta 1 was estimated using PeptideMass on the ExPASy server

The following conditions were selected for the estimation:
Selected enzyme: Trypsin
Two missed cleavages
All cysteines have been treated with Iodoaceamide to form carbamidomethyl-cysteine (Cys_CAM)
Methionines have not been oxidized
Using monoisotopic masses of the occurring amino acid residues and peptide masses as [M+H]+.

Table 3.3. Peptide mass of SUMO-1

Lysine in SUMO-1 where trypsin is cleaving	Peptide sequence	Theoretical Mass (monoisotopic mass)
K78	ELGMEEEDVIEVYQEQTGG	2154.9383

Table 3.3. The peptide mass of the SUMO-1 peptide was estimated using PeptideMass on the ExPASy server

The following conditions were selected for the estimation:
Selected enzyme: Trypsin
Zero missed cleavages
All cysteines have been treated with Iodoaceamide to form carbamidomethyl-cysteine (Cys_CAM)
Methionines have not been oxidized
Using monoisotopic masses of the occurring amino acid residues and peptide masses as [M+H]+.

Table 3.4. Theoretical mass of SUMO-modified CK1 delta peptides

SUMO site	Theoretical mass of CK1/ SUMO peptide	Mass/charge (m/z) 2 charges	Mass/charge (m/z) 3 charges	Mass/charge (m/z) 4 charges	Mass/charge (m/z) 5 charges
K14	4973.4426	n/a	1658.481	1244.111	995.488
K38	5148.4616	n/a	1716.821	**1287.865**	1030.492
K130	3569.6840	n/a	**1190.561**	893.171	714.737
K140	3697.7789	n/a	1233.259	**925.195**	740.356
K154	3686.8323	n/a	1229.611	922.458	738.166
K155	4005.9968	n/a	1335.999	1002.249	801.999
K217	5265.5348	n/a	1755.844	1317.132	1053.907
K221	2938.4276	1469.714	980.143	735.357	588.485
K224	2859.3167	n/a	**953.772**	715.579	572.663
K263	3554.5969	n/a	1185.532	889.399	711.719
K294	4567.0558	n/a	**1523.019**	1142.514	914.211

Table 3.4. The theoretical mass of the different SUMO-modified CK1 delta peptides

The mass was done using the following calculation. Mass of CK1 peptide + mass of SUMO-1 peptide - 1 (1 charge) -18 (H_2O) = the theoretical mass of the CK1 delta/SUMO-1 peptide.

The mass spectra of the peptides can be found in Figures 3.69-71 and an overview of the modified peptides is shown at the bottom of each spectra. These results confirmed some of the SUMO-modification sites using the SUMOplot prediction server from Abgent and it looked very promising together with the results from Figure 3.67. All the lysines were checked in the CK1 delta structure (PDB: 4jjr) and found to be on the outside of the protein, except for K38, and therefore available for modification (Figures 3.72 and 3.73). K38 is in the active site, K130 is in front of the active site or in the catalytic loop and K224 in the docking site for p53.

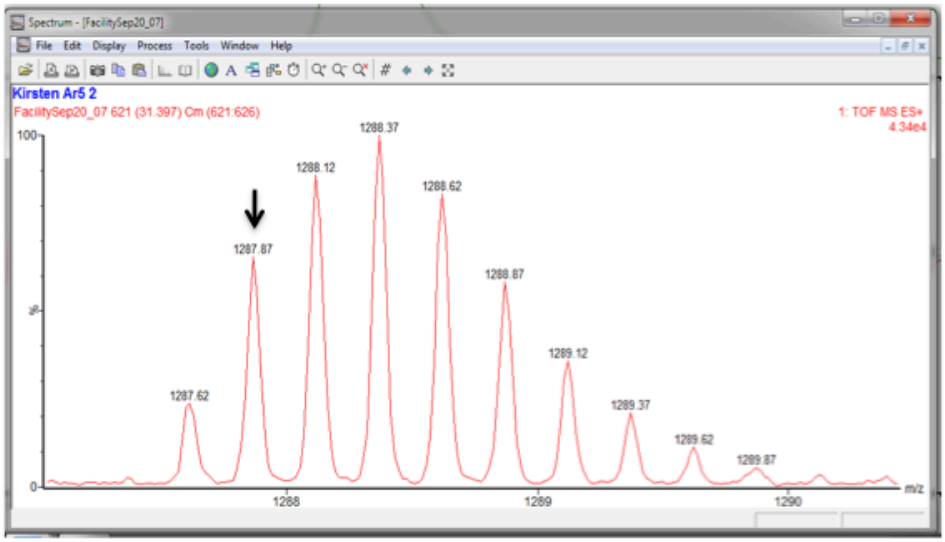

K38. Theoretical mass: 1287.865 m/z – 4 charges

K38 peptide IGSGSFGDIYLGTDIAAGEEVAIKLECVK
SUMO peptide ELGMEEEDVIEVYQEQTGG

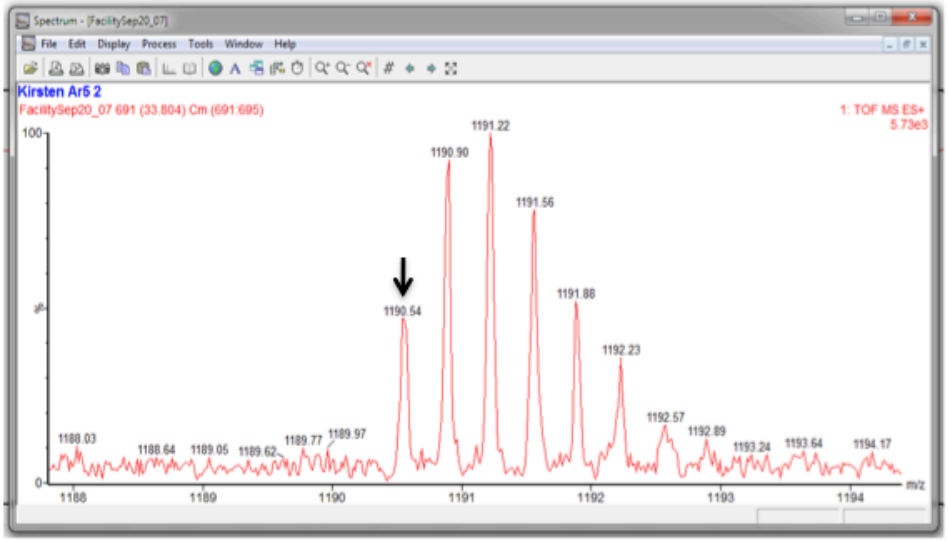

K130. Theoretical mass: 1190.561 m/z – 3 charges

K130 peptide DVKPDNFLMGLGK
SUMO peptide ELGMEEEDVIEVYQEQTGG

Figure 3.69. Mass spectra of SUMO-modified CK1 delta peptide K38 and K130

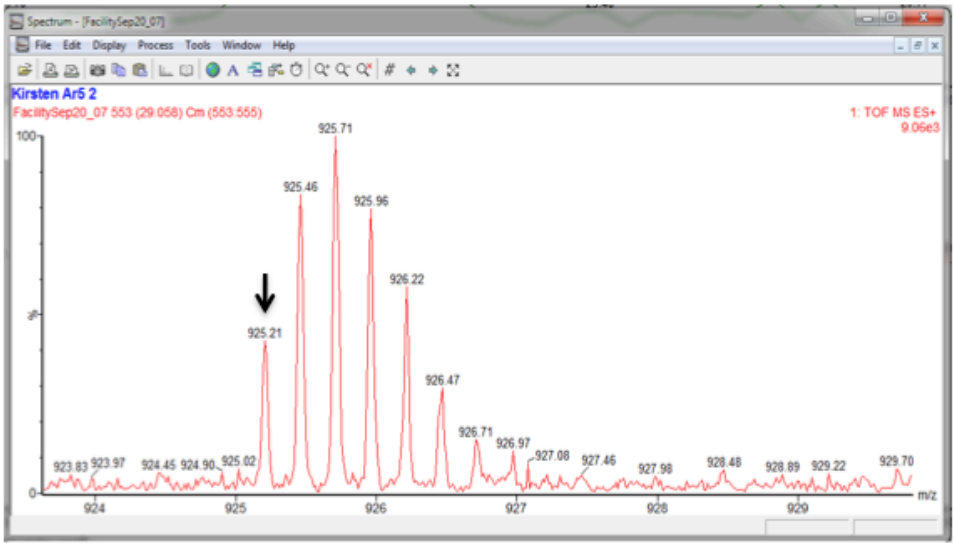

K140. Theoretical mass: 925.195 m/z – 4 charges

K140 peptide DVKPDNFLMGLGKK
SUMO peptide ELGMEEEDVIEVYQEQTGG

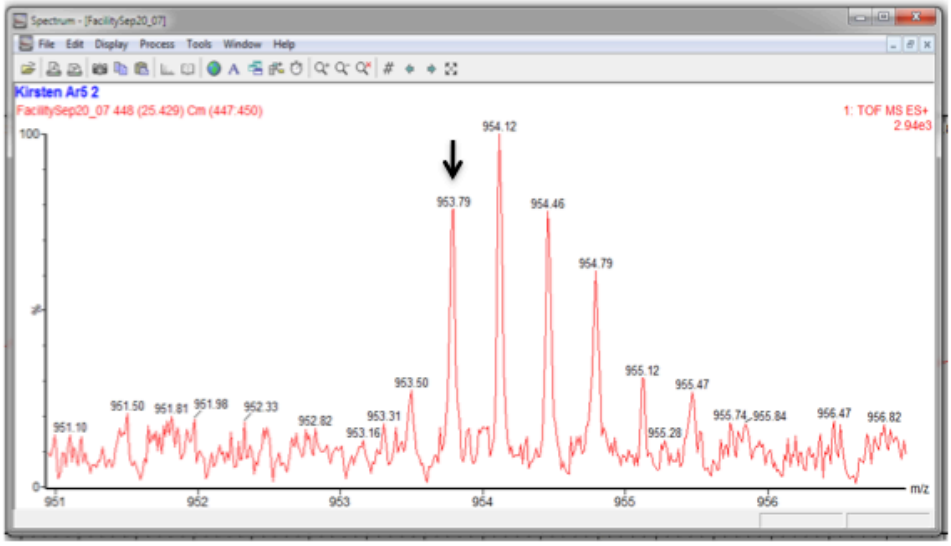

K224. Theoretical mass: 953.772 m/z – 3 charges

K224 peptide QKYER
SUMO peptide ELGMEEEDVIEVYQEQTGG

Figure 3.70. Mass spectra of SUMO-modified CK1 delta peptide K140 and K224

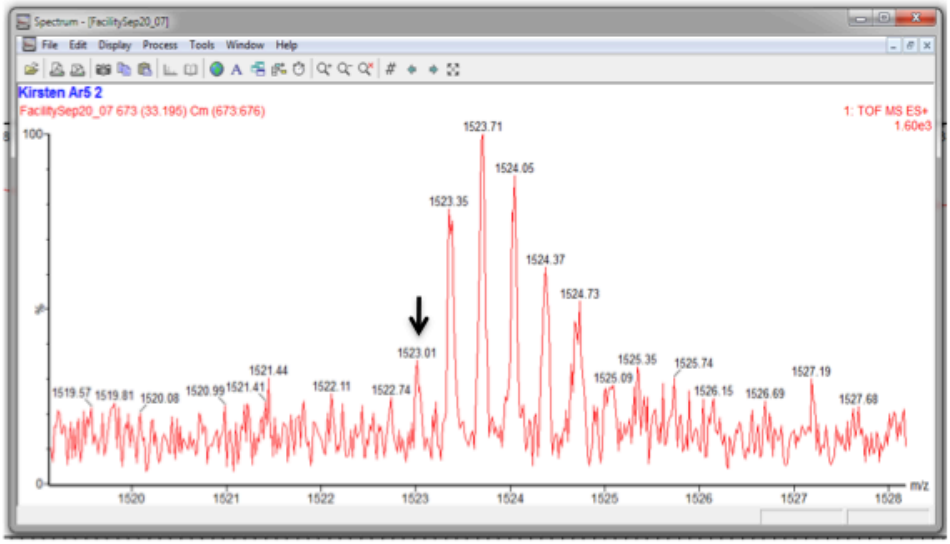

K294. Theoretical mass: 1523.019 m/z – 3 charges

K294 peptide QGFSYDYVFDWNMLKFGASR
SUMO peptide ELGMEEEDVIEVYQEQTGG

Figure 3.71. Mass spectrum of the SUMO-modified CK1 delta K294 peptide

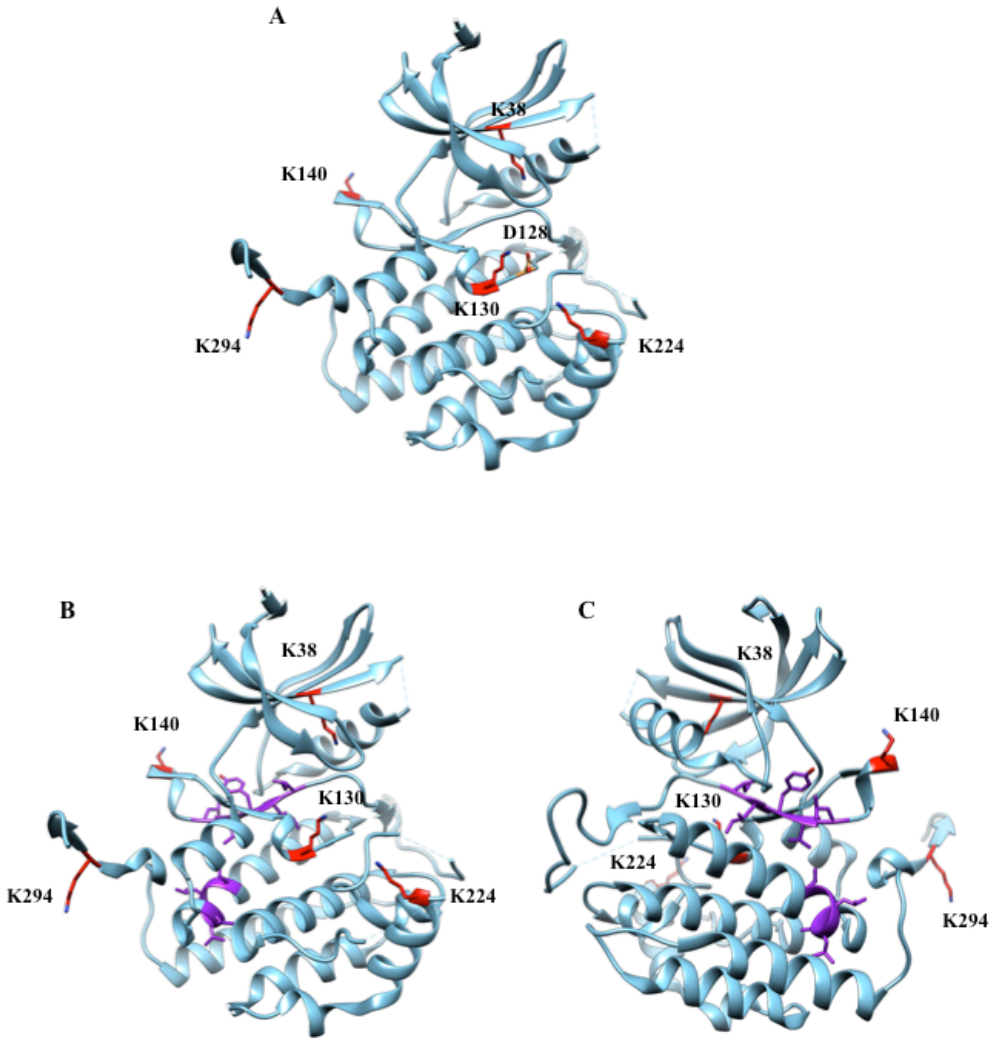

Figure 3.72. Highlighting the lysines in CK1 delta 1-317 which can be SUMO-modified according to the mass spectrometry results

UCSF Chimera was used for the analysis (UCSF- a visualization system for exploratory research and analysis. Pettersen EF, Goddard TD, Huang CC, Couch GS, Greenblatt DM, Meng EC, Ferrin TE. *J Comput Chem.* 2004 Oct; 25(13):1605-12). PDB reference: Casein kinase 1d, 4jjr.
Lysines are marked in red. The aspartic acid D128 important for proton transfer is marked in orange in A. The potential SIMs are marked in purple in B and C. With kind help from Dr Rajeka Perera.

K38 conserved in all CK1 isoforms (α,γ,δ,ε)	K38 is in the active site
K130 conserved in all CK1 isoforms	K130 in front of the active site/in the catalytic loop
K140 conserved in CK1 γ, δ and ε	K140 ?
K224 conserved in α, δ and ε	K224 is in the docking site for p53
K294 conserved in α, δ and ε	K294 ?

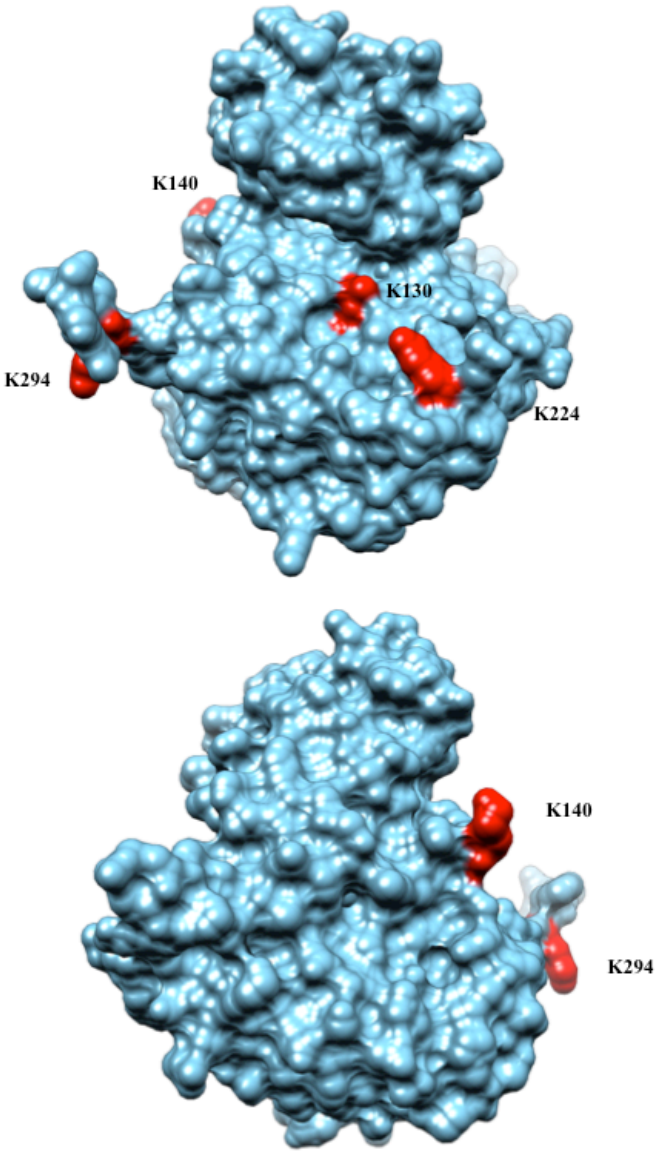

Figure 3.73. Highlighting the lysines in CK1 delta 1-317 which can be SUMO-modified according to the mass spectrometry results

UCSF Chimera was used for the analysis (UCSF- a visualization system for exploratory research and analysis. Pettersen EF, Goddard TD, Huang CC, Couch GS, Greenblatt DM, Meng EC, Ferrin TE. *J Comput Chem.* 2004 Oct; 25(13):1605-12). PDB reference: Casein kinase 1d, 4jjr.
Lysines are marked in red. K46 is not on the surface but might still be available to SUMO-modification because of the C-terminal GG-finger in SUMO. With kind help from Dr Rajeka Perera.

3.5.9 Kinase activity of CK1 delta and SUMO-modified CK1 delta

Kinase activity studies of CK1 delta 1-317 were performed in parallel to mapping the lysines involved in SUMO-modification. Because some of the SUMO-modified lysines in CK1 delta could provide some potential inhibition of the kinase activity and therefore be involved in the regulation of the kinase activity, kinase assay experiments were performed.

The ADP-Glo kinase assay from Promega was used and an overview of the principles employed in the assay method is shown in Figure 3.74.

A preliminary experiment was performed and the results can be seen in Figure 3.75. As expected, the activity of SUMO-modified CK1 delta 1-317 was lower than the unmodified kinase when used at a concentration of 20 ng. A purified CK1 delta 1-317 from NEB was used as a positive control. Two different concentrations of the purified proteins were tested in the assay. For unmodified CK1 delta there was no difference in activity between 20 ng and 100 ng of protein. For the modified version of the kinase the activity went up when 100 ng was used, which was expected. Several experiments followed to optimise the conditions for the assay. The length of the kinase assay was varied from 20-40 minutes. The length of the assay depends on the ATP concentration used in the assay and the amount of ATP was varied from 50-150 μM (Supplementary Figures 6.2, 6.3 and 6.4). The optimised conditions chosen were 13 ng protein + 240 μM substrate + 150 μM ATP. It was important to make sure that nothing was limiting the assay. These experiments were done in parallel to mapping the SUMO-modified lysines in CK1 delta 1-317, so the protein purification optimisation also influenced the kinase assay. In Figure 3.76 it can be seen that the activity of the purified proteins went down compared to the bought kinase. This was due to changes in the purification protocol and taking out the Triton X-100. It did not appear to be a problem as the difference between the unmodified and the modified CK1 kinase was the important point of interest and the tendency remained the same.

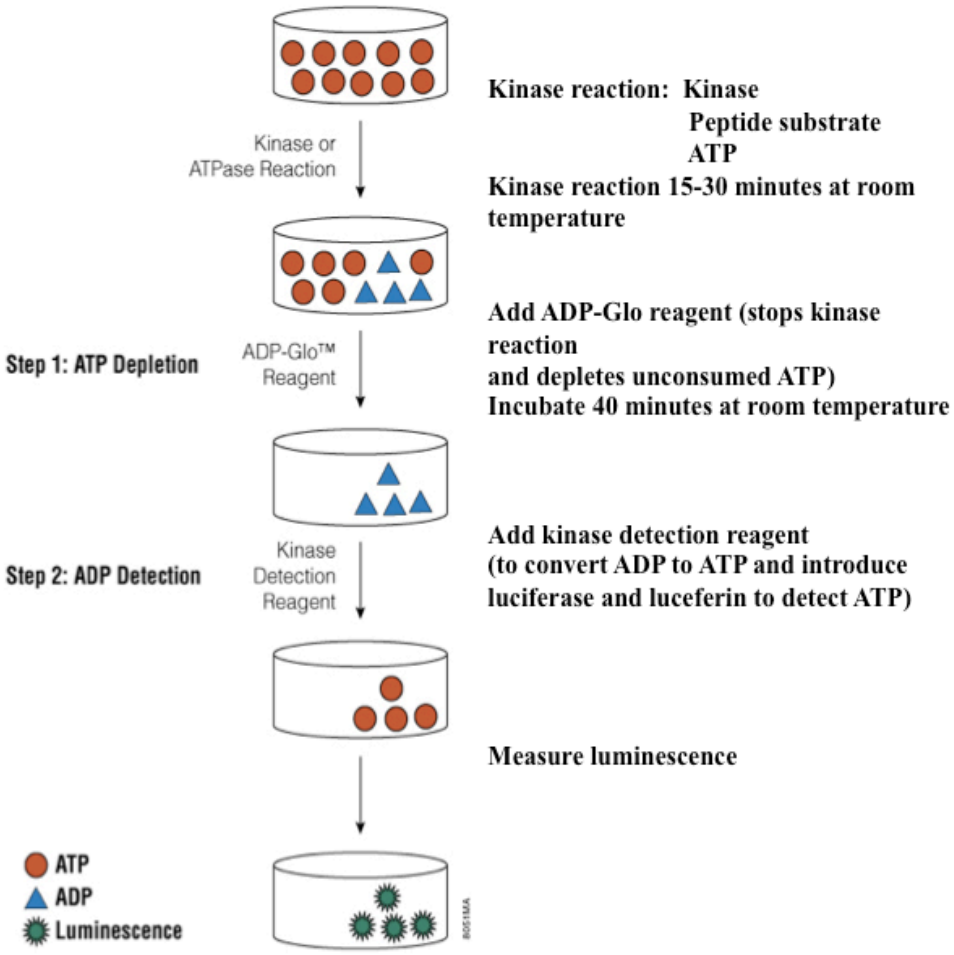

Figure 3.74. Overview of ADP-Glo assay (figure adapted from Promega)

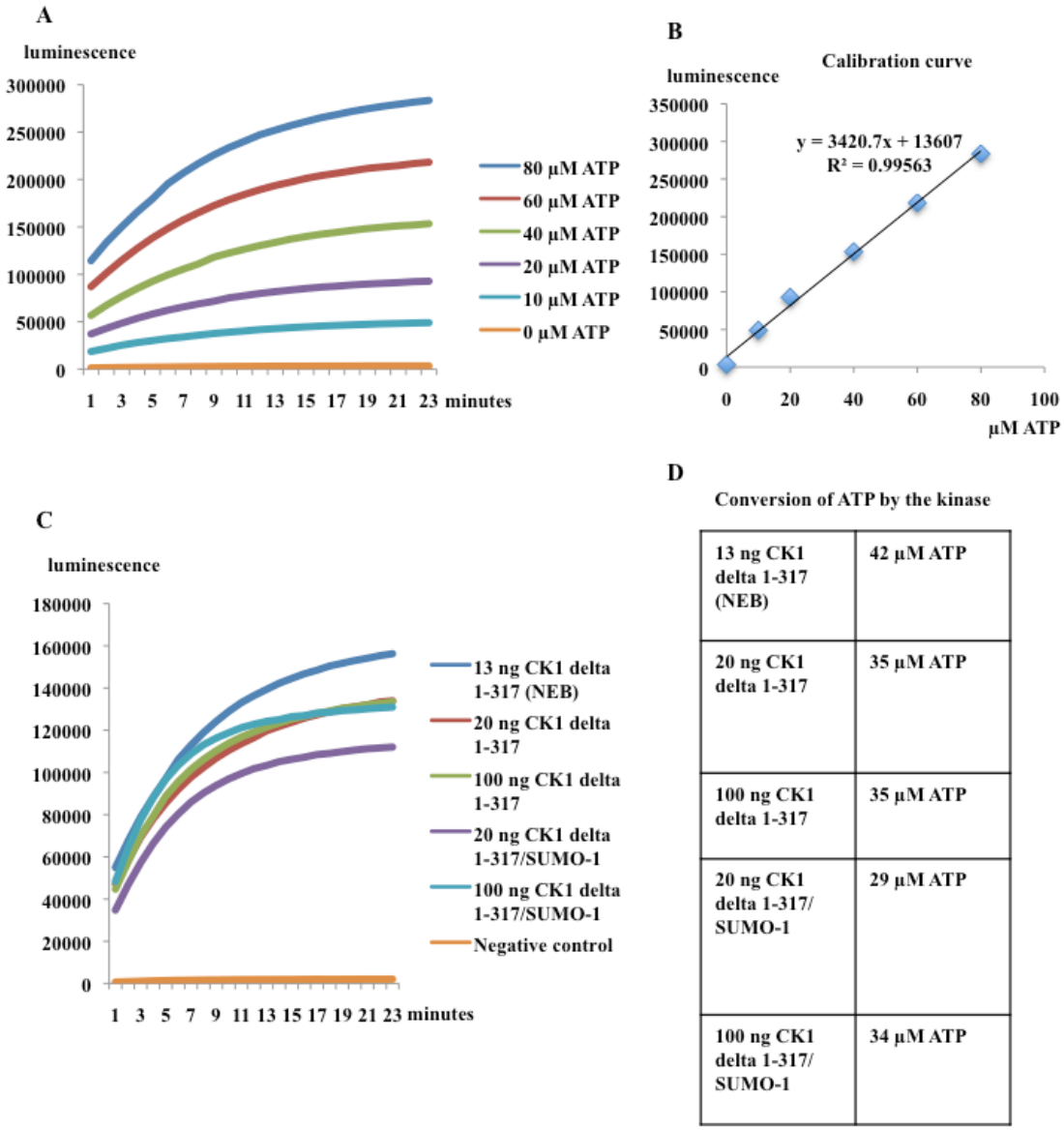

13 ng CK1 delta 1-317 (NEB)	42 µM ATP
20 ng CK1 delta 1-317	35 µM ATP
100 ng CK1 delta 1-317	35 µM ATP
20 ng CK1 delta 1-317/ SUMO-1	29 µM ATP
100 ng CK1 delta 1-317/ SUMO-1	34 µM ATP

Figure 3.75. Kinase assay with CK1 delta 1-317 and SUMO-1 modified CK1 delta 1-317

Kinase reaction: 13/26 ng CK1 + 240 µM CK1 peptide substrate [pS7} + 40 µM ATP
Kinase reaction 30 minutes at room temperature
ADP-Glo added
Incubated 40 minutes at room temperature
Kinase detection reagent added
Luminescense measured for 23 minutes

A: Standard curve
B: Calibration curve created using the standard curve
C: Kinase activity measured as luminescence
D: ATP converted by the kinase - calibration curve (B) used to convert luminescence from (C) into ATP concentrations

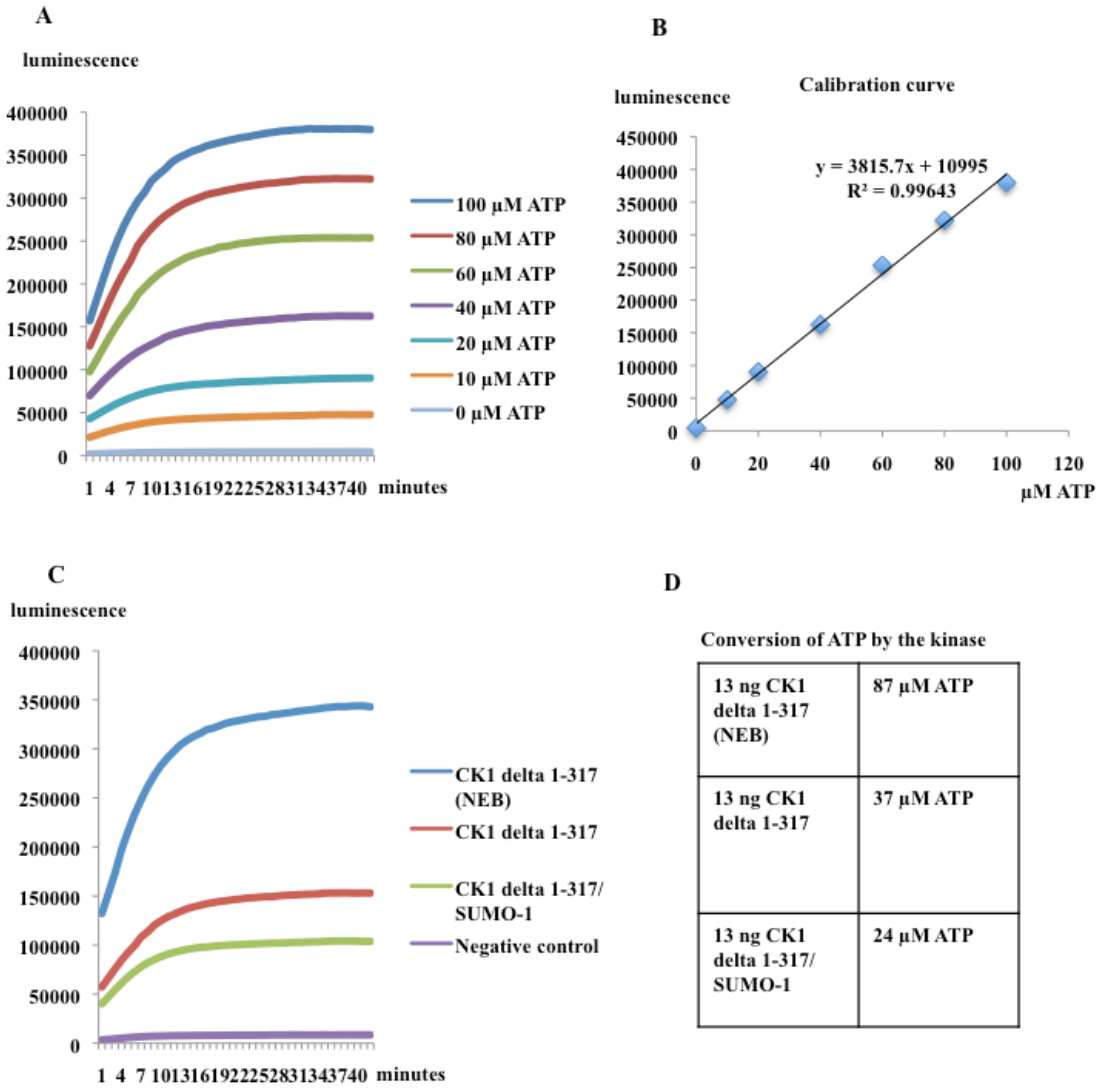

Figure 3.76. Kinase assay with CK1 delta 1-317 and SUMO-1 modified CK1 delta 1-317

Kinase reaction: 13 ng CK1 + 240 µM CK1 peptide substrate [pS7} + 150 µM ATP
Kinase reaction 30 minutes at room temperature
ADP-Glo added
Incubated 40 minutes at room temperature
Kinase detection reagent added
Luminescense measured for 40 minutes

A: Standard curve
B: Calibration curve created using the standard curve
C: Kinase activity measured as luminescence
D: ATP converted by the kinase - calibration curve (B) used to convert luminescence from (C) into ATP concentrations

Because it proved difficult to map the modified lysines in the CK1 delta 1-317 kinase in the *E.coli* system, the planned experiments were slightly altered. It had been intended to mutate all the lysines important for SUMO-modification in CK1 delta 1-317, then check the kinase activity and after that add the SUMO site back into the protein sequence, modify the kinase and check the activity again. That way it would have been possible to see how much each modified lysine inhibits the activity of CK1 delta. It proved to be difficult not only because one of the modified lysines was in the active site in CK1 delta but also because SUMO modified other lysines in the *E.coli* system when CK1 delta 1-317 was mutated.

The next step was to take the purified and modified CK1 kinase and use a purified SUMO protease to de-modify it and then to measure the activity before and after in the kinase assay. Some optimisation experiments were performed to find the length of time for the de-modification but also to see if the SUMO protease would cleave in the buffer needed for the following kinase experiment. It was even possible to see the cleavage in a Coomassie Blue stain although only faintly (Supplementary Figure 6.5A). Another experiment was performed and this time the cleavage was checked in a western blot (Supplementary Figure 6.5B).

For the final experiment the unmodified and modified CK1 delta 1-317 protein was purified again, then checked in a western blot (Figure 3.77A). The fractions marked with an arrow were concentrated and a SUMO protease assay performed (Figure 3.77B). The protein before and after protease cleavage was used in the kinase assay (Figure 3.78). Again, as observed in all kinase experiments, the activity of the modified kinase was lower than the unmodified kinase. Surprisingly and very unexpectedly the activity went up for both the modified and unmodified kinase after treatment with SUMO protease. Another experiment was done to see if that would be the case for CK1 delta kinase from NEB as well. As can be seen in Figure 3.79, this was not the case. Here the activity went down after treatment with the SUMO protease. This is due to dilution of the kinase when adding the protease. One possible explanation could be that the purified kinase was not folded so well after taking away the Triton X-100 in the elution buffer.

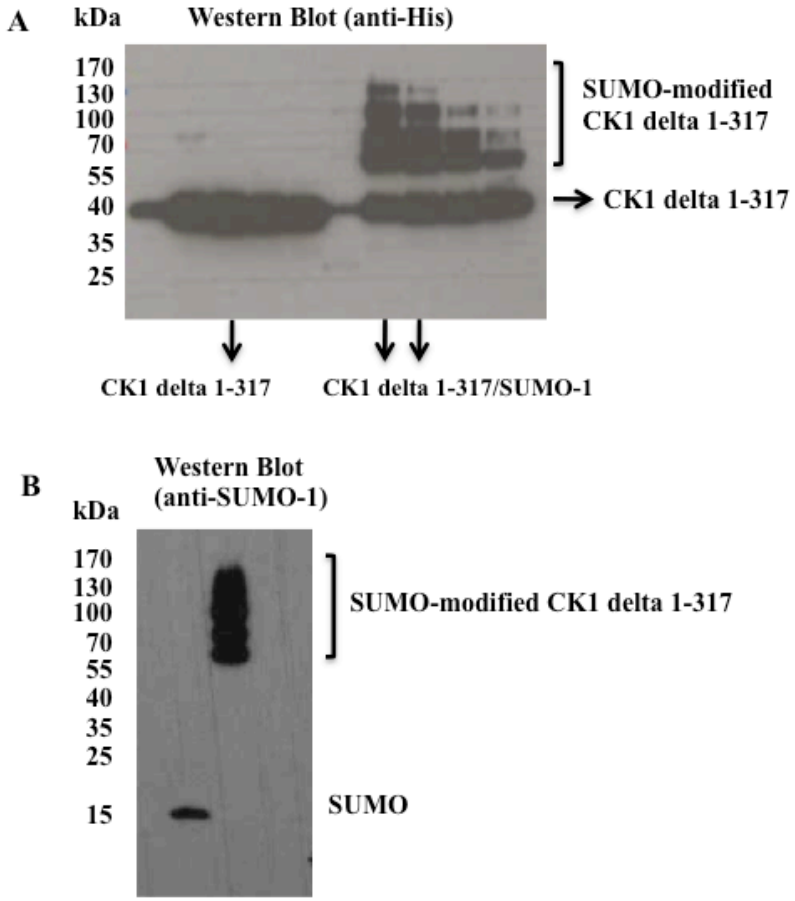

Figure 3.77. SUMO protease cleavage of SUMO-modified CK1 delta 1-317

BL21-Gold(DE3) cells co-transformed with pET-28a CK1 delta 1-317 SUMO mutant and pT-Trx-AU(E1)-Ubc9(E2)-SUMO-1 were induced with 0.2 mM IPTG and left to grow overnight at 22 ˚C. Proteins were purified and several fractions were loaded onto a 4-20% polyacrylamide gradient gel, transferred onto a nitrocellulose membrane and the expressed proteins were detected using an anti-His mAb (A) or polyclonal rabbit anti-SUMO-1 antibodies after 4 hours' cleavage with the SUMO protease at room temperature (B).

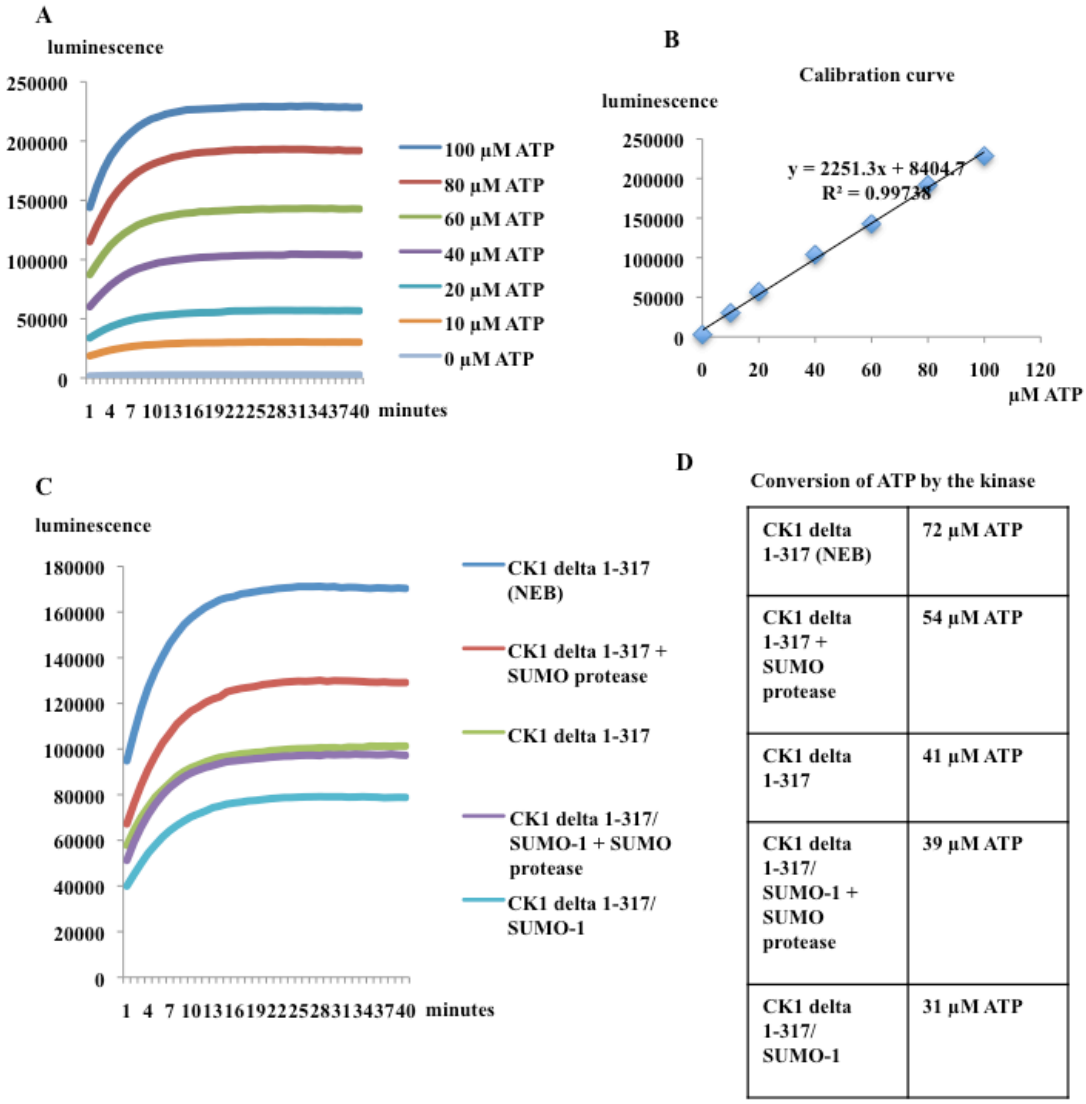

CK1 delta 1-317 (NEB)	72 µM ATP
CK1 delta 1-317 + SUMO protease	54 µM ATP
CK1 delta 1-317	41 µM ATP
CK1 delta 1-317/ SUMO-1 + SUMO protease	39 µM ATP
CK1 delta 1-317/ SUMO-1	31 µM ATP

Figure 3.78. Kinase assay with CK1 delta 1-317, SUMO-1 modified CK1 delta 1-317 and SUMO-1 modified CK1 delta treated with SUMO protease

Kinase reaction: 13 ng CK1 + 240 µM CK1 peptide substrate [pS7} + 150 µM ATP
Kinase reaction 30 minutes at room temperature
ADP-Glo added
Incubated 40 minutes at room temperature
Kinase detection reagent added
Luminescense measured for 40 minutes

A: Standard curve
B: Calibration curve created using the standard curve
C: Kinase activity measured as luminescence
D: ATP converted by the kinase - calibration curve (B) used to convert luminescence from (C) into ATP concentrations

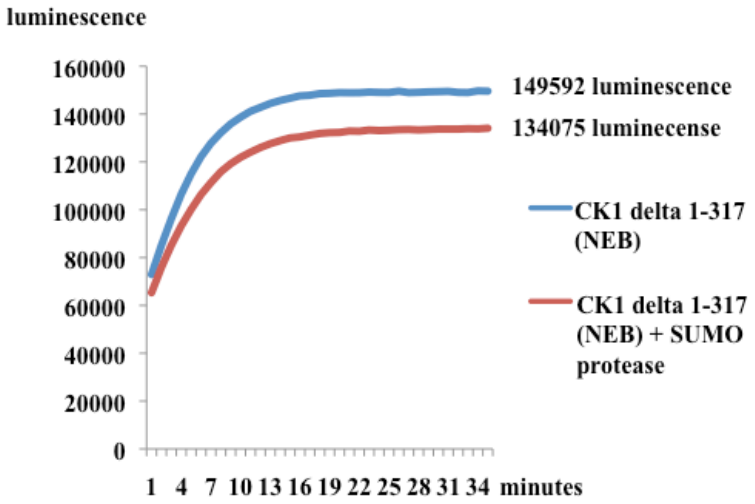

Figure 3.79. Activity of CK1 delta from NEB before and after treatment with the SUMO protease

Kinase reaction: 13 ng CK1 + 240 µM CK1 peptide substrate [pS7} + 150 µM ATP
Kinase reaction was left 20 minutes at room temperature
ADP-Glo added
Incubated 40 minutes at room temperature
Kinase detection reagent added
Luminescense measured for 35 minutes

3.5.10 Summary

- **SuPr-1 colocalised with DEFs where it hydrolysed SUMO from the filaments**
- **SuPr-1 did not colocalise with the DEFs formed by the FADD phosphorylation mutants**
- **The CK1 alpha LS protein has a very short half life in mammalian cells and mapping of the lysines necessary for SUMO modification was not possible**
- **CK1 alpha LS and CK1 alpha splice variants were insoluble when expressed in *E.coli***
- **Lysines important for SUMO modification in CK1 alpha are conserved in CK1 delta and mapped in this isoform**
- **Mass spectrometry analysis showed that CK1 delta 1-317 was SUMO-modified at K38, K130, K140, K224 and K294.**
- **SUMO modification of CK1 delta inhibited its kinase activity and could potentially regulate the localisation of the kinase**

3.5.11 Conclusion and hypothesis

CK1 alpha was insoluble when expressed in *E.coli* and instead the necessary lysines for SUMO-modification were mapped in CK1 delta, which is 76% identical to the amino acid level of CK1 alpha. The important and highly predicted lysines important for SUMO-modification are conserved in the isoforms. Mass spectrometry analysis was used to map the SUMO-modified lysines in CK1 delta 1-317. SUMO-modification of the kinase inhibited its kinase activity and could potentially regulate the localisation of the kinase.

3.5.12 Summary of the of the colocalisation studies

DEFs were formed by overexpressed FADD and were used here to mimic interactions and functionality. DEFs localised to the ICD where they colocalised with NLS-vimentin. PML NBs also localise to the ICD. Soon after the transfection of FADD and during early stages of the formation of the DEFs they colocalised with the PML NBs without disrupting them. At a later stage the results showed that a protein, which

could potentially be CK1 alpha, was recruited to the filaments and SUMO-modified. CK1 might be recruited there already modified, although the results indicated that it occurs at a later time point. Early after transfection of FADD, CK1 was observed localising to the DEFs without colocalisation of SUMO. The colocalisation of CK1 alpha and SUMO increased over time. This led to SUMO colocalising with the DEFs in the nucleus, which again led to other SUMO-modified proteins leaving the PML NBs all at different time points. When a SUMO-specific protease colocalised to DEFs there was no disruption of the PML NBs. This suggested that SUMO is needed for the disruption of the PML NBs.

4 Discussion

4.1 The role of PML and PML NBs in FADD-mediated apoptosis

4.1.1 Introduction

In the following chapter all the results retrieved during my PhD are considered and used to try to explain the role of PML and PML NBs in FADD-mediated apoptosis. The FADD protein is involved in death receptor-mediated apoptosis and when overexpressed forms DEFs which are used here to mimic interactions and functionality. Phosphorylation of FADD, which is involved in cell cycle arrest, is highly regulated by the CK1 alpha kinase. A new role for PML and PML NBs in regulating kinase activity and therefore phosphorylation of proteins is proposed.

4.1.2 Signal transduction pathways as part of a PML regulatory cascade

As a part of functional studies of the PML protein done by Boddy et al., 1996, TFAF-1 was identified as an interacting partner with PMLVI in a yeast two-hybrid assay. Nothing else had been published about TFAF-1 at the time and it was only when I started my project that this interaction began to be investigated further.

Only a partial coding sequence of TFAF-1 was available at the beginning of my PhD studies and it is tempting to think that this clone was identified as a yeast two-hybrid interaction partner with TRAF4, hence the name 'TRAF4-associated factor 1' (TFAF-1). However, this has not been corroborated experimentally. An anti-peptide antibody was generated against the TFAF-1 protein and used in colocalisation studies with PML. Neither endogenous nor overexpressed TFAF-1 colocalised with PML at PML NBs. TFAF-1 showed a diffuse distribution in the nucleus and the cytoplasm. A small fraction of PML is soluble in the nucleoplasm and this might be that fraction interacting with TFAF-1. The TFAF-1 protein contains a coiled-coil domain and this is probably the domain interacting with the coiled-coil domain in the PML protein. An interesting observation is that the domain structure of PML is very similar to the domain structure of TRAF4 and the family of TRAF proteins (Arch et al., 1998). All proteins contain the RING finger, several zinc finger motifs and a coiled-coil domain. When TFAF-1 was expressed as a fusion protein with the DsRed protein it formed

cytoplasmic filaments. These filaments were shown to be a part of the microtubule cytoskeleton and co-localised in the cytoplasm with DEFs formed by the FADD protein. This suggested that TFAF-1 could be involved in Fas-mediated apoptosis. The DsRed protein has strong oligomerisation properties and has been shown to form at least a tetramer or even a weak octamer (Baird et al., 2000). This could be the reason, together with TFAF-1 probably also being able to homo-oligomerize through its coiled-coil domain, for the DsRed/TFAF-1 filament formation. TFAF-1 oligomerisation is unlikely on its own to form the filaments. The filament formation should then be observed when TFAF-1 is expressed with the FLAG-tag as well, yet this was not the case. Because the main interest was to investigate PML and PML nuclear bodies involved in apoptosis – and especially death receptor-mediated apoptosis – the colocalisation studies with the DEFs were investigated further.

During the course of this study other publications have reported on TFAF-1, which now has alternate names such as FLJ14502, HSD11, chromosome 15 open reading frame 23 and SKAP (for Small Kinetochore Associated Protein). TFAF-1/SKAP is shown to be a microtubule-associated protein and localises to kinetochores and the mitotic spindle during mitosis. This localisation suggests a function in mitosis (Fang et al., 2009; Schmidt et al., 2010; Dunsch et al., 2011). Depletion of TFAF-1/SKAP delays the metaphase to anaphase transition, causes elongated spindle and partial segregation of chromosomes, and in some cells multipolar spindles are observed (Fang et al., 2009; Schmidt et al., 2010; Dunsch et al., 2011).
It could be interesting to go back to the PML/TFAF-1 interaction studies, especially because it has been shown that PML -/- cells show abrogation in the mitotic entry and in the response to spindle depolymerisation (Daniels et al., 2004).

4.1.3 PML nuclear bodies and death-effector filaments

It was observed that pDsRed/TFAF-1 filaments colocalise in the cytoplasm with DEFs formed by FADD. Although the DsRed/TFAF-1 filaments were shown to be cytoplasmic filaments, the PML NB formation seemed to be altered in some of the pDsRed/TFAF-1-expressing cells. It was also observed that the DEFs formed by FADD changed the pattern of PML NBs, in that the DEFs took PML into small tracks. It was shown that DEFs are not only cytoplasmic filaments as published earlier (Siegel et al., 1998) but also went through the nucleus, where they localised to the

interchromosomal domains (ICD). PML has been shown to localise to the ICD together with other nuclear body components like Cajal bodies (Bridger et al., 1998). The DEFs did not disrupt Cajal bodies, HIPK2 bodies or nucleoli and the disruption seemed to be specific for PML NBs.

Many different cell lines were tested after transfection of FADD but it did not seem to make any obvious difference to the formation of DEFs or track/filament formation of PML NBs. No difference was observed between U2OS and Saos-2 (p53 null cell line) cells. This suggested that p53 was not involved in the filament formation of DEFs and in the track/filament formation of PML NBs. A third cell line, HT1080 cells, were used in the studies but also here no difference was observed in the formation of DEFs or track/filament formation of PML NBs.

Other major PML NB constituents such as SUMO, Sp100 and Daxx were also taken into the DEFs. SUMO associated with the DEFs in longer filaments and is probably the first member of the constituents to change from bodies to filaments. SUMO was already disrupted 24 hours after tranfection of FADD and so was PML, whereas Sp100 and Daxx followed later, around 48 hours after transfection. PML tracks and SUMO filaments colocalised in DEFs and PML NB disruption increased over time. Shortly after the transfection of FADD the DEFs formed along the ICD and PML NBs associated with them before disruption. DEFs were formed by overexpressing the FADD protein and were used here to mimic functionality.

It was important to know if not only overexpressed FADD but also endogenous levels could disrupt the PML NBs. When cells were treated with apoptotic inducers FADD formed some kind of filaments which could be DEFs, but they did not disrupt the PML NBs. These filaments appeared to localise to the cytoplasm and therefore would be unable to disrupt the PML NBs.

Caspase-8 has been shown to be recruited to the DEFs (Siegel et al., 1998). Full-length caspase-8 cannot form DEFs; only the caspase-8 DED-AB and caspase-8 DED-B are able (Siegel et al., 1998). It was interesting to see whether the PML NB disruption was dependent on the recruitment of caspases. This did not seem to be the case as filament/track formation of SUMO and PML was still observed in FADD-transfected cells after treatment with caspase inhibitor z-VAD-fmk. When caspase-8 DED-AB was overexpressed as a fusion protein with GFP it formed DEFs localising to the cytoplasm and therefore did not disrupt the PML NBs. Another observation made to confirm that the formation of DEFs and disruption of PML NBs was

independent of caspases was when FADD transfections were done with CrmA. CrmA is a serpin-like protease inhibitor and blocks the activities of many caspases. Also here there was no difference in the formation of DEFs or in the disruption of PML NBs.

Many viral proteins also disrupt PML NBs and the disruption observed here by the DEFs reminded one of the PML track formation caused by Ad5 E4 Orf3. DEFs and filaments/tracks formed by Ad5 E4 Orf3 showed a partial colocalisation, which meant PML tracks formed by the aforementioned proteins could be the same. PML II has been shown to interact with Ad5 E4 Orf3 (Hoppe et al., 2006) and maybe there was a possible but as yet unidentified interaction between the FADD DED and PML II.

DEFs seemed to target the PML NBs specifically. PML -/- cells did not have PML NBs and in these cells the DEF formation appeared a little different. The DEFs were shorter and non-continuous and it was almost as if the formation was disrupted, which could suggest that PML or PML NBs are needed for the formation. Co-transfection of FADD and SUMO did not change the formation of DEFs in PML -/- cells, which suggested that it was not SUMO alone that was needed for the DEF formation.

Phosphorylation of FADD has been shown to be involved in the non-apoptotic properties of FADD (Alappat et al., 2005) and PML -/- cells are protected from apoptosis induced by Fas and TNF (Wang et al., 1998b). It was therefore interesting to look at phosphorylation of FADD in PML -/- cells. Surprisingly, there was less phosphorylated FADD found in PML -/- cells compared to NIH/3T3 cells. This experiment might not be conclusive because two different cell lines from two different mouse strains were used. This was done because the PML wild type cell line was not available to us at the time when the experiments were performed. Phosphorylated FADD localises to the nucleus and not at the death receptors and is usually associated with its non-apoptotic properties (Zhang et al., 2008). As mentioned above, it was difficult to draw any conclusion from the experiment here. Another experiment was conducted in a PMLIII-inducible cell line but there was no difference detected in phosphorylation of transfected FADD before and after induction of PML. There was only one PML isoform expressed in the inducible cell line and a much better experiment would have been to deplete PML and then observe whether there was a difference in FADD phosphorylation and formation of DEFs before and after depletion. It was attempted to make a stable cell line where PML was depleted but it was not achieved during the studies.

4.1.4 PML nuclear bodies and FADD

PML -/- KO mice and cells have an altered response to death receptor ligands so it was very interesting to observe that DEFs change the pattern of PML NBs. It was tempting to think that it was a direct interaction between PML and FADD. PML could associate with the DEFs and because PML is needed for the NB formation the other constituents could co-associate with PML. But this did not seem to be the case, at least not for the PML isoform tested here. No interaction was found between FADD and PML IV (personal communication with T.G. Hofmann). A better option would probably have been to test for an interaction between the isoform PML II and FADD after finding a partial colocalisation of the the DEFs and the filaments formed by Ad5 E4 Orf3.

Truncated FADD constructs and FADD mutants were made to try to map the domain in FADD necessary for the disruption of the PML NBs. The FADD DED was sufficient to change the localisation of PML and Sp100. The pattern of PML and Sp100 looked very much like the PML tracks formed by Ad5 E4 Orf3. The dominant negative mutant FADD-DN containing the death domain (DD) and the C-terminus of FADD showed a diffuse distribution and did not change the localisation of PML NBs. These results suggesed that the DED and the formation of DEFs were necessary for the disruption of the PML NBs. Earlier results suggested that caspase activation was not important for PML NB disruption. This was confirmed again by transfecting the mutant FADD F25G. This mutant has a mutation in the DED and reduced binding to caspase-8. It was able to form DEFs in some of the transfected cells and to disrupt the PML NBs. Again, caspase activation did not seem to be necessary for the disruption of the PML NBs.

Because SUMO colocalised to the DEFs in the nucleus it was conjectured that it could be FADD getting SUMO-modified. Two potential lysines, K35 which is a part of a potential NLS, and K125, were mutated to arginines but no change in the PML NB track/filament formation was detected. Nuclear fractions from FADD-transfected cells were loaded onto a polyacrylamide gel and a western blot was done using anti-FADD antibodies, but also here no SUMO-modified FADD was observed. This concurs with the literature where no interaction or SUMO-modification of FADD has

been reported and suggested that another protein was being recruited to the DEFs and then SUMO-modified, or that it could be recruited already SUMO-modified.

Independent studies using only the C-terminus of FADD containing the DD result in the dominant negative mutant FADD-DN which can bind the death receptor but not caspase-8 because of the missing DED. It is possible to disrupt this interaction with the death receptor Fas by mutating the alanine A174 in the DD to a proline. A174P is still able to bind to two other interacting partners, TRADD and RIP, but is unable to induce apoptosis (Morgan et al., 2001). This mutation is also in the kinase-binding domain of FADD and the mutant FADD-DN A174P has been shown to be less phosphorylated compared to wild-type FADD (Alappat et al., 2005). Interestingly this mutant FADD A174P localised partially to PML NBs. A possible explanation could be that FADD might be recruited to PML NBs under certain conditions where it interacts with CK1 alpha before getting phosphorylated. FADD A174P could still be recruited to PML NBs but the phosphorylation is disrupted and FADD stays in the PML NBs.

Phosphorylation of FADD is mapped to the serine 194 (Scaffidi et al., 2000). Phosphorylation of FADD is important for cell cycle arrest in G_2/M and thereby in regulating the apoptotic properties of FADD (Alappat et al., 2003). The serine was mutated to an alanine to create a phospho-dead mutant. Two other two mutants were made as well, serine to glutamic acid or aspartic acid, to mimic phosphorylation. The interesting results showed that FADD had to be phosphorylated to disrupt the PML NBs. The DEFs formed by the phospho-mutants were still nuclear and the PML NBs colocalised with the filaments but they were not disrupted. No obvious difference between phosphorylated and unphosphorylated DEFs was detected. Phosphorylation of the DEFs seemed to be necessary for the disruption of the PML NBs. These results also suggested that the disruption of the PML NBs is specific and is not just the DEFs penetrating the nucleus. Had the latter been the case one would have expected it to occur with the unphosphoryltated DEFs as well. The DEFs mimic interactions and functionality but filament formation probably only occurs when FADD is overexpressed and not with endogenous levels of the FADD protein.

4.1.5 The role of PML in FADD phosphorylation

HIPK3 was the first kinase published to phosphorylate FADD (Rochat-Steiner et al., 2000). HIPK3 is shown to partially colocalise with PML and also phospho-FADD.

This was the perfect candidate to phosphorylate FADD maybe even at the PML NBs, but unfortunately it was not possible to reproduce the original results.

The focus was therefore on casein kinase 1 alpha (CK1 alpha), a serine/threonine kinase and the second candidate to be published to phosphorylate FADD (Alappat et al., 2005). CK1 alpha is expressed as four different splice variants with or without two inserts, L and S. The L insert contains a potential NLS and the longest isoform LS was chosen for this study. All four splice variants have been shown to phosphorylate FADD. CK1 alpha LS localises to splicing speckles when overexpressed (Gross et al., 1999). The CK1 family of proteins is highly conserved and has been shown to be involved in cell cycle progression, cell differentiation and proliferation, DNA repair and chromosome segregation (Knippschild et al., 2005).

Both overexpressed and endogenous CK1 alpha was recruited to the DEFs where it colocalised with SUMO in many of the transfected cells. SUMO was not always detected in the filaments and this suggested that it could be a cell cycle-dependent phenomenon or that SUMO could be recruited later, after phosphorylation of FADD. Interestingly, CK1 alpha was not recruited to any of the DEFs formed by the phospho-FADD mutants. It was expected that CK1 alpha LS would colocalise with the phospho-mutant DEFs but just not phosphosrylate FADD. The serine 194 is not localised in the kinase binding domain so why would it interrupt the binding? These results were consistent with the observation that FADD had to be phosphorylated to disrupt the PML NBs and further strengthened the enquiry. Is it SUMO-modified CK1 alpha observed in the DEFs? SUMO modification of the kinase, potentially at PML NBs, could regulate the localisation and the activity of the kinase.

4.1.6 SUMO-modification of CK1 alpha LS in mammalian cells

By using servers to predict SUMO-modification sites in the CK1 alpha LS protein, several potential sites were found. SUMO-modification of CK1 alpha LS can be another way of regulating localisation and activity of CK1 just as autophosphorylation has been shown to regulate the activity of several CK1 family members (Budini et al., 2009; Rivers et al., 1998). A SUMO-specific protease named SuPr-1 is recruited to the DEFs and the colocalisation of SuPr-1 and DEFs resulted in no disruption of the PML NBs. This suggested that SUMO is needed for the disruption of PML NBs. It is probably a case of SUMO leaving the PML NBs first and then all other NB

components following. The inactive mutant SuPr-1 C466S colocalised to the DEFs but it did not hydrolyse SUMO from them and the PML NB disruption was still observed. As expected, neither the active SUMO protease nor the inactive form were recruited to the DEFs formed by the phospho-FADD mutants.

From all the colocalisation studies it was clear that the colocalisation of the DEFs and the PML NBs increased over time. The DEFs are forming in the ICD and the PML NBs are colocalising with the DEFs. A protein is recruited to the DEFs, which might be CK1 alpha, and is being SUMO-modified. This causes SUMO to leave the bodies and all the other SUMO-modified PML NB components follow at different times (Summary in Figure 4.1).

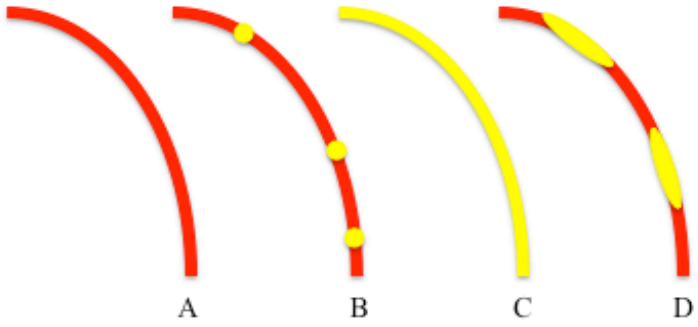

Figure 4.1. Overview of DEF formation and PML NB disruption

A: DEFs are forming in the ICD.

B: DEFs colocalise with PML NBs in the ICD.

C: A protein, possibly CK1 alpha, is recruited to the DEFs and is being SUMO-modified. This results in colocalisation of SUMO and DEFs.

D: SUMO is recruited away from the PML NBs and other PML NB components follow. This results in colocalisation of other SUMO-modified PML NB components and DEFs.

CK1 alpha LS was overexpressed with or without SUMO in different mammalian cell lines to try and confirm the predicted SUMO-modification of CK1 alpha. SUMO-1,2 and 3 were tested together with eleven CK1 alpha LS SUMO mutants, but the results were inconclusive. Higher migrating bands, which could be SUMO-modified CK1 alpha, were detected after cotransfection of CK1 alpha LS and either EGFP-SUMO-1

or MLV-SUMO-1. It proved to be very difficult to map the lysines involved in the SUMO modification of CK1 alpha LS using mammalian cells because the CK1 alpha LS splice variant has a very short half-life of only 100 minutes (Burzio et al., 2002). This resulted in very little difference observed between the many mutants tested with and without SUMO in western blots. Only one mutant showed any difference in immunofluorescence studies. CK1 alpha LS K138R caused an increase in SUMO filaments after co-transfection with FADD. This could be due to the mutant being more active and phosphorylating FADD more efficiently and then following that, becoming SUMO-modified.

These experiments could possibly be repeated with inhibitors of deSUMOylases. This could lead to a more conclusive result. Another experiment, such as co-immunoprecipitation studies between CK1 and SUMO, could also lead to more specific results. Inhibitors of deSUMOylases were not used routinely when the experiments were conducted for this study.

4.1.7 Expression and SUMO-modification of CK1 alpha LS in *E.coli*

A new SUMO-modification system using *E.coli* was set up to try to map the necessary lysines in CK1 alpha LS. In this system the SUMO-modification machinery is expressed from one plasmid and the protein of interest from another plasmid. Full-length CK1 alpha LS and three other shorter constructs – CK1 alpha aa 1-325 (the shortest splice variant); a mutant CK1 alpha aa 1-325 S313G; and a truncated CK1 alpha aa 1-301 – were all tested under many different conditions. Cell-free expression systems were tested to avoid potential degradation or toxicity. Different temperatures were tested for better protein folding, but no matter what changes were made the CK1 alpha isoform stayed mainly insoluble and therefore unable to be SUMO-modified. A mutant strain of BL21 which has been optimised for expression of insoluble proteins in a soluble form was tested but also here the CK1 alpha remained insoluble.

CK1 alpha is known to be 76% identical to the amino acid level of CK1 delta (Gross and Anderson, 1998) and most of the lysines important for SUMO modification are conserved through the CK1 family as well. CK1 delta has been used for crystallisation studies and this isoform was chosen for the SUMO-modification studies (Longenecker et al., 1996; Zeringo et al., 2013).

In the meantime it is possible to buy purified CK1 alpha S protein. The CK1 alpha S protein is expressed in insect cells, which suggest that the CK1 protein needs post-

translational modification that is not available in *E.coli* for proper protein folding and solubility.

4.1.8 Expression and SUMO-modification of CK1 delta in *E.coli*

CK1 delta 1-317 was soluble and SUMO-modified by SUMO-1 and SUMO-3 in the *E.coli* expression system. SUMO-1 was chosen for the expression and SUMO-modification studies as SUMO-1 does not make SUMO-chains (Bayer et al., 1998), and the higher molecular bands would each count for one SUMO attachment.

Optimisation of expression and SUMO-modification of CK1 delta 1-317 was conducted and a better purification was seen using a Cobalt-affinity column, which has a very low non-specific binding. After adding a C-terminal His-tag to the protein as well as having the N-terminal His-tag, a much better binding to the affinity column was found. This could be due to folding of the CK1 delta protein and the N-terminal His-tag not being properly exposed. The protocol used from (Burzio et al., 2002) uses 1 % Triton X-100 in the elution buffer. This caused the purified protein to produce an indisctict band pattern when run on a polyacrylamide gel and made it very difficult to distinguish between the higher-migrating SUMO-modified bands. Therefore the elution buffer was used without Triton X-100. This causes the protein to be more likely to aggregate and all assays were carried out on the same day of purification or on the day after.

Several CK1 delta 1-317 SUMO mutants were created in the hope of being able to map the lysines involved in the modification. Many overnight expression and modification experiments were performed but it became clear from the western blots that as soon as mutations were introduced into CK1 delta 1-317, SUMO started to modify other non-specific lysines in the CK1 delta 1-317 protein. Because of this, mass spectrometry of the SUMO-modifed CK1 delta protein was used to identify the crucial lysines. In parallel, expression and SUMO-modifications studies were continued at shorter time points as this made it less likely to force-modify the protein and SUMO less likely modify other unspecific lysines. After 5-6 hours' expression instead of overnight, (as described by Uchimura et al., 2004 and Saitoh et al., 2009) it looked far more promising, although it was still not exactly clear which lysines are modified. It was only after analysis of the mass spectrometry data was performed that a much clearer result appeared.

4.1.9 Mass spectrometry of SUMO-modified CK1 delta 1-317 from *E.coli*

The mass spectrometry of SUMO-modifed CK1 delta 1-317 was undertaken by Dr Paul Hitchen in the CISBIO Mass Spectrometry Core Facility at Imperial College London, but all the data analyses calculating potential charges and masses I conducted manually and checked them in the mass spectrometry dataset. CK1 delta was found to be SUMO-modified at K38, which is the active site and involved in binding of ATP. When looking at the surface structure of the CK1 delta protein in Figure 3.73 (p. 171) it is clear that this lysine is hidden in the active site, but because the GG-finger in SUMO-1 is quite long and flexible it still appears to be possible to modify K38. K38 is a SUMO consensus site and will probably be modified if the lysine is exposed and available to the SUMO-modification machinery. This was the only lysine that was easily mapped as SUMO-modified in the *E.coli* system using western blotting. The other lysines detected in the mass spectrometry analysis are all exposed and on the surface of the CK1 delta protein. K130 is located in the catalytic pocket and very close to the aspartic acid D128 (Figure 3.72A, p. 170), which is the catalytic base (Longenecker et al., 1996; Hanks, 2003). SUMO-modification at K130 could regulate the activity of the kinase by interfering with the catalytic domain. This is consistent with the observation of the CK1 alpha LS K138R mutant where more SUMO filaments are formed after co-transfection of FADD, likely due to higher activity of this mutant. Absence of SUMO modification at this lysine in CK1 results in less inhibition of the catalytic loop and therefore higher kinase activity. K224 is next to a region that is disordered (Figure 3.72, p. 170) and this region is thought to be able to adopt conformation to unphosphorylated substrates (Longenecker et al., 1996). Interestingly, this region has been mapped as a docking site for p53 (Venerando et al., 2010). Both CK1 delta and CK1 alpha phosphorylate p53 at the N-terminus (Venerando et al., 2010). CK1 phosphorylation of p53 stabilises p53 through inhibition of MDM2 (Bode and Dong, 2004). This SUMO-modification site, K224, could potentially regulate the phosphorylation of p53 and therefore its activity. Interestingly, K224 is an arginine in the CK1 gamma isoform and this isoform does not phosphorylate p53 (Venerando et al., 2010) and therefore does not need this regulation. Another interesting observation is that K224 is a part of a potential NLS. Lysines involved in SUMO-modification are often part of a NLS, as shown for K490 in PML (Duprez et al., 1999). SUMO modification of the last two lysines, K140 and K294, do not show any obvious regulation, yet these sites could potentially under

certain conditions be modified by SUMO-2/3 and thus potentially be targeted for degradation. This is similar to PML, which is modified by SUMO-2/3 at K160 after arsenic treatment and targeted for degradation (Lallemand-Breitenbach et al., 2008). RNF4 was found to bind to and ubiquitinate SUMO-2 chains (Tatham et al., 2008). This could be another way of regulating the kinase activity and therefore protein phosphorylation.

All 11 potential SUMO-modifications sites in CK1 delta were checked in the mass spectrometry dataset but only five were found. These five sites are all predicted using the SUMOplot analysis program from Abgent. The sites K38, K130 and K224 are sites that correspond to the sites predicted in the isoform CK1 alpha.

CK1 delta contains three potential SIMs, two of them overlapping. CK1 delta could interact with SUMO and at the same time be covalently modified, as suggested for the yeast kinase SNF1 (Simpson-Lavy and Johnston, 2013). SUMO could potentially interact with CK1 delta and at the same time covalently modify a lysine in another CK1 protein and thereby inactivate the kinase. The CK1 alpha protein also contains a SIM and the proposed regulation could be the same for this isoform.

4.1.10 Kinase activity of CK1 delta and SUMO-modified CK1 delta.

Kinase activity of CK1 delta and SUMO-modified CK1 delta was tested using the ADP-Glo kinase assay from Promega. A purified CK1 delta protein bought from NEB was used as a positive control. As expected, the SUMO-1-modified CK1 delta kinase showed less activity compared to the unmodified kinase. It was not possible to modify CK1 delta fully. Usually around 50 % of the kinase is modified by SUMO but only two out of the six sites detected in MS interfere with the active site. This correlates with the inhibition measured in the kinase assay where a reduction in Figure 3.75 (p. 174) was detected from 35 µM ATP for CK1 delta 1-317 to 29 µM ATP for CK1 delta 1-317/SUMO-1. SUMO-modification varied slightly between each purification but the tendency was always consistent. The inhibition by SUMO of the kinase activity varied from 17% to 35%. It would have been preferable to purify 100% SUMO-modified CK1 delta and measure it together with the unmodified kinase in the assay, perhaps by expressing a His-tagged SUMO protein. However, this is not possible because SUMO modifies a large variety of proteins and the purification would end up with not only SUMO-modified CK1 delta but also many others being purified.

It would have been ideal to mutate every single lysine detected in the mass spectrometry analysis as a SUMO-modification site and then test the activity of the kinase with and without this lysine modified to see how much SUMO-modification at each particularly lysine inhibits the activity of the kinase. This was unfortunately not possible as SUMO started modifying other lysines in the mutated CK1 delta kinase in the *E.coli* system. The activity was therefore tested with the SUMO-modified kinase and compared to the unmodified kinase and then compared again after treatment with a SUMO-specific protease to de-modify the kinase. The activity of the modified CK1 delta kinase was then expected to rise to the level of the unmodified kinase after de-modification. This was the case for the modified CK1 delta kinase: the activity went up after protease treatment by 25%. The problem was that the activity also went up by 32% for the unmodified kinase when the protease was added. This was probably due to the purified CK1 kinases not being absolutely folded or more likely aggregating due to the exclusion of Triton X-100 from the elution buffer. Another experiment was performed to see if the activity increases for the bought CK1 delta after treatment with the SUMO protease as well, but this was not the case. After adding the protease to the bought CK1 delta the activity went down by 10%, probably due to dilution of the kinase by adding the protease. Further experiments are planned to optimise the protein purification for the kinase assay to ensure that the purified protein is well-folded and not aggregating. The protease treatment of the SUMO-modified kinase can then be repeated under optimal conditions.

Preliminary data showed that CK1 delta is SUMO-modified and the modification alters the activity. Because the protein sequence is highly conserved throughout the CK1 family it is tempting to assume that the lysines modified in CK1 delta could be modified in CK1 alpha as well. SUMO-modification might alter not only the activity of the kinase but also the localisation. SUMO modification could potentially also regulate autophosphorylation of the kinases and thus also regulate the kinase activity. These results add an entirely new level to the regulation of the CK1 kinase activity.

Further mass spectrometric experiments are planned which will select for the peptides of interest identified in the first round of MS experimentation. The peptides will be selected for tandem mass spectrometry (MS/MS) in order to obtain sequence information on the peptides of interest, thus confirming the presence of any SUMO modification on the peptide, as predicted by the observed peptide molecular mass in the first round of experimentation.

Futher in vivo studies should be done to confirm the SUMO modification of CK1. Colocalisation studies in different mammalian cell lines should be performed and co-immunoprecipitations should be conducted using overexpressed and endogenous CK1 and SUMO. Again, these experiments could possibly be repeated with inhibitors of deSUMOylases.

5 Conclusion

Preliminary data showed CK1 delta is modified by SUMO-1 in the *E.coli* system. The crucial lysines are conserved in the CK1 alpha isoform as well. SUMO-modification alters the activity of the kinase, and PML NBs might be where SUMO modification takes place. FADD is phosphorylated by CK1 alpha. CK1 alpha might be modified by SUMO to regulate the activity of the kinase. The SUMO-modification of CK1 alpha might be altered in PML -/- cells because of the missing PML NBs and this could result in a deregulation of phosphorylated FADD. This again could potentially lead to the altered Fas-mediated apoptosis in PML -/- cells. Another factor which could contribute to the altered response in PML -/- cells is that the missing PML is not interacting with the Fas receptor and is thereby destabilising the Fas/FADD/Procaspase-8 complex, as speculated by (Tao et al., 2011). Another possibility is an unidentified interaction between PML II and FADD DED, which is consistent with the speculation above. The B-box in PML could interact with the Fas receptor and the C-terminus of PML II could interact with the DED in FADD, stabilising the Fas/FADD/Procaspase-8 complex.

It could potentially be two separate events observed when the DEFs are disrupting the PML NBs: one where CK1 alpha is SUMO-modified after phosphorylation of FADD causing the other PML NB component to leave the bodies as well. The other event could potentially be FADD DED interacting with the C-terminus of PML II causing the disruption of the bodies.

Another positive aspect of the results here is that PML has been shown to interact with CK1 delta in cells after treatment with the DNA damage-inducing reagent Doxorubicin. CK1 delta is recruited to the PML NBs upon DNA damage where it interacts with PML and p53, facilitating phosphorylation of p53 and protecting p53 from inhibition by Mdm2 (Alsheich-Bartok et al., 2008). Also here it could be speculated that CK1 delta might be SUMO-modified after phosphorylation of p53 or that CK1 is SUMO-modified first and is then taken to the PML NBs. SUMO might potentially modify not only the active site K38 but also the active pocket K130 as well as K224 in the p53 docking site, which could play very important roles here and regulate phosphorylation of p53 and p53 activity.

The overall conclusion is that preliminary results show an unexplored area where the SUMO-modification of kinases adds a new regulation and therefore alters phosphorylation of proteins. This regulation might take place at PML NBs and this also adds another interesting aspect to the already very complex story of PML NBs and PML NB constituents. (SUMO-modification of CK1 isoforms and proposed regulations summarised in Figure 5.1.)

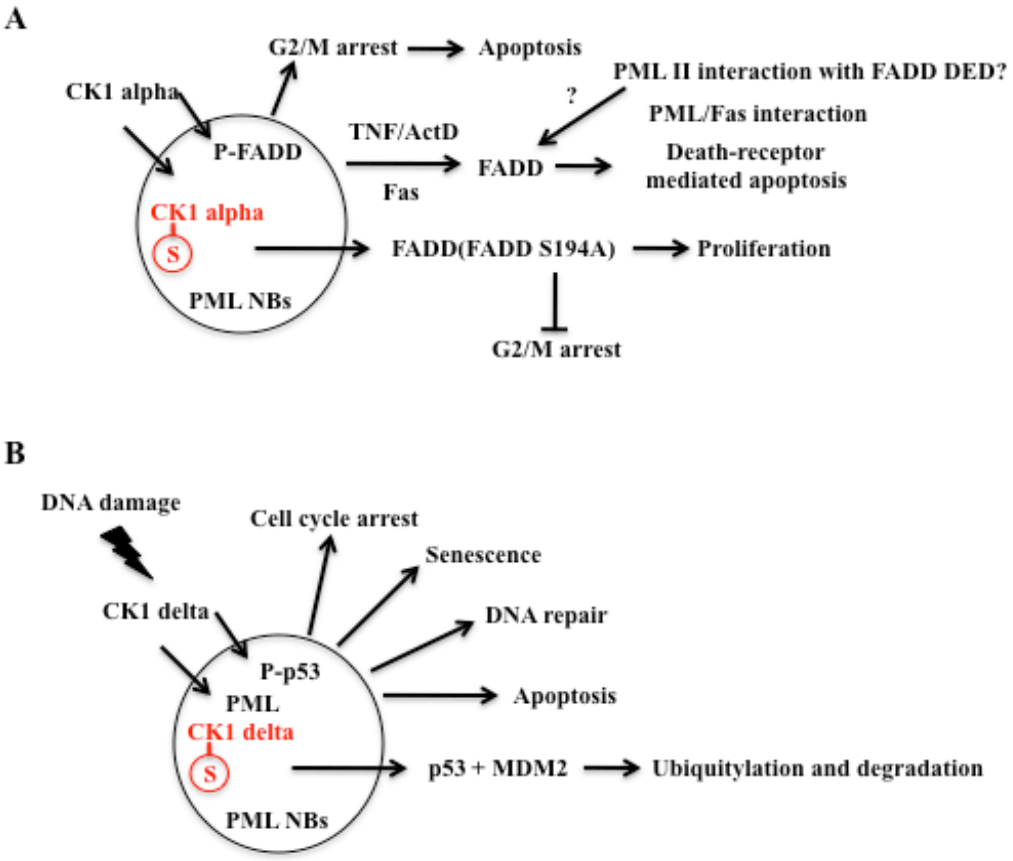

Figure 5.1. SUMO-modification of CK1 members and proposed regulations

A: SUMO-modification of CK1 alpha might take place at PML NBs. This could potentially regulate phosphorylation of FADD and therefore cell cycle arrest and apoptosis.
B: SUMO-modification of CK1 delta might take place at PML NBs. This could potentially regulate the phosphorylation of p53 and therefore cell cycle arrest, senescence, DNA repair and apoptosis.

6 Supplementary material

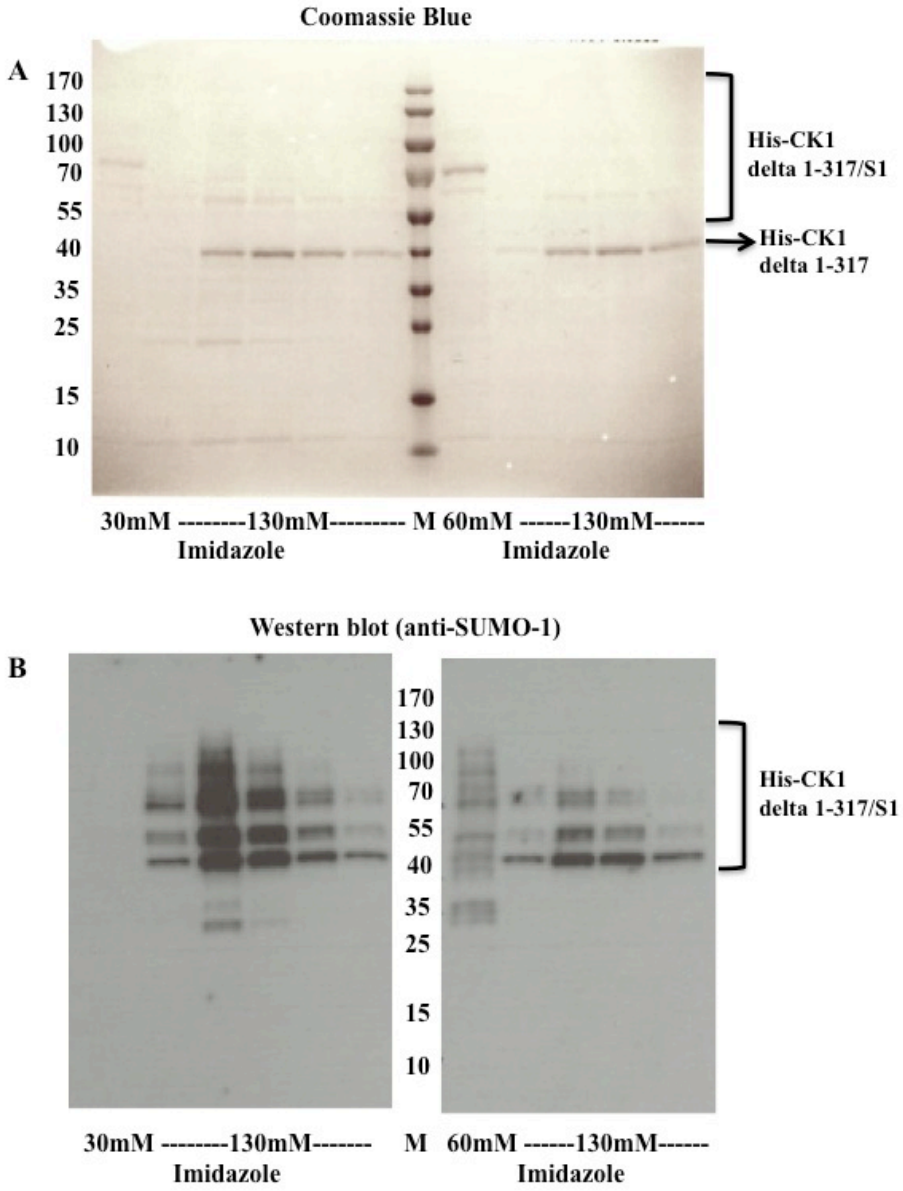

Supplementary Figure 6.1. Testing wash and elution conditions of SUMO-modified CK1 delta 1-317

BL21-Gold(DE3) cells transformed with pET-28a CK1 delta 1-317 with or without pT-Trx-AU(E1)-Ubc9(E2)-SUMO-1, induced with 0.2 mM IPTG and left to grow overnight at 15 ˚C. Protein was purified and several fractions were loaded onto a 4-20% polyacrylamide gradient gel and stained with either Coomassie Blue (**A**) or proteins were transferred onto a nitrocellulose membrane and detected using a rabbit anti-SUMO-1 antibody (**B**).

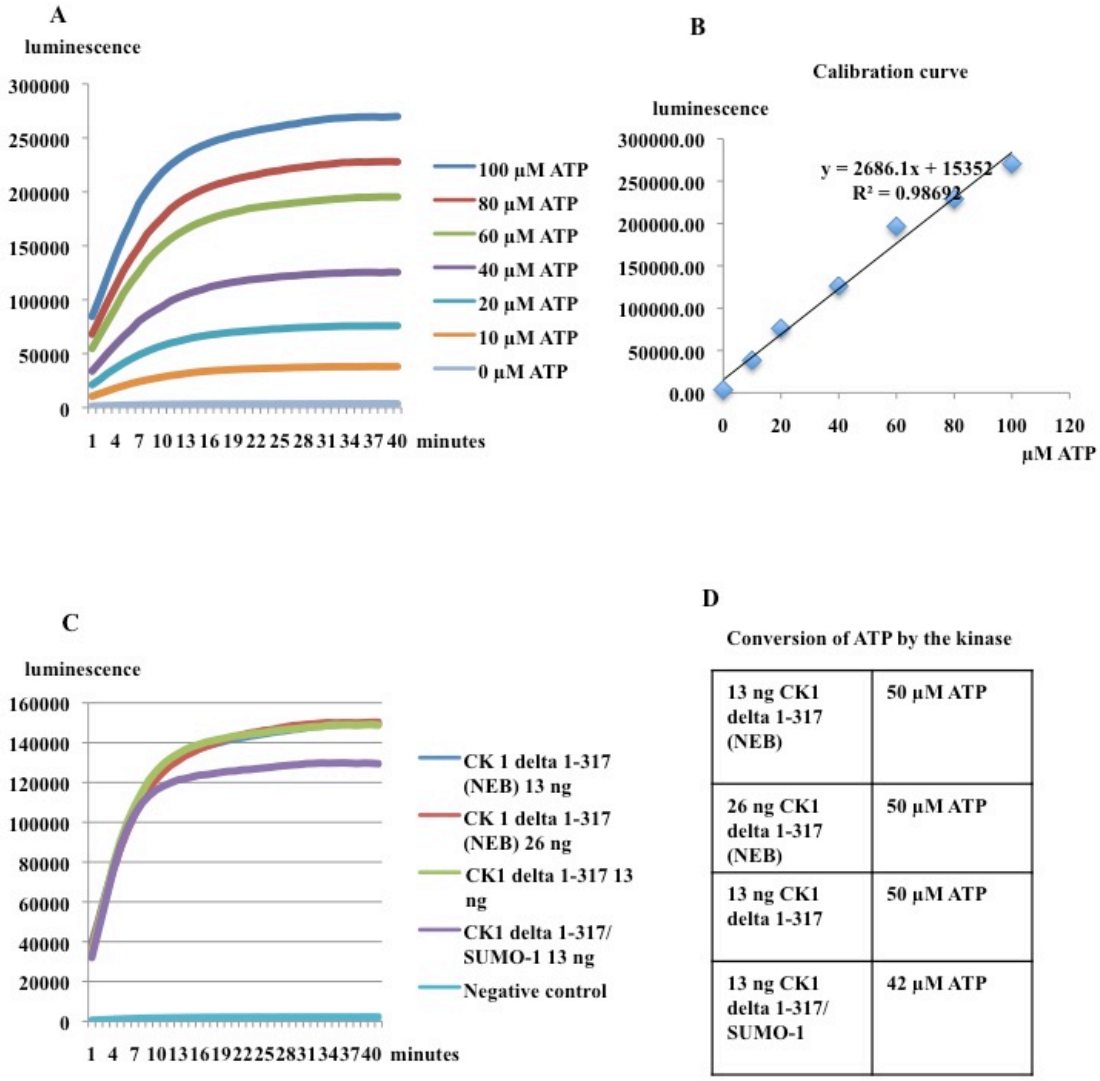

Supplementary Figure 6.2. Testing protein concentrations with CK1 delta 1-317 and SUMO-1 modified CK1 delta 1-317

Kinase reaction: 13/26 ng CK1 + 240 µM CK1 peptide substrate [pS7} + 40 µM ATP
Kinase reaction 30 minutes at room temperature
ADP-Glo added
Incubated 40 minutes at room temperature
Kinase detection reagent added
Luminescense measured for 40 minutes

A: Standard curve
B: Calibration curve created using the standard curve
C: Kinase activity measured as luminescence
D: ATP converted by the kinase - calibration curve (B) used to convert luminescence from (C) into ATP concentrations

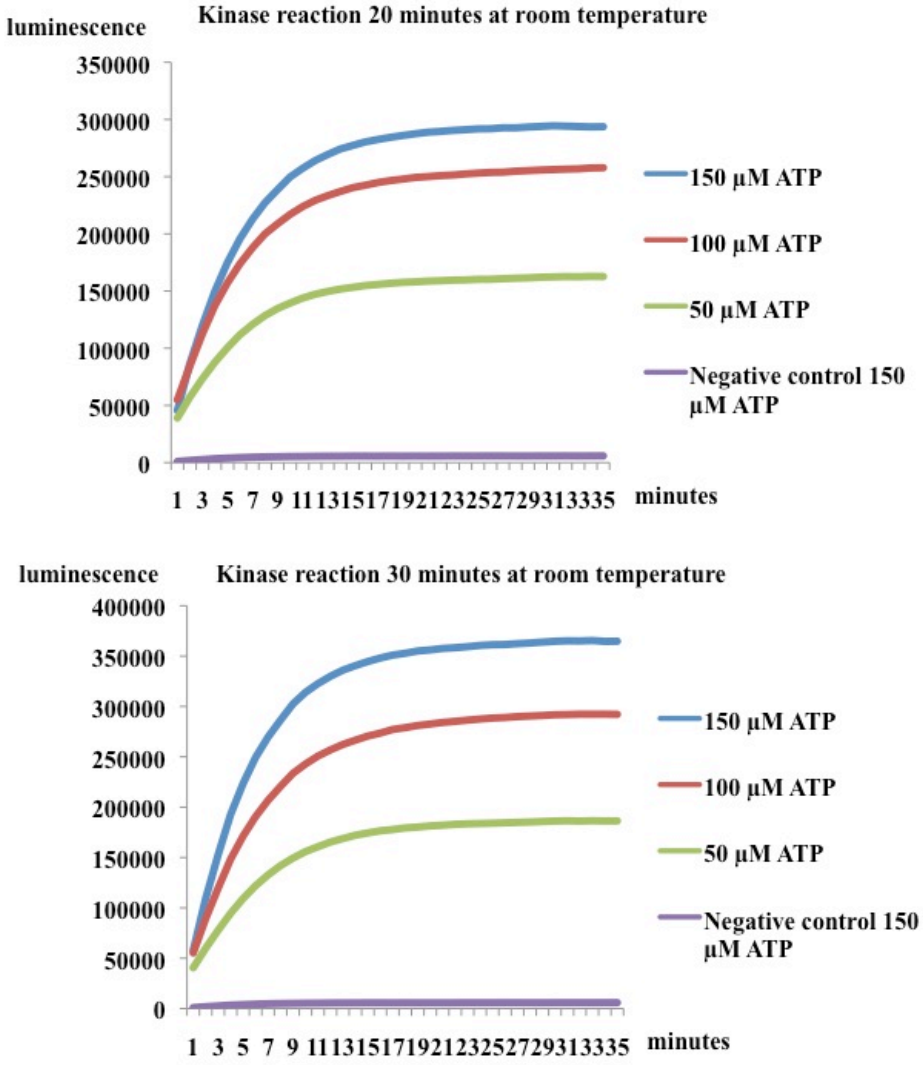

Supplementary Figure 6.3. Testing the length of the kinase reaction and concentration of ATP in a kinase assay with CK1 delta 1-317 (NEB)

Kinase reaction: 13 ng CK1 + 240 µM CK1 peptide substrate [pS7} + 50, 100, 150 µM ATP
Kinase reaction 20 or 30 minutes at room temperature
ADP-Glo added
Incubated 40 minutes at room temperature
Kinase detection reagent added
Luminescense measured for 35 minutes

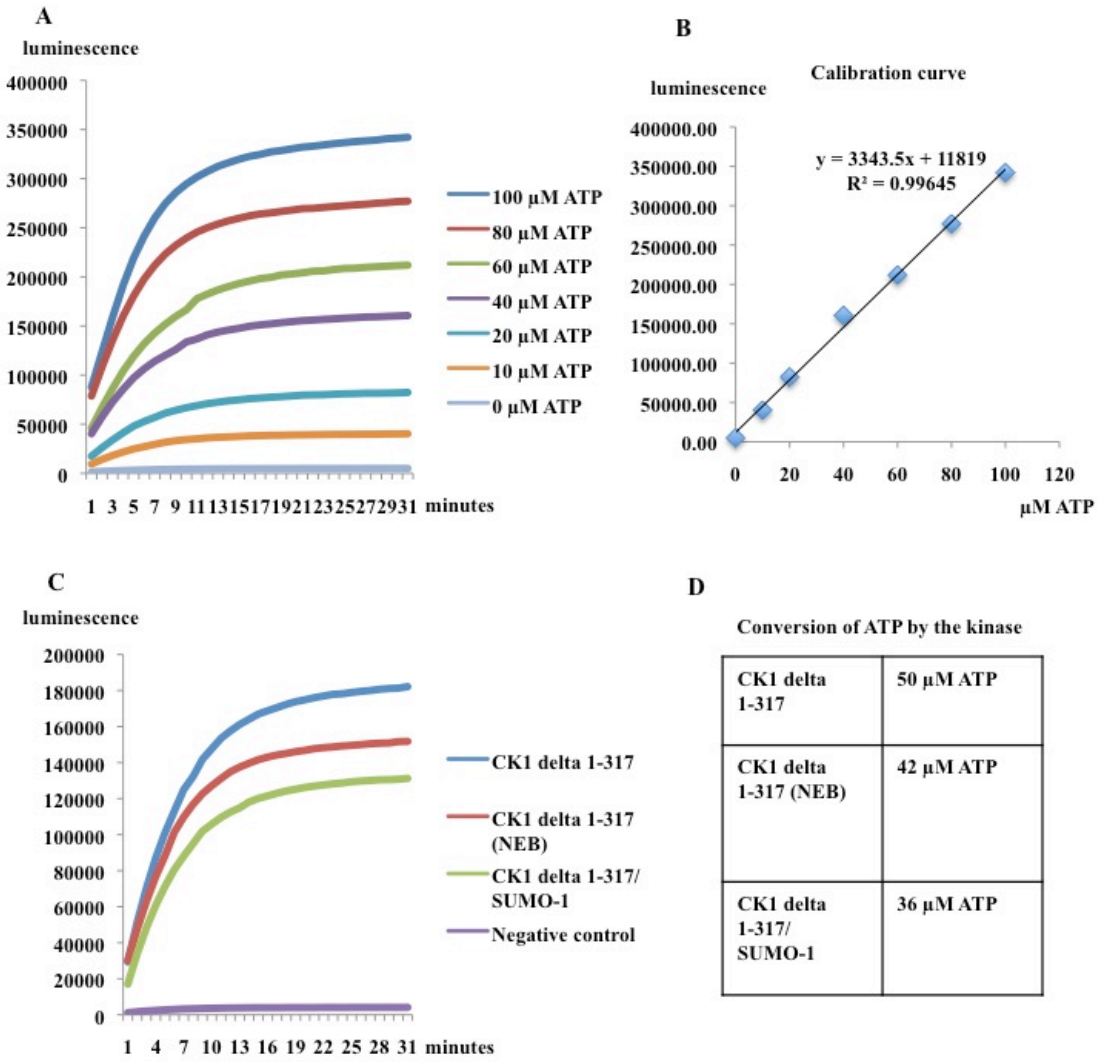

Supplementary Figure 6.4. Kinase assay with CK1 delta 1-317 and SUMO-1 modified CK1 delta 1-317

Kinase reaction: 13 ng CK1 + 240 µM CK1 peptide substrate [pS7} + 80 µM ATP
Kinase reaction 15 minutes at room temperature
ADP-Glo added
Incubated 40 minutes RT
Kinase detection reagent added
Luminescense measured for 31 minutes

A: Standard curve
B: Calibration curve created using the standard curve
C: Kinase activity measured as luminescence
D: ATP converted by the kinase - calibration curve (B) used to convert luminescence from (C) into ATP concentrations

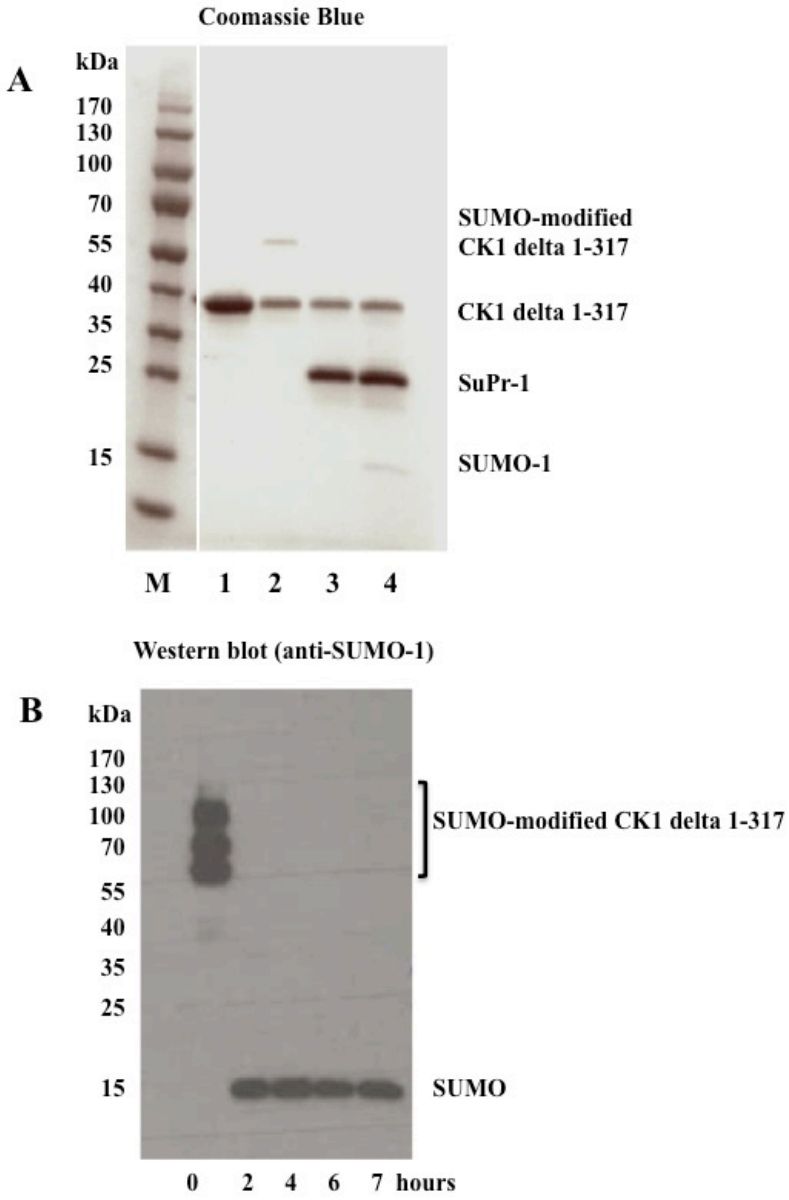

Supplementary Figure 6.5. SUMO protease cleavage of SUMO-modified CK1 delta 1-317

BL21-Gold(DE3) cells co-transformed with pET-28a CK1 delta 1-317 SUMO mutant and pT-Trx-AU(E1)-Ubc9(E2)-SUMO-1 were induced with 0.2 mM IPTG and left to grow overnight at 22 ˚C. (**A**) Proteins were purified and several fractions were concentrated (A: lane 1 and 2). SUMO protease cleavage of the purified proteins was performed (A: lane 3 and 4) and loaded onto a 4-20% polyacrylamide gradient gel and stained with Coomassie Blue. (**B**) A time course was done to find the optimal time needed for full cleavage of the SUMO-modified CK1 delta 1-317. Uncleaved and cleaved protein was loaded onto a 4-20% polyacrylamide gradient gel, transferred onto nitrocellulose and proteins were detected using rabbit anti-SUMO-1 antibodies.

7 References

AGGARWAL, B. B. 2003. Signalling pathways of the TNF superfamily: a double-edged sword. *Nat Rev Immunol,* 3, 745-56.

ALAPPAT, E. C., FEIG, C., BOYERINAS, B., VOLKLAND, J., SAMUELS, M., MURMANN, A. E., THORBURN, A., KIDD, V. J., SLAUGHTER, C. A., OSBORN, S. L., WINOTO, A., TANG, W. J. & PETER, M. E. 2005. Phosphorylation of FADD at serine 194 by CKIalpha regulates its nonapoptotic activities. *Mol Cell,* 19, 321-32.

ALAPPAT, E. C., VOLKLAND, J. & PETER, M. E. 2003. Cell cycle effects by C-FADD depend on its C-terminal phosphorylation site. *J Biol Chem,* 278, 41585-8.

ALAYED, K. M., MEDEIROS, L. J., PHAN, D., OJIAKU, C., PATEL, J., YAP, J. P., MCCORD, Y., WOODS, J. S., KONOPLEV, S., BUESO-RAMOS, C. E. & REYES, S. R. 2013. Immunostaining for rapid diagnosis of acute promyelocytic leukemia with the tetramethylrhodamine-5-isothiocyanate-conjugated anti-promyelocytic leukemia monoclonal antibody PG-M3. *Arch Pathol Lab Med,* 137**,** 1669-73.

ALSHEICH-BARTOK, O., HAUPT, S., ALKALAY-SNIR, I., SAITO, S., APPELLA, E. & HAUPT, Y. 2008. PML enhances the regulation of p53 by CK1 in response to DNA damage. *Oncogene,* 27, 3653-61.

ANTON, L. C., SCHUBERT, U., BACIK, I., PRINCIOTTA, M. F., WEARSCH, P. A., GIBBS, J., DAY, P. M., REALINI, C., RECHSTEINER, M. C., BENNINK, J. R. & YEWDELL, J. W. 1999. Intracellular localization of proteasomal degradation of a viral antigen. *J Cell Biol,* 146, 113-24.

ARCH, R. H., GEDRICH, R. W. & THOMPSON, C. B. 1998. Tumor necrosis factor receptor-associated factors (TRAFs)--a family of adapter proteins that regulates life and death. *Genes Dev,* 12, 2821-30.

ARNOULD, C., PHILIPPE, C., BOURDON, V., GR GOIRE, M. J., BERGER, R. & JONVEAUX, P. 1999. The signal transducer and activator of transcription STAT5b gene is a new partner of retinoic acid receptor alpha in acute promyelocytic-like leukaemia. *Hum Mol Genet,* 8, 1741-9.

BAIRD, G. S., ZACHARIAS, D. A. & TSIEN, R. Y. 2000. Biochemistry, mutagenesis, and oligomerization of DsRed, a red fluorescent protein from coral. *Proc Natl Acad Sci U S A,* 97, 11984-9.

BAYER, P., ARNDT, A., METZGER, S., MAHAJAN, R., MELCHIOR, F., JAENICKE, R. & BECKER, J. 1998. Structure determination of the small ubiquitin-related modifier SUMO-1. *J Mol Biol,* 280, 275-86.

BELLODI, C., KINDLE, K., BERNASSOLA, F., COSSARIZZA, A., DINSDALE, D., MELINO, G., HEERY, D. & SALOMONI, P. 2006. A cytoplasmic PML mutant inhibits p53 function. *Cell Cycle,* 5, 2688-92.

BERNARDI, R. & PANDOLFI, P. P. 2003. Role of PML and the PML-nuclear body in the control of programmed cell death. *Oncogene,* 22, 9048-57.

BERNARDI, R. & PANDOLFI, P. P. 2007. Structure, dynamics and functions of promyelocytic leukaemia nuclear bodies. *Nat Rev Mol Cell Biol,* 8, 1006-16.
BERNARDI, R., PAPA, A. & PANDOLFI, P. P. 2008. Regulation of apoptosis by PML and the PML-NBs. *Oncogene,* 27, 6299-312.
BESNAULT-MASCARD, L., LEPRINCE, C., AUFFREDOU, M. T., MEUNIER, B., BOURGEADE, M. F., CAMONIS, J., LORENZO, H. K. & VAZQUEZ, A. 2005. Caspase-8 sumoylation is associated with nuclear localization. *Oncogene,* 24, 3268-73.
BEST, J. L., GANIATSAS, S., AGARWAL, S., CHANGOU, A., SALOMONI, P., SHIRIHAI, O., MELUH, P. B., PANDOLFI, P. P. & ZON, L. I. 2002. SUMO-1 protease-1 regulates gene transcription through PML. *Mol Cell,* 10, 843-55.
BIRNBOIM, H. C. & DOLY, J. 1979. A rapid alkaline extraction procedure for screening recombinant plasmid DNA. *Nucleic Acids Res,* 7, 1513-23.
BODDY, M. N., DUPREZ, E., BORDEN, K. L. & FREEMONT, P. S. 1997. Surface residue mutations of the PML RING finger domain alter the formation of nuclear matrix-associated PML bodies. *J Cell Sci,* 110, 2197-205.
BODDY, M. N., HOWE, K., ETKIN, L. D., SOLOMON, E. & FREEMONT, P. S. 1996. PIC 1, a novel ubiquitin-like protein which interacts with the PML component of a multiprotein complex that is disrupted in acute promyelocytic leukaemia. *Oncogene,* 13, 971-82.
BODE, A. M. & DONG, Z. 2004. Post-translational modification of p53 in tumorigenesis. *Nat Rev Cancer,* 4, 793-805.
BOLDIN, M. P., GONCHAROV, T. M., GOLTSEV, Y. V. & WALLACH, D. 1996. Involvement of MACH, a novel MORT1/FADD-interacting protease, in Fas/APO-1- and TNF receptor-induced cell death. *Cell,* 85, 803-15.
BONILLA, W. V., PINSCHEWER, D. D., KLENERMAN, P., ROUSSON, V., GABOLI, M., PANDOLFI, P. P., ZINKERNAGEL, R. M., SALVATO, M. S. & HENGARTNER, H. 2002. Effects of promyelocytic leukemia protein on virus-host balance. *J Virol,* 76, 3810-8.
BORDEN, K. L., BODDY, M. N., LALLY, J., O'REILLY, N. J., MARTIN, S., HOWE, K., SOLOMON, E. & FREEMONT, P. S. 1995. The solution structure of the RING finger domain from the acute promyelocytic leukaemia proto-oncoprotein PML. *Embo J,* 14, 1532-41.
BORDEN, K. L., LALLY, J. M., MARTIN, S. R., O'REILLY, N. J., SOLOMON, E. & FREEMONT, P. S. 1996. In vivo and in vitro characterization of the B1 and B2 zinc-binding domains from the acute promyelocytic leukemia protooncoprotein PML. *Proc Natl Acad Sci U S A,* 93, 1601-6.
BOUTELL, C., CUCHET-LOURENCO, D., VANNI, E., ORR, A., GLASS, M., MCFARLANE, S. & EVERETT, R. D. 2011. A viral ubiquitin ligase has substrate preferential SUMO targeted ubiquitin ligase activity that counteracts intrinsic antiviral defence. *PLoS Pathog,* 7, e1002245.
BRADLEY, J. R. & POBER, J. S. 2001. Tumor necrosis factor receptor-associated factors (TRAFs). *Oncogene,* 20, 6482-91.
BRAND, P., LENSER, T. & HEMMERICH, P. 2010. Assembly dynamics of PML nuclear bodies in living cells. *PMC Biophys,* 3, 3.
BRIDGER, J. M., HERRMANN, H., MUNKEL, C. & LICHTER, P. 1998. Identification of an interchromosomal compartment by polymerization of nuclear-targeted vimentin. *J Cell Sci,* 111 (Pt 9), 1241-53.

BUDINI, M., JACOB, G., JEDLICKI, A., PEREZ, C., ALLENDE, C. C. & ALLENDE, J. E. 2009. Autophosphorylation of carboxy-terminal residues inhibits the activity of protein kinase CK1alpha. *J Cell Biochem,* 106, 399-408.

BURZIO, V., ANTONELLI, M., ALLENDE, C. C. & ALLENDE, J. E. 2002. Biochemical and cellular characteristics of the four splice variants of protein kinase CK1alpha from zebrafish (Danio rerio). *J Cell Biochem,* 86, 805-14.

CARRACEDO, A., ITO, K. & PANDOLFI, P. P. 2011. The nuclear bodies inside out: PML conquers the cytoplasm. *Curr Opin Cell Biol,* 23, 360-6.

CARRINGTON, P. E., SANDU, C., WEI, Y., HILL, J. M., MORISAWA, G., HUANG, T., GAVATHIOTIS, E. & WERNER, M. H. 2006. The structure of FADD and its mode of interaction with procaspase-8. *Mol Cell,* 22**,** 599-610.

CASTAIGNE, S., CHOMIENNE, C., DANIEL, M. T., BALLERINI, P., BERGER, R., FENAUX, P. & DEGOS, L. 1990. All-trans retinoic acid as a differentiation therapy for acute promyelocytic leukemia. I. Clinical results. *Blood,* 76, 1704-9.

CHAN, J. Y., CHIN, W., LIEW, C. T., CHANG, K. S. & JOHNSON, P. J. 1998. Altered expression of the growth and transformation suppressor PML gene in human hepatocellular carcinomas and in hepatitis tissues. *Eur J Cancer,* 34, 1015-22.

CHANG, C. C., NAIK, M. T., HUANG, Y. S., JENG, J. C., LIAO, P. H., KUO, H. Y., HO, C. C., HSIEH, Y. L., LIN, C. H., HUANG, N. J., NAIK, N. M., KUNG, C. C., LIN, S. Y., CHEN, R. H., CHANG, K. S., HUANG, T. H. & SHIH, H. M. 2011. Structural and functional roles of Daxx SIM phosphorylation in SUMO paralog-selective binding and apoptosis modulation. *Mol Cell,* 42, 62-74.

CHELBI-ALIX, M. K., QUIGNON, F., PELICANO, L., KOKEN, M. H. & DE THE, H. 1998. Resistance to virus infection conferred by the interferon-induced promyelocytic leukemia protein. *J Virol,* 72, 1043-51.

CHEN, Z., BRAND, N. J., CHEN, A., CHEN, S. J., TONG, J. H., WANG, Z. Y., WAXMAN, S. & ZELENT, A. 1993. Fusion between a novel Kruppel-like zinc finger gene and the retinoic acid receptor-alpha locus due to a variant t(11;17) translocation associated with acute promyelocytic leukaemia. *EMBO J,* 12, 1161-7.

CHINNAIYAN, A. M., O'ROURKE, K., TEWARI, M. & DIXIT, V. M. 1995. FADD, a novel death domain-containing protein, interacts with the death domain of Fas and initiates apoptosis. *Cell,* 81, 505-12.

CHINNAIYAN, A. M., TEPPER, C. G., SELDIN, M. F., O'ROURKE, K., KISCHKEL, F. C., HELLBARDT, S., KRAMMER, P. H., PETER, M. E. & DIXIT, V. M. 1996. FADD/MORT1 is a common mediator of CD95 (Fas/APO-1) and tumor necrosis factor receptor-induced apoptosis. *J Biol Chem,* 271, 4961-5.

CHU, Y. & YANG, X. 2011. SUMO E3 ligase activity of TRIM proteins. *Oncogene,* 30, 1108-16.

CHUNG, J. Y., PARK, Y. C., YE, H. & WU, H. 2002. All TRAFs are not created equal: common and distinct molecular mechanisms of TRAF-mediated signal transduction. *J Cell Sci,* 115, 679-88.

CONDEMINE, W., TAKAHASHI, Y., ZHU, J., PUVION-DUTILLEUL, F., GUEGAN, S., JANIN, A. & DE THE, H. 2006. Characterization of

endogenous human promyelocytic leukemia isoforms. *Cancer Res,* 66, 6192-8.

CREMER, T. & CREMER, C. 2001. Chromosome territories, nuclear architecture and gene regulation in mammalian cells. *Nat Rev Genet,* 2, 292-301.

CUCHET-LOURENCO, D., BOUTELL, C., LUKASHCHUK, V., GRANT, K., SYKES, A., MURRAY, J., ORR, A. & EVERETT, R. D. 2011. SUMO pathway dependent recruitment of cellular repressors to herpes simplex virus type 1 genomes. *PLoS Pathog,* 7, e1002123.

DANIELS, M. J., MARSON, A. & VENKITARAMAN, A. R. 2004. PML bodies control the nuclear dynamics and function of the CHFR mitotic checkpoint protein. *Nat Struct Mol Biol,* 11, 1114-21.

DE THE, G., RIVIERE, M. & BERNHARD, W. 1960. Examen au microscope electronique de la tumeur VX2 du lapin domestique derivee du papillome de Shope. *Bull.Cancer,* 47, 570-584.

DE THE, H. & CHEN, Z. 2010. Acute promyelocytic leukaemia: novel insights into the mechanisms of cure. *Nat Rev Cancer,* 10, 775-83.

DE THE, H., LAVAU, C., MARCHIO, A., CHOMIENNE, C., DEGOS, L. & DEJEAN, A. 1991. The PML-RAR alpha fusion mRNA generated by the t(15;17) translocation in acute promyelocytic leukemia encodes a functionally altered RAR. *Cell,* 66, 675-84.

DJAVANI, M., RODAS, J., LUKASHEVICH, I. S., HOREJSH, D., PANDOLFI, P. P., BORDEN, K. L. & SALVATO, M. S. 2001. Role of the promyelocytic leukemia protein PML in the interferon sensitivity of lymphocytic choriomeningitis virus. *J Virol,* 75, 6204-8.

DOS SANTOS, G. A., KATS, L. & PANDOLFI, P. P. 2013. Synergy against PML-RARa: targeting transcription, proteolysis, differentiation, and self-renewal in acute promyelocytic leukemia. *J Exp Med,* 210**,** 2793-802.

DRANE, P., OUARARHNI, K., DEPAUX, A., SHUAIB, M. & HAMICHE, A. 2010. The death-associated protein DAXX is a novel histone chaperone involved in the replication-independent deposition of H3.3. *Genes Dev,* 24**,** 1253-65.

DUNSCH, A. K., LINNANE, E., BARR, F. A. & GRUNEBERG, U. 2011. The astrin-kinastrin/SKAP complex localizes to microtubule plus ends and facilitates chromosome alignment. *J Cell Biol,* 192, 959-68.

DUPREZ, E., SAURIN, A. J., DESTERRO, J. M., LALLEMAND-BREITENBACH, V., HOWE, K., BODDY, M. N., SOLOMON, E., DE THE, H., HAY, R. T. & FREEMONT, P. S. 1999. SUMO-1 modification of the acute promyelocytic leukaemia protein PML: implications for nuclear localisation. *J Cell Sci,* 112, 381-93.

EBERSTADT, M., HUANG, B., CHEN, Z., MEADOWS, R. P., NG, S. C., ZHENG, L., LENARDO, M. J. & FESIK, S. W. 1998. NMR structure and mutagenesis of the FADD (Mort1) death-effector domain. *Nature,* 392, 941-5.

EUN JEOUNG, L., SUNG HEE, H., JAESUN, C., SUNG HWA, S., KWANG HUM, Y., MIN KYOUNG, K., TAE YOON, P. & SANG SUN, K. 2008. Regulation of glycogen synthase kinase 3beta functions by modification of the small ubiquitin-like modifier. *Open Biochem J,* 2, 67-76.

EVERETT, R. D. 2001. DNA viruses and viral proteins that interact with PML nuclear bodies. *Oncogene,* 20, 7266-73.

EVERETT, R. D. & CHELBI-ALIX, M. K. 2007. PML and PML nuclear bodies: implications in antiviral defence. *Biochimie,* 89, 819-30.

EVERETT, R. D., LOMONTE, P., STERNSDORF, T., VAN DRIEL, R. & ORR, A. 1999. Cell cycle regulation of PML modification and ND10 composition. *J Cell Sci,* 112 (Pt 24), 4581-8.

FAGIOLI, M., ALCALAY, M., PANDOLFI, P. P., VENTURINI, L., MENCARELLI, A., SIMEONE, A., ACAMPORA, D., GRIGNANI, F. & PELICCI, P. G. 1992. Alternative splicing of PML transcripts predicts coexpression of several carboxy-terminally different protein isoforms. *Oncogene,* 7, 1083-91.

FALINI, B., FLENGHI, L., FAGIOLI, M., LO COCO, F., CORDONE, I., DIVERIO, D., PASQUALUCCI, L., BIONDI, A., RIGANELLI, D., ORLETH, A., LISO, A., MARTELLI, M. F., PELICCI, P. G. & PILERI, S. 1997. Immunocytochemical diagnosis of acute promyelocytic leukemia (M3) with the monoclonal antibody PG-M3 (anti-PML). *Blood,* 90**,** 4046-53.

FANG, L., SEKI, A. & FANG, G. 2009. SKAP associates with kinetochores and promotes the metaphase-to-anaphase transition. *Cell Cycle,* 8, 2819-27.

FENAUX, P., CHASTANG, C., CHEVRET, S., SANZ, M., DOMBRET, H., ARCHIMBAUD, E., FEY, M., RAYON, C., HUGUET, F., SOTTO, J. J., GARDIN, C., MAKHOUL, P. C., TRAVADE, P., SOLARY, E., FEGUEUX, N., BORDESSOULE, D., MIGUEL, J. S., LINK, H., DESABLENS, B., STAMATOULLAS, A., DECONINCK, E., MALOISEL, F., CASTAIGNE, S., PREUDHOMME, C. & DEGOS, L. 1999. A randomized comparison of all transretinoic acid (ATRA) followed by chemotherapy and ATRA plus chemotherapy and the role of maintenance therapy in newly diagnosed acute promyelocytic leukemia. The European APL Group. *Blood,* 94, 1192-200.

FERNANDEZ-MIRANDA, G., PEREZ DE CASTRO, I., CARMENA, M., AGUIRRE-PORTOLES, C., RUCHAUD, S., FANT, X., MONTOYA, G., EARNSHAW, W. C. & MALUMBRES, M. 2010. SUMOylation modulates the function of Aurora-B kinase. *J Cell Sci,* 123, 2823-33.

FLENGHI, L., FAGIOLI, M., TOMASSONI, L., PILERI, S., GAMBACORTA, M., PACINI, R., GRIGNANI, F., CASINI, T., FERRUCCI, P. F., MARTELLI, M. F. & ET AL. 1995. Characterization of a new monoclonal antibody (PG-M3) directed against the aminoterminal portion of the PML gene product: immunocytochemical evidence for high expression of PML proteins on activated macrophages, endothelial cells, and epithelia. *Blood,* 85**,** 1871-80.

FU, Z., CHAKRABORTI, T., MORSE, S., BENNETT, G. S. & SHAW, G. 2001. Four casein kinase I isoforms are differentially partitioned between nucleus and cytoplasm. *Exp Cell Res,* 269, 275-86.

GAMBACORTA, M., FLENGHI, L., FAGIOLI, M., PILERI, S., LEONCINI, L., BIGERNA, B., PACINI, R., TANCI, L. N., PASQUALUCCI, L., ASCANI, S., MENCARELLI, A., LISO, A., PELICCI, P. G. & FALINI, B. 1996. Heterogeneous nuclear expression of the promyelocytic leukemia (PML) protein in normal and neoplastic human tissues. *Am J Pathol,* 149, 2023-35.

GAREAU, J. R. & LIMA, C. D. 2010. The SUMO pathway: emerging mechanisms that shape specificity, conjugation and recognition. *Nat Rev Mol Cell Biol,* 11, 861-71.

GENG, Y., MONAJEMBASHI, S., SHAO, A., CUI, D., HE, W., CHEN, Z., HEMMERICH, P. & TANG, J. 2012. Contribution of the C-terminal regions of promyelocytic leukemia protein (PML) isoforms II and V to PML nuclear body formation. *J Biol Chem,* 287, 30729-42.

GEOFFROY, M. C. & CHELBI-ALIX, M. K. 2011. Role of promyelocytic leukemia protein in host antiviral defense. *J Interferon Cytokine Res,* 31, 145-58.

GEOFFROY, M. C., JAFFRAY, E. G., WALKER, K. J. & HAY, R. T. 2010. Arsenic-induced SUMO-dependent recruitment of RNF4 into PML nuclear bodies. *Mol Biol Cell,* 21, 4227-39.

GIORGI, C., ITO, K., LIN, H. K., SANTANGELO, C., WIECKOWSKI, M. R., LEBIEDZINSKA, M., BONONI, A., BONORA, M., DUSZYNSKI, J., BERNARDI, R., RIZZUTO, R., TACCHETTI, C., PINTON, P. & PANDOLFI, P. P. 2010. PML regulates apoptosis at endoplasmic reticulum by modulating calcium release. *Science,* 330**,** 1247-51.

GODDARD, A. D., BORROW, J., FREEMONT, P. S. & SOLOMON, E. 1991. Characterization of a zinc finger gene disrupted by the t(15;17) in acute promyelocytic leukemia. *Science,* 254, 1371-4.

GROSS, S. D. & ANDERSON, R. A. 1998. Casein kinase I: spatial organization and positioning of a multifunctional protein kinase family. *Cell Signal,* 10, 699-711.

GROSS, S. D., LOIJENS, J. C. & ANDERSON, R. A. 1999. The casein kinase Ialpha isoform is both physically positioned and functionally competent to regulate multiple events of mRNA metabolism. *J Cell Sci,* 112 (Pt 16), 2647-56.

GROTZINGER, T., JENSEN, K., GULDNER, H. H., STERNSDORF, T., SZOSTECKI, C., SCHWAB, M., SAVELYEVA, L., REICH, B. & WILL, H. 1996a. A highly amplified mouse gene is homologous to the human interferon-responsive Sp100 gene encoding an autoantigen associated with nuclear dots. *Mol Cell Biol,* 16, 1150-6.

GROTZINGER, T., STERNSDORF, T., JENSEN, K. & WILL, H. 1996b. Interferon-modulated expression of genes encoding the nuclear-dot-associated proteins Sp100 and promyelocytic leukemia protein (PML). *Eur J Biochem,* 238, 554-60.

GULDNER, H. H., SZOSTECKI, C., GROTZINGER, T. & WILL, H. 1992. IFN enhance expression of Sp100, an autoantigen in primary biliary cirrhosis. *J Immunol,* 149, 4067-73.

GULDNER, H. H., SZOSTECKI, C., SCHRODER, P., MATSCHL, U., JENSEN, K., LUDERS, C., WILL, H. & STERNSDORF, T. 1999. Splice variants of the nuclear dot-associated Sp100 protein contain homologies to HMG-1 and a human nuclear phosphoprotein-box motif. *J Cell Sci,* 112 (Pt 5), 733-47.

GURRIERI, C., CAPODIECI, P., BERNARDI, R., SCAGLIONI, P. P., NAFA, K., RUSH, L. J., VERBEL, D. A., CORDON-CARDO, C. & PANDOLFI, P. P. 2004. Loss of the tumor suppressor PML in human cancers of multiple histologic origins. *J Natl Cancer Inst,* 96, 269-79.

HA, H., HAN, D. & CHOI, Y. 2009. TRAF-mediated TNFR-family signaling. *Curr Protoc Immunol,* Chapter 11**,** Unit11 9D.

HAKLI, M., KARVONEN, U., JANNE, O. A. & PALVIMO, J. J. 2005. SUMO-1 promotes association of SNURF (RNF4) with PML nuclear bodies. *Exp Cell Res,* 304, 224-33.

HAKLI, M., LORICK, K. L., WEISSMAN, A. M., JANNE, O. A. & PALVIMO, J. J. 2004. Transcriptional coregulator SNURF (RNF4) possesses ubiquitin E3 ligase activity. *FEBS Lett,* 560, 56-62.

HANKS, S. K. 2003. Genomic analysis of the eukaryotic protein kinase superfamily: a perspective. *Genome Biol,* 4, 111.

HANNICH, J. T., LEWIS, A., KROETZ, M. B., LI, S. J., HEIDE, H., EMILI, A. & HOCHSTRASSER, M. 2005. Defining the SUMO-modified proteome by multiple approaches in Saccharomyces cerevisiae. *J Biol Chem,* 280, 4102-10.

HAYASHI, N., SHIRAKURA, H., UEHARA, T. & NOMURA, Y. 2006. Relationship between SUMO-1 modification of caspase-7 and its nuclear localization in human neuronal cells. *Neurosci Lett,* 397, 5-9.

HECKER, C. M., RABILLER, M., HAGLUND, K., BAYER, P. & DIKIC, I. 2006. Specification of SUMO1- and SUMO2-interacting motifs. *J Biol Chem,* 281, 16117-27.

HENDERSON, B. R. & ELEFTHERIOU, A. 2000. A comparison of the activity, sequence specificity, and CRM1-dependence of different nuclear export signals. *Exp Cell Res,* 256, 213-24.

HOPPE, A., BEECH, S. J., DIMMOCK, J. & LEPPARD, K. N. 2006. Interaction of the adenovirus type 5 E4 Orf3 protein with promyelocytic leukemia protein isoform II is required for ND10 disruption. *J Virol,* 80, 3042-9.

INADA, H., IZAWA, I., NISHIZAWA, M., FUJITA, E., KIYONO, T., TAKAHASHI, T., MOMOI, T. & INAGAKI, M. 2001. Keratin attenuates tumor necrosis factor-induced cytotoxicity through association with TRADD. *J Cell Biol,* 155, 415-26.

ISHOV, A. M., SOTNIKOV, A. G., NEGOREV, D., VLADIMIROVA, O. V., NEFF, N., KAMITANI, T., YEH, E. T., STRAUSS, J. F., 3RD & MAUL, G. G. 1999. PML is critical for ND10 formation and recruits the PML-interacting protein daxx to this nuclear structure when modified by SUMO-1. *J Cell Biol,* 147, 221-34.

ISHOV, A. M., VLADIMIROVA, O. V. & MAUL, G. G. 2004. Heterochromatin and ND10 are cell-cycle regulated and phosphorylation-dependent alternate nuclear sites of the transcription repressor Daxx and SWI/SNF protein ATRX. *J Cell Sci,* 117**,** 3807-20.

ITO, K., BERNARDI, R., MOROTTI, A., MATSUOKA, S., SAGLIO, G., IKEDA, Y., ROSENBLATT, J., AVIGAN, D. E., TERUYA-FELDSTEIN, J. & PANDOLFI, P. P. 2008. PML targeting eradicates quiescent leukaemia-initiating cells. *Nature,* 453**,** 1072-8.

JANG, M. S., RYU, S. W. & KIM, E. 2002. Modification of Daxx by small ubiquitin-related modifier-1. *Biochem Biophys Res Commun,* 295, 495-500.

JEANNE, M., LALLEMAND-BREITENBACH, V., FERHI, O., KOKEN, M., LE BRAS, M., DUFFORT, S., PERES, L., BERTHIER, C., SOILIHI, H., RAUGHT, B. & DE THE, H. 2010. PML/RARA oxidation and arsenic binding initiate the antileukemia response of As2O3. *Cancer Cell,* 18**,** 88-98.

JENSEN, K., SHIELS, C. & FREEMONT, P. S. 2001. PML protein isoforms and the RBCC/TRIM motif. *Oncogene,* 20, 7223-33.

JOHNSON, E. S. & BLOBEL, G. 1999. Cell cycle-regulated attachment of the ubiquitin-related protein SUMO to the yeast septins. *J Cell Biol,* 147, 981-94.

KAISER, T. E., INTINE, R. V. & DUNDR, M. 2008. De novo formation of a subnuclear body. *Science,* 322, 1713-7.

KAKIZUKA, A., MILLER, W. H., JR., UMESONO, K., WARRELL, R. P., JR., FRANKEL, S. R., MURTY, V. V., DMITROVSKY, E. & EVANS, R. M. 1991. Chromosomal translocation t(15;17) in human acute promyelocytic leukemia fuses RAR alpha with a novel putative transcription factor, PML. *Cell,* 66, 663-74.

KAMITANI, T., KITO, K., NGUYEN, H. P., FUKUDA-KAMITANI, T. & YEH, E. T. 1998a. Characterization of a second member of the sentrin family of ubiquitin-like proteins. *J Biol Chem,* 273, 11349-53.

KAMITANI, T., KITO, K., NGUYEN, H. P., WADA, H., FUKUDA-KAMITANI, T. & YEH, E. T. 1998b. Identification of three major sentrinization sites in PML. *J Biol Chem,* 273, 26675-82.

KAMITANI, T., NGUYEN, H. P., KITO, K., FUKUDA-KAMITANI, T. & YEH, E. T. 1998c. Covalent modification of PML by the sentrin family of ubiquitin-like proteins. *J Biol Chem,* 273, 3117-20.

KAUFMANN, M., BOZIC, D., BRIAND, C., BODMER, J. L., ZERBE, O., KOHL, A., TSCHOPP, J. & GRUTTER, M. G. 2002. Identification of a basic surface area of the FADD death effector domain critical for apoptotic signaling. *FEBS Lett,* 527, 250-4.

KIM, H. J., SONG, D. E., LIM, S. Y., LEE, S. H., KANG, J. L., LEE, S. J., BENVENISTE, E. N. & CHOI, Y. H. 2011. Loss of the promyelocytic leukemia protein in gastric cancer: implications for IP-10 expression and tumor-infiltrating lymphocytes. *PLoS One,* 6, e26264.

KISCHKEL, F. C., HELLBARDT, S., BEHRMANN, I., GERMER, M., PAWLITA, M., KRAMMER, P. H. & PETER, M. E. 1995. Cytotoxicity-dependent APO-1 (Fas/CD95)-associated proteins form a death-inducing signaling complex (DISC) with the receptor. *EMBO J,* 14, 5579-88.

KNIPPSCHILD, U., GOCHT, A., WOLFF, S., HUBER, N., LOHLER, J. & STOTER, M. 2005. The casein kinase 1 family: participation in multiple cellular processes in eukaryotes. *Cell Signal,* 17, 675-89.

KNIPSCHEER, P., FLOTHO, A., KLUG, H., OLSEN, J. V., VAN DIJK, W. J., FISH, A., JOHNSON, E. S., MANN, M., SIXMA, T. K. & PICHLER, A. 2008. Ubc9 sumoylation regulates SUMO target discrimination. *Mol Cell,* 31, 371-82.

KNIPSCHEER, P., VAN DIJK, W. J., OLSEN, J. V., MANN, M. & SIXMA, T. K. 2007. Noncovalent interaction between Ubc9 and SUMO promotes SUMO chain formation. *EMBO J,* 26, 2797-807.

KOKEN, M. H., LINARES-CRUZ, G., QUIGNON, F., VIRON, A., CHELBI-ALIX, M. K., SOBCZAK-THEPOT, J., JUHLIN, L., DEGOS, L., CALVO, F. & DE THE, H. 1995. The PML growth-suppressor has an altered expression in human oncogenesis. *Oncogene,* 10, 1315-24.

LALLEMAND-BREITENBACH, V. & DE THE, H. 2010. PML nuclear bodies. *Cold Spring Harb Perspect Biol,* 2, a000661.

LALLEMAND-BREITENBACH, V., JEANNE, M., BENHENDA, S., NASR, R., LEI, M., PERES, L., ZHOU, J., ZHU, J., RAUGHT, B. & DE THE, H. 2008. Arsenic degrades PML or PML-RARalpha through a SUMO-triggered RNF4/ubiquitin-mediated pathway. *Nat Cell Biol,* 10, 547-55.

LALLEMAND-BREITENBACH, V., ZHU, J., CHEN, Z. & DE THE, H. 2012. Curing APL through PML/RARA degradation by As2O3. *Trends Mol Med,* 18, 36-42.

LALLEMAND-BREITENBACH, V., ZHU, J., PUVION, F., KOKEN, M., HONORE, N., DOUBEIKOVSKY, A., DUPREZ, E., PANDOLFI, P. P., PUVION, E., FREEMONT, P. & DE THE, H. 2001. Role of promyelocytic leukemia (PML) sumolation in nuclear body formation, 11S proteasome recruitment, and As2O3-induced PML or PML/retinoic acid receptor alpha degradation. *J Exp Med,* 193, 1361-71.

LAMOND, A. I. & EARNSHAW, W. C. 1998. Structure and function in the nucleus. *Science,* 280, 547-53.
LANCTOT, C., CHEUTIN, T., CREMER, M., CAVALLI, G. & CREMER, T. 2007. Dynamic genome architecture in the nuclear space: regulation of gene expression in three dimensions. *Nat Rev Genet,* 8, 104-15.
LAPENTA, V., CHIURAZZI, P., VAN DER SPEK, P., PIZZUTI, A., HANAOKA, F. & BRAHE, C. 1997. SMT3A, a human homologue of the S. cerevisiae SMT3 gene, maps to chromosome 21qter and defines a novel gene family. *Genomics,* 40, 362-6.
LAVAU, C., MARCHIO, A., FAGIOLI, M., JANSEN, J., FALINI, B., LEBON, P., GROSVELD, F., PANDOLFI, P. P., PELICCI, P. G. & DEJEAN, A. 1995. The acute promyelocytic leukaemia-associated PML gene is induced by interferon. *Oncogene,* 11, 871-6.
LE, X. F., YANG, P. & CHANG, K. S. 1996. Analysis of the growth and transformation suppressor domains of promyelocytic leukemia gene, PML. *J Biol Chem,* 271, 130-5.
LEE, H. E., JEE, C. D., KIM, M. A., LEE, H. S., LEE, Y. M., LEE, B. L. & KIM, W. H. 2007. Loss of promyelocytic leukemia protein in human gastric cancers. *Cancer Lett,* 247, 103-9.
LEPPARD, K. N., EMMOTT, E., CORTESE, M. S. & RICH, T. 2009. Adenovirus type 5 E4 Orf3 protein targets promyelocytic leukaemia (PML) protein nuclear domains for disruption via a sequence in PML isoform II that is predicted as a protein interaction site by bioinformatic analysis. *J Gen Virol,* 90, 95-104.
LIN, D. Y., HUANG, Y. S., JENG, J. C., KUO, H. Y., CHANG, C. C., CHAO, T. T., HO, C. C., CHEN, Y. C., LIN, T. P., FANG, H. I., HUNG, C. C., SUEN, C. S., HWANG, M. J., CHANG, K. S., MAUL, G. G. & SHIH, H. M. 2006. Role of SUMO-interacting motif in Daxx SUMO modification, subnuclear localization, and repression of sumoylated transcription factors. *Mol Cell,* 24, 341-54.
LIN, H. K., BERGMANN, S. & PANDOLFI, P. P. 2004. Cytoplasmic PML function in TGF-beta signalling. *Nature,* 431, 205-11.
LONGENECKER, K. L., ROACH, P. J. & HURLEY, T. D. 1996. Three-dimensional structure of mammalian casein kinase I: molecular basis for phosphate recognition. *J Mol Biol,* 257, 618-31.
MANNEN, H., TSENG, H. M., CHO, C. L. & LI, S. S. 1996. Cloning and expression of human homolog HSMT3 to yeast SMT3 suppressor of MIF2 mutations in a centromere protein gene. *Biochem Biophys Res Commun,* 222, 178-80.
MAO, Y. S., ZHANG, B. & SPECTOR, D. L. 2011. Biogenesis and function of nuclear bodies. *Trends Genet,* 27, 295-306.
MARTIN-MARTIN, N., SUTHERLAND, J. D. & CARRACEDO, A. 2013. PML: Not all about Tumor Suppression. *Front Oncol,* 3**,** 200.
MATERA, A. G., IZAGUIRE-SIERRA, M., PRAVEEN, K. & RAJENDRA, T. K. 2009. Nuclear bodies: random aggregates of sticky proteins or crucibles of macromolecular assembly? *Dev Cell,* 17, 639-47.
MATIC, I., MACEK, B., HILGER, M., WALTHER, T. C. & MANN, M. 2008. Phosphorylation of SUMO-1 occurs in vivo and is conserved through evolution. *J Proteome Res,* 7, 4050-7.
MATUNIS, M. J., COUTAVAS, E. & BLOBEL, G. 1996. A novel ubiquitin-like modification modulates the partitioning of the Ran-GTPase-activating protein

RanGAP1 between the cytosol and the nuclear pore complex. *J Cell Biol,* 135, 1457-70.
MCNALLY, B. A., TRGOVCICH, J., MAUL, G. G., LIU, Y. & ZHENG, P. 2008. A role for cytoplasmic PML in cellular resistance to viral infection. *PLoS One,* 3, e2277.
MEDEMA, J. P., SCAFFIDI, C., KISCHKEL, F. C., SHEVCHENKO, A., MANN, M., KRAMMER, P. H. & PETER, M. E. 1997. FLICE is activated by association with the CD95 death-inducing signaling complex (DISC). *EMBO J,* 16, 2794-804.
MICHAELSON, J. S., BADER, D., KUO, F., KOZAK, C. & LEDER, P. 1999. Loss of Daxx, a promiscuously interacting protein, results in extensive apoptosis in early mouse development. *Genes Dev,* 13, 1918-23.
MILOVIC-HOLM, K., KRIEGHOFF, E., JENSEN, K., WILL, H. & HOFMANN, T. G. 2007. FLASH links the CD95 signaling pathway to the cell nucleus and nuclear bodies. *EMBO J,* 26, 391-401.
MINTY, A., DUMONT, X., KAGHAD, M. & CAPUT, D. 2000. Covalent modification of p73alpha by SUMO-1. Two-hybrid screening with p73 identifies novel SUMO-1-interacting proteins and a SUMO-1 interaction motif. *J Biol Chem,* 275, 36316-23.
MISTELI, T. 2001. Protein dynamics: implications for nuclear architecture and gene expression. *Science,* 291, 843-7.
MISTELI, T. 2007. Beyond the sequence: cellular organization of genome function. *Cell,* 128, 787-800.
MISTELI, T. 2008. Cell biology: Nuclear order out of chaos. *Nature,* 456, 333-4.
MISTELI, T. 2010. Higher-order genome organization in human disease. *Cold Spring Harb Perspect Biol,* 2, a000794.
MOILANEN, A. M., POUKKA, H., KARVONEN, U., HAKLI, M., JANNE, O. A. & PALVIMO, J. J. 1998. Identification of a novel RING finger protein as a coregulator in steroid receptor-mediated gene transcription. *Mol Cell Biol,* 18, 5128-39.
MORGAN, M., THORBURN, J., PANDOLFI, P. P. & THORBURN, A. 2002. Nuclear and cytoplasmic shuttling of TRADD induces apoptosis via different mechanisms. *J Cell Biol,* 157, 975-84.
MORGAN, M. J., THORBURN, J., THOMAS, L., MAXWELL, T., BROTHMAN, A. R. & THORBURN, A. 2001. An apoptosis signaling pathway induced by the death domain of FADD selectively kills normal but not cancerous prostate epithelial cells. *Cell Death Differ,* 8, 696-705.
MULLER, S., MATUNIS, M. J. & DEJEAN, A. 1998. Conjugation with the ubiquitin-related modifier SUMO-1 regulates the partitioning of PML within the nucleus. *Embo J,* 17, 61-70.
NAGATA, S. 1999. Fas ligand-induced apoptosis. *Annu Rev Genet,* 33, 29-55.
NASR, R., GUILLEMIN, M. C., FERHI, O., SOILIHI, H., PERES, L., BERTHIER, C., ROUSSELOT, P., ROBLEDO-SARMIENTO, M., LALLEMAND-BREITENBACH, V., GOURMEL, B., VITOUX, D., PANDOLFI, P. P., ROCHETTE-EGLY, C., ZHU, J. & DE THE, H. 2008. Eradication of acute promyelocytic leukemia-initiating cells through PML-RARA degradation. *Nat Med,* 14, 1333-42.
NEGOREV, D. & MAUL, G. G. 2001. Cellular proteins localized at and interacting within ND10/PML nuclear bodies/PODs suggest functions of a nuclear depot. *Oncogene,* 20, 7234-42.

OKURA, T., GONG, L., KAMITANI, T., WADA, T., OKURA, I., WEI, C. F., CHANG, H. M. & YEH, E. T. 1996. Protection against Fas/APO-1- and tumor necrosis factor-mediated cell death by a novel protein, sentrin. *J Immunol,* 157, 4277-81.

PANDOLFI, P. P., GRIGNANI, F., ALCALAY, M., MENCARELLI, A., BIONDI, A., LOCOCO, F. & PELICCI, P. G. 1991. Structure and origin of the acute promyelocytic leukemia myl/RAR alpha cDNA and characterization of its retinoid-binding and transactivation properties. *Oncogene,* 6, 1285-92.

PERCHERANCIER, Y., GERMAIN-DESPREZ, D., GALISSON, F., MASCLE, X. H., DIANOUX, L., ESTEPHAN, P., CHELBI-ALIX, M. K. & AUBRY, M. 2009. Role of SUMO in RNF4-mediated promyelocytic leukemia protein (PML) degradation: sumoylation of PML and phospho-switch control of its SUMO binding domain dissected in living cells. *J Biol Chem,* 284, 16595-608.

PRUDDEN, J., PEBERNARD, S., RAFFA, G., SLAVIN, D. A., PERRY, J. J., TAINER, J. A., MCGOWAN, C. H. & BODDY, M. N. 2007. SUMO-targeted ubiquitin ligases in genome stability. *EMBO J,* 26, 4089-101.

QUIGNON, F., DE BELS, F., KOKEN, M., FEUNTEUN, J., AMEISEN, J. C. & DE THE, H. 1998. PML induces a novel caspase-independent death process. *Nat Genet,* 20, 259-65.

REDNER, R. L., RUSH, E. A., FAAS, S., RUDERT, W. A. & COREY, S. J. 1996. The t(5;17) variant of acute promyelocytic leukemia expresses a nucleophosmin-retinoic acid receptor fusion. *Blood,* 87, 882-6.

REGAD, T. & CHELBI-ALIX, M. K. 2001. Role and fate of PML nuclear bodies in response to interferon and viral infections. *Oncogene,* 20, 7274-86.

REINEKE, E. L. & KAO, H. Y. 2009. Targeting promyelocytic leukemia protein: a means to regulating PML nuclear bodies. *Int J Biol Sci,* 5, 366-76.

REYMOND, A., MERONI, G., FANTOZZI, A., MERLA, G., CAIRO, S., LUZI, L., RIGANELLI, D., ZANARIA, E., MESSALI, S., CAINARCA, S., GUFFANTI, A., MINUCCI, S., PELICCI, P. G. & BALLABIO, A. 2001. The tripartite motif family identifies cell compartments. *EMBO J,* 20, 2140-51.

RIVERS, A., GIETZEN, K. F., VIELHABER, E. & VIRSHUP, D. M. 1998. Regulation of casein kinase I epsilon and casein kinase I delta by an in vivo futile phosphorylation cycle. *J Biol Chem,* 273, 15980-4.

ROCHAT-STEINER, V., BECKER, K., MICHEAU, O., SCHNEIDER, P., BURNS, K. & TSCHOPP, J. 2000. FIST/HIPK3: a Fas/FADD-interacting serine/threonine kinase that induces FADD phosphorylation and inhibits fas-mediated Jun NH(2)-terminal kinase activation. *J Exp Med,* 192, 1165-74.

RYU, S. W., CHAE, S. K. & KIM, E. 2000. Interaction of Daxx, a Fas binding protein, with sentrin and Ubc9. *Biochem Biophys Res Commun,* 279, 6-10.

SAITOH, H., UWADA, J. & AZUSA, K. 2009. Strategies for the expression of SUMO-modified target proteins in Escherichia coli. *Methods Mol Biol,* 497, 211-21.

SALOMONI, P. 2013. The PML-Interacting Protein DAXX: Histone Loading Gets into the Picture. *Front Oncol,* 3**,** 152.

SALOMONI, P. & BELLODI, C. 2007. New insights into the cytoplasmic function of PML. *Histol Histopathol,* 22, 937-46.

SALOMONI, P. & KHELIFI, A. F. 2006. Daxx: death or survival protein? *Trends Cell Biol,* 16, 97-104.

SAMBROOK, J., FRITSCH, E. F., AND MANIATIS, T. 1989. *Molecular Cloning: A Laboratory Manual, (Nolan, C., and Ford, N., eds) 2nd Ed.* Cold Spring Harbor, NY: Cold Spring Harbor Laboratory.

SANCHEZ-PULIDO, L., VALENCIA, A. & ROJAS, A. M. 2007. Are promyelocytic leukaemia protein nuclear bodies a scaffold for caspase-2 programmed cell death? *Trends Biochem Sci,* 32, 400-6.

SANDU, C., MORISAWA, G., WEGORZEWSKA, I., HUANG, T., ARECHIGA, A. F., HILL, J. M., KIM, T., WALSH, C. M. & WERNER, M. H. 2006. FADD self-association is required for stable interaction with an activated death receptor. *Cell Death Differ,* 13**,** 2052-61.

SCAFFIDI, C., FULDA, S., SRINIVASAN, A., FRIESEN, C., LI, F., TOMASELLI, K. J., DEBATIN, K. M., KRAMMER, P. H. & PETER, M. E. 1998. Two CD95 (APO-1/Fas) signaling pathways. *EMBO J,* 17, 1675-87.

SCAFFIDI, C., VOLKLAND, J., BLOMBERG, I., HOFFMANN, I., KRAMMER, P. H. & PETER, M. E. 2000. Phosphorylation of FADD/ MORT1 at serine 194 and association with a 70-kDa cell cycle-regulated protein kinase. *J Immunol,* 164, 1236-42.

SCAGLIONI, P. P., YUNG, T. M., CAI, L. F., ERDJUMENT-BROMAGE, H., KAUFMAN, A. J., SINGH, B., TERUYA-FELDSTEIN, J., TEMPST, P. & PANDOLFI, P. P. 2006. A CK2-dependent mechanism for degradation of the PML tumor suppressor. *Cell,* 126, 269-83.

SCHMIDT, J. C., KIYOMITSU, T., HORI, T., BACKER, C. B., FUKAGAWA, T. & CHEESEMAN, I. M. 2010. Aurora B kinase controls the targeting of the Astrin-SKAP complex to bioriented kinetochores. *J Cell Biol,* 191, 269-80.

SEELER, J. S. & DEJEAN, A. 2003. Nuclear and unclear functions of SUMO. *Nat Rev Mol Cell Biol,* 4, 690-9.

SESSLER, T., HEALY, S., SAMALI, A. & SZEGEZDI, E. 2013. Structural determinants of DISC function: new insights into death receptor-mediated apoptosis signalling. *Pharmacol Ther,* 140**,** 186-99.

SHEN, T. H., LIN, H. K., SCAGLIONI, P. P., YUNG, T. M. & PANDOLFI, P. P. 2006. The mechanisms of PML-nuclear body formation. *Mol Cell,* 24, 331-9.

SHEN, Z., PARDINGTON-PURTYMUN, P. E., COMEAUX, J. C., MOYZIS, R. K. & CHEN, D. J. 1996. UBL1, a human ubiquitin-like protein associating with human RAD51/RAD52 proteins. *Genomics,* 36, 271-9.

SHIRAKURA, H., HAYASHI, N., OGINO, S., TSURUMA, K., UEHARA, T. & NOMURA, Y. 2005. Caspase recruitment domain of procaspase-2 could be a target for SUMO-1 modification through Ubc9. *Biochem Biophys Res Commun,* 331, 1007-15.

SIEGEL, R. M., MARTIN, D. A., ZHENG, L., NG, S. Y., BERTIN, J., COHEN, J. & LENARDO, M. J. 1998. Death-effector filaments: novel cytoplasmic structures that recruit caspases and trigger apoptosis. *J Cell Biol,* 141, 1243-53.

SIMPSON-LAVY, K. J. & JOHNSTON, M. 2013. SUMOylation regulates the SNF1 protein kinase. *Proc Natl Acad Sci U S A,* 110, 17432-7.

SONG, J., DURRIN, L. K., WILKINSON, T. A., KRONTIRIS, T. G. & CHEN, Y. 2004. Identification of a SUMO-binding motif that recognizes SUMO-modified proteins. *Proc Natl Acad Sci U S A,* 101, 14373-8.

STADLER, M., CHELBI-ALIX, M. K., KOKEN, M. H., VENTURINI, L., LEE, C., SAIB, A., QUIGNON, F., PELICANO, L., GUILLEMIN, M. C., SCHINDLER, C. & ET AL. 1995. Transcriptional induction of the PML

growth suppressor gene by interferons is mediated through an ISRE and a GAS element. *Oncogene,* 11, 2565-73.

STERNSDORF, T., JENSEN, K., REICH, B. & WILL, H. 1999. The nuclear dot protein sp100, characterization of domains necessary for dimerization, subcellular localization, and modification by small ubiquitin-like modifiers. *J Biol Chem,* 274, 12555-66.

STERNSDORF, T., JENSEN, K. & WILL, H. 1997. Evidence for covalent modification of the nuclear dot-associated proteins PML and Sp100 by PIC1/SUMO-1. *J Cell Biol,* 139, 1621-34.

SUN, H., LEVERSON, J. D. & HUNTER, T. 2007. Conserved function of RNF4 family proteins in eukaryotes: targeting a ubiquitin ligase to SUMOylated proteins. *EMBO J,* 26, 4102-12.

SZOSTECKI, C., GULDNER, H. H., NETTER, H. J. & WILL, H. 1990. Isolation and characterization of cDNA encoding a human nuclear antigen predominantly recognized by autoantibodies from patients with primary biliary cirrhosis. *J Immunol,* 145, 4338-47.

TANG, D., LAHTI, J. M., GRENET, J. & KIDD, V. J. 1999. Cycloheximide-induced T-cell death is mediated by a Fas-associated death domain-dependent mechanism. *J Biol Chem,* 274, 7245-52.

TANG, J., XIE, W. & YANG, X. 2005. Association of caspase-2 with the promyelocytic leukemia protein nuclear bodies. *Cancer Biol Ther,* 4, 645-9.

TAO, R. H., BERKOVA, Z., WISE, J. F., REZAEIAN, A. H., DANILUK, U., AO, X., HAWKE, D. H., KARP, J. E., LIN, H. K., MOLLDREM, J. J. & SAMANIEGO, F. 2011. PMLRARalpha binds to Fas and suppresses Fas-mediated apoptosis through recruiting c-FLIP in vivo. *Blood,* 118, 3107-18.

TATHAM, M. H., GEOFFROY, M. C., SHEN, L., PLECHANOVOVA, A., HATTERSLEY, N., JAFFRAY, E. G., PALVIMO, J. J. & HAY, R. T. 2008. RNF4 is a poly-SUMO-specific E3 ubiquitin ligase required for arsenic-induced PML degradation. *Nat Cell Biol,* 10, 538-46.

TATHAM, M. H., JAFFRAY, E., VAUGHAN, O. A., DESTERRO, J. M., BOTTING, C. H., NAISMITH, J. H. & HAY, R. T. 2001. Polymeric chains of SUMO-2 and SUMO-3 are conjugated to protein substrates by SAE1/SAE2 and Ubc9. *J Biol Chem,* 276, 35368-74.

TORII, S., EGAN, D. A., EVANS, R. A. & REED, J. C. 1999. Human Daxx regulates Fas-induced apoptosis from nuclear PML oncogenic domains (PODs). *Embo J,* 18, 6037-49.

TOURNEUR, L. & CHIOCCHIA, G. 2010. FADD: a regulator of life and death. *Trends Immunol,* 31**,** 260-9.

TUSSIE-LUNA, M. I., ROZO, L. & ROY, A. L. 2006. Pro-proliferative function of the long isoform of PML-RARalpha involved in acute promyelocytic leukemia. *Oncogene,* 25, 3375-86.

UCHIMURA, Y., NAKAMURA, M., SUGASAWA, K., NAKAO, M. & SAITOH, H. 2004. Overproduction of eukaryotic SUMO-1- and SUMO-2-conjugated proteins in Escherichia coli. *Anal Biochem,* 331, 204-6.

ULLMAN, A. J., REICH, N. C. & HEARING, P. 2007. Adenovirus E4 ORF3 protein inhibits the interferon-mediated antiviral response. *J Virol,* 81, 4744-52.

UZUNOVA, K., GOTTSCHE, K., MITEVA, M., WEISSHAAR, S. R., GLANEMANN, C., SCHNELLHARDT, M., NIESSEN, M., SCHEEL, H., HOFMANN, K., JOHNSON, E. S., PRAEFCKE, G. J. & DOHMEN, R. J.

2007. Ubiquitin-dependent proteolytic control of SUMO conjugates. *J Biol Chem,* 282, 34167-75.

VENERANDO, A., MARIN, O., COZZA, G., BUSTOS, V. H., SARNO, S. & PINNA, L. A. 2010. Isoform specific phosphorylation of p53 by protein kinase CK1. *Cell Mol Life Sci,* 67, 1105-18.

VICKERS, M., JACKSON, G. & TAYLOR, P. 2000. The incidence of acute promyelocytic leukemia appears constant over most of a human lifespan, implying only one rate limiting mutation. *Leukemia,* 14, 722-6.

WANG, Z. G., DELVA, L., GABOLI, M., RIVI, R., GIORGIO, M., CORDON-CARDO, C., GROSVELD, F. & PANDOLFI, P. P. 1998a. Role of PML in cell growth and the retinoic acid pathway. *Science,* 279, 1547-51.

WANG, Z. G., RUGGERO, D., RONCHETTI, S., ZHONG, S., GABOLI, M., RIVI, R. & PANDOLFI, P. P. 1998b. PML is essential for multiple apoptotic pathways. *Nat Genet,* 20, 266-72.

WEIDTKAMP-PETERS, S., LENSER, T., NEGOREV, D., GERSTNER, N., HOFMANN, T. G., SCHWANITZ, G., HOISCHEN, C., MAUL, G., DITTRICH, P. & HEMMERICH, P. 2008. Dynamics of component exchange at PML nuclear bodies. *J Cell Sci,* 121, 2731-43.

WELLS, R. A., CATZAVELOS, C. & KAMEL-REID, S. 1997. Fusion of retinoic acid receptor alpha to NuMA, the nuclear mitotic apparatus protein, by a variant translocation in acute promyelocytic leukaemia. *Nat Genet,* 17, 109-13.

WILKINSON, K. A. & HENLEY, J. M. 2010. Mechanisms, regulation and consequences of protein SUMOylation. *Biochem J,* 428, 133-45.

XIE, P. 2013. TRAF molecules in cell signaling and in human diseases. *J Mol Signal,* 8**,** 7.

XU, R. M., CARMEL, G., SWEET, R. M., KURET, J. & CHENG, X. 1995. Crystal structure of casein kinase-1, a phosphate-directed protein kinase. *EMBO J,* 14, 1015-23.

YANG, X., KHOSRAVI-FAR, R., CHANG, H. Y. & BALTIMORE, D. 1997. Daxx, a novel Fas-binding protein that activates JNK and apoptosis. *Cell,* 89, 1067-76.

YEN, C. C., TSAO, Y. P., CHEN, P. C., WU, Y. C., LIU, J. H., PAN, C. C., LIU, C. Y., TZENG, C. H., CHEN, P. M., CHEN, Y. J., LIN, C. H. & HSU, W. H. 2011. PML protein as a prognostic molecular marker for patients with esophageal squamous cell carcinomas receiving primary surgery. *J Surg Oncol,* 103, 761-7.

YOON, G. S. & YU, E. 2001. Overexpression of promyelocytic leukemia protein and alteration of PML nuclear bodies in early stage of hepatocarcinogenesis. *J Korean Med Sci,* 16, 433-8.

ZELENT, A., GUIDEZ, F., MELNICK, A., WAXMAN, S. & LICHT, J. D. 2001. Translocations of the RARalpha gene in acute promyelocytic leukemia. *Oncogene,* 20, 7186-203.

ZERINGO, N. A., MURPHY, L., MCCLOSKEY, E. A., ROHAL, L. & BELLIZZI, J. J., 3RD 2013. A monoclinic crystal form of casein kinase 1 delta. *Acta Crystallogr Sect F Struct Biol Cryst Commun,* 69, 1077-83.

ZHANG, P., CHIN, W., CHOW, L. T., CHAN, A. S., YIM, A. P., LEUNG, S. F., MOK, T. S., CHANG, K. S., JOHNSON, P. J. & CHAN, J. Y. 2000. Lack of expression for the suppressor PML in human small cell lung carcinoma. *Int J Cancer,* 85, 599-605.

ZHANG, X., VALLABHANENI, R., LOUGHRAN, P. A., SHAPIRO, R., YIN, X. M., YUAN, Y. & BILLIAR, T. R. 2008. Changes in FADD levels, distribution, and phosphorylation in TNFalpha-induced apoptosis in hepatocytes is caspase-3, caspase-8 and BID dependent. *Apoptosis,* 13, 983-92.

ZHONG, S., MULLER, S., RONCHETTI, S., FREEMONT, P. S., DEJEAN, A. & PANDOLFI, P. P. 2000. Role of SUMO-1-modified PML in nuclear body formation. *Blood,* 95, 2748-52.

ZHU, J., GIANNI, M., KOPF, E., HONORE, N., CHELBI-ALIX, M., KOKEN, M., QUIGNON, F., ROCHETTE-EGLY, C. & DE THE, H. 1999. Retinoic acid induces proteasome-dependent degradation of retinoic acid receptor alpha (RARalpha) and oncogenic RARalpha fusion proteins. *Proc Natl Acad Sci U S A,* 96, 14807-12.

ZHU, J., KOKEN, M. H., QUIGNON, F., CHELBI-ALIX, M. K., DEGOS, L., WANG, Z. Y., CHEN, Z. & DE THE, H. 1997. Arsenic-induced PML targeting onto nuclear bodies: implications for the treatment of acute promyelocytic leukemia. *Proc Natl Acad Sci U S A,* 94, 3978-83.

ZHU, J., ZHOU, J., PERES, L., RIAUCOUX, F., HONORE, N., KOGAN, S. & DE THE, H. 2005. A sumoylation site in PML/RARA is essential for leukemic transformation. *Cancer Cell,* 7**,** 143-53.